CRANFIELD INSTITUTE OF TECHNOLOGY

COLLEGE OF AERONAUTICS

PhD THESIS

VIBRATION OF STRUCTURES WITH NON-LINEAR DAMPING

by

B. S. Gabri M.Sc.

Supervisor: Dr. C. L. Kirk

March 1978

TEXT CUT OFF IN ORIGINAL

TEXT BOUND INTO THE SPINE

Summary

The work reported here is directed towards the problem of measuring and modeling non-linear damping in steel space frame civil engineering structures. In order to gain a better understanding of the damping mechanism in such structures, tests were performed on a full scale bolted lattice structure and the results of section A show that the joint damping can be represented approximately in the form:

$$F_D = C\,(1 + \varepsilon\,|\dot{x}|^n)\dot{x}$$

where n = 1.

Other situations where this form of non-linear damping occurs is in the case of fluid flow past a solid body. In offshore structures the hydro-dynamic force due to drag effects are found to be proportional to velocity squared. For non linear material damping, n, takes a value of 6.

In section B, various methods of solution to the non-linear dynamical system under random excitation were studied and it was found that the 'Equivalent Non-Linear Differential Equation' (ENL) method yields a better measure of the response of the non-linear system to white noise excitation than other approximate methods. Analytical expressions are derived for the mean-square response, probability density function and level crossing rates. With the modified 'ENL' method (MENL) it is shown how one can extract the non-linear damping and excitation power spectral density. A good correlation is obtained between experimental and theoretical results.

SECTION A

CONTENTS

FIGURES

TABLES

NOTATION

A	Actuator piston area (in^2)
a_4	Flatness factor
B_1	Bandwidth (Frequency resolution)
B_c	Bulk modulus of the hydraulic oil (lb/in^2)
C	$= 2\beta_o\omega_o$
C^*	Generalised structural damping
C_D	Drag coefficient
C_{xy}	Co-spectral density function
D	Specific damping energy (in lb/cu-in cycle)
D_o	Total damping energy (in lb/cycle)
E	Energy stored in the tower
$E(X^2)$	Essemble mean square value if displacement
F	Generalised force (lb)
F_D	Damping force
f_r	rth resonant frequency of the tower (Hz)
F(t)	Force acting on the SDOF system
G(s)	Open loop transfer function
$G_c(s)$	Closed loop transfer function
$\|H(f)\|$	Modulus of transfer function
i	Servovalve current (mA)
J	Material constant
K_1	Gain of the servovalve (mA/volt)
K_3	$2\mathfrak{J}/\omega_n$
K_4	$1/\omega_n^2$
K_5	Gain of load cell and amplifier (volts/lb)

K_o	Spring stiffness (lb/in)
K	Open loop gain (1/s)
K^*	Generalised stiffness of the tower (lb/in)
K_h	Hydraulic stiffness (lb/in)
K_v	Value gain (Cls/mA)
M^*	Generalised mass of the tower (lb $in^{-1}s^2$)
M(Y)	Mass per limit length at point Y
n	Material constant
P_L	Load pressure (lb/in^2)
$P(X\dot{X})$	Joint probability density of displacement and velocity
P(X)	Probability density of displacement
Q_{XY}	Quad-spectral density
q	Flow through the servovalve (cis)
$R_{XX}(\tau)$	Autocorrelation function
s	Laplace Operator
S	Stress amplitude
S_e	Reference stress amplitude
S_X	Power spectral density of displacement
S_{FX}	Cross-spectral density of force&displacement
S_o^*	Double sided power spectral density of generalised force
T	Time
t	time
V_y	wind velocity at height y above ground level
V_o	Output of bridge amplifier (volts)
V_t	Volume of fluid in the actuator (in^3)

W_o	Single sided power spectral density of force
X	Displacement (in)
$\dot{X}$	Velocity (in/s)
$\ddot{X}$	Acceleration (in/s^2)
$\overline{X}$	Mean displacement
Y	Displacement
Z	Displacement
β	Critical damping ratio
β_o	Critical damping ratio at zero amplitude
γ	Material constant
δ_a	Aerodynamic logarithmic decrement
ϵ	Non-linear damping parameter
ϵ^*	Non-dimensional non-linearity parameter
ϵ_r	Normalised standard error
ϵ_b	Bias error
θ	Strain measured by the strain gauge
λ	Non-dimensional displacement
μ	Coefficient of friction
π	= 3.14159
ρ	Density of air
Σ	Summation
$\phi_r(y)$	rth mode shape of the tower
Ψ_x^2	mean square displacement

ω	Frequency of the tower in rad/s
ω_o	Frequency of the tower with linear damping
ω_n	Apparent natural frequency of the servovalve (rad/s)
ω_s	Fundamental frequency of the tower (rad/s)
ω_c	Combined frequency (rad/s)
ω_h	Hydraulic frequency (rad/s)
δ_o	$= \sqrt{\frac{\pi S_o}{2\beta_o \omega_o}}$

SECTION A

Introduction

In the past, considerable interest has been shown in the problem of wind excited vibrations of large structures. There have been many published papers (1-5) describing such aspects as the power spectra of wind, the mechanism of wind induced forces and the response of large structures to turbulent wind and earthquake excitations etc. However little work has been done on investigating damping mechanisms in full scale structures.

The response of a structure to dynamic loading is strongly dependent on such basic properties as the natural frequencies of vibration and the damping in the structure. The increase in size and flexibility of many modern structures and the corresponding decrease in their natural frequencies has made them more prone to excitation by natural vibration exciting influences. For example, television transmission towers and masts (6) water towers, suspension bridges (7) and tall multi-storey buildings (8) can be adversely affected by random excitation due to wind and earthquakes.

The response of such structures to deterministic or random excitation usually shows some degree of non-linearity. This non-linear behaviour is a result of either non-linear damping or non-linear stiffness or combination of both. The problem of non-linear stiffness has been studied extensively both in aircraft and civil engineering structures. From the point of view of the calculation of structural response to random excitation, a damping non-linearity is more important than a stiffness non-linearity. Lyon (9) has shown that stiffness non-linearity becomes significant when exciting jet noise pressure level exceeds 143 db but the damping non-linearity should be taken into account even at 20db below this level. Crandall (10) has shown that non-linear damping has more profound effect on the fatigue life of a structure , yet there has been little work done, in the study of non-linear damping in civil engineering structures.

When structures are subjected to vibration they dissipate energy. Although considerable information is available on the individual damping mechanism, i.e. material damping, joint damping and aerodynamic damping etc., there is little information available on the overall non-linear damping in built-up civil engineering structures which consists of various members jointed together.

Unlike the stiffness and the mass properties of a structure, the damping characteristics cannot be determined with such ease. In formulating a mathematical model of non-linear damping, it is important that some experimental results of damping of a structure are available. Since tests on real structures of necessity are usually conducted at relatively low amplitudes, little information is found from such tests on the non-linear behaviour. Moreover, tests of existing structures yields data on the overall damping capacity, a capacity which may vary to a large extent from one structure to another. They cannot as such provide basic information on the actual sources of energy dissipation. It is also not possible in the case of the model studies to simulate the structure on a reduced scale and it has been shown (11) that damping increases as the model scale is reduced. Thus caution should be used in extrapolating damping data obtained from small models to full scale structures. Bearing this in mind, in the present investigation, the dynamic tests were conducted on a full scale self supporting flood lighting tower and were made at amplitudes large enough to produce the desired non-linear effects.

Section A of this thesis is devoted to experimental work and section B to solving the non-linear differential equation of motion of the structure to random excitation.

In section A a brief review is given on the various sources of damping in structures. Free, steady state and random vibration tests were performed on a 30ft. high self supporting flood lighting tower to study the non-linear damping in such structures.

In section B a brief review is given of the method of analysis of the response of non-linear structure to random excitation. A method used in this thesis is called the 'Equivalent Non-linear Differential Equation' method, which combines an exact solution of the Fokker-Planck equation of a particular form of non-linear differential equation with the equivalent linearisation technique. Originally suggested by Caughey, this method has been used by Kirk (12) for the case of velocity squared damping and is described in detail, together with the derivation of Fokker-Planck equation for the case of linear plus non-linear damping of the form $\epsilon C|\dot{X}|^{n}\dot{X}$. The steady state solution of the Fokker-Planck equation for the equivalent non-linear system is calculated, from which the statistical properties of the system are calculated and compared with exact statistical properties calculated from analogue computer simulation and other approximate methods. To the author's knowledge, there is no published literature which describes the extraction of non-linear damping parameter from random response and excitation measurements. With the modified equivalent non-linear differential equation (MENL) method, it is shown how this parameter can be determined.

The limitations of the analytical approach are

(1) It can only be applied to a single degree of freedom system. For practical purposes, however the representation of a structure by a single degree of freedom system is justified in most cases on the grcund that in most designs, the response of the first mode of the multi-degree of freedom system is usually considered.

(2) In the specification of the random force (i.e. Gaussian White Noise).

(3) In the representation of the non-linear damping force $C (1 + \epsilon | \dot{X} |^{n}) \dot{X}$, i.e. the damping force is proportional to some power of velocity).

2.0 Damping in Steel Structures

The various sources of damping which affect the response of a steel structure are:-

1) Ambient damping

2) Material damping

3) Joint damping

and 4) Foundation damping

2.1 Ambient Damping (Aerodynamic Damping)

A structure vibrating in air is subjected to aerodynamic forces tending to damp the vibrations. In still air these forces will be due mainly to the viscosity of the air disturbed by the vibrating structure. The damping of this nature is insignificant compared with other sources of damping. If, however, the air is flowing past the structure, the principal aerodynamic forces acting will be those from drag and lift. If the structure is oscillating, fluctuating components of drag and lift forces will be induced tending to oppose and hence damp out the motion. This form of damping has been investigated in Ref. (13).

The logarithmic aerodynamic damping decrement is given by the expression

$$\delta_a = \frac{\Delta E}{2E} \qquad (2.1)$$

where ΔE is the work done per cycle against drag forces and E is the total elastic strain energy stored in the structure. Consider the tower vibrating in rth mode $(\phi_r(y))$ then velocity of the tower at a point y is

$$\dot{X} = 2\pi f_r \phi_r(y) \sin(2\pi f_r t)$$

where f_r is the natural frequency is the rth mode. The drag force on area dA in a steady wind velocity V_y is

$$\Delta D = \frac{1}{2} \rho C_D (V_y + \dot{X})^2 \, dA \qquad (2.2)$$

where C_D is the drag coefficient

The drag coefficient C_D is not a constant but varies with Reynold's number, which is function of velocity.

The fluctuating component of this drag is

$$d\,(\Delta D) = \frac{1}{2}\,\rho\, C_D dA\,(2V_y\dot{X}+\dot{X}^2) \qquad (2.3)$$

The work done per cycle on the area dA is then

$$d\,(\Delta E) = \oint_{cycle} d\,(\Delta D)\; d\,X \qquad (2.4)$$

The total energy in the tower is given by kinetic energy at the mid-position of oscillation

$$d\,(E) = \frac{1}{2}\, m\,(y)\, \dot{X}^2 dy \qquad (2.5)$$

where m(y) is the mass per unit length at point y.

Therefore for entire structure

$$\delta_a = \frac{\int_o^L d(\Delta E)}{2\int_o^L d(E)} = \frac{1}{2}\,\frac{\rho C_D B}{f_r}\,\frac{\int_o^L V_y \phi_r^2(y)\, dy}{\int_o^L m(y)\,\phi_r^2(y)\, dy} + \frac{2}{3\pi}\,\frac{\rho C_D B}{f_r}\,\frac{\int_o^L \phi^3(y)\, dy}{\int_o^L m(y)\,\phi^2(y)\, dy} \qquad (2.6)$$

where dA has been assumed to be equal to Bdy

This is the basic expression for the aerodynamic decrement due to the motion of the tower in a steady wind velocity V_y.

Assuming that V_y and m(y) are constant along the height of the tower, the expression for the δ_a reduces to

$$\delta_a = \frac{1}{2} \frac{\rho c_D B V}{f_r m} + \frac{2}{3\pi} \frac{\rho c_D B}{f_r m} \frac{\int_o^L \phi^3 (y)\, dy}{\int_o^L \phi^2 (y)\, dy} \qquad (2.7)$$

In ref.(14), aerodynamic damping in the case of a simulated bridge deck was investigated by attaching plywood to the surface of the truss. Logarithmic decrement with and without the plywood plates attached showed that no change could be measured. This shows that the second term

in equation (2.7) is negligible and hence reduces to

$$\delta a = \frac{1}{2} \frac{\rho C_D B V}{f_r m} \qquad (2.8)$$

Equation (2.8) shows that δa varies directly as the mean wind velocity, V, and inversely as the frequency of vibration, f_r. This implies that the higher modes are lightly damped aerodynamically. Since the tests were carried out in still air, the contribution of the aerodynamic damping to the total critical damping ratio measured is negligible.

2.2 Material Damping

Material damping is a general name for the mechanism by means of which energy is dissipated within a material under cyclic load. Structural materials are not perfectly elastic even at very low stress levels. Inelasticity exists in materials in a variety of different ways. Under cyclic stress, for example, inelastic behaviour takes form of a stress-strain hysteretic loop as shown below the area of which is proportional to the energy dissipated per cycle.

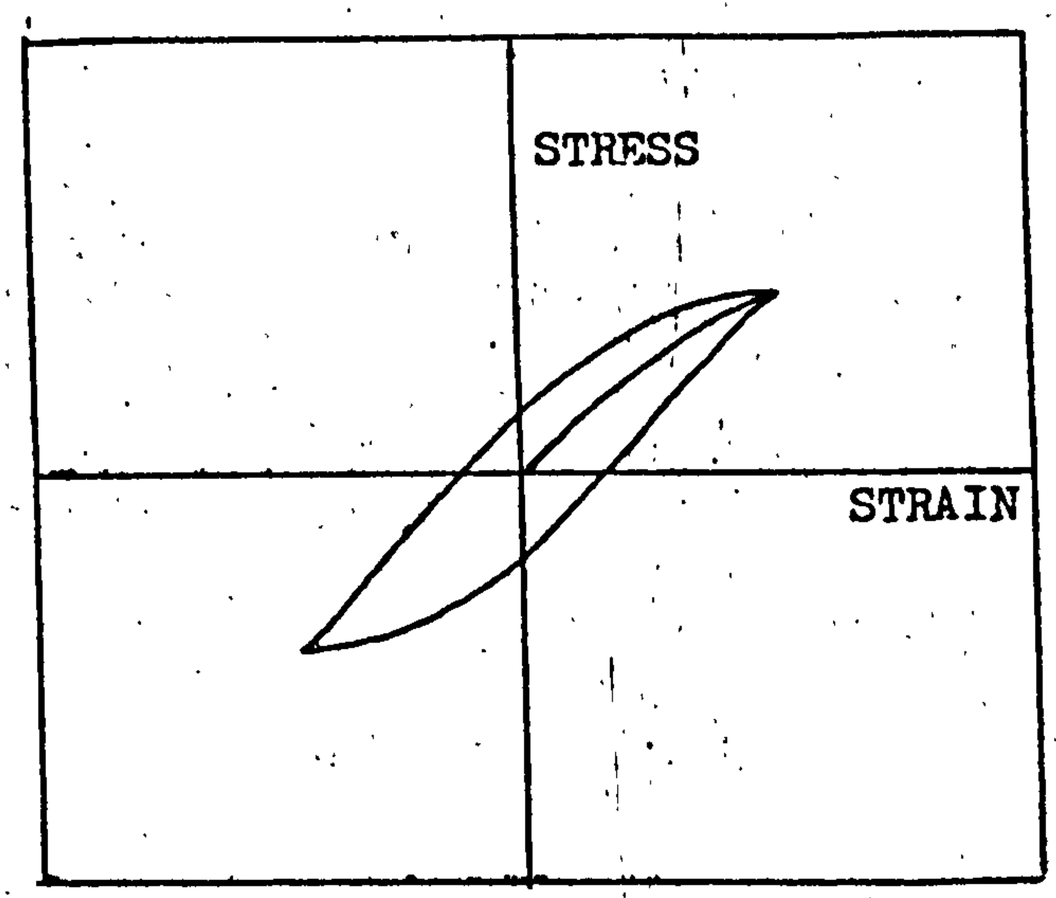

Although such loops are always present at stresses of engineering interest they are often too narrow to be observed by conventional methods. The shape of the loop depends on the damping mechanism operative. The various mechanisms involved in material damping are discussed in Ref.(15).

The damping properties of materials are commonly investigated by subjecting specimens to harmonically varying stress of constant amplitude. The energy dissipated per cycle of stress, per unit volume of material is known as the specific damping energy, D. Thus knowing its variation with stress amplitude, one can predict the material damping of a structure vibrating harmonically in a known mode (as shown in section 2.6).

Several investigations have shown that for most materials, the energy dissipated per cycle of stress is independent of frequency and proportional to the square of the stress amplitude. Kimbell and Lovell Ref.(16) have shown that for a frequency range of 2 cycles per minute to 50 cycles per second, at low stress amplitudes, the expression which best fitted their data is

$$D \propto S^2$$

The low stress range is defined as the range between 0-10 % of fatigue strength (S_e), the intermediate range as 10-30 % of S_e and high range as that above 30 % S_e . The specific damping energy loss for a large number of materials has been generalised to the form

$$D = J(S/S_e)^n \qquad (2.9)$$

where s is the stress amplitude, and J and n are material constants. Since the total damping energy D_o, is the integral of D over the stressed volume, D_o exhibits no dependence on frequency. Ref.(16) indicates that this independence of the total material damping on the frequency is reasonably general at low stress range and over a large frequency range.

Equation (2.9), however, is not valid for high stress levels as illustrated by the damping energy versus stress plot (fig. 1a from Ref.17), for typical structural materials. Goodman and Lazan, Ref.(17) have shown that the energy loss per stress cycle is independent of frequency but nonlinearly dependent on stress amplitude. The empirical relationship between the energy loss per cycle per unit volume and stress for variety of structural material is represented approximately by

$$D = (S/S_e)^{2.3} + 6(S/S_e)^8 \qquad (2.10)$$

This equation follows closely the geometric mean of a band within which are located most of their test-data points. An alternative formula suggested in Ref.(18) is

$$D = J(S/S_e)^2 + \gamma(S/S_e)^{n+2} \qquad (2.11)$$

where J, γ and n are material constants.

In the low stress range, when the first term predominates, it is seen that the specific damping is linear, but in the higher stress range, it becomes highly non-linear. This information allows one to calculate the material damping in a structure. It is seen that stresses above the design working level must be induced in order to obtain higher specific damping values. This may be satisfatory for a small number of cycles but permanent fatigue damage may result from continuously oscillating state.

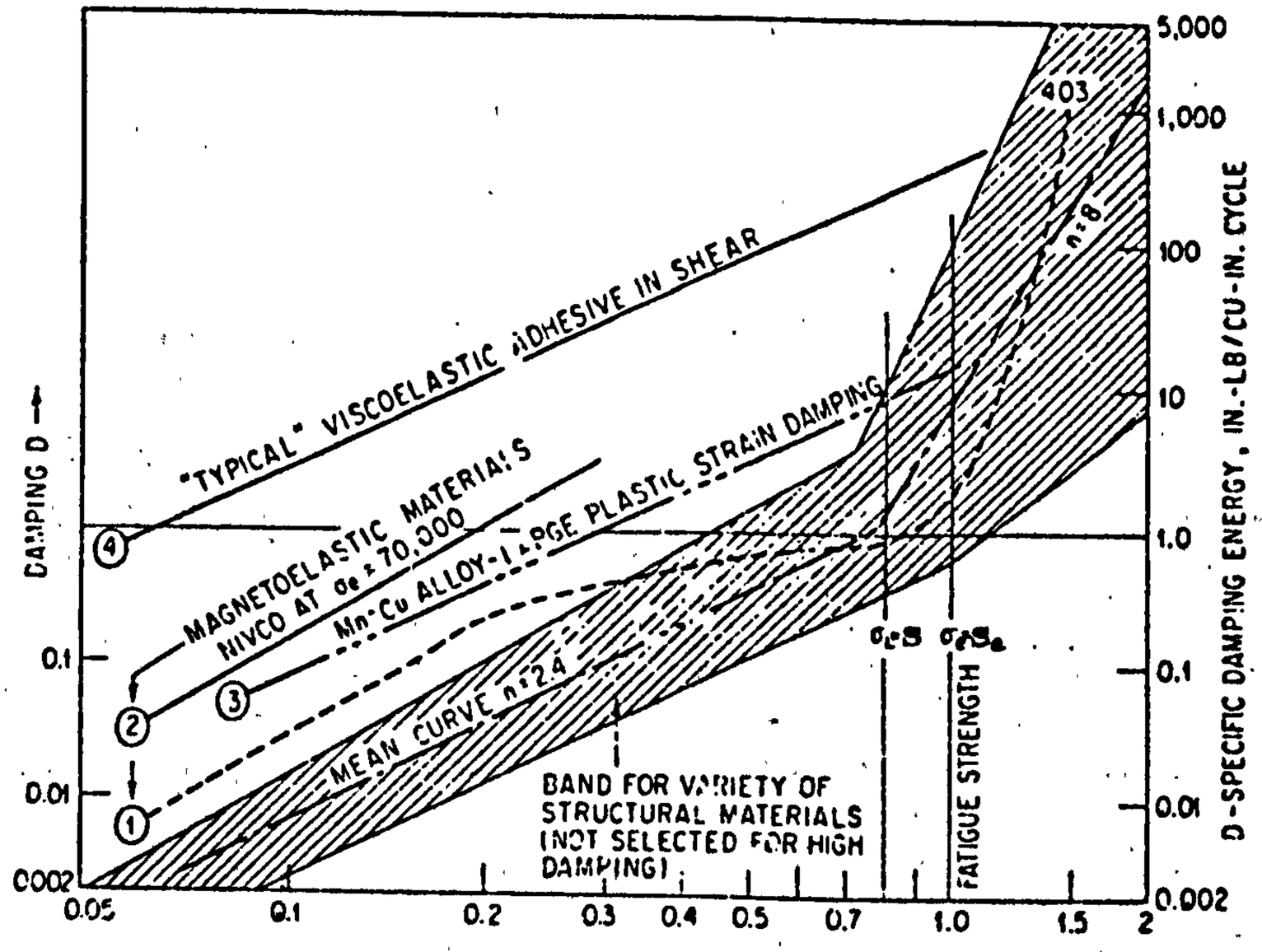

FIGURE 1a (FROM REF.17)

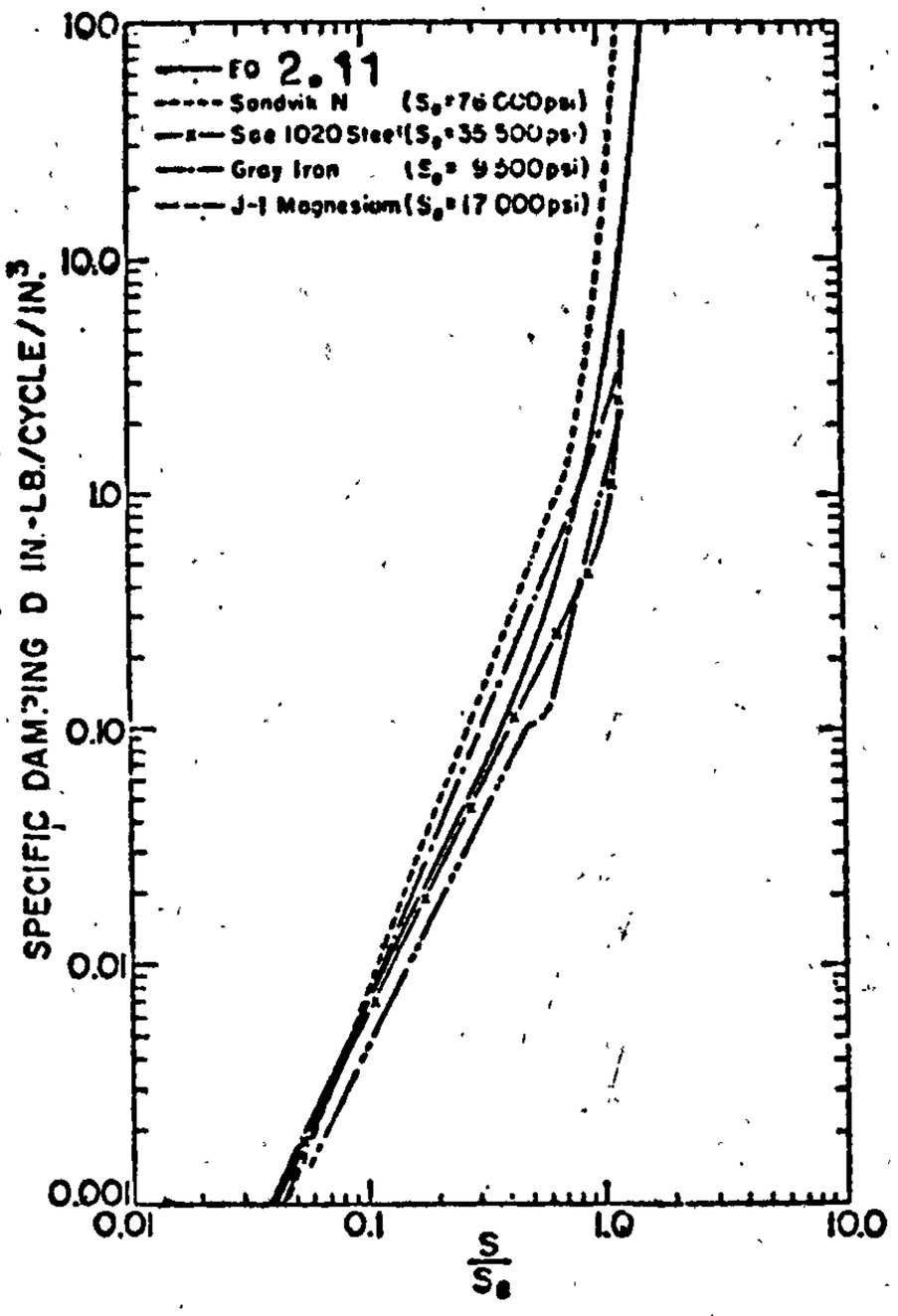

FIGURE 1b (FROM REF.18)

DAMPING ENERGY VERSUS STRESS FOR TYPICAL STRUCTURAL MATERIALS

FIGURE 1

It is important to bear in mind however, that non-linearity of damping is a common feature in structural material, particularly in members undergoing intermediate or high stresses and even in many instances at low stress. For example, SAE 1020 steel which is a linear material at stress level below its cyclic stress sensitivity limit, S_L $(.856S_e)$, where undergoing stresses above this limit, it exhibits a very large non-linearity (i.e. damping energy is proportional to σ^{30}(Ref.(17)).

2.3 Bolted Joint Damping

Measurements of damping in built-up structures have shown that material damping absorbs a small part of energy compared to the total energy dissipated. The major part of the energy dissipation takes place in some form of friction damping from slip or working of the joints. Friction damping has been used in the past in car suspension dampers and also in the Lanchester damper to reduce torsional oscillation in shafts. In contrast to Coulomb damping which does not occur until a given force is reached, slip damping occurs as soon as any bending moment is applied to the structure. The slippage occurs over a restricted region of the joint and has the effect of increasing slightly the deflection of the structure compared with solidly jointed structure.

The damping characteristics of simple built-up structures were first studied in some detail by Pian and Hallowell (19). They analysed I-beams with narrow plates bolted to the flanges through oversize holes so that the bolts would not make contact with the cylinderical surfaces of the holes. The bolts provided essentially only normal forces at the interface between the beam and cover plates. These normal forces determine the limiting static friction forces. The analysis was carried out by investigating where this limiting force is exceeded and slippage occurs and by calculating from this information the energy dissipated per cycle. Experimental results were found to agree quite well with theoretical predictions.

Pian (20), later extended the previous built-up cantilever beam analysis to the case where sliding between the beam flanges and capping plates is prevented by the tight fit of the screws. He again obtained reasonable agreement between theory and experiment, using experimentally determined valves of shear joint stiffness and friction force.

A structure whose damping action is closely related to that of a built-up beam was investigated by Goodman and Klumpp (21). They dealt with a cantilever composed of two identical leaves held together by a uniform pressure and were able to obtain a general insight into the damping of their system and to verify theoretical conclussions by experiments.

Dynamic testing of materials and built-up structures (22) has shown that joint damping as measured by the resonant amplification factor, depends on the clamping pressure and that an optimum value of the pressure exists at which minimum amplification is obtained.

Analysis of all these problems shows that effective joint stiffness is amplitude dependent and the cyclic energy dissipation varies as the cube of the exciting force amplitude and there exists an optimum interface pressure for maximum damping. This appears reasonable when it is considered that the energy dissipation is proportional to the product of the interface shearing force and relative tangential motion. Theoretically, energy dissipation due to this type of damping is zero, for zero or a large interface pressure. It attains a maximum value when the pressure is somewhere inbetween these extremes. When slippage does occur it is usually limited to only a portion of the interface. Analysis based on assumption of partial slippage (23) shows that the energy dissipation is essentially proportional to the third power of the force amplitude. Therefore the joint damping is basically non-linear.

Slippage of the joints does not usually occur at low stresses. Thus in the low stress range material damping accounts entirely for the structural damping present, and a linear assumption for the analysis is perhaps acceptable. Any non-linearity present in this range is however due to joint damping. When the stress level is high, both non-linear material and joint damping contribute to the dissipation of energy. Therefore as the excitation intensity increases, the structural damping departs appreciably from linearity. Other factors affecting the joint damping is the lubrication of the contact surfaces. Lubricating the contact surfaces increases the damping (24).

2.4 Foundation Damping

There are two important sources of energy dissipation in the soil. The hysteretic component of damping, which is due to inelastic behaviour of the soil and radiation damping which is due to the energy which is radiated away from the foundation-soil system by elastic shear wave propagation. Many structures have had their total damping measured but unfortunately there is little published information on their foundation damping. Table (1) from Ref. (25) gives approximate factors, for three different types of foundations, by which the logarithmic decrement of the structure is modified.

In order to reduce the effect of foundation damping on the total damping measured, the tower was erected on a massive (15 ton) concrete foundation block (see appendix J). It is assumed that the forces on the tower are small so that the moments and forces transmitted will cause negligible rotation and translation of the block and hence produce negligible radiation damping. The vibration response of the foundation block was measured during the dynamic testing and it was found to be negligible. In view of this the foundation was considered to be rigid and its damping negligible compared with other damping sources.

2.5 Mathematical Modelling of the Tower

The formulation of a mathematical model of a structure first requires the idealisation of the structure into a lumped mass model. The differential equation of motion governing the dynamical behaviour of the linear lumped mass model can be written as

$$[M]\{\ddot{X}\} + [C]\{\dot{X}\} + [K]\{X\} = \{F\} \qquad (2.12)$$

where

$[M]$ is the mass matrix
$[C]$ is the damping matrix
$[K]$ is the stiffness matrix
$\{X\}$ is a vector of displacement
$\{F\}$ is a vector of forces

For dynamical analysis the tower was modelled mathematically as a discrete system of 64 masses lumped at the nodal points (Fig.2). The nodes were joined by beam elements having six degrees of freedom per node. (3 translational and 3 rotational). The beam element does not allow for the effects of shear deformation and rotary inertia. The shear centre of the cross-section and the point of the intersection of the two principal axes of the cross-section must lie on the line joining the two nodes at the ends of the element. The mass between the mid-height above and below a nodal point was concentrated at the nodal point. The masses of the bolts and the cover plates were calculated from structural drawing and are tabulated in table (2).

The eigenvalue problem

$$\left[K - \omega^2 M\right]\{X\} = 0 \qquad (2.13)$$

was solved by standard techniques to yield the mode shapes ϕ_r and the associated natural frequencies. The first three bending frequencies were found to be 6.718Hz, 32.68Hz and 66.19Hz. The corresponding mode shapes are shown in figure (24b). The first two torsional frequencies were 20.744Hz and 56.098Hz.

In general the mode shapes and the natural frequencies of a tower are similar to those of a cantilever beam but modified by the following factors:-

1) Attachments, which may offer constraints.
2) Heavy loads at the top of the tower, which lower the frequencies and effect the mode shapes.
3) The foundation is never infinitely rigid, and hence, reduces the natural frequencies.

The effect of the added mass on the mode shape and natural frequencies was investigated and the mode shapes for various added masses are as shown in Fig.(26). It is seen that added mass does not effect the fundamental mode shape significantly.

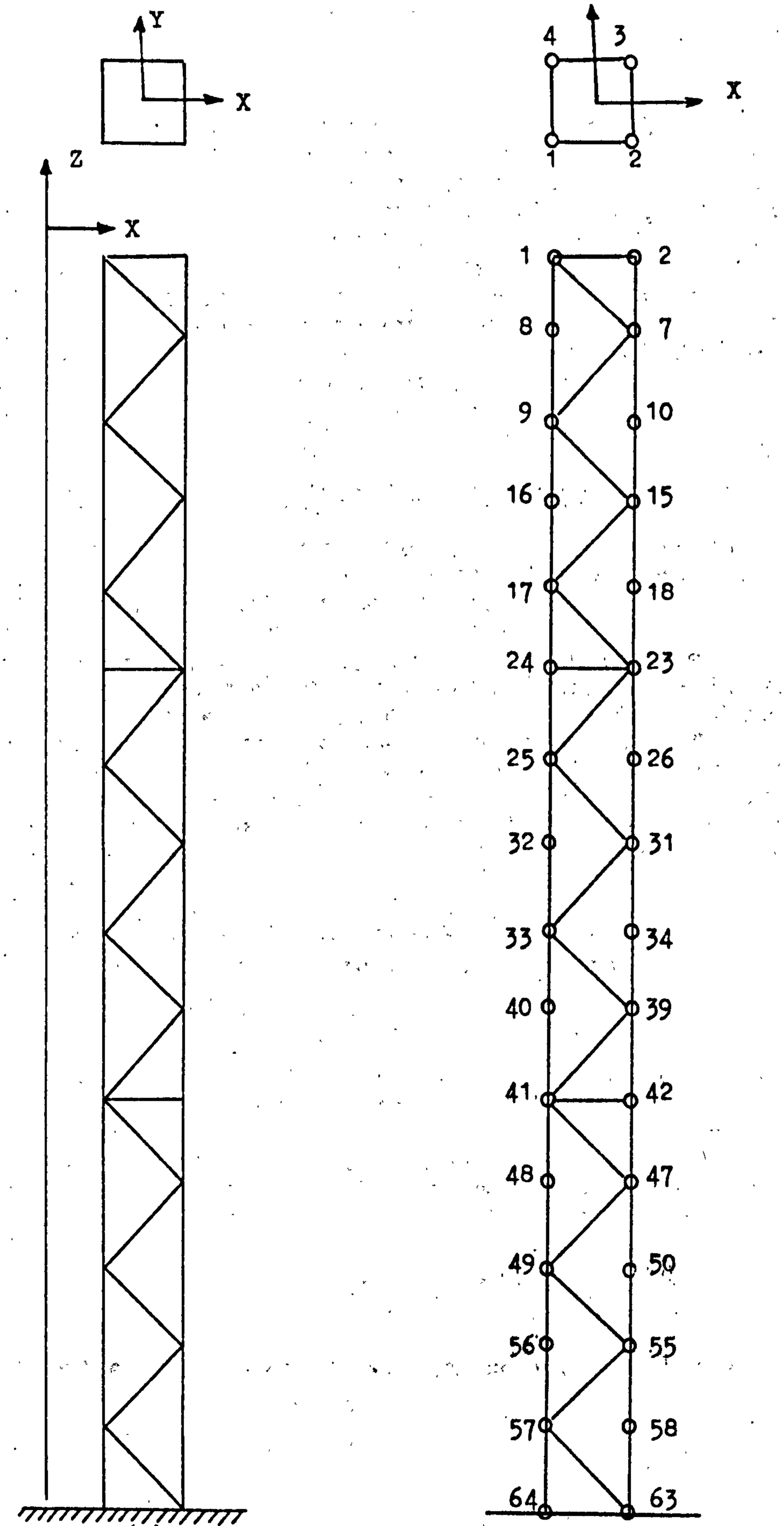

(a)
LATTICE TOWER

(b)
LUMPED MASS MODEL OF (a)

FIGURE 2

Since the tower has two axes of symmetry the frequencies in the two orthogonal bending planes are equal. In the eigenvector extraction programme, the bending modes in these orthogonal planes showed coupling effect. A similar behaviour was observed in the experimental test tower. In order to remove the coupling, so that vibration could be imparted to the tower in one plane only, the frequency in the plane orthogonal to the plane of interest was lowered by removing a bracing member near the base. This solution also gave satisfactory results in the experimental test tower.

2.6 Determination of Material Damping Constants

A lightly damped structure excited by random excitation, vibrates in one or more of its normal modes. The cyclic energy loss due to internal material damping at each of these modes can be calculated using the dissipation law given by equation (2.11) provided the stress in the various structural members is known. Since the damping is light, it is assumed that stresses are in-phase throughout the structure and depend on position and mode of vibration. It is also assumed that the material is linearly elastic so that the stresses can be taken as proportional to a single generalised deflection variable $X_r(t)$. In this analysis $X_r(t)$ is taken to be the displacement at the top of the tower.

During steady state vibrations at a natural frequency ω_r, the generalised velocity variable will be

$$\dot{X}_r(t) = X_r\omega_r \mathrm{Sin}\ (\omega_r t+\theta) \qquad (2.14)$$

The total energy loss, E, per cycle is obtained by summing the specific damping of all the members of the structure. It has been suggested in Ref.(18) that a cyclic energy loss similar to equation (2.11), having the same amplitude dependence can be obtained by assuming that the generalised velocity given by equation (2.14) is resisted by a generalised damping force of the form

$$F_r(t) = C\dot{X}_r(1+\epsilon\left|\dot{X}_r\right|^n) \qquad (2.15)$$

Where C and ϵ are material constants and n has the same value as that in equation (2.11).

The corresponding energy loss per cycle is, Ref.(18),

$$E = \int_0^{\frac{2\pi}{\omega_r}} F(t)\dot{X}dt$$

$$= \pi C\omega_r X^2 \left(1+2\pi^{-\frac{1}{2}}\epsilon X_r{}^n \omega_r{}^n \Gamma\left(\frac{n+3}{2}\right)/\ \Gamma\left(\frac{n+4}{2}\right)\right) \quad (2.16)$$

The first term in equation (2.16) represents the energy loss due to the linear damping force and the second term is that due to non-linear material damping. The cyclic energy loss due to the generalised force will be the same as that due to material damping at any amplitude provided the parameter C and ϵ are chosen as follows

$$C = \frac{\sum_{i=1}^{N} J(S/Se)_i^2 Vol_i}{\pi\omega_r X_r^2} \quad (2.17)$$

and

$$\epsilon = \frac{\sum_{i=1}^{N} J\gamma(S/Se)_i^{n+2} Vol_i\ \Gamma\left(\frac{n+4}{2}\right)}{2\sqrt{\pi}\omega_r^{n+1} X_r^{n+2}\ \Gamma\left(\frac{n+3}{2}\right)} \quad (2.18)$$

It is seen that C and ϵ depend on the material constants J, r and n and on the spatial distribution of the stresses in the members for the mode shape under consideration and also on the reference deflection X_r and the frequency ω_r. This equivalence is only correct for a simple harmonic motion at frequency ω_r. Since a single degree of freedom system under random excitation has a response centred around the resonant frequency, it is assumed to apply also in this case. When the structure vibrates randomly, the same damping mechanism dissipate vibrational energy and govern the vibrational level. If predictions of the random vibration level are to be made it is necessary to know the relationship between the energy dissipation under harmonic conditions and the energy dissipated under random conditions. When the structure is subjected to random vibration, the stress amplitude cannot be described in forms of a particular amplitude but rather in terms of the r.m.s. value stress. In order to compare damping

under random and harmonic conditions, it is therefore more appropriate to compare them on the basis of equal r.m.s. stress (or amplitude) level. Thus the viscous damping ratio measured from the transfer function derived from random testing is compared with viscous damping ratio calculated from free vibration test at the same r.m.s. response level.

In order to calculate material damping coefficients, one needs to know the stress distribution in the structure. A space frame programme (appendix F) was developed to calculate the stresses in the members of the tower. For values of J = 0.7 in-lb/in^3/cycle γ = 6.0, n = 6 and Se = 35,000 lb/in^2, the material damping parameters calculated for the fundamental mode are

$$C = 0.1692$$

and hence $\beta = 0.245E-2$

and $\epsilon = 0.2729E-13$

Similarly β and ϵ can be calculated for higher modes.

3.0 Full Scale Experimental Apparatus

A full scale, self supporting floodlighting tower, $2\frac{1}{4}$ feet square by 30 feet high (as shown in figure 13) was used in this investigation. The tower height was reduced from 50 feet to 30 feet due to the limited height of the building in which it was erected. This increased the natural frequencies but as this increase in frequencies was still in the range of the electrohydraulic actuator system, it was considered not too serious. The tower was constructed from mild steel angle section members bolted together with high tensile steel bolts. As the interfaces at the joints have a considerable effect on damping, all the 132 bolts were tightened to a constant torque using a torque wrench. The tension-torque characteristics of the bolt and nut assembly were investigated and are given in appendix (I). One other factor affecting the damping and the natural frequencies of the structure is the foundation. In order to reduce the effect of foundation as much as possible, the tower was erected on a masive concrete foundation, the details of which are given in appendix (J). The effects of various foundation damping are given in table (1).

The main problem in testing large structures are:-

1) Method of controlled force application.

2) Method of measuring the resulting structural response.

The force applied should be representative of that met in practice and it should be measurable and controllable. Originally, the loading on the structure was programmed to be applied simultaneously at three levels on the tower using three electro-hydraulic actuators which were mounted on the masive building frame-work. The multi-point excitation was however, not under taken as it was found difficult to control the three actuators simultaneously. Even for a single point excitation, it was found that initially, the force control system was unable to apply a constant force in the frequency range of interest (0-10 Hz). Considerable time was spent in devising a suitable method for applying constant magnitude forces to the tower. The details of this investigation are given in section (4).

3.1 Dynamic Tests

The main dynamic tests that were performed on the tower structure are summarised below.

1. Free vibration tests
2. Forced vibration tests
   a) Resonance
   b) Random vibration

3.1.1 Free vibration tests

The simplest type of dynamic test consists of deflecting the structure with a winch and wire and suddenly releasing it, thus causing the structure to oscillate primarily in its fundamental mode. In this investigation the initial deflection was applied by pushing the tower with the top actuator and then suddenly pulling the actuator back. One drawback with this method was that the amplitude was limited by the maximum force that can be applied with the actuator and the maximum velocity at which it can be pulled back. Amplitudes up to 0.6 inch. were the maximum that could be achieved.

Free vibrations can also be set up in a structure by initial velocity rather than by initial displacement. This can be done by impact forces caused by falling weights or by a pendulum that can strike a horizontal blow. Impulsive loads for structural tests have also been generated by explosive cartridges. In such impulsive tests the total time duration of the applied force has to be short compared with the natural period of the structural modes so that the resulting motions are function of total impulse or the initial velocity, rather than the force amplitude.

One common source of error in the measurement of damping of wind sensitive structures is that the measurements are not made under still conditions. With the tower being indoors it was possible to eliminate this sort of error. Another problem with exciting a structure is that an oscillation excited in one plane processes round. This behaviour is normally observed in many tall buildings (27) with symmetrical cross-section. It is believed that this coupling is due to a consequence of equal frequencies in the two orthogonal planes.

The motion in the initial plane of oscillation decrease more rapidly than if the precession does not occur and this can lead to false reading of structural damping. The motion of the tower was measured in two orthogonal directions and it was found that the tower oscillated in one plane only. This was achieved by carefully ensuring that the stiffness and mass axes of the tower coincided and that the two orthogonal frequencies were slightly different.

3.1.2 Measurement and recording of data

A dynamic time history from a single transducer does not necessarily contain all the information needed to describe the system completely. If the measurement is taken at a node line, for example, information on that mode will be missing. Thus the resolution of the measurement needed to extract information on a particular mode is highly dependent on transducer location. If a single transducer is to be used, then a point must be found which has sufficient amplitude in all the modes of interest (i.e. accelerometer should be placed near the top of the tower and strain gauge near the base (Fig.15) for the fundamental mode).

For measurement of free vibration, the tower was instrumented as follows:-

1. Two accelerometers were mounted at the top of the tower, so that accelerations could be measured in two mutually perpendicular directions (in line of the initial displacement and at right angles).

2. One strain gauge was mounted on the base leg of the tower just above the holding down base plate so that strains could be measured in the same plane as the accelerometer.

3. A displacement transducer was mounted on the top cover plate so that it measured the tower displacement relative to the ceiling of the hanger.

Any one of the above three vibration measurement techniques could have been used alone and values of the logarithmic decrement obtained, but all three were used simultaneously so that consistency of the results could give added confidence to the conclusions reached. Several trial runs were made after the tower had been instrumented to check normal operation of the instruments. With the ladder attached to the inside of the tower, it was found that this introduced non-planar motion when the tower was excited in

one plane, Since the objective of this study was to measure the damping characteristics of the tower when it oscillates in one plane, the ladder was removed and Fig. 16 shows the typical records from the accelerometers.

As the objective of the tests is to determine the damping in a bolted structure, all the bolts were tightened to constant torque with a torque wrench. Static forces were applied at the top with the hydraulic actuator and the resulting displacement and strain were measured. Fig. 17 shows one such force - deflection curve from which the static stiffness of the tower can be calculated.

The static deflection applied was suddenly released and the outputs from the accelerometers, displacement transducer and the strain gauge was recorded on a Sangamo FM tape recorder. This was repeated for a range of bolt torque and displacements. For large deflections, the structure was deflected using a turn buckle with a mechanical fuse. The fuse consisted of a pin which was broken in double shear. This design has the advantage over other fuses in that the applied load does not influence the breaking point which depends only on the diameter and the material of the pin. The fuse system is shown in appendix (J). The problem with this type of mechanical fuse, however, is that it requires an adjacent structure to which it can be attached.

When the structure is excited in this manner many modes are excited. The second mode of the structure is 27.7 Hz. Even if the higher modes are completely filtered out by the electronic equipment, they are still present in the structure and so dissipate more energy. However, if it is assumed that the same logarithmic decrement for higher modes as for the first bending mode apply, then the second bending mode will have decreased to a negligible amplitude after a few cycles of the first bending mode. For this reason, the first few points were ignored in the calculation of the logarithmic decrement.

The recorded data was then digitised and since the damping ratio is basically small (less than 0.01) the logarithmic decrement and the critical damping ratio was calculated from the relationship for linear damping

i.e.
$$\delta = \frac{1}{N} \ln \left(\frac{X_n}{X_{n+N}}\right) \qquad (3.1)$$

$$\beta = \frac{\delta}{2\pi} \qquad (3.2)$$

where X_n is the amplitude at which the counting started and X_{n+N}, is the amplitude at which it stopped. Initially, the ratio of the start to stop was maintained at approximately 1:07. The calculations were also repeated for 1:0.9. Since the damping was measured over a band X_n and X_{n+N}, the logarithmic decrement is specified as the average over this band (i.e. $((X_n+X_{n+N})/2)$. Figures 18a, b and c shows the results of all the tests performed on this tower. The typical calue of the total critical damping ratio at zero amplitude is 0.215/100 and it increases to 0.56/100 at mean amplitude of 0.5 inches for a bolt torque of 40 lb. ft. and to a value of 0.365/100 for a bolt torque of 120 lb. ft.

3.2 Results of Free Vibration Tests

The series of free vibration tests were carried out a) to discover the dependence of the damping on frequency, amplitude of vibration and bolt torque (interface pressure), and b) for predicting these dependencies theoretically.

As the tower was initially erected on a steel frame made of universal I beams (Fig. 13), the results of Fig. 18 to 32 pertain to this set up, in which case the fundamental frequency of the tower was 5.49 Hz. This set up seemed satisfactory for small vibration levels of the tower but as the vibration levels were increased, rotation of the base beams could be detected and hence a more rigid concrete base was designed and the free vibration tests were repeated for a few values of bolt torque. It was found that the fundamental frequency of the tower increased from 5.49 Hz to 6.109 Hz but the dependence of critical damping ratio remained similar to previous tests. All forced vibration tests were performed with the tower erected on the concrete base.

All the tests were performed under approximately constant temperature of 15°C. The effect of temperature on the damping characteristics of the tower was not investigated. For the build-up structures, the penetration of the water into the joint in cold weather and subsequent freezing may result in changes in the frictional characteristics of the joint and hence the damping. Rusty joints would also have an unpredictable influence on damping. Initially, these free vibration tests were performed with the increasing bolt

torque setting to comply with industrial practice on bolt torque tightening procedure. After these initial tests, the nut and bolt combinations were tightened and loosened several times before final assembly in order to decrease the spread in the torque-tension characteristics in accordance with test results described in appendix (I).

3.2.1 Effect of Vibration Amplitude

Figure (18) shows that the results of the series of measurement of the total damping in terms of the critical damping ratio as a function of vibration amplitude for various values of bolt torque. For the range of amplitudes investigated (0 to 0.6 inches) the total damping exhibits an approximately linear increase with amplitude. Since the total damping represents not only losses in the joints but also due to material damping, further test were done to determine whether the joint damping amplitude is dependent.

The tests were repeated at various bolt torques and it is seen that the slopes of all the lines decrease with increase of torque, a variable affecting joint damping only. This fact suggests that structures with bolted joints have damping which increases linearly with increase in amplitude.

In the range of vibration amplitudes studied, the material non-linear damping due to stress to the power of eight is negligible. A single degree of freedom system on analogue computer with non-linear joint and non-linear material damping showed that a two inch deflection of the tower is required before any non-linear material damping can be detected from free vibration tests. Since the tests were performed below this amplitude it seems reasonable to assume that material non-linear damping is negligible.

3.2.2 Effect of Torque

The total damping is also presented as a function of bolt torque. These curves in figure 19, are a cross-plot of damping ratio versus amplitude plots. As might be expected, it was found that the more tightly the joints are bolted up, the less is the damping, particularly at higher amplitudes. If it is assumed that a change in torque has no effect on the extraneous sources of damping, the increase in damping over and above the zero amplitude must be due to bolted joints. The magnitude of the joint damping at a

particular torque amplitude is determined by subtracting the respective zero amplitude damping and the results are as shown in Fig. 20.

In the construction of this tower, the bolts were fitted through clearance holes. A question arises as to what might be the damping characteristics of the tower, if the bolts were fitted through non-clearance holes. In Ref. 14 this aspect was investigated and it was found that as far as the damping characteristics of the truss were concerened, the tighness with which the connections were bolted up was of more importance than the fit of the bolts in the bolt holes. This shows that total slip does not occur.

3.2.3 Effect of Frequency

The effect of frequency on the damping was investigated using free vibration test-technique. Free vibrations of the tower at frequencies below its basic fundamental frequency were obtained with added masses firmly attached to the cover plate. The masses have to be firmly attached because the movement caused by inertia force would dissipate energy and hence lead to higher damping ratios.

The total damping in terms of the damping ratio was calculated for one bolt torque setting for three values of frequencies and the results are as shown in Fig. 21. The effect of the decrease in frequency is to decrease the slope of the damping versus amplitude plot, showing that the joint damping is frequency dependent.

3.2.4 Variation of Joint Damping With Time

Energy of vibration is dissipated by microscopic slip on interfaces where elements are jointed (Ref.21). The cyclic energy loss to micro-shear between the two surfaces of a joint is a wear process and gives rise to fretting. Such wear results in a change in the interfacial contact conditions so that after a long period of vibration, the rate of energy loss changes. In order to investigate this long term effect, the tower was excited at amplitudes up to 1.2 inches peak to peak for various lengths of time and the logarithmic decrement measured after each such interval as shown in Fig. 22. The logarithmic decrement

taken before and after the tower had performed approximately 8×10^5 oscillations showed a decrease corresponding to 7.5 % in logarithmic decrement due to joint damping. This reduction may be due to wear of the contract surface, thus reducing the normal force or due to reduction in the effective coefficient of friction. To check if the normal force and hence the torque on the bolts had reduced during this test, the bolt torque was measured and it was found that there was no noticeable change in torque.

Of importance from a practicle view point is the capability of a bolted joint to maintain its performance over a long period of time. Provided such changes do not move the joints too far from optimum damping conditions, then this can be acceptable. Bolted joints made according to current industrial practice, however, are by no means optimissed with respect to damping. The design of such joints is generally governed by consideration of static and fatigue strength.

3.3 Analytical Representation of Damping

One of the main reasons for undertaking the series of free vibration tests described above was to obtain information that would shed light on to the mechanism involved in energy dissipation in the structure and to find a model which would accurately define this mechanism analytically.

A generalised non-linear damping force which can be described mathematically as being proportional to the power of the velocity is

$$F_D = C_n |\dot{X}|^n \text{ sign } (\dot{X}) \qquad (3.3)$$

where a damping coefficient, C_n, and the exponent, n, can have any positive value. For example a value of n = o represents Coulomb damping where coefficient C_o equals the dry friction force, which is equal to μ times the normal force between the two surfaces, where μ is the coefficient of friction. It is a characteristic of Coulomb friction that the coefficient varies with relative velocity between the two surfaces as shown in figure (3), from Ref. (29). A value of n = 1, represents linear viscous damping coefficient which is commonly used in structural dynamic

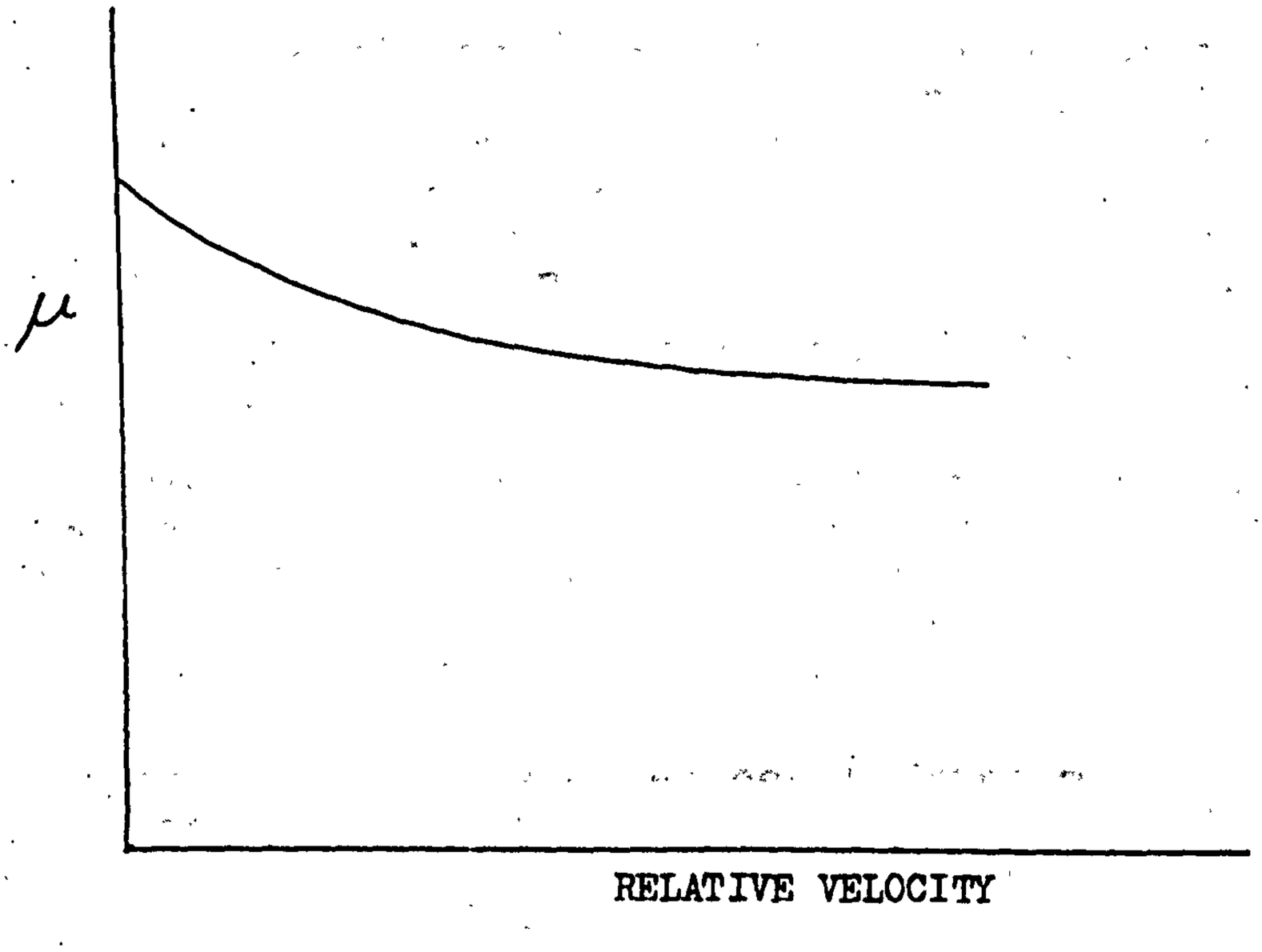

VARIATION OF COEFFICIENT OF FRICTION WITH RELATIVE VELOCITY
(FROM REF.29)

FIGURE 3

calculations. A value of n = 2, represents quadratic damping. Other values of the exponent, n, can be selected to represent non-linear damping characteristics applicable for a given physical damping. For example n = 7 Ref. (17) for non-linear material damping.

In some engineering mechansims, stick-slip oscillation due to friction occur, where a joint slips and then sticks. At the beginning dry friction prevails and amplitude decays linearly with relative amplitude. As the amplitude decreases, the slip ceases and then the amplitude decays exponentially. In this case the damping force F_D can be considered to be a sum of coulomb force and viscous damping force.

Various non-linear models were tried to fit the experimental data and the one which accurately describes the observed behaviour was found to be

$$F_d = C_1 \quad (1+\epsilon|\dot{X}|)\ \dot{X} \qquad (3.4)$$

Free vibration of a single-degree-of freedom system with this damping model was studied in detail, using Runge-Kutta numerical integration on a digital computer and the results are as shown in Fig. 23.

3.3.1 Energy Loss Per Cycle

A useful technique in studying different analytical representations of damping is to compare the energy loss per cycle (ΔE/cycle). This is obtained by integrating the damping force and displacement over vibration cycle.

$$\Delta E/\text{cycle} = \int_{\text{cycle}} F(t)dx \qquad (3.5)$$

$$= \int_{\text{period}} F(t)\ \frac{dx}{dt}\ dt$$

If $x = X_o \sin(\omega t+\theta)$ (i.e. nonlinear damping does not effect sinusoidal wave form of motion)

Where

X_o is the amplitude

θ is the phase angle

The velocity becomes

$$\dot{X} = X_o \omega \cos(\omega t+\theta) \qquad (3.6)$$

Substituting equations (3.4) and (3.6) in (3.5) yields,

$$\Delta E/\text{cycle} = C_1 \pi \omega X_o^2 + \frac{8}{3}\epsilon C_1 \omega^2 X_o^3 \qquad (3.7)$$

The energy dissipated by an equivalent viscous damping coefficient, C_{eq} is

$$\frac{\Delta E}{\text{cycle}} = \pi C_{eq} \omega X_o^2 \qquad (3.8)$$

Equating (3.7) to (3.8) yields

$$C_{eq} = C_1 \left(1+ \frac{8\epsilon}{3\pi} \omega X_o\right)$$

$$\therefore \quad \beta_{eq} = \beta_1 \left(1+ \frac{8}{3\pi}\epsilon \omega X_o\right) \qquad (3.9)$$

Thus plotting β_{eq} against X_o (mean displacement) yields a straight line with a slope of $\frac{8\omega\beta_1\epsilon}{3\pi}$.

$$\therefore \quad \epsilon = 3\pi \frac{\text{slope}}{8\omega\beta_1} \qquad (3.10)$$

Thus by measuring β_1, which is equal to β_{eq} at $X_o=0$, and the slope, it is possible to measure the non-linear damping (ϵ) from equation (3.10).

For example, from figure (18c) for torque = 40 lb.ft.

$$\beta_1 = 0.215/100$$

$$\text{slope} = \frac{0.69}{100} \quad (\frac{1}{in})$$

$$\therefore \quad \epsilon = \frac{3\pi \times 0.69 \times 100}{8 \times 100 \times 0.215 \ \omega} = 0.1096 \quad (in^{-1} \ s)$$

ω = resonance frequency

The measured non-linear damping coefficients at the various torques are tabulated in Table (3).

The equation of motion of a single degree of freedom system with non-linear joint damping becomes

$$\ddot{X} + 2\beta_1\omega_o(1+\epsilon|\dot{X}|)\dot{X}+\omega_o{}^2 X = f(t) \qquad (3.11)$$

3.4 Measurement of Mode Shape

Once the fundamental frequency of the structure has been found, the mode shape can be determined. For this test the tower was excited at a single point. Five accelerometers which were initially calibrated so that $\pm$ 1 g produced an output of $\pm$ 1.0 V, were mounted on the tower at 6 feet intervals. Since there was not enough accelerometers to measure the vibration amplitudes at all

the required points simultaneously, after recording the amplitude at five points the accelerometer positions were shifted to new positions and the tower brought to resonance. This was repeated until the vibration amplitude of all required points had been recorded. The structure may not vibrate at exactly the same amplitude at precisely the same frequency on each run. Therefore one accelerometer and displacement transducer were used as reference. Subsequently all the amplitudes were adjusted to constant modal amplitudes. The fundamental mode shape is as shown in Fig.(24).

3.5 Effect of Added Mass

The affect of additional mass at the top of the tower on the fundamental frequency was investigated. The mass was added to the tower on the top cover plate and firmly bolted in position. The fundamental frequency was determined for various additonal masses. The resulting frequency was then compared with Dunkerley's empirical formula which permits a theoretical evaluation of the fundamental frequency of the combined system.

$$\frac{1}{\omega^2} = \frac{1}{\omega_1^2} + \frac{1}{\omega_2^2} \qquad (3.12)$$

where ω = fundamental frequency of combined system

ω_1 = fundamental frequency of tower alone

ω_2 = fundamental frequency of massless tower with lumped mass at free end

Figure 25 shows the variation of the frequency with added mass. It shows that there is good correlation between measured and predicted frequencies. The effect of added mass was also investigated using a finite element programme and good agreement was also obtained for the percentage change in the natural frequencies due to the added mass.

3.6 Generalised Mass and Stiffness of the Tower

The generalised mass of a particular mode can be determined experimentally by adding a known quantity of mass to the structure and measuring the consequent reduction in the resonant frequency. The mass must be sufficient to

lower the resonant frequency by an amount that can be measured accurately. **However, it should not alter the mode** shape of the structure. So the added masses at each point should be proportional to the original mass at that point. If the masses are not added in this manner to maintain the same mode shape, a method to correct the error due to this is described in Ref.(28). The finite element analysis was used to investigate the effects of adding a concentrated mass at the top of the tower on the mode shapes. It was found that the fundamental mode shape remains unaltered but the second mode shape changes due to this concentrated mass placed at the top. The mode shapes are plotted in Fig.(26). Since the **generalised stiffness of the structure remains unaltered with addition of the extra mass**

$$M_i \omega_i^2 = K_i = (M_i + \Delta M_i)(\omega_i - \Delta\omega_i)^2$$

$$M_i \omega_i^2 = (M_i + \Delta M_i)(\omega_i^2 - 2\omega_i\Delta\omega_i + \Delta\omega_i^2)$$

$$\therefore M_i = -\frac{1}{2}\Delta M_i \frac{\omega_i}{\Delta\omega_i} + \text{higher order terms} \qquad (3.13.a)$$

The negative signes show that the frequency decreases, as to be expected.

This technique implies that the additional mass be added at the position where mode shape is normalised to one. Or in general

$$M_i = -\frac{1}{2}\Delta M_i \frac{\omega_i}{\Delta\omega_i}\left(\frac{x_a}{x_r}\right)^2 \qquad (3.14)$$

where X_r is a reference displacement and X_a is the displacement at a point on the structure where the small added mass is attached. The added mass however, should be small so that higher powers of small quantities can be neglected in equation (3.13).

The advantage of this method is that knowledge of neither the mode shape nor the mass distribution is required. There are, however, two important requirements and these are

i) That the added mass shall produce no change of mode shape.

and ii) that a **pure** mode is being excited.

Theoretically, it is impossible to satisfy the first of these requirements, since the addition of discrete

masses to a continuous structure, other than at node must result in a change in mode shape. In practice, if values of added mass are such that the variation of frequency with added mass is linear, it may be assumed that any change of mode shape is negligible.

It is not necessary, however, to attach masses to the structure, since the same dynamic effect may be produced by applying appropriately-phased forces to the structure either through the exciters that are used for mode excitation or through separate exciters. The force on a structure due to the attachment of a small added mass M_a, at point where the oscillatory displacement is X_a and the frequency is ω_i, is given by

$$F_a = -M_a \ddot{X}_a = \omega_i^2 M_a X_a \qquad (3.15)$$

Substituting this is equation (3.14) yields

$$M_i = -\frac{1}{2\omega_i}\left(\frac{X_a}{X_r^2}\right)\left(\frac{dF_a}{d\omega_i}\right) \qquad (3.16)$$

If a force F is applied to the structure instead of a mass M_a, the force must be in anti-phase with the acceleration of the structure and therefore in quadnature with the external excitation forces.

A mass of 0.1449 lb. $in^{-1}s^2$ was added to the tower cover plate and the frequency of the fundamental mode decreased to 5.545 Hz. from 6.04 Hz. Thus substituting the added mass and change in frequency in equation (3.11) yield

$$M_1 = 0.884 \text{ lb.in}^{-1}\text{s}^2$$

If the mass distribution of the structure is known, the generalised mass can also be calculated from measured mode shape

$$M_i = \Sigma M_i \phi_i^2 \qquad (3.17)$$

and generalised stiffness can be obtained from

$$K_i = M_i \omega_i^2 \qquad (3.18)$$

The generalised mass calculated from computed mode shape and mass distribution of the tower is $M_1 = 0.862$ lb. in $^{-1}s^2$.

3.7 Steady state Resonance Tests

Although the free vibration tests described appear to have the virtue of relative simplicity, forced vibration tests usually provide more complete and accurate information. A steady state resonance test involves the application of sinusoidally varying uni-directional force whose frequency can be held accurately constant at one value while measurements are made of the resulting motion of the structure. The frequency is then adjusted to a new value and the measurements repeated so as to cover the whole frequency range of interest. From these measurements a frequency response function of the structure can be plotted and accurate values of the natural frequencies and damping ratios can be obtained. By varying the magnitude of the exciting force, various non-linear characteristics of the structure if present, can be studied. The set up for this test is as shown in Fig.27.

The excitation signal was derived from a signal generator which gave a frequency readout to $\pm$ 0.001 Hz. The displacement amplitude was measured with LVDT type displacement transducer which has infinite resolution. A tracking filter was used to perform peak amplitude detection. The tracking filter was first adjusted to make sure that it didn't introduce any phase shift between input and output in the frequency range of interest. The phase relationship between the force and the displacement was measured with an analogue phase meter. The input signal amplitudes applied to the phase meter were adjusted and maintained approximately constant for each test to minimise errors. Several trial tests were done to eliminate abnormal instrumental behaviour such as drift, noise etc.

As the free vibration tests performed earlier showed that the effect of the bolt torque was to reduce the slope of damping ratio versus amplitude plots, the tests were performed for one bolt torque setting only. The frequency response function was measured for various levels of force input and results are as plotted in figure (28a). The ratio of peak response to peak force levels are plotted in figure (28b). It is seen that the tower does not have a unique frequency response function, i.e. D/F is not constant as in the case of linear system but decreases with increase in input force level. This shows that the tower has non-linear damping. In the range of response amplitudes studied, the fundamental frequency of the tower decreases by

0.35 % for 138.6 % increase in response. The static test figure (17), shows that the tower is statically linear but figure (28) shows that it is non-linear dynamically. Since the non-linear damping only effects the properties of the transfer function near the resonant frequency, it can be used to determine which model best fits the measured transfer function, Ref. (30).

3.8 Random Vibration Tests

The study of random vibration of linear systems subjected to stationary random excitation is well developed and requires only a knowledge of the frequency response function of the system and the spectral density of the excitation. In the physical world most systems exhibit non-linear behaviour. For non-linear systems it is not possible to apply in a direct manner the spectral density technique used for linear systems in order to determine the rms response. The reason for this is that in non-linear systems the frequency response function relating sinusoidal response to sinusoidal excitation is not constant at a given frequency. It can thus be seen that the random vibration of non-linear systems under stationary excitation can in general only be studied by approximate methods.

One of the effects of non-linearity in random vibration relates to the probability density function P(X) of the response. In linear systems the frequency response function is unique and when it is excited by a Gaussian distributed force, the probability distribution of the response will also be Gaussian. Non-linear systems do not, however, have a unique frequency response function. As a result of this when a non-linear system is excited by a Gaussian distributed force, the response is non-Gaussian (see section 5).

3.8.1 Random Excitation

The quantitative definition of the excitation experienced by the structure is important in measuring the dynamic response. It should be representative of that met in practice and should be measurable and controllable experimentaly and also be capable of analytical representation.

As in the present investigation the interest is to study the vibration under random loading conditions, an approximation is made regarding the variation of mean velocity with height. The turbulence is considered to be fully correlated with height (coherence of unity), i.e. the wind velocity is in the same sense at all heights at any given time. Secondly the power spectral density of the input force is considered to be constant in the frequency range of interest. Such an excitation, of course, does not exist in nature. However, a study of the response of this idealised random excitation should at least in a qualititive sence, give insight into the random response to other forms of random excitation.

In practical cases, the lowest natural frequency of a structure is always higher than the range over which high ordinates of the excitation spectrum occur. The response of the structure to wind excitation is as shown in figure (29a). The corresponding power spectrum of the fluctuating component of the response is shown in figure (29b), which illustrates the 'broad band' and the 'narrow band' components. The broad band response is effectively quasi-static and the narrow band represents the modulated response at the natural frequency. As the damping is most civil engineering structures is low, the bandwidth in the excitation spectrum that significantly influences the narrow band response component is extremely narrow. Thus the assumption mentioned above is not too severe. This allows the results of experimental study to be compared with those derived from the Fokker-Planck equation in which a white noise input is assumed.

In order to study the non-linear behaviour of the tower under random excitation the structure was excited with Gaussian, band limited white noise. Due to the limitation imposed by the spring stiffness on the maximum force application, the structure could not be excited to a large enough amplitude to investigate the non-linear material damping under random conditions. Thus the non-linearity investigated is due to joint damping.

The preliminary random loading tests showed that the spring that could be used, without effecting the dynamic response, was spring of stiffness 781.3 lb/in. The resonance frequency of the tower was measured from random vibration tests and compared with the free vibration tests. Two showed no change in the fundamental frequency. The input force was measured with a load cell which was connected in series with the actuator and the response was

measured using three transducers. The accelerometer and the displacement transducer was located at the tower cover-plate and the strain gauge near the base, on one main leg of the tower. The strain gauge was used for monitoring the maximum stress level.

3.8.2 Calibration

Accurate measurement in any experiment requires calibration of the equipment. Thus before any experimental data could be recorded several precautions were taken to ensure that each instrument was properly calibrated. The calibration of the transducer was measured with pre-amplifier and filters in series so that the output voltage could be converted to physical units straight away. The frequency response characteristics of the filters were also measured so that the effect of filtering could be estimated. Fig. 30 shows that the calibration of the load cell and the displacement transducer.

3.8.3 Duration of Random Testing

The length of the test in random analysis influences the statistical reliability of the measured data; the shorter the test length, the lower the reliability. However, long tests require long processing time and a compromise has to be made between long test-length and practical limitations regarding recording and computer storage requirements. The reliability of the spectral density estimates is characterised by the normalised standard error or the number of degree of freedom. In practice, the statistical scatter in power spectral density can be reduced by either ensemble average or frequency averaging.

The normalised standard error of power spectral density estimates is a function of record length T and the resolution bandwidth, B_e. This implies that the record length needed to provide a specified normalised error ϵ_r in power spectral density estimates can be predicted by $T=(B_e \epsilon_r^2)^{-1}$ where B_e is a known parameter of the analysis procedure rather than an unknown parameter of data. The resolution bandwidth B_e is a primary factor in the bias portion of the spectral density error. The bias error can be calculated for spectral measurements at resonant frequencies in terms of a ratio of the resolution bandwidth B_e to the half power point bandwidth B_r of the structure. Fig. 4 from Ref. 31 shows that the relationship between bias error

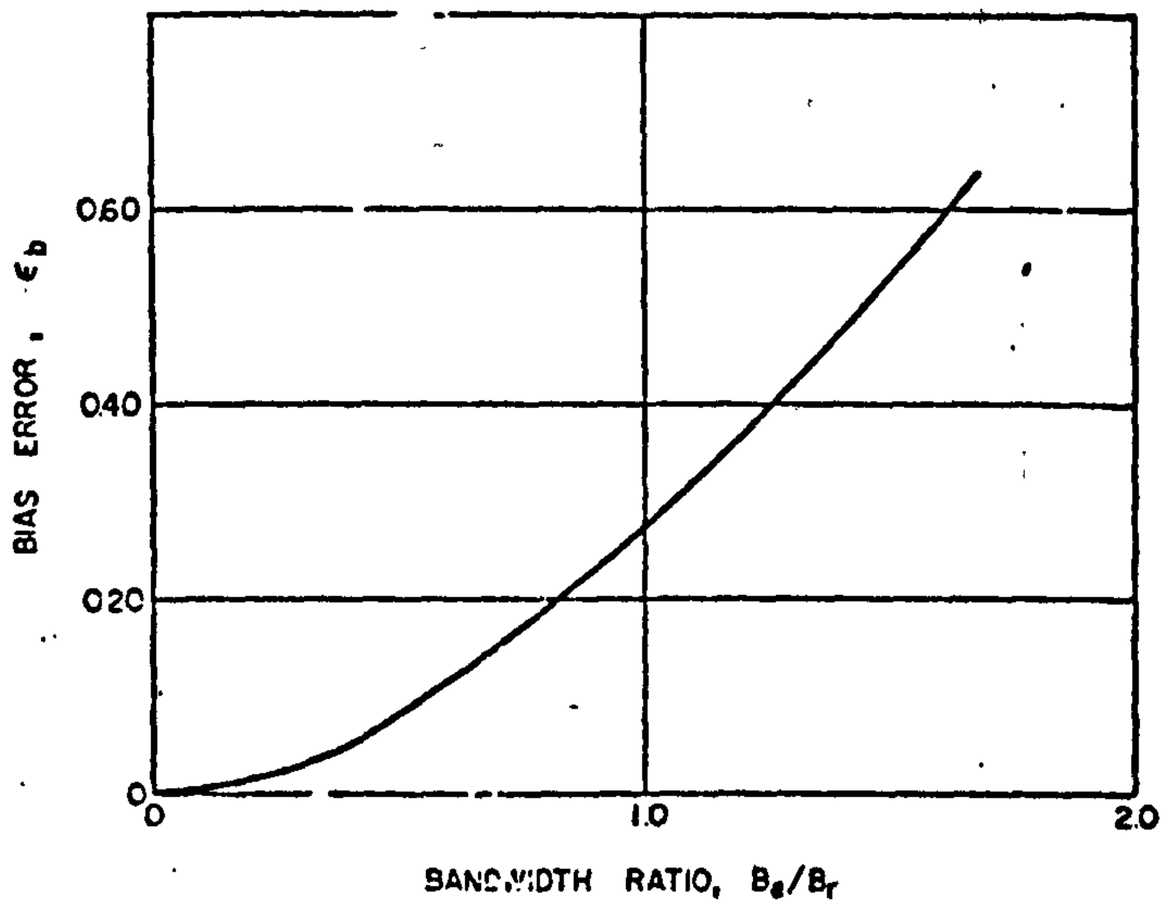

BIAS ERROR FOR SECOND ORDER SYSTEM (REF.31)

FIGURE 4

and bandwidth ratio. The spectral density peakes are always underestimated. For a 2048 point fourier transforms the frequency resolution for a maximum frequency of 10 Hz = 0.009765 Hz. The half power point bandwidth ($2\beta_o f_o$) of the structure is 0.0258 Hz. Hence from figure (4), the bias error in response spectral peaks is less than 0.05. For a statistical error less than 0.141, the record length required is

$$T = (B_e \epsilon_r^2)^{-1} = \left[0.009765 \times 0.141^2\right]^{-1} = 5150.9 \text{ sec}$$

$$= 85.84 \text{ minutes.}$$

The two main parameter measured from random testing as far as measuring damping non-linearities is concerned are the mean square response, $E(X^2)$, and the power spectral density of the force, W(f). Since W(f) is fairly uniform in the frequency range of interest (0-10 Hz), its statistical error can be further reduced by frequency smoothing. The statistical error becomes $\bar{\epsilon}_r = \epsilon_r \sqrt{\frac{1}{SM}}$ where SM is the number of neighbouring frequency components used in smoothing. The random excitation force and the resultant random response of the tower were recorded and later analysed using a digital computer. The typical force and response plots are as shown in figure (32).

3.9 Digital Data Analysis

The method of analysis used here is well established and is described in many text books (Ref. 31 and 32). As the understanding of the digital procedure in random signal analysis is essential a brief description of the various parameters measured is given here.

3.9.1 Power Spectral Density

The power spectral density gives the frequency composition of the random variable in terms of its mean square value. The average square value will approach an exact mean square value as the observation time T approaches infinity. Thus for a variable X(t, f), the mean square value in the range f and f+Δf is given by

$$\psi_x^2(f,\Delta f) = \lim_{T\to\infty} \frac{1}{T} \int_0^T x^2(t,f,\Delta f)dt. \qquad (3.19)$$

For small Δf, the power spectral density $W_x(f)$ is defined as

$$W_x(f) = \frac{\psi_x^2(f,\Delta f)}{\Delta f}$$

$$= \lim_{\Delta f\to o} \frac{\psi_x^2(f,\Delta f)}{\Delta f} = \lim_{\Delta f\to o} \left(\frac{1}{\Delta f}\right)\left[\lim_{T\to\infty}\frac{1}{T}\int_o^T x^2(t,f,\Delta f)dt\right]$$

(3.20)

$W_x(f)$ is always, a real valued, non-negative function. If $X(t)$ represents white noise, its power spectral density has a constant magnitude over the entire frequency range.

A real spectrum containing positive frequencies only is referred to as a single-sided spectrum. A spectrum in which both positive and negative frequencies are included is called 'double-sided' spectrum. The inclusion of negative frequencies is a mathematical notation which makes possible the expression of a Fourier series and integrals in exponential form. Correct interpretation of expressions involving negative frequencies is necessary for real physical problems. Single and double sided spectral density functions are as shown in figure (5). Their relationship is

$$W_x(f) = 2S_x(f) (\text{for } 0<f<\infty) \qquad (3.21)$$

Practical density evaluation derive $W_x(f)$ and it is necessary to include the scaling factor when referring to mathematical calculations in which intergration over negative frequency takes place.

Since $S_x(f) = 2\pi S_x(\omega)$

$$\therefore \quad S_x(\omega) = \frac{1}{2\pi}\left(\frac{1}{2} W_x(f)\right) \qquad (3.22)$$

Figure 33a and 33b show the typical measured power spectral densities of excitation and response. Knowing the spectral density of the input S_y and the output S_x, the transfer function of the system can be calculated from

$$|H(\omega)| = \sqrt{\frac{S_x(\omega)}{S_y(\omega)}} \qquad (3.23)$$

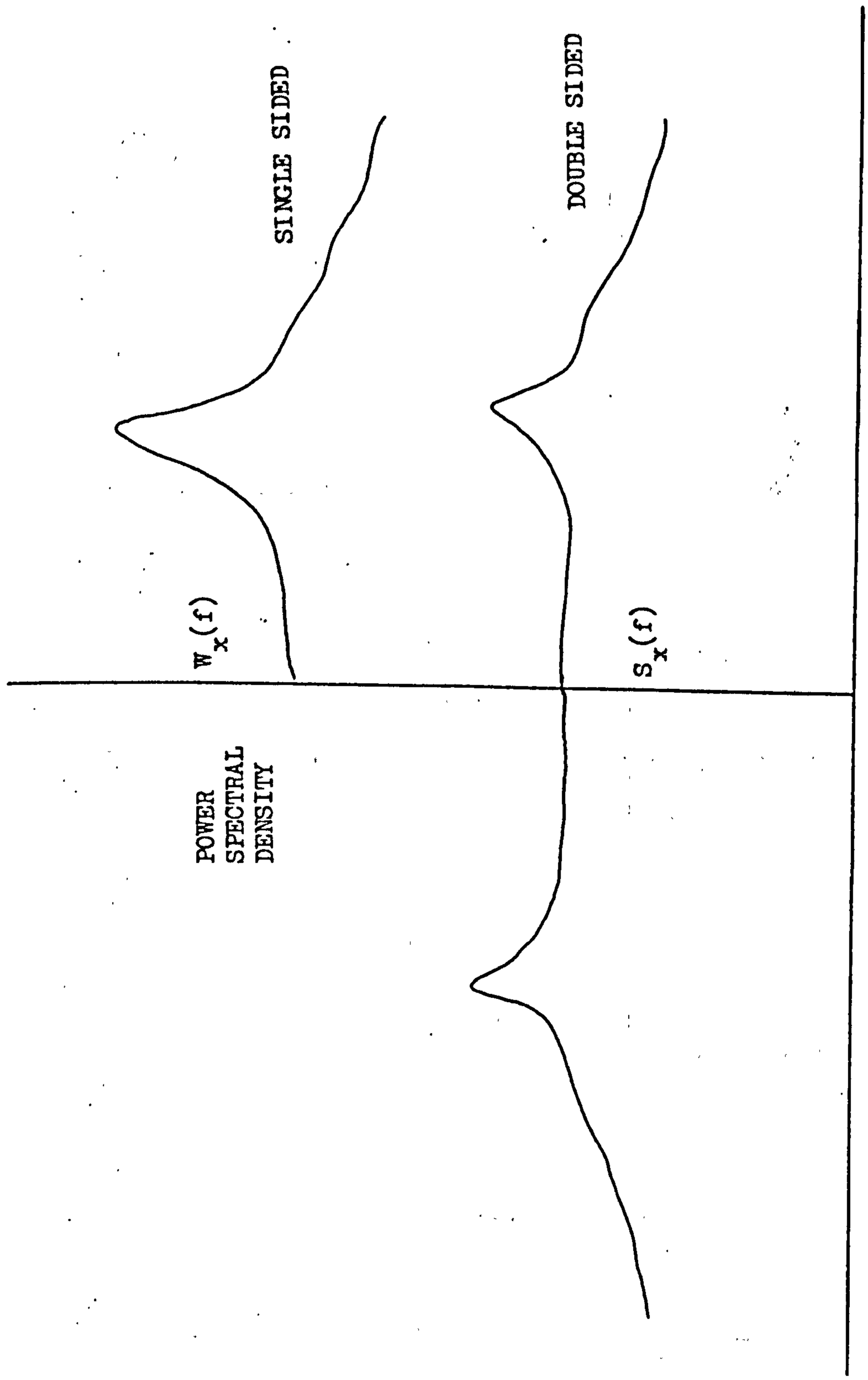

SINGLE AND DOUBLE SIDED SPECTRUM

FIGURE 5

where $|H(\omega)|$ denotes the modulus of the transfer function. In this relation the phase information is lost. On the other hand, the cross-spectral density function which is in-general complex, gives the phase information also.

$$S_{xy}(\omega) = C_{xy}(\omega) - iQ_{xy}(\omega) \qquad (3.24)$$

and
$$H(\omega) = \frac{S_{xy}(\omega)}{S_{xx}(\omega)} \qquad (3.25)$$

The phase angle between X and Y is given by

$$\theta_{xy} = \tan^{-1} \left(\frac{Q_{xy}(\omega)}{C_{xy}(\omega)}\right. \qquad (3.26)$$

where $C_{xy}(\omega)$ = co-spectral density function

$Q_{xy}(\omega)$ = quad spectral density function

Both of these methods can be used for evaluating the transfer, but the latter method is used in the present analysis.

3.9.2 Correlation and Coherence Functions

These are equivalent descriptions in the time and frequency domain respectively. The auto-correlation function describes the general dependence of the value of the data at one time of the value at another time. It is defined as

$$R_{xx}(\tau) = \lim_{T\to\infty} \frac{1}{T} \int_0^T X(t)\, X(t+\tau)\, dt \qquad (3.27)$$

where τ is the time delay. Typical plots of autocorrelation are shown in figure (6). The information that can be obtained from study of autocorrelation is:-

1) Nature of the variable as to its randomness, and harmonic content and their relative amplitudes.

2) The period of the fundamental frequency content (This is given by four times the time delay for the first zero crossing of the autocorrelation)..

3) Non-linearity and damping in the system if the variable is a response signal. The autocorrelation would be similar to figure (6c), if the system is lightly damped. The decay is proportional to twice the logarithmic decrement. This method has been

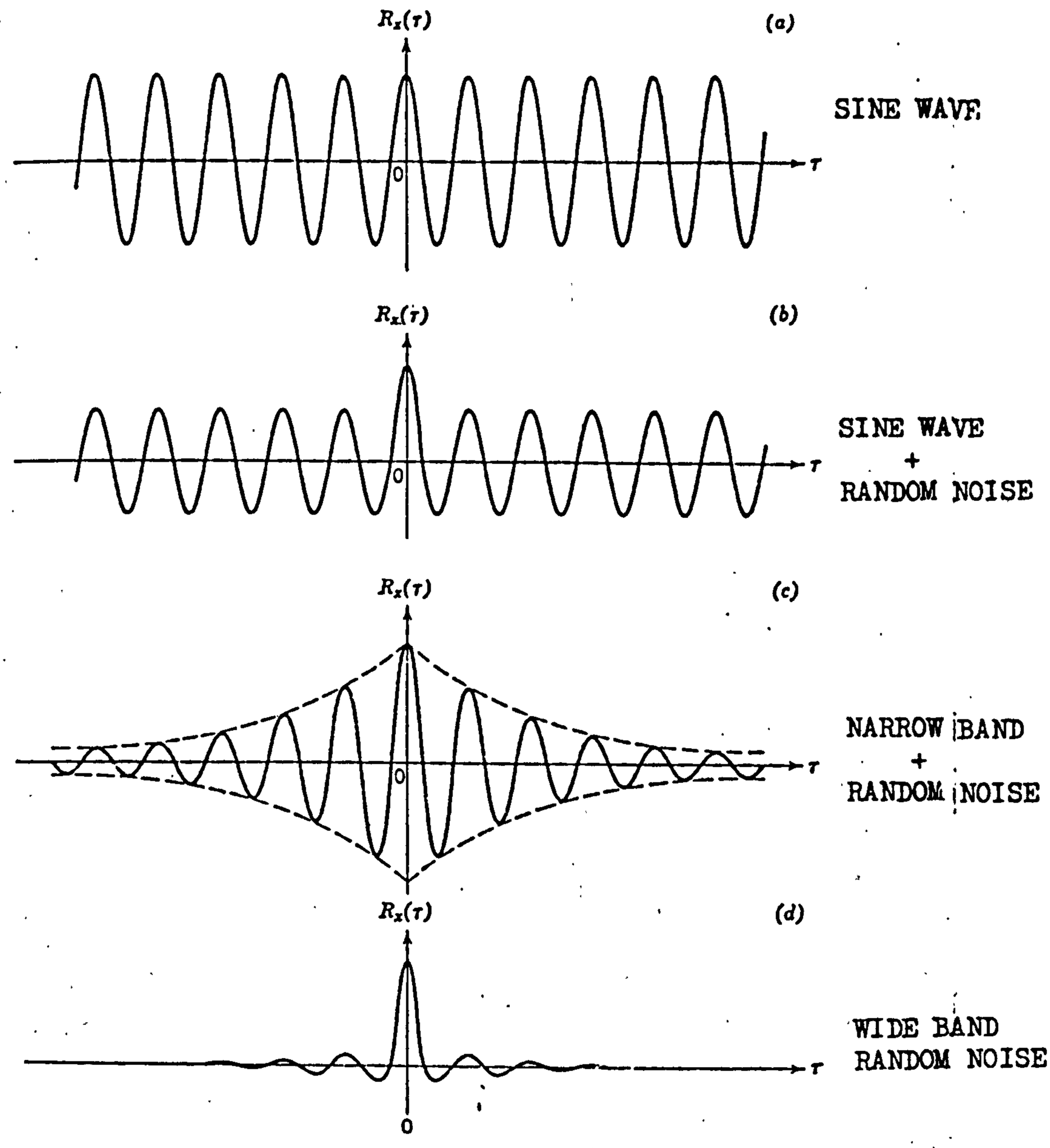

AUTOCORRELATION FUNCTIONS

FIGURE 6

used in Ref.(33) to extract damping value from random response signals of linear systems.

4) The mean square value is given by

$$\psi^2 = R_{xx}(0) \qquad (3.28)$$

and mean value $\bar{X}$ by

$$\bar{X} = \sqrt{R_{xx}(\infty)} \qquad (3.29)$$

Coherence between the force F(t) and the response X(t) is a real value function defined by

$$\gamma_{Fx}(f) = \frac{|S_{Fx}(f)|^2}{S_{FF}(f) S_{xx}(f)} \qquad (3.30)$$

and satisfies the relation $0 < \gamma^2_{Fx}(f) < 1$, provided that mean value is zero. For a linear system with well defined 'one to one' relation between the input and response, $\gamma^2_{Fx}(f) = 1$ over all frequencies. The coherence function is less than unity if

1) extremeous noise is present
2) the system is non-linear
3) F(t) does not completely describe the excitation force.

When $\gamma^2_{Fx} = 0$, force and response are incoeherent, i.e. there is no transmission path for the force at the given frequency. The typical coherence function is as shown in figure (34)

3.9.3 Transfer Functions

The frequency response function is a special case of the transfer function. For physically reliable and stable system, the frequency response function may replace the transfer-function with no loss of useful information. It is generally a complex valued quantity which may be conveniently thought of in terms of a magnitude and an associated phase angle. In polar notation

$$H(f) = H(f)\, e^{-j\phi(f)} \qquad (3.31)$$

where the absolute value H(f) is called the system 'gain factor' and the associated plane angle $\phi(f)$ is called the system 'phase factor'. It is important to note that the frequency response function H(f) of a constant parameter

linear system is a function of only frequency and is not a function of either time or the excitation. If the system were non-linear, H(f) would also be a function of the applied input. If the parameter of the system are not constant, H(f) would also be function of time. Figure 35 shows the typical measured transfer function. Figure 36 and 37 show the corresponding modulus, $|H(f)|$ and phase angle, respectively.

3.9.4 Probability Density Function

The time history of a random signal is never repeated exactly, therefore, for a mathematical standpoint the instantaneous amplitude at any future time cannot be predicted. The only thing that can be said about a future occurence is that a signal within certain amplitude limits will occur with a certain probability. The method of displaying this probability of occurence is the amplitude density curve and gives a statistical description of the amplitude characteristics of the random signal. For a stationary random signal the probability density function $P(X)$ is

$$P(X) = \lim_{\substack{T\to\infty \\ \Delta X\to\infty}} \frac{1}{T}\,\frac{1}{\Delta X}\sum_{n=1}^{n=\infty} t_n(X, X+\Delta X) \qquad (3.32)$$

where the quantity t_n is the time spent by the signal within the narrow range X_n to $X+\Delta X$ and T is the total time of observation.

The most common probability density function found in nature is Gaussian or 'Normal' distribution curve, given by

$$P(X) = \frac{1}{\sqrt{2\pi}\delta_x} e^{-\frac{1}{2}\left(\frac{X-\overline{X}}{\delta_x}\right)^2} \qquad (3.33)$$

where δ_X is the rms value about the mean, $\overline{X}$. The important properties of the probability density function are:-

$$1) \qquad \overline{X} = \int_{-\infty}^{\infty} XP(X)dX$$

and

$$2) \qquad \delta_X^2 = \int_{-\infty}^{\infty} (X-\overline{X})^2 P(X)dX \qquad (3.34)$$

i.e. the first and the second moments of the probability density function are the mean and the variance of the variable respectively.

The joint probability density function of two random sample records describes the probability that both sample records will simultaneously assume values within some defined pair of ranges at any instant of time, i.e.

$$P(XY) = \lim_{\substack{\Delta X \to 0 \\ \Delta Y \to 0 \\ T \to \infty}} \frac{1}{(\Delta X)(\Delta Y)} \frac{1}{T} \left[\sum_{n=1}^{n=\infty} t_n(X, X+\Delta X \text{ and } Y, Y+\Delta Y) \right] \qquad (3.35)$$

When the two phenomena in question are statistically independent, then the joint probability density function is given by

$$P(X, Y) = P(X)P(Y). \qquad (3.36)$$

In computing the pdf, the number of class intervals has to be supplied. Based on the assumption that a chi-square Goodness-of-fit test for normality is to be made, Ref.(34) gives for 95 % confidence level

$$\text{No of class interval } (K) = 1.87\ (N-1)^{2/5} - 2 \qquad (3.37)$$

$\therefore$ The bandwidth $= \frac{(b-a)}{K}$ Where a and b are minimum and maximum values required in histrogram

Figures 38a and 38b show the typical measured pdf for the excitation and response respectively.

3.9.5 Test for Stationarity

The correct procedures for analysising random data, are strongly influenced by certain basic characteristics which may or may not be exhibited by the data. The most important of these is the stationarity of the data because the analysis procedures required for non-stationarity data are generally more complicated than those which are appropriate for stationary data. The stationary data can be tested by using the run test (see Ref.(31)).

To test the stationarity of the tower response, the response data was divided into 50 segments of equal length and standard deviation was computed for each segment. The typical power spectral densities of excitation and response

of the first 30 segments (as this was the maximum number of segments that could be plotted) are as shown in figures 39a and 39b, respectively. The number of runs about the mean value are then calculated. From table (3) of Ref.(31), the hypothesis of stationarity would be accepted at $\alpha = 0.05$ level of significance if the number of runs observed in the sequence are at least 19 but not more than 32. From data it was found that there are 20 runs in the sequence. Hence the hypothesis of stationarity is accepted at the 5 per cent level of significance.

3.10 Digital Data Reduction

The analogue data from FM tape recorder was analysed using 'Random Signal Analysis' facilities at ESRU. First the analogue signal is converted to digital form using an analogue to digital converter (ADC). The analogue signal could be either digitised separately or multiplexed. If multiplexed, lag errors are introduced in correlation, transfer function and coherence function analysis. However, the error can be minimised in multiplexing by spacing the related channels close to each other. It can be eliminated altogether by recording a reference trigger signal on one channel such that each channel can be individually triggered from the same starting point.

3.10.1 Digital Sampling Rate

The question of what sampling rate to choose is governed by the higher frequency component present. Shannons Theorem (Ref.(35)) states that to avoid aliasing the sample rate must be at least twice as high as the highest frequency component present. Thus, if there are frequencies present which are greater than the Nyguist or cut-off frequency ($\frac{1}{2}$x sampling rate) than the spectrum will be folded about the Nyguist frequency. No amount of digital filtering will overcome this problem as the data would have been already sampled. It is thus essential to use a low pass analogue filter to filter the higher frequency components.

Let the spectrum have non-negligible values at frequencies considerable above f_{max} (maximum frequency of interest). It would appear therefore that a sampling rate of at least twice f_{max} be used after first passing the signal through a low pass filter set to f_{max}. However, if the filter has a cut off rate of 24 db per octave, then the spectrum received by the ADC may not have decayed to about

2 % of its value at$2f_{max}$ (i.e. a 60 db drop) until a frequency f_1, which is 2.5 octaves above f_{max}. It may thus be necessary to use a sampling rate of $2f_1$, if aliasing is to be avoided (i.e. $f_s = 5f_{max}$) In practice however, a figure of 4 f_{max} is usually found to be sufficient. The sampling rate requirement will also be dependent on the degree of resolution desired. For spectral analysis this sampling rate is adequate but for damping measurement analysis from free vibration curve, a sampling rate of 80 times the frequency of the mode of interest is desirable.

3.10.2 Accuracy of Measurement

The accuracy of computation depends on the number of samples taken. Normalised standard error and confidence level required furnish this information.

The normalised standard error, ϵ_s of some statistical parameter, X, may be defined as the ratio of the standard deviation of the estimate of X and the true value of X. In the particular case where spectral analysis is being used

$$\hat{\epsilon}_s^2 = \delta \frac{|\hat{G}(\omega)|}{G(\omega)}$$

Where $\hat{G}(\omega)$ = Final estimate of spectral density

$G(\omega)$ = True power spectral density.

For Gaussian distribution this is approximated to

$$\epsilon_s = \frac{1}{\sqrt{B\,T}} \qquad (3.48)$$

where B is the bandwidth or frequency resolution requirement

T is the length of sample necessary to calculate the result to the desired accuracy.

Having defined the standard error, ϵ_s and the maximum frequency requirement, record length T and number of samples can be calculated.

If instead of specifying standard error, if confidence level is specified then the number of degree of freedom necessary for prescribed confidence level, based on chi-square test can be calculated

$$n = 2\,B\,T \qquad (3.49)$$

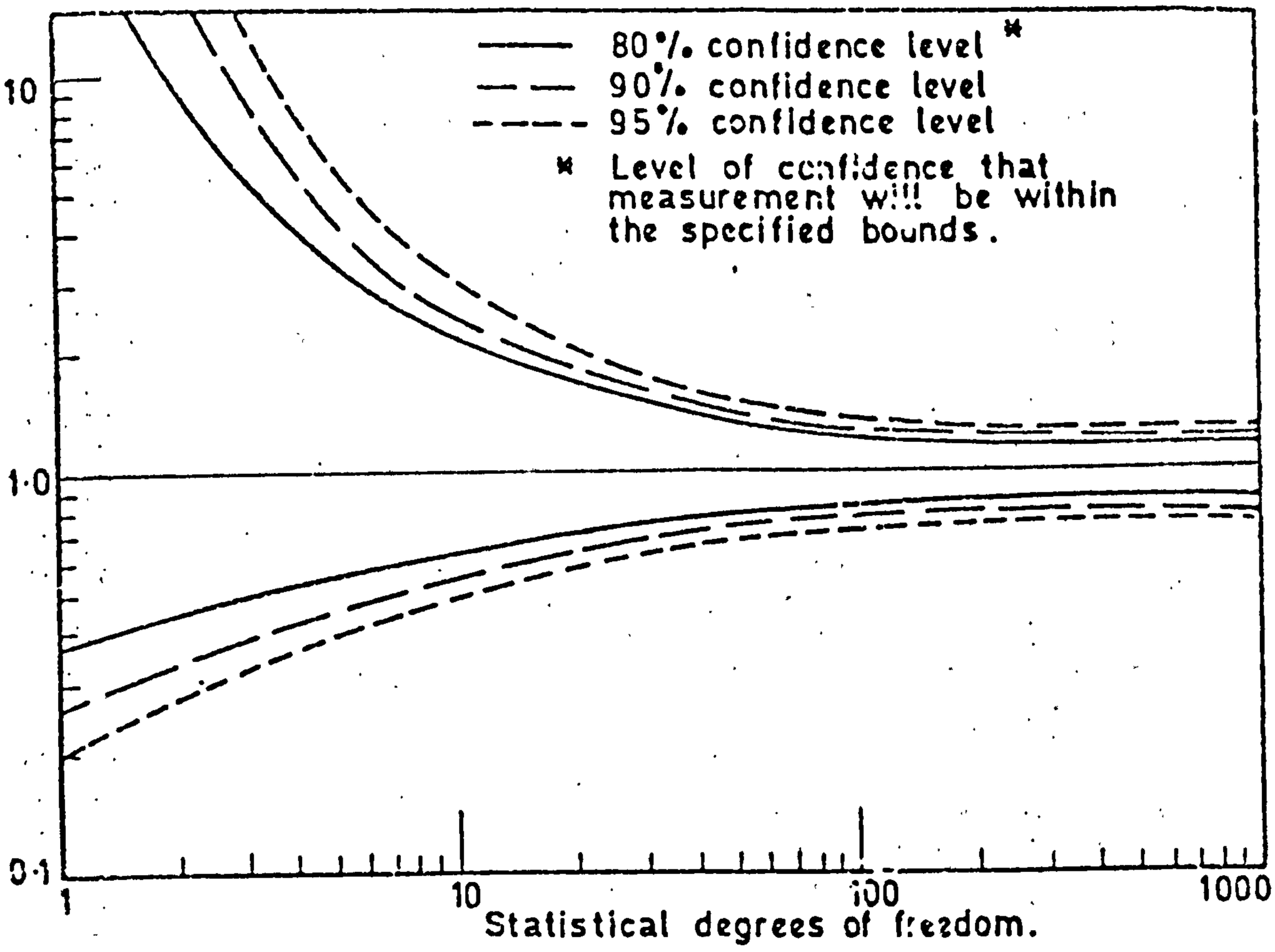

STATISTICAL DEGREES OF FREEDOM
FIGURE 7

The advantage of specifying a confidence level is that it can be applied to situations where the underlaying probability density function of the sample is not known. The relationship between the estimated values and the exact values as a function of degree of freedom is illustrated in figure (7) for several confidence level.

3.11 Set-up for Random Testing

The set-up for measuring random vibration response of the tower is as shown in figure (31a). The random Gaussian force was generated by feeding a random signal from a Solartron random signal generator, to the input of the electro-hydraulic control system. The output of the signal generator was first passed through a low pass filter in order to control the energy input in the frequency bandwidth (i.e. 0-10 Hz). Although the actuator was driven with a flat spectrum the tower was excited by a force spectrum (lb^2/Hz), which has a notch at the resonant frequency of the tower (See section 4). As a result of this, the signal from the low pass filter was passed through a specially designed filter which compensates for the reduction of power input near resonance of the tower. This arrangement although provided a fairly flat spectrum, required extensive calibration before each test. This method required preliminary tests to set the filter gain and bandwidth in order to maintain a constant force spectrum (lb^2/Hz) from 0 to 10 Hz. A typical force spectrum is shown in figure 33a. Ideally what is required is a computer controlled system as depicted in figure (31b), in which the input force spectrum is measured on-line and compared with reference (flat) spectrum. If the reference spectrum is not achieved, the excitation to actuator is altered until the required spectrum is achieved. This method was looked into, but latter discarded due to lack of suitable mini-computer. The author Ref.(36) has developed a computer controlled random testing system which is now being implemented on the ESRU computer.

The response of the tower was measured using

a) accelerometers

b) displacement transducer

and c) strain gauge

The force was measured using a strain gauge force transducer. The voltage signals corresponding to the measured force and response were each passed through a d.c amplifier with low pass filters, before recording them on an FM tape recorder.

The purpose of the d.c amplifier was to provide a satisfactory impedance matching between the units and to adjust the voltage levels to be within the linear range (±2V) of the magnetic tape recorder. In order to reduce the statistical errors, inherent, is random data analysis, long time histories of the signals are required. Normally, 50 ensemble averages (i.e. 100 degree of freedom) are considered adequate. For low frequency work this means long test duration. For example, in order to calculate the statistical properties of excitation and response of the tower to 0.14 standard deviation, in the frequency range of 0-10 Hz, required each test to be of 85.84 minutes duration. In order to be able to store this large amount of data, the signals were recorded at $3^3/_4$ in/S so that severals runs could be recorded on one analogue tape. During the data processing, the recorded force and response signals were simultaneously digitised using ADC's and converted to digital data with appropriate engineering units and stored on digital magnetic tapes. In order to reduce the digitising time, the recorded data was replayed at 60 in/S, thus reducing the digitising time by a factor of 16.

3.11.1 Response of Single-Degree of Freedom System to Random Excitation

The generalised mass of the tower calculated from the measured mode shape is 0.862 $lb.in^{-1}S^2$. The force was applied to the tower at a height of 10 feet above the base where the normalised mode shape amplitude is $\phi = 0.169$. Thus the generalised force applied to the tower becomes

$$F^*(t) = 0.169 * F(t) \qquad (3.50)$$

where F(t) is the force measured by the transducer at its point of application. The response amplitudes in the random tests were small (±0.5 in peak) compared to the response amplitudes required to produce non-linear material damping. Hence the non-linear damping present is mainly due to joint damping. Thus the equation of motion of the tower in the fundamental mode with non-linear joint damping can be written as

$$\ddot{X} + \gamma\,(1+\epsilon\,|\dot{X}|)\dot{X} + \omega_o^2 X = \frac{\phi}{M^*}\,F(t) = \frac{F^*(t)}{M^*} \qquad (3.51)$$

The power spectral density of the generalised, random excitation force $F^*(t)$ is

$$S_o^* = \phi^2\,\frac{W_o}{4\pi}$$

where W_o is the magnitude of the power spectral density of the measured force in Lb^2/Hz

(3.52)

Thus the power spectral density/unit mass becomes

$$S_o^* = \frac{\phi^2}{M^{*2}} \quad \frac{W_o}{4\pi} \qquad (3.53)$$

Substituting the value of ϕ and M^* in equation (3.53) yields

$$S_o^* = 0.0156\ W_o \quad lb^2/Rad/S/(lb\ in^{-1}s^2)^2 \qquad (3.54)$$

$\therefore$ Mean square displacement response for a single degree of freedom linear system becomes

$$\therefore \quad E(X^2) = \frac{\pi S_o}{2\beta_c \omega_o^3}\left(\frac{\phi}{M}\right)^2 \qquad (3.55)$$

$W_o(lb^2/Hz)$ was measured from the recorded data and substituted in equation (3.54) to yield the power spectral density of excitation. The mean square displacement response of the tower of the point where the mode shape was normalised to unity (top of the tower) was measured from the recorded displacement and the accelerometers signals. The results on the random vibration tests are as tabulated in Table (4). The mean square displacement was plotted against power spectral density, W_o, as shown in Figure (40).

3.12 Discussion on Random Vibration Tests

Using the digital analysis techniques discussed in section (3.10), the power spectral density of excitation force (lb^2/Hz) and the mean square displacement response (in^2) from both displacement and accelerometer tranducers were measured. Since the power spectral density of the force is fairly flat, in the range 0-10 Hz, (figure 33a), the statistical fluctuation can be further reduced using frequency smoothing. A frequency smoothing of five was used which resulted in the standard error of 0.045 in spectral density measurements. The purpose of measuring r.m.s stress was to make sure that the tower remained in the linear stress range and also that the non-linear damping due to material can be calculated. For the r.m.s stress levels measured in the excitation range of these tests, the non-linearity due to material damping is negligible.

The plots of mean square displacements versus power spectral density of excitation (W_o, lb^2/Hz) are as shown in figure (40). To make a consistant evaluation of damping, using various methods, it is essential that no change in damping, due to bolt torque occurs when excitation changes from discrete frequency testing to random vibration testing.

This can be achieved with certainty, if all the tests are carried out one after the other. Thus prior to random testing, a free vibration test was carried out to measure the damping parameters β and ϵ, as shown in section (3.3).

Corresponding to these values, a theoretical curve is drawn and it is seen that within the limits of experimental errors, the agreement between the measured and computed response values is quite good. The extraction of non-linearity parameter, ϵ, from random testing is discussed in section (5).

The viscous damping coefficient calculated from transfer function measured from random vibration tests was found to be 0.00258. This is roughly 30 % highter than that measured from free vibration tests at same r.m.s displacement amplitude. The discrepancy between the two methods is due to lack of frequency resolution. To measure the transfer function and hence an approximate viscous damping coefficient from the half power bandwidth of the transfer function generated from the random excitation tests requires at least 6 to 8 points in the half power bandwidth. The bandwidth of the tower is $B = 2\beta f_n = 0.024$ Hz. For a 2048 point FFT transform, the frequency resolution is 0.0097 Hz. A typical transfer function measured from random tests shown in firgure (35). The frequency resolution of this transfer function can be improved by using 8192 point FFT transform which results in frequency resolution of 0.0024 Hz, thus giving approximately 10 points in the half power bandwidth.

Another method of increasing frequency resolution is by using 'Band Selectable Fourier Analysis' (BSFA), the so called 'zoom' transform. BSFA is a measurement technique in which the fourier transform is performed over a frequency band whose lower and upper limit are independently selectable. This is in contrast to standard fourier analysis, which is always computed over a frequency range from zero frequency to same maximum frequency, F_{max}.

4.0 Force Control Excitation

4.1 Introduction

The two forms of exciters that will produce random forces are:-

1) Electro-magnetic
2) Electro-hydraulic

The main problem with electro-magnetic exciters, as far as their use in civil engineering is concerned, is that their low frequency range response is very poor.

In this investigation, electro-hydraulic actuators were used for applying forces to the 30 feet high bolted lattice structure. It was initially found that this electro-hydraulic force controlled system was unable to apply a constant force over the frequency bandwidth of interest. Secondly, the force input to the structure at its resonant frequency becomes noisy and unmeasurable. This condition has been observed by users of hydraulic actuators but they restrict themself to frequency below the -3db point. As in this experimental investigation of tower response to random force inputs required a constant force level at all frequencies, a theoretical study was undertaken to investigate this behaviour.

A review of published literature shows that most of the analytical work is electro-hydraulic actuators has been limited to displacement controlled systems and only a small portion of work has been done on the force controlled system (Ref.37), and this has been confined to the frequency range well below the resonant frequency of the structure.

4.2 Electro-hydraulic Loading System

The loading system has three loading channels. Each channel is comprised of a three term controller, a servovalve amplifier, electro-hydraulic servovalve, a hydraulic actuator and a load cell which measures the applied load on the tower. The three term controller receives the command signal and the applied load signal from the load cell. The resulting error signal is applied, after amplification, to the servovalve which adjusts the rate of oil flow to and from the hydraulic actuator until the required load is achieved on to the structure. The control system consists of a hydraulic and an electrical system. Figure (41) shows

the schematic diagram of the hydraulic system and figure (42) shows the schematic diagram of the electrical system. Details of the hydraulic and electrical components are given in appendices C and D.

4.2.1 System Transfer Functions

To make a theoretical assessment of the system's performance, expressions for the open and closed loop response of a single channel to sinusoidal input are derived for the system under force control. The difference between the displacement and force control system is that in the case of a position feedback system the output component takes up a position proportional to the input signal and is independent of the external force applied to it. In the case of the force feedback system, the force opposing the actuating component is compared with the input signal and the output component tends to take up a position in which it meets an opposing force equal to that demanded by the input.

Figure (43) shows the control system block diagram. In this system the servovalve amplifier transfer function G1 and the load cell transfer function G4 are assumed constants. Hence only the hydraulic valve transfer function G2 and the actuator and load transfer G3 remains to be derived. In order to derive the transfer function of the actuator and load, following assumptions are made:-

1) The tower and its connecting structure is a system of many degrees of freedom. As its fundamental frequency is of real interest, the tower is approximated by a simple system of one degree of freedom.

2) The mass of the piston is assumed to be zero.

3) The actuator piston is assumed to be initially in the centre position.

4) The servovalve has zero overlap or underlap.

5) There is no friction or leakage present in the actuator.

Two attachment configurations are considered:-

1) Elastic connection between the actuator and the tower.

2) Rigid connection between the actuator and the tower.

The simplified diagram of the system of case (1) is shown as in Figure (44).

With the above assumptions, the flow equation of the actuator becomes

$$q = A(\dot{X} - \dot{Z}) + \frac{V_t}{2B} \dot{P}_L \qquad (4.1)$$

The flow to the actuator is a function of two variables, the servovalve current and load pressure.

$$\begin{aligned} q &= f(i, P_L) \\ &= \frac{\partial q}{\partial i} i + \frac{\partial q}{\partial P_L} P_L \\ &= K_v i + R_v P_L \end{aligned} \qquad (4.2)$$

where K_v = Valve sensitivity to input current (cis/mA)

R_v = Valve sensitivity to load pressure (cis/psi)

Although the hydraulic valve is inherently non-linear a reasonably good approximation to its tranfer function can be obtained if the operation of the system is limited to small loads and small input signals. For this condition the operation of the valve is confined to a small region near the origin of its pressure - flow characteristics at which point the valve flow gains are almost independent of the control signal and load pressure. If the operation of the valve is also limited to low frequencies (less than 50 Hz) its transfer function is found to be (Ref.31).

$$\frac{q}{i} = \frac{K_v}{\left[1+2\zeta/\omega_n\, s + (s/\omega_n)^2\right]}$$

$$q = \frac{K_v\, i}{(K_4 s^2 + K_3 s + 1)} \qquad (4.3)$$

where K_v = valve static gain at zero load pressure (cis/mA)
ω_n = apparent natural frequency (rad/sec)
$K_3 = 2\zeta/\omega_n$
$K_4 = 1/\omega_n{}^2$
ζ = apparent damping ratio

One of the lags in equation (4.3) is due to time constant of torque motor field and the other arises as a result of spool motion. Standard moog valves are available in several sizes and the value of the valve sensitivity K_v, depends upon the rated flow and the valve current.

The actuator is subjected to an external generalised force comprising inertia, viscous damping and stiffness.

$$F = F^*/\phi = (M^* s^2 + C^* s + K^*)\ Y/\phi \qquad (4.4)$$

Let

$$M^* s^2 + C^* s + K^* = U^*$$

$$\therefore \quad F = U^*\ Y/\phi \qquad (4.5)$$

This force is balanced in the actuator by the pressure P and the piston area A

$$F = A.P \qquad (4.6)$$

The support reaction is

$$-K_e Z = F \qquad (4.7)$$

where K_e is the stiffness of the actuator support.

The actuator is subjected to the force, F, through a spring of stiffness K_o.

$$F = K_o\ (X - Y\phi) \qquad (4.8)$$

where $(X-Y\phi)$ is the net compression of the spring K_o.

From equations (4.5) and (4.8)

$$X = \frac{U^* Y}{\phi K_o} + Y\phi = Y\phi \left[1 + \frac{U^*}{K_o \phi^2}\right] \qquad (4.9)$$

From equation (4.7)

$$Z = -\,{}^{F}/_{K_e}$$

Substituting these in equation (4.1) gives

$$q = As\left[Y\phi \left(1+ \frac{U^*}{K_o \phi^2}\right)+ \frac{U^* Y}{K_e \phi} + \frac{F V_t}{2BA^2}\right]$$

$$\therefore \frac{F}{q}(s) = \frac{M^* s^2 + C^* s+K^*}{As\left[s^2 \left(\frac{M^*}{K_e} + \frac{M}{K_o} + \frac{M^* V_t}{2BA^2}\right)+ s\left(\frac{C^*}{K_e} + \frac{C^*}{K_o} + \frac{V_t C^*}{2BA^2}\right)\right.}$$

$$\left. + \left(\phi^2 + \frac{K^*}{K_o}+ \frac{K^*}{K_e}+ \frac{V_t K^*}{2BA^2}\right)\right] \qquad (4.10)$$

The term $\frac{V_t}{2BA^2}$ can be regarded as the stiffness K_h of the entrapped oil. K_h is not only dependent upon the bulk modulus B of the oil, but it is also a function of the actuator geometry. It can be shown that it is also a function of the position of the actuator piston.

$$\therefore \frac{F}{q}(s) = \frac{K^*\left(\frac{M^*}{K^*} s^2+ \frac{C}{K^*} s+1\right)}{As\left[\left(\frac{M^*}{K_e} + \frac{M^*}{K_h} + \frac{M^*}{K_o}\right)s^2+s\left(\frac{C^*}{K_e} + \frac{C}{K_o} + \frac{C^*}{K_h}\right)\right.}$$

$$\left. + \left(\phi^2 + \frac{K^*}{K_e}+ \frac{K^*}{K_o}+ \frac{K^*}{K_h}\right)\right] \qquad (4.11)$$

The transfer function of the servovalve is

$$\frac{i}{V_e}(s) = K_1 \qquad (4.12)$$

where i = output current of the amplifier (mA)

V_e = error voltage (volts)

K_1 = gain of the amplifier (mA/volts)

The transfer function of the load cell and amplifier is

$$\frac{V_o}{F}(s) = K_5 \qquad (4.13)$$

where F = force measured by the load cell (lb)

K_5 = gain of the load cell amplifier (volts/lb)

V_o = output voltage from the amplifier (volts)

Overall open loop transfer function G(s) of the system becomes

$$G(s) = \frac{F}{q} \cdot \frac{q}{i} \cdot \frac{i}{V_e} \cdot \frac{V_o}{F} = \frac{V_o}{V_e} \qquad (4.14a)$$

Substituting the valves of $\frac{F}{q}$, $\frac{q}{i}$, $\frac{L}{V}$ and $\frac{V_o}{F}$ from equations (4.11), (4.3), (4.12) and (4.13) respectively yields

$$G(s) = \frac{K\left[\frac{s^2}{\omega_s^2} + \frac{2\beta}{\omega_s}s+1\right]}{s\left[\frac{s^2}{\omega_c^2} + \frac{2\beta_c}{\omega_c}s+\alpha\right]\left[\frac{s^2}{\omega_n^2} + \frac{2\zeta}{\omega_n}s+1\right]} \qquad (4.14)$$

where

$$K = \frac{K_1 K_V K_5 K^*}{A}$$

$$\omega_s = \sqrt{\frac{M^*}{K^*}}$$

$$\frac{1}{\omega_c^2} = \left(\frac{M^*}{K_o} + \frac{M}{K_e} + \frac{M}{K_h}\right) = \left(\frac{1}{\omega_o^2} + \frac{1}{\omega_e^2} + \frac{1}{\omega_h^2}\right)$$

where ω_s is the fundamental frequency of the tower. ω_c is the combined frequency of the spring K_o, spring K_h and spring K_e.

$$\alpha = \phi^2 + \frac{K^*}{K_o} + \frac{K^*}{K_e} + \frac{K^*}{K_h}$$

$$\beta_c = \frac{\beta\ \omega_s}{\omega_c}$$

The attachment stiffness K_e is large compared with K_h, therefore the open loop transfer function simplifies to

$$G(s) = \frac{K\left[\frac{s^2}{\omega_s^2} + \frac{2\beta}{\omega_s}s + 1\right]}{s\left[\frac{s^2}{\omega_c^2} + \frac{2\beta_c}{\omega_c}s+\alpha\right]\left[\frac{s^2}{\omega_n^2} + \frac{2\zeta}{\omega_n}s+1\right]} \qquad (4.15)$$

where $\frac{1}{\omega_c^2} = \frac{1}{\omega_o^2} + \frac{1}{\omega_h^2}$ and $\alpha = \phi^2 + \frac{K^*}{K_o} + \frac{K^*}{K_h}$

The value of ω_n should be as large as possible. For the existing actuator, the equation

$$\omega_h = \sqrt{\frac{2BA^2}{V_t\ M^*}}$$

shows that (A and V_t given) the increase in ω_n can be achieved only by decreasing the mass of the load M^* or by increasing the bulk modulus, B, both of which are seldom possible in practice.

4.2.2 Closed Loop Frequency Response

The closed loop frequency of a system with unity feedback gain is given by the expression

$$G_c(s) = \frac{G(s)}{1+G(s)}$$

Therefore the closed loop transfer function of the system becomes

$$G_c(s) = \frac{K\left[\frac{s}{\omega_s^2} + \frac{2\beta}{\omega_s}s+1\right]}{\left[\frac{s^5}{\omega_c^2\,\omega_n^2} + s^4\left(\frac{2\beta_c}{\omega_n\,\omega_c} + \frac{2\zeta}{\omega_c\,\omega_n}\right) + s^3\left(\frac{1}{\omega_c^2} + \frac{\alpha}{\omega_n^2} + \frac{4\beta\zeta}{\omega_c\,\omega_n}\right)\right.}$$

$$\left. + s^2\left(\frac{2\beta_c}{\omega_c} + \frac{\alpha 2\zeta}{\omega_n} + \frac{K}{\omega_s^2}\right) + s\left(\alpha + \frac{2\beta}{\omega_s}K\right) + K\right] \qquad (4.16)$$

4.2 3 Transfer Function Of The System In Case 2

In this case $K_o = \infty$. The analysis is similar to case (1). Therefore replacing $K_o = \infty$ in the open loop transfer function of case (1), the open loop transfer function of case (2) becomes

$$G(s) = \frac{K\left[\frac{s^2}{\omega_s^2} + \frac{2\beta}{\omega_s}s + 1\right]}{S\left[\frac{s^2}{\omega_h^2} + \frac{2\beta_h}{\omega_h}s + \eta\right]\left[\frac{s^2}{\omega_n^2} + \frac{2\zeta}{\omega_n}s + 1\right]} \qquad (4.17)$$

where

$$\omega_h = \sqrt{\frac{K_h}{M^*}}$$

$$\beta_h = \frac{\beta\,\omega_s}{\omega_h}$$

and

$$\eta = \phi^2 + \frac{K^*}{K_h}$$

The closed loop transfer function becomes

$$G_c(s) = \frac{K\left[\frac{s^2}{\omega_s^2} + \frac{2\beta}{\omega_s}s+1\right]}{\left[\frac{s^5}{\omega_h^2\,\omega_n^2} + s^4\left(\frac{2\beta_h}{\omega_n\,\omega_h} + \frac{2\zeta}{\omega_h\,\omega_n}\right) + s^3\left(\frac{1}{\omega_h^2} + \frac{\alpha}{\omega_n^2} + \frac{4B\zeta}{\omega_c\,\omega_n}\right)\right.}$$

$$\left. + s^2\left(\frac{2\beta_h}{\omega_h} + \frac{2\eta\zeta}{\omega_n} + \frac{K}{\omega_s^2}\right) + s\left(\eta + \frac{2\beta K}{\omega_s}\right) + K\right] \qquad (4.18)$$

4.3 Stability Analysis

Stability is probably the most important performance characteristic of a servo system. The design of the loop dynamic performance is usually centered around the requirement for stability. Compared with Root locus and Nyquist diagrams, the Nichol's chart method of stability analysis is the most useful in hydraulic control because parameters tend to vary. As the Nichol's diagram can be sketched rapidly, stability can be investigated for a wide range of parameter variations.

The Nichol's diagram is a plot of open loop transfer function

$$G(s) = \frac{K\left(\frac{s^2}{\omega_s^2} + \frac{2\beta}{\omega_s}s + 1\right)}{s\left(\frac{s^2}{\omega_c^2} + \frac{2\beta_c}{\omega_c}s + c\right)\left(\frac{s^2}{\omega_n^2} + \frac{2\beta_n}{\omega_n}s + 1\right)} \qquad (4.19)$$

where K (s^{-1}) is the open loop gain constant (also called velocity constant). The free s in the denominator indicates an integration so that this electrohydraulic servo loop is of type 1. If the servo valve is assumed to have a fast response (servo valve transfer function assumed constant), the above transfer function can be approximated by

$$G(s) = \frac{K\left(\frac{s^2}{\omega_s^2} + \frac{2\beta}{\omega_s}s + 1\right)}{s\left(\frac{s^2}{\omega_c^2} + \frac{2\beta_c}{\omega_c}s + \alpha\right)} \qquad (4.20)$$

For low values of damping (β), the ratio of the trinomials in equation (4.20) adds a loop to the vertical straight line which represents the integration on the Nichols chart. This loop is situated on the right of the vertical line representing integration. The angular frequency (ω_s) in the numerator which reduces the amplitude and advances the phase is less than the angular frequency ($\omega_c\sqrt{\alpha}$), which increases the amplitude and retards the phase. The open loop transfer functions are as shown in figure (45) for various values of spring stiffnesses (K_o).

4.3.1 Routh's Stability Criteria

The characteristic equation of the system in case 1 becomes

$$A_1s^5 + B_1s^4 + C_1s^3 + D_1s^2 + E_1s + F_1 = 0 \qquad (4.21)$$

where

$$A_1 = 1/(\omega_c^2\ \omega_n^2\ K)$$

$$B_1 = \left(\frac{2}{\omega_c\ \omega_n\ K}\right)(\beta_c + \zeta)$$

$$C_1 = \left(1/\omega_c^2 + \alpha/\omega_n^2 + \frac{4\beta\zeta}{\omega_n\ \omega_c}\right)/K$$

$$D_1 = \left(2\beta_c/\omega_c + \frac{2\zeta\alpha}{\omega_n} + K/\omega_s^2\right)/K$$

$$E_1 = \left(\alpha + 2\beta K/\omega_s\right)/K$$

$$F_1 = 1$$

Applying Routh's stability criteria to this equation yields the condition for absolute stability

$$\frac{2}{\omega_c\ \omega_n}(\beta_c + \zeta)\left(\frac{1}{\omega_c^2} + \frac{\alpha}{\omega_n^2} + \frac{4\beta\zeta}{\omega_n\ \omega_c}\right) > \frac{1}{\omega_c^2\omega_n^2}\left(\frac{2\beta_c}{\omega_c} + \frac{2\zeta\alpha}{\omega_n} + \frac{K}{\omega_s^2}\right) \qquad (4.22)$$

To illustrate the various factors which influence the stability of the electrohydraulic system, the above condition was evaluated for various loop gains (K), position (ϕ)of the attachment for the actuator to the tower, spring stiffness (K_β) and structural damping (β). The results are as tabulated in Table 5.

4.3.2 Measured Characteristics of the Electrohydraulic System

The characteristics of a closed loop electrohydraulic system which need determining are

1) Forward gain

2) Loop gain

3) Amplitude ratio

and 4) Phase angle

The forward gain can be determined statistically by putting a certain specified input (command voltage) and measuring the output force accurately. Usually all that is necessary is to measure the input and feedback voltages, the feedback voltage having previously calibrated in terms of force. The rest of the characteristics can be obtained by measuring the frequency response to a sinusoidal input. This was measured using Solartron TFA. The TFA consists of a signal generator which has a sinusoidal output with a constant peak voltage. The output of the system taken from the feedback load cell is fed into the Resolved Components Indicator, which

measures the peak to peak value (with input) and the quadrature (90° out-of-phase) components of the force signal. These data plotted directly are a Nyquist plot of the closed loop. They can then be reduced to a Bode plot by measuring the length and angle of the vector reprented by each frequency. Figure (46) shows the Nyquist plot and (47) shows the Bode plot of the measured closed loop response.

4.3.3 Theoretical Open Loop and Closed Loop Transfer Functions

From equations (4.15) and (4.17), Bode plots of the open loop transfer functions of the two cases were calculated and are shown in Figure (48). The corresponding Nichols plots are shown in Figure (49). Closed loop Bode plot can be plotted from the open loop Nochols Plot but the process becomes tedious. The Bode plots of the closed loop were calculated from equations (4.16) and (4.18) and are shown in Figure (50). The corresponding Nyquist plots are as shown in Figure (51). It is seen from these plots that the response of the control system deteriorates at the resonant frequency of the tower. These plots are similar to the measured frequency response (Figure (47)) of the control system. It is seen that this drop in response is more when the actuator is rigidly connected to the tower compared with when it is connected through a spring. On the actual system it was found that it was practically impossible to measure the force input to the tower as its resonant frequency when the actuator is rigidly connected to it. In similar test with the load applied through a spring it was found that it is possible to measure the applied force. This is due to the fact that the spring allows a phase difference to exist between the actuator ram and the tower displacements. Figure (52) shows the phase relationships between the actuator ram displacement, tower displacement and the force. Figure (53) shows the measured phase relationships near the resonant frequency of the tower.

At frequencies below the natural frequency of the tower, the phase difference between the force and the tower displacement and the actuator and the tower is small, but near the resonance of the tower a large phase change occurs between the actuator and the tower. This can only exist without effecting the force measurement if a flexible linkage exists between the two components. A spring of stiffness, K_o, provides this linkage.

The dip in the force measurement is an inherent property of the force control system. Under deterministic conditions, i.e. when applying a sinusoidally varying force, the reductions in the force can be restored to the desired value by increasing the command signal manually. As the system has to be used for applying random loads with a flat spectrum over the frequency range 0 - 15 Hz., this becomes impossible. To overcome this attenuation in such applications a filter with a frequency response, that is inverse of the frequency response of the control system was introduced outside the control loop.

4.4 Shaping Filter

Various filter designs were tried which had the required frequency. It was found that in most of them it was not possible to change parameters of the filter easily. One which was found to be most appropriate for this system is as described in Appendix B. The transfer function of the filter is

$$\frac{V_{OUT}}{V_{IN}} = \frac{s^2 + (a + c)\, s + b}{s^2 + a\, s + b}$$

$$= \frac{s^2 + \left(\frac{1}{R_1\ C_1} + \frac{1}{R_4\ C_1}\right) s + \frac{1}{R_3\ R_2\ C_1\ C_2}\ \frac{R_6}{R_5}}{s^2 + \frac{1}{R_1\ C_1}\ s + \frac{1}{R_2\ R_3\ C_1\ C_2}\ \frac{R_6}{R_5}} \qquad (4.23)$$

The resonant frequency ω_f of the filter can be changed by altering one resistor, namely R_3 and its peak amplitude by R_1.

Modified Closed Loop Transfer Function

The modified transfer function of the control system becomes

$$G(s) = \frac{K \left[\frac{s^2}{\omega_s^2} + \frac{2\beta}{\omega_s} s + 1\right]\left[s^2 + \gamma s + \omega_f^2\right]}{\left[A_1 S^5 + B_1 S^4 + C_1 S^3 + D_1 S^2 + E_1 S + F_1\right]\left[s^2 + \mu s + \omega_f^2\right]} \qquad (4.24)$$

Figure (57) shows the closed loop response of the system with and without the filter. To select the gain and the bandwidth of the filter, first the transfer function of the control system is measured with the filter switched off. Then the parameter of the filter are selected such that inverse transfer function matches the transfer of the control system.

4.5 Random Input Testing

To investigate the performanne of the system under random input conditions, the force applied to the tower was measured for various spring stiffnesses. Figure (58) shows the power spectral density of the force applied to the tower when the actuator is rigidly connected and figure (59) shows when it is elastically connected. It is seen from these plots that the attenuation of force with elastic connection at resonant frequency of the tower is less than that with rigid connection. Figure (60) shows the effect of the filter on the psd of the force applied to the tower. The bandwidth of the system under these conditions is approximately 8 Hz. In order to study the effect of

stiffness on the bandwidth, the force applied to the tower was measured using various spring stiffnesses. Figure 61 to 63 shows that increasing the stiffness increases the bandwidth of the system.

4.6 Discussion

Table 5 shows that the gain of the system can be increased appreciably without effecting the stability, when the force is applied to the tower through a spring. On the test rig, the maximum proportional gain that could be applied when the actuator was rigidly connected was 0.03, whereas with the spring this gain could be increased to 0.4 without affecting the stability of the system. Figure (53) shows the Nichols plots of the open loop transfer function of the system in case 1, for three valves of proportional gain.

The attenuation in the force level at tower resonance is small and the force is measurable in case 1 compared with case 2. This is due to the spring allowing phase changes to occur between displacements of the actuator ram (X) and the tower (Y). Figure (52) shows that the phase difference between X and Y is small below resonance and goes to 180^{o} above resonance.

The maximum static force that can be generated by the actuator is 1000 lb, but the amount that can be transferred to the tower in case 1 depends on the spring stiffness K_s. Apart from controlling the static force, it also controls the bandwidth of the system in the dynamic case. Figures (61 to 63) shows that increasing the stiffness of the spring increases the bandwidth over with constant force level can be applied.

To investigate the effect of the position of the actuator to the tower, on the response of the system, the closed loop transfer of the system was calculated for various attachment positions. The results are as shown in figure (56). The attenuation of the force level is large when the actuator is connected at the top compared with when connected near the base of the tower. As the force input to the tower for a given displacement at the increases as the attachment position is moved towards the base, the actuators were connected at 2, 6 and 10 feet from the ground level so that required loads could be applied depending on the particular test requirements.

In any resonance tests, consideration should be given to the effect that the exciter has on the dynamic properties of the structure. In a resonance test on an aircraft it is usual to assume that the influence of the exciter

characteristics on the modes of the aircraft is negligible. With lighter structures this assumption may no longer be valid and with very light aeroelastic models the effect of attaching an exciter may be considerable. In such cases it is essential to have an excitation control system in which the unwanted characteristics of the exciter can be removed by applying forces to the exciter that will compensate the forces due to the added mass and damping effects of the exciter.

The damping measured from the transfer function derived from random excitation gave results comparable with those obtained from free vibration tests. This shows that the spring and actuator does not introduce unwanted damping into the system.

4.7 Conclusion

1) The analysis and the results from the test rig shows that when applying dynamic forces to a structure around or at its natural frequencies using electrohydraulic system, one should apply the force through a flexible linkage which allows phase variations between force and displacement to exist.

2) The point of application of the force should be close to the node of the resonance mode being excited so that the actuator displacement is small and in the operating range of the system.

SECTION B

5.0 Introduction

The non-linear nature of damping motivates an examination of solution methods for systems with non-linear differential equations. The various methods that can be used in analysising non-linear dynamical system under random excitation are,

1) Perturbation techniques
2) The Equivalent Linearisation method
3) The Fokker-Planck equation

and 4) Functional analysis methods.

There are, however, limitations and advantages in applying these methods to a particular problem. The perturbation was first developed by Crandall (45) for simple one and two degree-of-freedom non-linear systems and it has been widely studied and applied since then (46 - 49). This approach has been applied to multi-degree of freedom systems by Tung (50) and is suitable for treating those cases in which the non-linear terms in the governing equations are small. The method is based on a series expansion in power of ϵ, the non-linearity parameter. No restriction on the type of random excitation is required in its application.

It can be used to treat both the non-linear stiffness and non-linear damping cases. So far perturbation method has been used only to compare the statistical properies such as the variance and spectral density of the response up to the first order perturbation terms. The analysis beyond the first order term is quite complex because of computational difficulties and as such will not be applied to the present problem.

The method of equivalent linearisation, which so far has had the widest range of applicability, was originated by Krylor and Bogoliubov (51) for deterministic inputs. It has been applied to single degree of freedom non-linear system and extended to multi-degree of freedom system with non-deterministic (random) inputs used by Caughey (52) and generalised by Foster (53) and Iwan and Yang (54). In this method, the linear part of the non-linear equations are uncoupled using modal analysis and the linearisation technique is applied to the resulting single degree of freedom equation separately. This is quite effective in certain applications but the conditions imposed on the instantaneous correlation matrix of excitation limits its use to rather special cases. In Foster's general approach, numerical methods must generally be used to obtain the equivalent linear damping and stiffness matrices. In Iwan and Yang's method, linear damping and stiffness matrices can be determined analytically. This approach is based on the concept of

decomposing the non-linear forces arising from both damping and stiffness of the actual system into sum of simpler approximate linear forces, each of which depends solely on the relative displacement and velocity between discrete masses of the system, In some cases, this method will yield a closed form solution. However, given a system of non-linear equations, the accuracy of the method depends on the choice of these approximate forces. Also when the masses are distributed, the identification of the forces is quite complex. This approach is well suited to lumped spring - mass type system.

The Fokker-Planck equation method has been extensively used in the study of both linear and non-linear system excited by random forces (55 and 56). This method is limited to purely random excitations.

Although a purely random process is not physically realisable, it may be used to approximate a real excitation process in a structural response computation under suitable conditions. This method, however, allows to obtain first and second order response moments from the system equations of motion. Existence of these moments permits the derivation of a diffusion equation for the joint probability density of the phase vector comprising the randomly varying system velocity and displacement. This diffusion equation is a partial differential equation of the first order in time and of the second order in the velocity - displacement phase space. For linear and certain non-linear systems, specifically those in which non-linearities involve displacement terms only, a solution is possible. Exact solutions exist in these situations because the resultant diffusion equation is linear and thus amendable to standard solution techniques. In the cases of the velocity - non-linear problem undertaken in this investigation, however, the Fokker-Planck diffusion equation is also non-linear which provides no simplification. An extensive historical background to the Fokker-Planck method is given in Ref.(57) and detailed discussion on the applicability of this method is given in Ref.(58).

The functional analysis method Ref.(64) is based on an iterative solution to a non-linear differential equation of the form $m\ddot{X} + C\dot{X} + KX + f(X) = N(t)$, where $f(X)$ is a non-linear function of X. An approximate closed form solution may be obtained by truncating the iteration at a certain point. To examine the convergence of the iteration the Lebesgne 'norm' is used and if the 'norm' of the difference between two successive approximations can be expressed as a Lipschitz condition

$$\left|\left|X_{n+1} - X_n\right|\right|_i \leq \lambda \left|\left| X_n - X_{n-1}\right|\right|_i$$

where $\lambda < 1$, then the iteration converges on a unique solution. This method has been applied to problems Ref.(64) where the non-linearity arises in the stiffness term and it can be extended to situation where non-linearity arises in damping terms.

The method used in analysing non-linear differential equations in this thesis is called the 'Equivalent Non-linear Differential Equation' method and it combines an exact solution of the Fokker-Planck equation of a particular form of non-linear differential equation with the equivalent linearisation technique. This method is described in details together with derivation of the Fokker-Planck equation for the case of non-linear damping of the form $C(1+\epsilon|\dot{x}|^n)$. and is modified so that a closed form of solution is possible for all valves of n.

5.1 Kolmorgorov - Fokker-Planck Equation

The Kolmorgorov - Fokker-Planck equation has been extensively used in the theoretical study of both linear and non-linear systems excited by random excitation.

Before proceeding with the application of Kolmogorov-Fokker-Planck equation to the dynamic system, some concept of Markoff process are recalled here. A Markoff process is a random process whose relationship to the past is confined only to the observation of the process that immediately precedes the present. For example, a stochastic process X(t) is called a Markoff process if for every n and

$$t_1 < t_2 < t_3 \ldots < t_n$$

$$P\left\{X(tn) \leqslant X_n \,\middle|\, X(tn-1), \ldots, X(t)\right\} = P\left\{X(tn) \leqslant X_n \,\middle|\, X(tn-1)\right\}$$

In other words, given the present state $X(t_o)$, the future ($t>t_o$) state is independent of the past state ($t<t_o$). Such processes are completely defined in the statisticalsense by their transitional or conditional probability laws. These laws are obtained as the fundamental solution to the Fokker-Planck equation pertaining to a particular dynamic system. It can be shown (Ref.59) that a stationary Gaussian random process is a particular case of a Markoff process when it has an exponential autocorrelation function.

5.2 Joint Probability Density Function

To formulate the concept of a Markoff process it is necessary to first define certain joint probability density functions (JPDF). Consider therefore, a random process X(t) at various sequential times $t_1, t_2 \ldots, t_n$ as shown in figure (8).

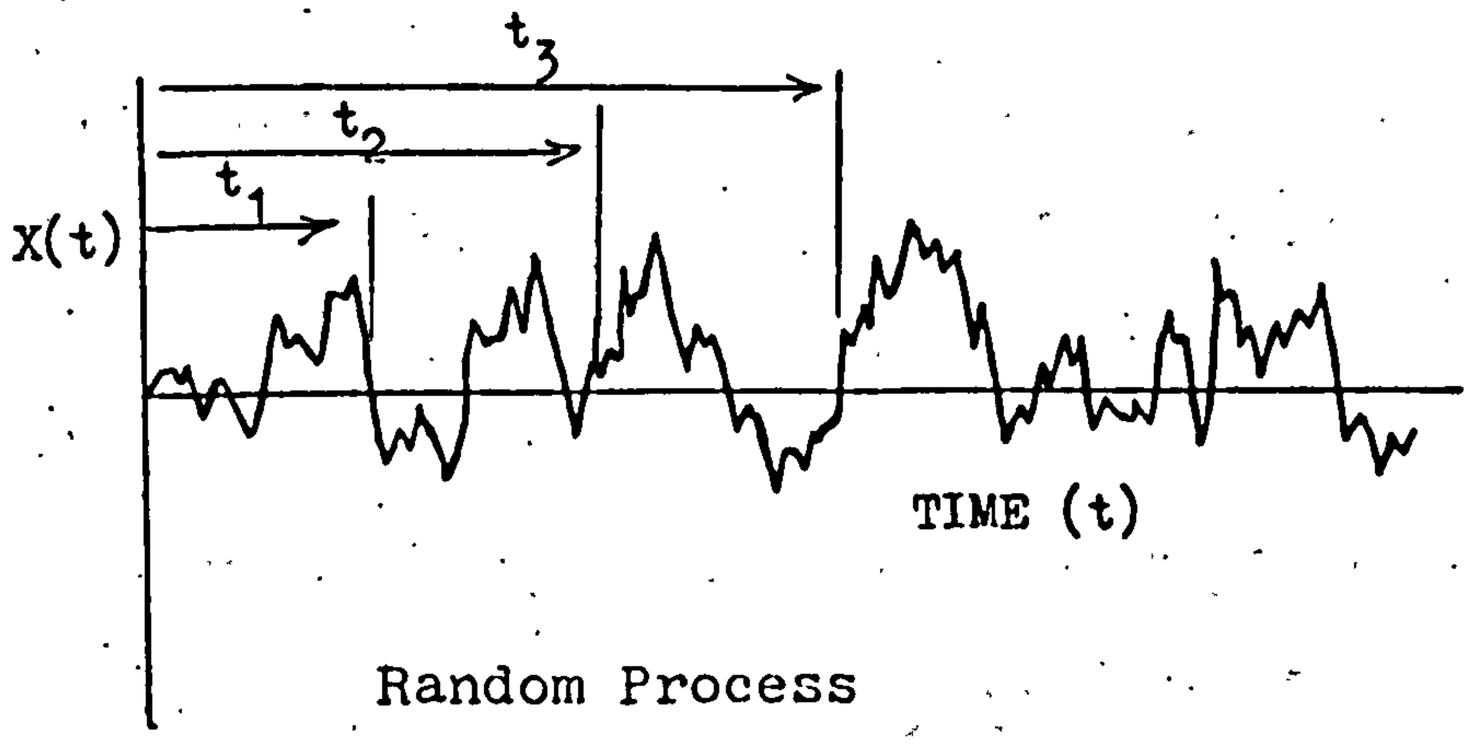

FIGURE 8

Let

$P_1(X_1 t_1)dX$ = the probability that X exists in the range X_1 to X_1+dX_1 at time t_1

$P_2(X_1 t_1, X_2 t_2)\ dX_1 dX_2$ = the joint probability that X exists in the range X_1 to X_1+dX_1 at t_1 and in the range X_2 to X_2+dX_2 at t_2

Therefore, the n dimensional jpdf can be written as

$P_n(X_1 t_1, X_2 t_2, \ldots X_n t_n)dX_1 dX_2 \ldots dX_n$ = the joint probability that X exists in the range X_1 to X_1+dX_1 at t_1,

..... and in the range X_n to X_n+dX_n at t_n

or

$$P_n(X_1 t_1, X_2 t_2 \ldots X_n t_n)\ dX_1 dX_2 \ldots dX_n$$

$$= \text{Prob}\left[X_1 < X_1(t_1) < X_1+dX_1, \ldots\ldots X_n < X_n(t_n) < X_n+dX_n\right] \qquad (5.1)$$

From equation (5.1), it can be seen that P_3 implies the existance of both P_1 and P_2 and that in general P_n implies all previous P_k, with $k<n$. In order to relate P_k to P_n, consider first, the case of two dimentional joint probability density function P(X,Y) which forms a surface in the X-Y plane.

Thus $$\int_{\infty}^{\infty} P(X)dX = \int_{-\infty}^{\infty}\int_{-\infty}^{\infty} P(X,Y)dxdy = 1 \qquad (5.2)$$

Differentiating equation (5.2) with respect to X yields

$$P(X) = \int_{-\infty}^{\infty} P(X,Y)dY \qquad (5.3)$$

Applying this principle to equation (5.1) yields

$$P_k(X_1 t_1, X_2 t_2 \ldots X_k t_k) = \int_{\infty}^{\infty}\int_{\ldots}^{\infty}\int_{n-k}^{\infty} P_n(X_1 t_1, X_2 t_2 \ldots X_n t_n)dX_{k+1}..dX_n \qquad (5.4)$$

fold

5.3 Conditional Probability Density Function

If at time $t = t_1$, $X = X_1$, then the conditional probability of finding X in the range X_2 to X_2+dX_2 at a time t_2-t_1 later is given by the expression

$$P_{c2}(X_1/X_2,\ t_2-t_1)\ dX_2 \qquad (5.5)$$

This situation is depicted in Fig.(9)

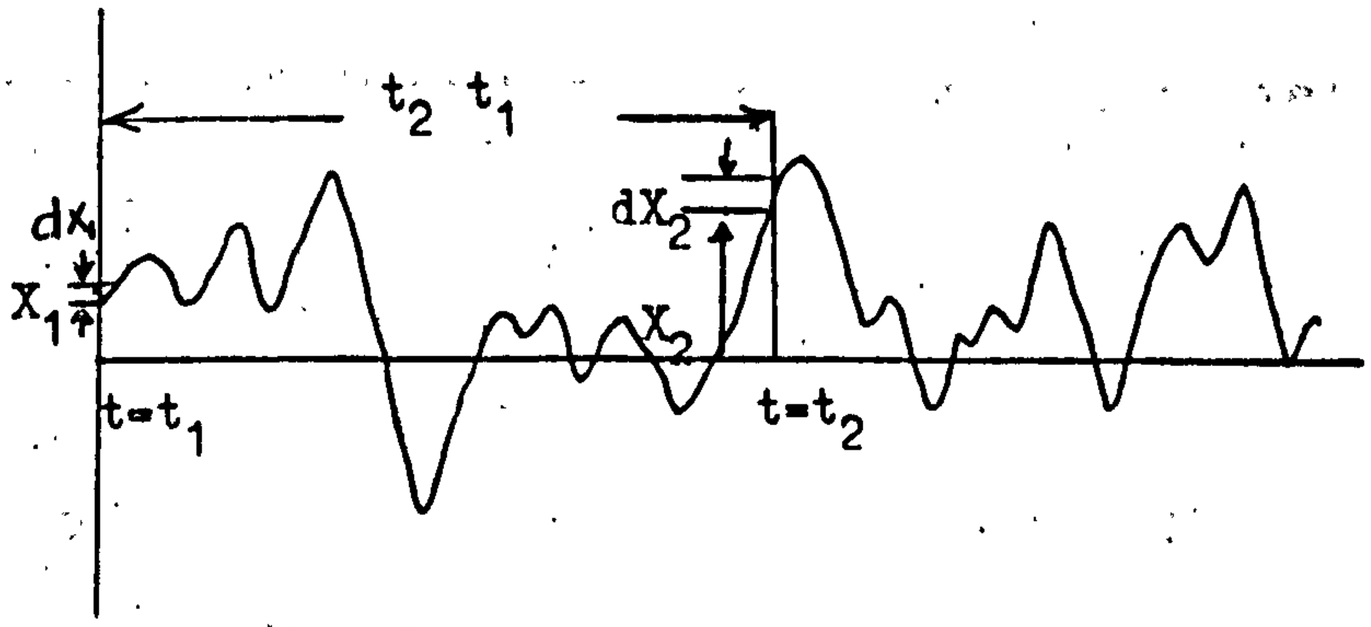

Random Process

FIGURE 9

In order to find $P_2(X_1t_1, X_2t_2)$, i.e. the joint probability that X exists in the range X_1 to X_1+dX_1 at time t_1 and in the range X_2 to X_2+dX_2 at time t_2, the following relation is used

$$P(s,q) = P(s)P_c(s/q) \qquad (5.6)$$

which defines the probability of events s and q occuring together, in terms of the product of the probabilities that s occurs and the conditional probability that q occurs when it is known that s has already occured. Thus using equation (5.6), yields

$$P_2(X_1t_1, X_2t_2) = P_1(X_1t_1).P_{c2}(X_1/X_2, t_2-t_1) \qquad (5.7)$$

Since $P_1(X_1t_1)$ is one-dimensional density function, P_2 is defined in terms of P_{c2}. The conditional probability density function integrates in the same way as an ordinary density function

$$\int_{-\infty}^{\infty} P_{c2}(X_1 | X_2, t)dX_2 = 1 \qquad (5.8)$$

From equation (5.4)

$$P_1(X_1t_1) = \int_{-\infty}^{\infty} P_2(X_1t_1, X_2t_2)dX_2 \qquad (5.9)$$

Exchanging X_2 for X_1 yields

$$P_1(X_2t_2) = \int_{-\infty}^{\infty} P_2(X_1t_1, X_2t_2)dX_1 \qquad (5.10)$$

Inserting (5.7)in (5.10) yields

$$P_1(X_2t_2) = \int_{-\infty}^{\infty} P_1(X_1t_1).P_{c2}(X_1/X_2,t_2-t_1)dX_1 \qquad (5.11)$$

By process of induction, equation(5.11) yields and integral equation which governs the transitional probability of a Markoff process as

$$P_{c2}(X_1/X_2,t)=\int_{-\infty}^{\infty} P_{c2}(X_1/X,t_o)P_{c2}\ (X/X_2,t-t_o)dX \quad (5.12)$$

Equation (5.12) is known as Smoluchowski or Chapman - Kolmogorov equation and it is basic equation of the theory of Markoff process.

5.4 Fokker-Planck Equation

Solutions of the Smoluchowski integral equation (5.12) are frequently obtained by solving an equivalent differential equation referred to as the Fokker-Planck equation. The solution of this equation yields the transitional probability density function of the Markoff random process. Method of Wang and Uhienbeck (Ref.(59) is used here to derive the Fokker-Planck equation.

From the elementary theory of probability in random process it is well known that the nth order moment of a process is given by

$$E[X^n] = \int_{-\infty}^{\infty} X^nP(X)dX \qquad (5.13)$$

where $E[\ ]$ denotes the ensemble average. Thus for example, when $n = 2$, equation (5.13) yields the mean square valve of the process. In the case of Markoff processes we are concerned with the transitional behaviour of a random process and in particular with the change of various moments of the process with time. Figure (10) shows a random process which has a given displacement X at time t and which changes by a small amount to a valve Z at time t+dt

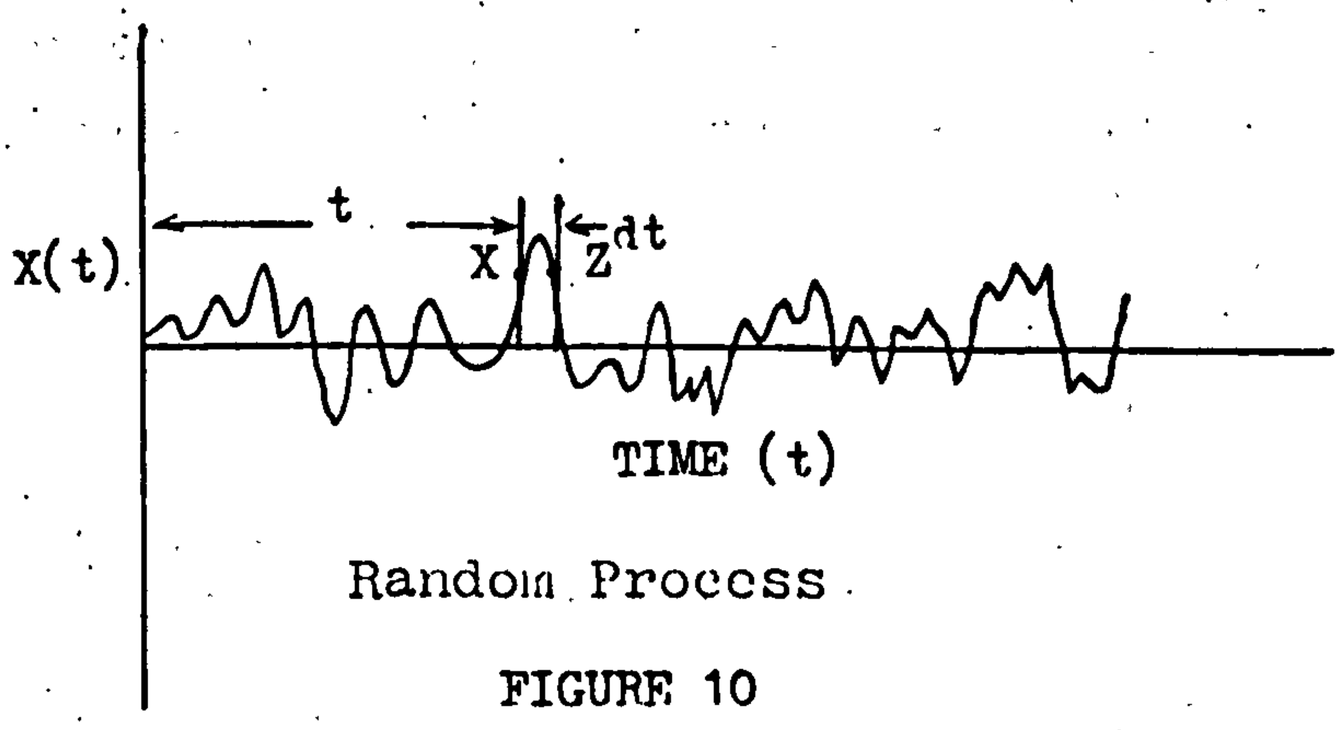

Random Process

FIGURE 10

The moments of change in the process in time dt, by analogy with equation (5.13) are defined for one-dimensional phase space by

$$a_n(Z,dt) = \int_{-\infty}^{\infty} (X-z)^n \, P(Z/X,dt) \, dX \qquad (5.14)$$

where n = 1,2,3 ....

As a result of Central Limit theorem (Ref.31), only the first and second order moments are assumed to exist in the limit as $dt \to 0$. This assumption implies that in a small time interval dt, the space co-ordinates of a random process only change by a small amount, hence the higher order moment, for $n > 2$, can be ignored. Thus the rates of change of the first two moments of increments in X(t) are

$$A(z) = \lim_{dt \to o} \frac{d}{dt} \left[a_1(z,t)\right] \text{ for } n=1 \qquad (5.15)$$

$$B(z) = \lim_{dt \to o} \frac{d}{dt} \left[a_2(z,t)\right] \text{ for } n=2 \qquad (5.16)$$

where $a_1(z,t)$ and $a_2(z,t)$ are given by equation (5.14).

Next consider the Smoluchowski integral equation (5.12) in the one-dimensional form

$$P_c(Y/X, t+dt) = \int_{-\infty}^{\infty} P_c(Y/Z, t) P_c(Z/X, dt) \, dZ \qquad (5.17)$$

Let R(X) be an arbitrary scalar function of variables $X_1, X_2, \ldots X_n$, which approaches zero sufficiently fast as X approaches $+\infty$ or $-\infty$. For example, R(X) could be a decaying exponential function. Multiplying equation (5.17) by R(X) and dropping the suffix C, integration over all the phase space yields

$$\int_{-\infty}^{\infty} R(X) P(Y/X,t) dX = \int_{-\infty}^{\infty} R(X) dX \int_{-\infty}^{\infty} P(Y/Z, t) \, P \, (Z/X, dt) dz \qquad (5.18)$$

Since the basic aim of the Fokker-Planck equation is to describe the variation of P(Y/X, t+dt) with time, we require to determine $\frac{\partial P}{dt}(Y/X,t)$. Thus from equation (5.18)

$$\int_{-\infty}^{\infty} R(X) \frac{\partial}{\partial t} P(Y/X, t) dX = \lim_{dt \to o} \frac{d}{dt} \left[\int_{-\infty}^{\infty} R(X) dX \int_{-\infty}^{\infty} P(Y/Z,t) P(Z/X, dt) dZ \right] \qquad (5.19)$$

Since Xand Z are close together, R(X) can be expanded in a Taylor series about the point X = Z i.e.

$$R(X) = R(Z) + (X-Z) \, R'(Z) + \frac{1}{2} (X-Z)^2 R''(Z) \; . \; . \qquad (5.20)$$

the higher order terms being ignord,

Substituting equation (5.20) in equation (5.19) and incorporating the limits of equation (5.15) and (5.16) yields

$$\int_{-\infty}^{\infty} R(X)\frac{\partial P}{\partial t}(Y/z,t)dX = \int_{-\infty}^{\infty} P(Y/z,t)\left[R'(z)A(z)+\frac{1}{2}R''(z)B(Z)\right] dZ \tag{5.21}$$

Integrating the right hand side of equation (5.21) by parts yields

$$\int_{-\infty}^{\infty} R(X)\frac{\partial P}{\partial t}\,dX = PA(X)R(X)\Big|_{-\infty}^{\infty} - \int_{-\infty}^{\infty} R(X)\frac{\partial}{\partial X}\left[A(X).P\right]dX+\frac{1}{2}R'(X).P.B(X)\Big|_{-\infty}^{\infty}$$

$$- R(X)\frac{\partial}{dX}\left[B(X).P\right]\Big|_{-\infty}^{\infty} + \int_{\infty}^{\infty} R(X)\frac{\partial^2}{\partial X}2\left[B(X).P\right]dX \tag{5.22}$$

Recalling that R(X) vanishes at the limits of integration, then by rearranging the terms in the equation (5.22) yields

$$\int_{-\infty}^{\infty} R(X)\left\{\frac{\partial P}{\partial t} + \frac{\partial}{\partial X}\left[A(X).P\right]-\frac{1}{2}\frac{\partial^2}{\partial X^2}\left[B(X).P\right]\right\}dX = 0 \tag{5.23}$$

Since R(X) is arbitrary, equation (5.23) must hold for any R(X). Thus the expression in bracket must be zero. From this condition, the Fokker-Planck equation is obtained, for the one-dimensional case as

$$\frac{\partial P}{\partial t} = -\frac{\partial}{\partial X}\left[A(X).P\right]+\frac{1}{2}\frac{\partial^2}{\partial x}\left[B(X).P\right] \tag{5.24}$$

Where A(X) and B(X) are the limits of the first and second order moments defined by equations (5.15) and (5.16). In the case of N dimension phase space, the equation (5.24)has been generalised to

$$\frac{\partial P}{\partial t} = -\sum_{i=1}^{N}\frac{\partial}{\partial X_i}(A_i(X)P) + \frac{1}{2}\sum_{i}^{N}\sum_{j}^{N}\frac{\partial^2}{\partial X_i \partial X_j}\left[B_{ij}(X).P\right] \tag{5.25}$$

Where A_i and B_{ij} are defined in a manner analogues to equations (5.15) and (5.16). Equation (5.25) is called Fokker-Planck equation and this will be used to determine the variance response of the dynamical system representing the structure.

5.5 Stationary Form of Fokker-Planck Equation

In certain situations it may happen that with the passage of time, the probability distribution $P_c(Y/X,t)$ tends to a limiting stationary distribution, independent of time and the initial conditions. Such a distribution represents the equilibrium state of the system after the initial transient motion has disappeared and may be obtained by letting $t \to \infty$ and writing $\frac{\partial P}{\partial t} = 0$ in equation (5.25), so that equation for $P(Y/X\ t)$ is

$$\frac{1}{2}\sum_{i=1}^{N}\sum_{j=1}^{N}\frac{\partial^2}{\partial X_i \partial X_j}\left[Bij(X)\ P(X)\right] - \sum_{i=1}^{N}\frac{\partial}{\partial X_i}\left[A_i(X)P(X)\right] = 0 \qquad (5.26)$$

where

$$P(X) = P_c(Y/X,t) \qquad (5.27)$$

5.6 Conditions Imposed on Random Input Function

To apply the random Markoff process technique to a dynamical system, some conditions must be imposed on the random force input. They are

1) $E[F(t)] = 0$
2) $E[F(t)F(t+\tau)] = 2\pi S.\delta(t)$ (i.e white noise auto correlation).
3) $F(t)$ to be a Gaussian distributed random function.

Condition (2) implies that the input function $F(t)$ has a white spectrum. Inspection of figure (11) reveals that the power spectrum of the effective random input $F(t)$ is almost flat over the frequency range $1 < f < 15$ Hz. If the frequency range is much larger than the system bandwidth and valve of α_1 (fig.11) is very small, the power spectrum of the effective random input can be considered as a white spectrum. In an actual case, if the power spectrum is uniform over a frequency range which is greater than the frequency range

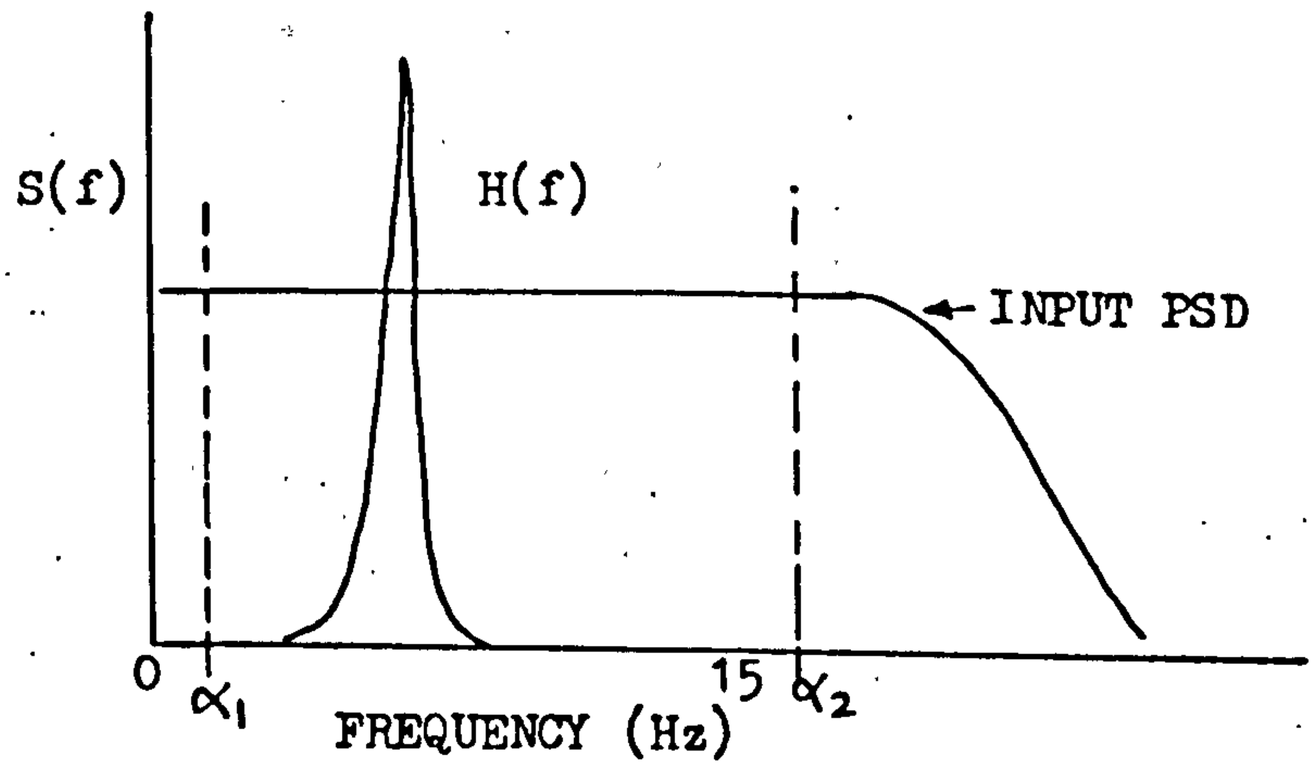

Input Spectrum

FIGURE 11

of the system, the power spectrum can be considered as white and band limited.

5.7 Application of Fokker-Planck Equation

Exact solutions of the Fokker-Planck equations have been found (Ref.58) for two types of stochastic differential equations:-

1) Systems of linear equations
2) Certain first order non-linear equations

Exact solutions for non-linear equations of second order excited by white noise have been found for the steady state probability density function for equation of the form (Ref.29)

$$\ddot{X} + \gamma f(H)\dot{X} + \omega_o^2 X = N(t) \qquad (5.28)$$

f(H) is a non-linear damping coefficient which is function of X and $\dot{X}$, and N(t) is a white noise stationary gaussian exciting force per unit mass. Equation (5.28) can be replaced by two first order equations by writing

$$\begin{aligned} X &= Y_1 \\ \dot{X} &= Y_2 \end{aligned} \qquad (5.29)$$

substituting these in equation (5.28) yields

$$\dot{Y}_1 = Y_2 \qquad (5.30a)$$

$$\dot{Y}_2 = -\gamma f(H)Y_2 - \omega_o^2 Y_1 + N(t) \qquad (5.30b)$$

This replacement of (5.28) by two first order equations is convenient for establishing conditions appropriate for relations like (5.32). The next procedure is to integrate equations (5.30) over at time dt which will latter be assumed short compared with the shortest characteristic time in X(t) and Y(t), yet very long compared with longest characteristic time is N(t).

In this case of single degree of freedom system, the phase space is two dimensional corresponding to the dimensions of Y_1 and Y_2. Thus in deriving the Fokker-Planck equation (5.26), $N = 2$ and $i, j = 1,2$. The average values of the first and second order moments for N = 2, corresponding to equation (5.14) which relates to the N = 1 are

$$a_i(Z,t) = \underset{N\ \text{fold}}{\int\int} (X_i - Z_i) P_c(Z/X, dt)\, dX_i \qquad (5.31)$$

$$b_{ij}(Z,t)=\int\int (X_i-Z_i)\ (X_j-Z_j)\ P_c(z/x,dt)\,dx_1$$

N fold

$$i,j = 1,2 \ldots N$$

In the limit A_i and B_{ij} are derived as follows

$$A_i = \lim_{dt\to 0}\left[\frac{da_i}{dt}\right] \tag{5.32}$$

$$B_{ij}= \lim_{dt\to 0}\left[\frac{db_{ij}}{dt}\right]$$

Furthermore, in the limit as $dt\to 0$, then $X_i\to Z_i$ and $P_c\to 1$. Noting also that $X_i-Z_i=dX_i$, it can be seen that

$$a_1 = E\left[dY_1\right]$$

$$a_2 = E\left[dY_2\right] \tag{5.33}$$

$$b_{11}= E\left[(dY_1)^2\right]$$

$$b_{12}= b_{21}=E\ \left[dY_1.dY_2\right]$$

$$b_{22}= E\ \left[(dY_2)^2\right]$$

Thus

$$A_1 = \lim_{dt\to 0}\ \frac{E\ [dY_1]}{dt} = E\left[Y_2\right]= E\left[\dot{X}\right]$$

$$A_2 = \lim_{dt\to 0}\ \frac{E\left[dY_2\right]}{dt}\ ,$$ which can be evaluated

from equation (5.30)

$$B_{11} = \lim_{dt\to 0}\ \frac{E\left[(dY_1)^2\right]}{dt} = \frac{E\left[(dX)^2\right]}{dt} \tag{5.34}$$

This is neglected since it is of second order of smallness.

$$B_{12} = B_{21} = \lim_{dt\to 0}\ E\left[\frac{(dY_1 dY_2)}{dt}\right] = E\left[\frac{d\dot{X}d\dot{X}}{dt}\right]= 0$$

Since for a stationary random process X and $\dot{X}$ are uncorrelated.

$$B_{22} = \lim_{dt \to 0} \frac{E\left[(dY_2)^2\right]}{dt}$$ which can be evaluated from (5.30).

To determine A_2 and B_{22}, equation (30b) is integrated over a short time dt to give

$$E\left[dY_2\right] = -E\left[\gamma f(H) Y_2\right] dt - E\left[\omega_o^2 X\right] dt + \int_t^{t+dt} E\left[N(\mathcal{J})\right] d\mathcal{J} \qquad (5.35)$$

Since $E\left[N(t)\right] = 0$, equation (5.35) becomes

$$E\left[dY_2\right] = - E\left[\gamma f(H) Y_2\right] dt - E\left[\omega_o^2 Y_1\right] dt$$

$$\therefore \quad A_2 = - E\left[\gamma f(H) Y_2\right] - E\left[\omega_o^2 Y_1\right] \qquad (5.36)$$

To determine B_{22}, equation (5.30b) is squared and averaged.

$$E\left[(dY_2)^2\right] = E\left[(-\gamma f(H) Y_2 dt - \omega_o^2 Y_1 + \int_t^{t+dt} N(\mathcal{J}) d\mathcal{J})^2\right] \qquad (5.37)$$

For stationary white noise excitation the autocorrelation function is given by

$$R(\tau) = 2\pi S_o \delta(\tau)$$

where $\delta(\tau)$ is the delta function and S_o denotes the constant power spectral density of white noise. Since $R(\tau) = 0$ when $\tau \neq 0$

$$R(0) = E\left[N^2(t)\right] = 2\pi S_o$$

Substituting these in for the expression for B_{22} yields

$$B_{22} = \lim_{dt \to 0} \frac{E\left[(dY_2)^2\right]}{dt} = 2\pi S_o \qquad (5.38)$$

Insertion of these values of A_1, A_2 and B_{22} in equation (5.25) yields

$$\frac{\partial P}{\partial t} = - \frac{\partial}{dY_1} (P Y_2) + \frac{\partial}{\partial Y_2}\left[(\gamma f(H) Y_2 + \omega_o^2 Y_1) P\right] + \pi S_o \frac{\partial^2 P}{\partial Y_2^2} \qquad (5.39)$$

This represents the associated Fokker-Planck equation to equation (5.28)

A random variable can be classified into two major classes, stationary and non-stationary process . The non-stationary process include data whose statistical properties vary with time. Thus the joint statistical properties at two time are functions of these particular times instead of their time difference. If it is assumed that after a long time, the process becomes stationary, (i.e. $\frac{\partial P}{\partial t} = 0$) and independent of initial conditions, the joint probability density function $P(Y_1 Y_2)$ then depends only on Y_1 and Y_2 and satisfies the following linear partial differential equation

$$- Y_2 \frac{dP}{dY_1} + \frac{\partial}{\partial Y_2}\left[(\gamma f(H) Y_2 + \omega_o^2 Y_1) P\right] + \pi S_o \frac{\partial^2 P}{\partial Y_2^2} = 0$$

or in the original variables

$$- \dot{X} \frac{\partial P}{\partial X} + \frac{\partial}{\partial \dot{X}}\left[(\gamma f(H)\dot{X} + \omega_o^2 X)\ P\right] + \pi S_o \frac{\partial^2 P}{\partial \dot{X}^2} = 0 \qquad (5.40)$$

Caughey (Ref.56) observed that this equation can be solved readily if the following separation is used

$$\left[\omega_o^2 X \frac{\partial P}{\partial \dot{X}} - \dot{X} \frac{\partial P}{\partial X}\right] + \frac{\partial}{\partial \dot{X}}\left[\gamma f(H)\dot{X} P + \pi S_o \frac{\partial P}{\partial \dot{X}}\right] = 0 \qquad (5.41)$$

i.e.
$$\omega_o^2 X \frac{dP}{d\dot{X}} - \dot{X} \frac{\partial P}{\partial X} = 0 \qquad (5.42)$$

and
$$\frac{\partial}{\partial \dot{X}}\left[\gamma f(H)\dot{X} P + \pi S_o \frac{\partial P}{\partial \dot{X}}\right] = 0$$

Equation (5.42), when integrated yields the J.P.D.F of displacement and velocity as

$$P(X\dot{X}) = C\ EXP\left[- \frac{\gamma}{\pi S_o} \int_o^H f(\eta)\, d\eta\right] \qquad (5.43)$$

For a linear system $P(X,\dot{X}) = P(X)P(\dot{X})$ but for a non-linear system in general this is no longer valid.

5.8 Equivalent Non-linear Differential Equation Method

The equation of motion of a single degree of freedom system with linear and non-linear damping is of the form

$$\ddot{X} + \gamma\ (1 + \epsilon |\dot{X}|^n)\dot{X} + \omega_o^2 X = N(t) \qquad (5.44)$$

Where n is an integer and ϵ is the non-linearity parameter. There is no analytical Fokker-Planck solution for equation (5.44). It can however be solved by a method of 'Equivalent non-linear differential equation' which yields an approximate joint probability density function from which the system variance can be calculated. This method combines an exact solution of the Fokker-Planck equation for a particular form of non-linear differential equation with equivalent linearisation technique. First suggested by Caughey this approach has been used in Ref.(60) for the case of quadratic damping.

The technique is to write the original non-linear differential equation in the form

$$\ddot{X} + \gamma\left(1+\epsilon_o\left(\frac{\dot{X}^2+\omega_o^2X^2}{2}\right)^{\frac{n}{2}}\right)\dot{X}+\omega_o^2X+\left\{\gamma\epsilon|\dot{X}|^n\dot{X} - \gamma\epsilon_o\dot{X}\left(\frac{\dot{X}^2+\omega_o^2X^2}{2}\right)^{\frac{n}{2}}\right\}$$

$$= N(t) \qquad (5.45)$$

Where the term in curly brackets constitutes the equation deficiency or error term.

$$e(X\dot{X}) = \gamma\epsilon\,\dot{X}^n\dot{X} - \gamma\epsilon_o\dot{X}\left(\frac{\dot{X}^2+\omega_o^2X^2}{2}\right)^{\frac{n}{2}} \qquad (5.46)$$

Since the aim is to obtain a good approximation to the solution of the original non-linear differential equation, we select ϵ_o, such that the error $e(X\dot{X})$ would be a minimum. Since $X\&\dot{X}$ are random, $e(X\dot{X})$ will be also random and hence its smallness might be subject to different interpretations. The method used here is to minimise the mean square value of $e(X\dot{X})$, i.e.

$$E\left[e^2(X\dot{X})\right]_{min}$$

For this to be true

$$\frac{d}{d\epsilon_o}\,E\left[(e(\dot{X}X)^2\right] = 0 \qquad (5.47)$$

Substituting (5.46) in (5.47) and interchanging the order of differentation and expectation yields

$$E\left[\frac{d}{d\epsilon_o}\left(\dot{X}\gamma\epsilon|\dot{X}|^n - \gamma\epsilon_o\left(\frac{\dot{X}^2+\omega_o^2X^2}{2}\right)^{\frac{n}{2}}\dot{X}\right)^2\right] = 0$$

$$E\left[-2\gamma^2\epsilon\left(\frac{\dot{X}^2+\omega_o^2X^2}{2}\right)^{\frac{n}{2}}\dot{X}^{n+2}+2\gamma^2\epsilon_o\left(\frac{\dot{X}^2+\omega_o^2X^2}{2}\right)^n\dot{X}^2\right] = 0$$

Solving for ϵ_o yields

$$\epsilon_o = \epsilon\frac{E\left[\left(\frac{\dot{X}^2+\omega_o^2X^2}{2}\right)^{\frac{n}{2}}\dot{X}^{n+2}\right]}{E\left[\left(\frac{\dot{X}^2+\omega_o^2X^2}{2}\right)^n\dot{X}^2\right]} \qquad (5.48)$$

From equation (5.48) it is seen that it is not an explicit expression for ϵ_o, since the expectation appearing on the right hand side depends on ϵ_o. To see whether it really leads to minimisation of the mean square error, differentiate equation (5.47) with respect to ϵ_o.

$$\frac{d^2}{d\epsilon_o^2} E\left[(e^2(X\dot{X})\right] = 2\chi^2 \left(\frac{\dot{X}^2+\omega_c^2X^2}{2}\right)^n \dot{X}^2 \quad \text{i.e.} \quad (+ve)$$

Equation (5.45) is solved using the Fokker-Planck method without the error term, i.e.

$$\ddot{X} + \gamma\left(1+\epsilon_o\left(\frac{\dot{X}^2+\omega_o^2X^2}{2}\right)^{\frac{n}{2}}\right)\dot{X} + \omega_o^2X = N(t) \qquad (5.49)$$

and hence the name, 'equivalent non-linear differential equation' method. This is a particular case of equation (5.28) where

$$f(H) = (1 + \epsilon_o(H)) \qquad (5.50)$$

$$H = \frac{1}{2}(\dot{X}^2+\omega_o^2X^2) \qquad (5.51)$$

This is the most general non-linear differential equation which can be solved by the Fokker-Planck method. Using equation (5.43), the unique steady state joint probability density becomes

$$P(X\dot{X}) = C\,EXP\left[-\frac{\gamma}{\pi S_o}\int_o^H (1 + \epsilon_o\eta)\,d\eta\right]$$

$$= C\ EXP\left[-\frac{\gamma}{\pi S_o}\left(\left(\frac{\dot{X}^2+\omega_o^2X^2}{2}\right)+\left(\frac{2\epsilon_o}{(n+2)}\right)\left(\frac{\dot{X}^2+\omega_o^2X^2}{2}\right)^{\frac{n+2}{2}}\right)\right] \qquad (5.52)$$

Where C is a normalising constant, given by

$$C = \left\{\int_{-\infty}^{\infty}\int_{-\infty}^{\infty} EXP\left[\frac{-\gamma}{\pi S_o}\left(\left(\frac{\dot{X}^2+\omega_o^2X^2}{2}\right)+\left(\frac{2\epsilon_o}{(n+2)}\right)\left(\frac{\dot{X}^2+\omega_o^2X^2}{2}\right)^{\frac{n+2}{2}}\right)\right]dX\,d\dot{X}\right\}^{-1} \qquad (5.53)$$

e.g equation (5.52) shows that $P(X\dot{X}) \neq P(X)P(\dot{X})$, i.e. displacement and velocity are not statistically independent. Since $P(X\dot{X})$ is not integrable in closed form it is not possible to write an explicit expression for C. Transforming to polar coordinates (see Appendix H) yields

$$C = \frac{\omega_o}{2\pi}\left[\int_o^\infty Exp\left(\frac{-\gamma}{\pi S_o}\left(\frac{r^2}{2}+\left(\frac{2\epsilon_o}{(n+1)}\right)\left(\frac{r^2}{2}\right)^{\frac{n+2}{2}}\right)\right)dr\right]^{-1} \qquad (5.54)$$

For non-linear damping, it is seen that the probability density function is non-Gaussain. Using this joint probability density function, in equation (5.48) yields

$$\epsilon_o = \frac{\epsilon\, 2^{\frac{n+2}{2}} \Gamma\left(\frac{n+3}{2}\right)}{\sqrt{\pi}\quad\quad \Gamma\left(\frac{n+4}{2}\right)} \qquad (5.55)$$

where Γ denotes the Gamma function.

5.9 Statistical Analysis

The statistical moments of X(t) can now be calculated using equation (5.52)

$$E\left[(X(t)^m\right] = \int_{-\infty}^{\infty}\int_{-\infty}^{\infty} x^m P(x\dot{x})\,dx\,d\dot{x}$$

$$= \frac{4\ I_m \int_o^{\infty} r^{m+1}\ EXP\left[-\left(a\left(r^2/2\right)+b\left(\frac{r^2}{2}\right)^{\frac{n+2}{2}}\right)\right] dr}{\omega_o{}^2 \int_o^{\infty} r\ EXP\left[-\left(a\left(\dot{r}^2/2\right)+b\left(r^2/2\right)^{\frac{n+2}{2}}\right)\right] dr} \qquad (5.56)$$

where $a = \frac{\gamma}{\pi S_o}$

$$b = \frac{2\epsilon_o \gamma}{\pi S_o (n+2)} \qquad \Big\} \quad (5.57)$$

$$I_m = \int_o^{\frac{\pi}{2}} \mathrm{Cos}^m\theta\ d\theta$$

for all even values of m. The moments of odd values of m are all zero.

5.10 Non-dimensional JPDF and Moments

For $\epsilon = 0$, the jpdf (equation (5.52) and the moments (equation 5.56) reduce to pdf and moments of linear system. In order to be able to observe what effect the non-linearity parameter has on the various statistical properties of X, they are calculated in nondimensional form

Let $$Y = \left(\frac{X}{\sigma_o}\right) \qquad (5.58)$$

$$Z = \left(\frac{\dot{X}}{\sigma_o}\right)$$

Where $\sigma_o = \sqrt{\frac{\pi S_o}{2\beta\omega}}\,3$, is the standard deviation of the response when $\epsilon = 0$.

The jpdf is the non-dimensional variables becomes

$$P(Y,Z) = C\ EXP\left[-\left(\left(\frac{Y^2+Z^2}{2}\right) + \alpha_n \epsilon_n^* \left(\frac{Y^2+Z^2}{2}\right)^{\left(\frac{n+2}{2}\right)}\right)\right] \tag{5.59}$$

where $C = \left[\int_{-\infty}^{\infty}\int_{-\infty}^{\infty} EXP\left[-\left(\left(\frac{Y^2+Z^2}{2}\right)+\alpha_n\ \epsilon_n^*\ \left(\frac{Y^2+Z^2}{2}\right)^{\frac{n+2}{2}}\right)\right] dYdZ\right]^{-1}$

$\epsilon_n^* = \epsilon_o \omega_o{}^n \sigma_o{}^n$ - non-dimensional non-linearity parameter

$$\alpha_n = \frac{2^{\frac{n+6}{2}}\ In+2}{\pi(n+2)}$$

$$I_n = \int_o^{\frac{\pi}{2}} Cos^n\ \theta d\theta \tag{5.60}$$

The moment in the non-dimesional variables are

$$E\left[Y^m\right] = \frac{2I_m}{\pi} \quad \frac{\int_o^{\infty} r^{m+1}\ EXP\left[-\left(\left(r^2/_2\right) + \alpha_n \epsilon_n^* \left(r^2/_2\right)^{\frac{n+2}{2}}\right)\right] dr}{\int_o^{\infty} r\ EXP\left[-\left(\left(r^2/_2\right) + \alpha_n \epsilon_n^* \left(r^2/_2\right)^{\frac{n+2}{2}}\right)\right] dr} \tag{5.61}$$

5.11 First Order Normalised Probability Density Function

Because it was the first order probability density that was measured from the analogue and experimental model, it can be readily found from the joint probability density function using the relation

$$P(Y) = \int_{-\infty}^{\infty} P(Y,Z)dZ \tag{5.62}$$

Where P(Y,Z) is given by equation (5.59)

In order to calculate the degree of peakedness of the distribution, usually, taken relative to normal distribution, the fourth moment about the mean was calculated. The dimensionless form of the fourth moment is called 'Kurtosis' (also called flatness factor)

$$a_4 = \frac{E(Y^4)}{\left[E(Y^2)\right]^2} = \frac{\left[\int_0^\infty r^5 \text{ EXP } \left[-((r^2/2)+\alpha_n \epsilon_n^*(r^2/2)^{\frac{n+2}{2}})\right]dr\right.}{\left[\int_0^\infty r^3 \text{ EXP } \left[-((r^2/2)+\alpha_n \epsilon_n^*(r^2/2)^{\frac{n+2}{2}})\right]dr\right]^2} \quad (5.63)$$

For the normal distribution, $a_4 = 3$. For a distribution which has a relatively high peak, $a_4 > 3$ and for a distribution which is less peaky, $a_4 < 3$. Theoretical and measured values of a_4 are as shown in Figure (71).

5.12 Average Level Crossing Rate

The basic parameters (i.e. rms) describing structural response under random excitation do not directly provide the specific information needed to predict a potential failure of the structure. The parameter of interest in failure prediction are, of course dependent upon the anticipated failure mechanism and for the complex structures the definition and modelling of possible failure mechanisms can be a difficult task (Ref.61). However, if attention is restricted to structures which serve only as load carrying function, then it is commonly assumed that failure will occur due to

a) the exceedance of a critical stress on displacement level.

or b) fatigue damage.

Level crossing statistics are of concern to the first type of failure modal while peak value statistics are of principal interest in the second case.

Average level crossing rates are also important in assessing wear rates in bolted joints. If the rate of level crossing is known then the time spent by a joint during slippage between different levels of displacement can be found. It would however, be necessary to assume

that the joint slip is a function of stress in adjacent members which in turn can be related to deflection of the tower.

It is seen from equation (5.61) that non-linear damping decreases the mean square level of response. From the view point of fatigue damage, this reduction in response level, hence stress level, is beneficial. The average number of crossing of some fixed level 'a' with positive slope is given by Rice's formula (Ref.62)

$$\gamma_{NL}^{+} = \int_{o}^{\infty} \dot{X}\, P(a,\dot{X})\, d\dot{X} \qquad (5.64)$$

where $P(a,\dot{X})$ is the joint probability density function of displacement and velocity given by equation (5.59). Substituting equation (5.59) in equation (5.64) yields

$$\nu_{NL}^{+} = \frac{\int_{o}^{\infty} Z\ \mathrm{EXP}\left[-\left(\left(\frac{Z^2+\lambda^2}{2}\right) + \alpha_n \epsilon_n^{*}\left(\frac{z^2+\lambda^2}{2}\right)^{\frac{n+2}{2}}\right]\right] dz}{2\pi \int_{o}^{\infty} r\ \mathrm{EXP}\left[-\left((r^2/2)+\alpha_n \epsilon_n^{*}\,(r^2/2)^{\frac{n+2}{2}}\right)\right] dr} \qquad (5.65)$$

where $\lambda = \left(\frac{a}{\sigma_o}\right)$

For linear system ($\epsilon^{*} = 0$), this reduce to

$$\nu_{L}^{+} = \frac{\omega_o}{2\pi}\ e^{\frac{-\lambda^2}{2}} \qquad (5.66)$$

Therefore

$$\frac{\nu_{NL}^{+}}{\nu_{L}^{+}} = \frac{e^{\lambda^2/2} \int_{o}^{\infty} Z\ \mathrm{EXP}\left[-\left(\left(\frac{z^2+\lambda^2}{2}\right)+\alpha_n \epsilon_n^{*}\left(\frac{z^2+\lambda^2}{2}\right)^{\frac{n+2}{2}}\right)\right] dz}{\int_{o}^{\infty} r\ \mathrm{EXP}\left[-\left(r^2/2 + \alpha_n \epsilon_n^{*}\,(r^2/2)^{\frac{n+2}{2}}\right)\right] dr} \qquad (5.67)$$

For n = 2 this reduces to

$$\frac{\nu_{NL}^{+}}{\nu_{L}^{+}} = e^{\frac{\lambda^2}{2}}\ \frac{(1-\mathrm{erf}\,(\wedge + \frac{1}{4\wedge}\lambda^2))}{(1-\mathrm{erf}\,(\wedge))} \qquad (5.68)$$

where

$$\wedge = \sqrt{\frac{1}{3\epsilon_2^{*}}}$$

When $\lambda = 0$ for any value of ϵ^* equation (5.68) reduces to

$$\nu_{NL}^{+} = \frac{\omega_o}{2\pi} = \nu_o^{+} \qquad (5.69)$$

This shows that ν_{NL}^{+} (zero level crossing) is independent of ϵ^* (non-linearity parameter). Similarly it can be shown that ν_{NL}^{+} (zero level crossing) is independent of ϵ^* for all values of n.

The computed variation of $\frac{\nu_{NL}^{+}}{\nu_o^{+}}$ with λ for n = 1 and n = 6 for various values of ϵ^* are shown in figure (72). The variations of the normalised level crossing with linear damping is also shown in the same figure . Since failure probabilities are often related to this statistic, (Ref.63), it can be seen that non-linear damping reduces the probability of first passage failure considerably.

5.13 Modified Equivalent Non-linear Differential Equation Method (MENL)

The mean square response of a non-linear system given by equation (5.61) is

$$E(Y^2) = \frac{2I_2}{\pi} \frac{\int_o^\infty r^3 \, EXP\left[-\left((r^2/2)+\alpha_n \epsilon_n^* (r^2/2)^{\frac{n+2}{2}}\right)\right]dr}{\int_o^\infty r \, EXP\left[-\left((r^2/2)+\alpha_n \epsilon_n^* (r^2/2)^{\frac{n+2}{2}}\right)\right]dr} \qquad (5.70)$$

It is found that apart from the case when n = 2, there is no closed form expression for $E(Y^2)$. It has to be solved numerically. For n = 2 it reduces to

$$E(Y^2) = \frac{\left[\sqrt{\frac{1}{\pi\alpha_2\epsilon_2^*}} \, EXP\left(-\frac{1}{\alpha_2\epsilon_2^*}\right) - \frac{1}{2\alpha_2\epsilon_2^*} \, erfc\left(\sqrt{\frac{1}{4\alpha_2\epsilon_2^*}}\right)\right]}{erfc\left(\sqrt{\frac{1}{4\alpha_2\epsilon_2^*}}\right)} \qquad (5.71)$$

Even in this case it is difficult to evaluate the non-linearity coefficient ϵ from the measured response and input power spectral density, S_o. Various other approximate

non-linear differential equations were studies and it was found that if the original equation was written in the form

$$\ddot{X} + \mu \left(\frac{\dot{X}^2+\omega_o^2X^2}{2}\right)^{\frac{n}{2}} \dot{X} + \omega_o^2X + \left\{\gamma(1+\epsilon|\dot{X}|^n)\dot{X} - \mu \left(\frac{\dot{X}^2+\omega_o^2X^2}{2}\right)^{\frac{n}{2}}\dot{X}\right\} = N(t) \tag{5.72}$$

where the error term is

$$e(X\dot{X}) = \left\{ \gamma(1+\epsilon|\dot{X}|^n)\dot{X} - \mu \left(\frac{\dot{X}^2+\omega_o^2X^2}{2}\right)^{\frac{n}{2}} \dot{X} \right\} \tag{5.73}$$

The Fokker-Planck solution to equation (5.72) without the error terms

$$P(X\dot{X}) = C\, e^{-\frac{2\mu\left(\frac{\dot{X}^2+\omega_o^2X^2}{2}\right)^{\frac{n+2}{2}}}{(n+2)\ \pi S_o}} \tag{5.74}$$

where the normalising constant C is

$$C = \frac{(n+2)\omega_o}{2\pi\Gamma\left(\frac{2}{n+2}\right)} \left[\frac{2\mu}{(n+2)\pi S_o 2^{\left(\frac{n+2}{2}\right)}}\right]^{\frac{2}{n+2}} \tag{5.75}$$

Using equation (5.74) in minimising the mean square error with respect to μ yields

$$\mu = \left\{A \left(\frac{\dot{\mu}}{S_o}\right)^{\frac{n}{n+2}} + B\,\epsilon\right\} \tag{5.76}$$

where

$$A = \gamma\,\Gamma\left(\frac{n+4}{n+2}\right) \left(\frac{2}{(n+2)\pi}\right)^{\frac{n}{n+2}}$$

$$B = \frac{2^{\frac{n+4}{2}}\, I_{n+2}{}^{\gamma}}{\pi}$$

The closed form expression for mean square response becomes

$$E(X^2) = \frac{1}{\omega_o^2} \frac{\Gamma\left(\frac{4}{n+2}\right)}{\Gamma\left(\frac{2}{n+2}\right)} \left[\left[\left(\frac{n+2}{2}\right)\right]\pi\right]^{\frac{2}{n+2}} \left(\frac{S_o}{\mu}\right)^{\frac{2}{n+2}} \tag{5.77}$$

From equation (5.76) it is seen that the first term in the bracket corresponds to linear damping and the second term corresponds to non-linear damping of the original equation.

For n = 0, the jpdf of the response is Gaussian. Since in this approximate solution to equation (5.44), the jpdf becomes non-Gaussian for $n > 0$, this requires that the linear damping term in equation (5.76) to be modified such that equation (5.77) reduces to a linear case for $\epsilon = 0$ and any value of $n > 0$. This modifying factor is obtained by substituting equation (5.76) into (5.77) and setting $\epsilon = 0$. The modified equation (5.76) becomes

$$\mu = \left\{ A \left(\mu/S_o\right)^{\frac{n}{n+2}} F(n) + B \epsilon \right\} \qquad (5.78)$$

where

$$F(n) = \frac{\Gamma\left(\frac{4}{n+2}\right)}{\Gamma\left(\frac{2}{n+2}\right)} \quad \frac{\left(\frac{n+2}{2}\right)}{\Gamma\left(\frac{n+4}{n+2}\right)}$$

is the modifying factor .

Using this approximation, the response of the system was calculated for various values of ϵ and n and compared with ENL, EL and analogue computer results. It was found that this modified solution yields a better approximate solution than EL for all values of n.

The agreement between MENL and ENL solutions is quite good. From equation (5.78) the expression for ϵ becomes

$$\epsilon = \frac{\mu}{B} - \frac{A}{B} \left(\frac{\mu}{S_o}\right)^{\frac{n}{n+2}} F(n) \qquad (5.79)$$

Knowing the mean square response, for a given input power spectral density, S_o, μ can be calculated from equation (5.77) and then substituted in equation (5.79) to yield ϵ, the non-linearity parameter as shown in section 7.

5.14 Equivalent Linearisation Method

An approximate solution to equation (5.44) can be obtained using Caughey's equivalent linearisation technique. In this method the non-linear equation of motion is replaced by a linear equation of motion

$$\ddot{X} + 2\beta_e \omega_o \dot{X} + \omega_o^2 X = N(t) \qquad (5.80)$$

The error introduced due to this linearisation is

$$e(X\dot{X}) = \gamma(1+\epsilon|\dot{X}|^n)\dot{X} - 2\beta_e \omega_o \dot{X} \qquad (5.81)$$

Minimising the mean square error yields

$$\beta_e = \frac{\gamma\, E\left[\dot{X}^2(1+\epsilon|\dot{X}|^n\right]}{2\omega_o\ E\left[\dot{X}^2\right]} \qquad (5.82)$$

Since N(t) is Gaussian white noise, the approximate displacement and velocity computed from (5.80) are also Gaussian. Calculating the expectations in (5.82) yields

$$\beta_e = \beta_o \left[1+\epsilon\sqrt{\frac{2}{\pi}}^{n+2} \omega_o{}^n \sigma^n \left[\left(\frac{n+3}{2}\right)\right]\right] \quad (5.83)$$

Since $\gamma = 2\beta\omega_o$

From linear theory, the mean square response is found to be

$$E[X^2] = \sigma_o^2 = \frac{\pi S_o}{2\beta_o\omega_o 3} \quad (5.84)$$

$$\therefore \quad \left(\frac{\sigma}{\sigma_o}\right)^2 = \frac{\beta_o}{\beta_e} \quad (5.85)$$

Substituting $\left(\frac{\beta_o}{\beta_e}\right)$ from equation (5.83) into (5.85) yields

$$\left(\frac{\sigma}{\sigma_o}\right)^2 = \frac{1}{\left[1 + \epsilon\sigma_o{}^n\omega_o{}^n\sqrt{\frac{2^{n+2}}{\pi}}\left(\frac{\sigma}{\sigma_o}\right)^n\left[\left(\frac{n+3}{2}\right)\right.\right.}$$

$$\therefore \quad C_1 \left(\frac{\sigma}{\sigma_o}\right)^{n+2} + \left(\frac{\sigma}{\sigma_o}\right)^2 - 1 = 0 \quad (5.86)$$

where

$$C_1 = \left[\left(\frac{n+3}{2}\right)\right. \quad \epsilon_n^* \quad \sqrt{\frac{2^{n+2}}{\pi}}$$

$$\epsilon_n^* = \epsilon\sigma_o{}^n\omega_o{}^n$$

Therefore the undimensional mean square response can be calculated from the algebric equation (5.86) for any value of n and ϵ.

6.0 Analogue and Digital Simulation of Non-Linear Dynamical System.

As there is no exact solution to equation (5.44), the purpose of the present study is to derive an approximate solution which can be used to measure the statistical properties of the response of the non-linear structure to random loading. The equivalent non-linear differential equation method was used and the relation between the mean square response and the power spectral density of the force is given by equation (5.70). Equation (5.44) was also

solved on an analogue computer to yield an exact solution and compared with the approximate solution.

The analysis is performed in the time domain by simulating generalised forces rather than in the frequency domain as usually done in the linear response analysis. The result of the analysis are shown in a diagram where the mean square response is plotted against the power spectral density of band limited white noise excitation. Since, however, the statistical fluctuation in the mean square of the simulated excitation process will undoubtedly reflect on the mean square of the simulated response process, both are measured by means of temporal average.

Theoretically, experiments involving random excitation should be carried out over an infinite time interval so that only the average characteristics of the excitation will affect the results. But every real measurement can only be made over a finite time. This means that, if random noise is used as a test signal, the result of an experiment will in general be different from its expected value, or if the experiment involving random input is repeated over and over, each repetition will yield a different result. The randomness of the noise introduces statistical variances into the results. Variance can be reduced by extending the measurement time, T, but it can never be made zero when random test signals are used.

What is needed, is a test signal which has the essential properties of random noise i.e. broad band, flat spectrum and resemblance to natural disturbances in waveform and probability density function.

This signal should be one that introduces no statistical variance into the results, even though the measurement is made over a finite time T. Pseudo Random Noise is one such signal which looks ans acts like random noise.

The circuit used for generating the pseudo random noise on the analogue computer is a shown in figure (G2) in appendix (G). Accuracy is a major concern when an analogue computer is used. Source of error are far more numerous than in digital computation. Possible sources of error can be the amplifiers, the non-linear elements and electrical noise. The main advantage is that the calculation time is almost independent of the complexity of the problem. Once a problem is patched, it can be solved continuously in a predetermined time scale (see appendix G). The response can be displaced on oscilloscope or plotted while the programme is running. Proper scaling is, however, important because the solution of the dynamical system is

represented by voltage outputs from the amplifiers, which have a range of +100V to -100V. If a mistake is made in scaling, it would lead to amplifier saturating, thus resulting in errors.

As the AD256 analogue computer, initially used in this study became obsolete, the analysis was carried out on the digital computer using SLAM - Simulation Language for Analogue Modeling. It is a high-level language based on Fortran and provides a frame work for simulation of a continuous system on digital computer. The flow chart and the listing, and results of typical run from the digital program are given in Appendix (G).

In the numerical integration of a differential equations error are directly related to some power of the length of the time step interval. Normally, the smaller the time interval, the smaller the error. Since the calculations are done at the terminal points of the time interval, the maximum response values may occur within the chosen interval and these values will not appear in the output. In order to find an optimum size of the time interval, Δt, a linear single degree of freedom system was subjected to random loading and integrated using fourth order Runge-Kutta integration method. It was found that time interval of $t=0.03/f_o$ seconds gives results which agree with theoretical results.

In digital simulation, two different schemes were used to represent the random force loading. Zero-order hold scheme is commonly used because it is easy to programme. In this case the force is held at a constant for one communication interval (CI) before changing to a new value at the next data point. First-order interpolation is also used in which the force is treated as a straight line between any two data points. The maximum frequency of the random loading is given by

$$f_{max} = \frac{1}{2\Delta t} \quad Hz$$

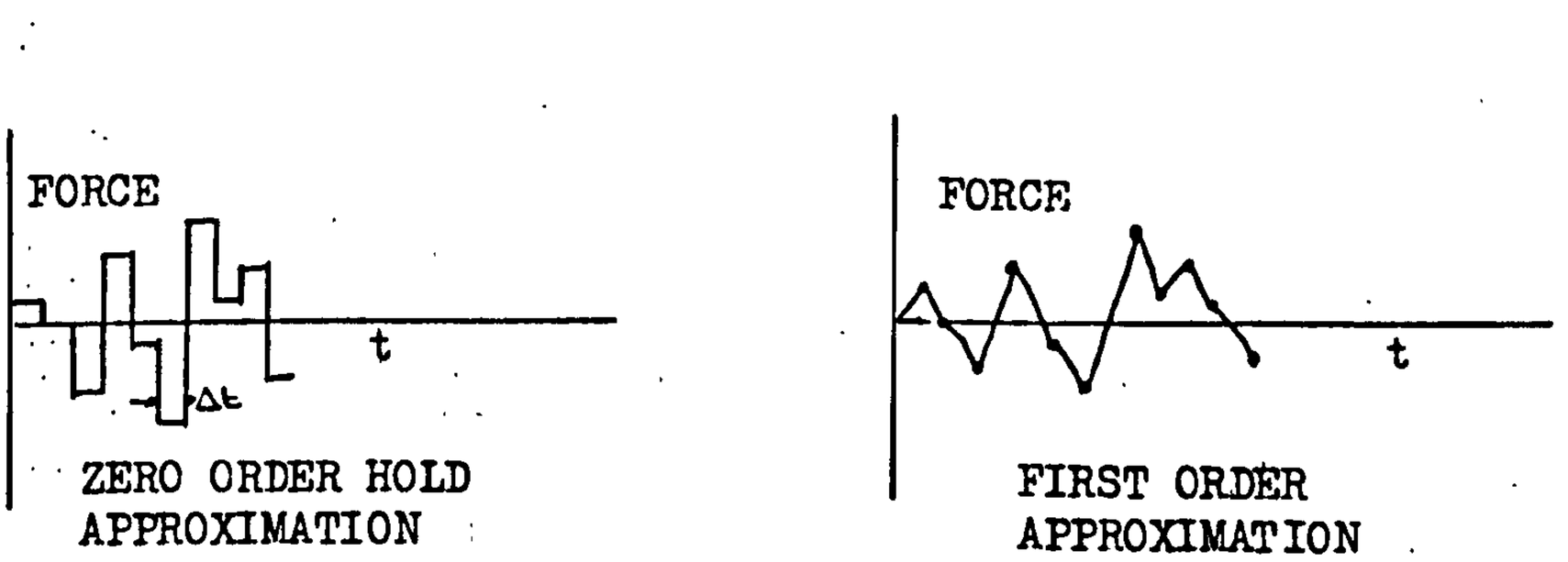

FORCING FUNCTIONS

FIGURE 12

The advantage of the digital computer is its high speed and its relatively simple programming. All the required results i.e. mean square value of response, power spectral density, probability density function and other theoretical calculation can be done in the same run. The typical time histories of force and response of the simulated system are shown in figures (73a and 73b) for n = 1 and n = 6 respectively.

The statistical properties of the non linear dynamical system were measured for various values of n and ϵ^4 and the results are discussed in section '8'

7.0. Determination of NON-Linear Parameter (ϵ) From Random Vibration Testing

A major objective of the present investigation is to provide a means of extracting non-linear damping coefficient from measured data for a fairly large value of n.

The equation of motion of a single degree of freedom system with linear and non-linear damping is of the form

$$\ddot{X} + \gamma\,(|+\epsilon|\dot{X}|^{n})\,\dot{X} + \omega_o^2 X = N(t) \qquad (7.1)$$

The solution of this equation by the method of MENL is given by equation (5.77) i.e. The mean square displacement response is

$$E(X^2) = \frac{1}{\omega_o}^2 \frac{\Gamma(\frac{4}{n+2})}{\Gamma(\frac{2}{n+2})} \left[(\frac{n+2}{2})\ \pi\right]^{\frac{2}{n+2}} (\frac{S_o}{\mu})^{\frac{2}{n+2}} \qquad (7.2)$$

where

$$\mu = \left[\ A(\frac{\mu}{S_o})^{\frac{n}{n+2}}\ F(n) + B\epsilon\right] \qquad (7.3)$$

$$A = \gamma\Gamma(\frac{n+4}{n+2})\ (\frac{2}{(n+2)\pi})^{\frac{n}{n+2}}$$

$$B = \frac{2^{\frac{n+4}{2}} I_{n+2}\,\gamma}{\pi},\quad F(n) = \frac{\Gamma(\frac{4}{n+2})}{\Gamma(\frac{2}{n+2})}\ \frac{(\frac{n+2}{2})}{\Gamma(\frac{n+4}{n+2})}$$

Solving equation (7.3) for ϵ yield

$$\epsilon = \frac{\mu}{B} - \frac{A}{B}(\frac{\mu}{S_o})^{\frac{n}{n+2}} F(n) \qquad (7.4)$$

$$\epsilon = \frac{S_o}{B} \left(\frac{C_1}{E(X^2)}\right)^{\frac{n+2}{2}} - F(n) \frac{A}{B} \left[\frac{C_1}{E(X^2)}\right]^{\frac{n}{2}} \qquad (7.5)$$

where $$C_1 = \frac{1}{\omega_o 2} \frac{\Gamma(\frac{4}{n+2})}{\Gamma(\frac{2}{n+2})} \left[(\frac{n+2}{2})\pi\right]^{\frac{2}{n+2}}$$

Equation (7.1) was simulated on a analogue computer for various values of ϵ and measured $E(X^2)$ for given S_o are as shown in table (6).

In order to measure the non-linear parameter, ϵ, consider the case when $\omega_o = 37.704$ Rad/S, $\beta = .0055$ ($\gamma = 2\beta\omega$), $n = 1$, $\epsilon = 0.1$ and $S_o = 4000$ lb^2/Rad/S.

Substituting these values in equation (7.5) yields

$$\epsilon = \frac{9.4594}{10^5} \frac{S_o}{\left[E(X^2)\right]^{3/2}} - \frac{0.017755}{\left[E(X^2)\right]^{1/2}} \qquad (7.6)$$

Substituting S_o and measured $E(X^2)$ in equation (7.6) yields

$$\epsilon = 0.0999$$

This was done for various values of S_o and the results are as shown in figure (74). Figures (40a and b show the measured mean square response of the tower for the various level of excitations. Using equation (7.5), the non-linear damping parameter, ϵ, was calculated and is tabulated in Table (7). This table also shows the non-linear damping parameter measured from free vibration tests.

7.1 Accuracy

The 'Equivalent Non-linear Differential Equation' method yields results which agree with the analogue computer results and as such can be considered to provide an exact solution of equation (7.1). The percentage error between Equivalent Non-linear Differential Equation' method and the other approximate methods can be defined as

$$\% \text{ error} = \left[\frac{E(X^2)_{approx} - E(X^2)_{ENL}}{E(X^2)_{ENL}}\right] \times 100$$

Since ENL method does not yield a closed form solution, except in case of n=2, the percentage error was calculated for the normalised response measurements for values of n=1 and n=6 only for various normalised non-linearity parameters, ϵ^*. The results are as tabulated in tables 8a and b.

8.0 Discussion

Comparison Between Approximate Solutions and Analogue Computer Results.

The results of the free vibration tests are as summerised in section (3). It is seen that joint damping is non-linear, i.e. it increases with amplitude of vibration. The analytical non-linear damping model which represents the results of the free vibration tests is given by equation (3.4). Since there is no analytical solution to the non-linear dynamical system represented by equation (3.11), the system was simulated on an analogue computer and the statistical properties measured and compared with those derived from approximate methods for various values of n and ϵ.

Mean Square Response.

The mean square value of the response of the non-linear dynamical system, to band limited white noise excitation was measured for n=1 and three values of ϵ, the non-linearity parameter. Figure (64) shows the comparison between approximate solutions and the simulation results. As there is no closed form solution to equation (5.61) it was solved numerically using the programmes given in appendix (L). It is seen that agreement between the ENL, MENL; EL and simulation results is very good. Figure (65) shows the corresponding mean square against the nondimensional non-linearity parameter ϵ^*.

In order to check the validity of the approximate solutions, the mean square response was calculated for higher values of n and the results are as summarised in figures (66) and (67). For n = 6, a non-linear damping model representing material non-linearity, the agreement between ENL, MENL and simulation results is fairly good but the EL gives a poor result. The reason for this is that for higher values of n, the response distribution is highly non-gaussian, whereas, EL assumes a gaussian response.

As the agreement between MENL and simulation results is fairly good for large values of n, it is possible to calculate the non-linearity parameter, ϵ, from the measured displacement response and power spectral density of the excitation, as shown in section 7. Figure 68 shows the comparison between the theoretical solutions for n=2. The effect of linear damping ratio (β) was also investigated and the results show that the agreement between simulation and ENL results is fairly good for small values of β (ie. 0.005) than for large values of β (ie. 0.05).

Stationarity of the Response

As there is no solution possible for the general Fokker-Planck equation given by (5.39), it was tactfully assumed that after long time the conditional probability $P_c(Y/X,t)$ will approach a limiting stationary probability density function, which is independent of subsequent time or the initial conditions, so that $\frac{\partial P}{\partial t} = 0$. To check this assumption, the stationary test (as described in section (3)) was applied to the simulated system and it was found that this assumption can be accepted at 5 per cent level of significance for all values of non-linearity parameter considered.

Probability Density Function

The solution of the Fokker-Planck method yields a joint probability density function of the response displacement and velocity and is given by equation (5.59). As this second order probability density function is time consumming to compute from experimental datathe first order probability density function of the displacement was calculated using equation (5.62). Figures (69 and 70) shows the measured variation of the nondimensioanl $P(X/_{\delta o})$ with (X/δ_o), for the ENL, MENL and that computed from simulation, for various value of ϵ^*. Also plotted are the corresponding gaussian probability density function for the same mean square valve as ENL. It is seen that there is very good agreement between ENL and simulated distributions, and that there is a pronounced deviation from the gaussian form in the tail of the distribution. Thus the effect of nonlinearity in damping is to reduce the probability of large excursions.

Flatness Factor (Kurtosis)

The flatness factor (a4) is a measure of deviation of the distribution from gaussian. For the normal distribution, a4 = 3. For a distribution which is peaky relative to gaussian distribution, a4 > 3 and for distribution which is less peaky a4 < 3. The measured and theoretical values of a4 are shown in figure (71).

Level Crossing Rate

As the first passage failure of lightly damped system can be related to the level crossing rate, the normalised level crossing rates were calculated and the results are as shown in figure (7 2). It is seen that there is good agreement between ENL method and simulation results.

Measurement of Non-linear Parameter

From the analogue simulation of the non-linear dynamical system it was found that when the mean square displacement response and input power spectral density were substituted in equation (7.5), ϵ, can be calculated with fair degree of accuracy as shown in figure (74). This analysis was repeated with measured displacement response and power spectral density of excitation on an actual tower structure and the results show that, ϵ, can be measured from random vibration tests with same degree of accuracy. The error in measuring W_o and $E(X^2)$ from random vibration tests introduces error in measurement of ϵ. In order to reduce the statistical error in measurement of W_o and $E(X^2)$, large number of ensemble averages are required. This leads to long testing time, especially for low frequency testing. However, the results of the present analysis (Figure 75) show that MENL method can be applied to engineering structures with reasonable degree of accuracy.

9.0 Conclusion

The main conclusion that can be derived from this study are:-

1) The non-linear damping arising in bolted civil engineering structure, is basically non-linear and can be modelled mathematically as

$$C\,(1+\epsilon|\dot{X}|^n)\dot{X} \quad \text{where } n = 1$$

2) The Fokker-Planck equation for the equivalent non-linear dynamical system excited by white noise yields a simple approximate expression for the stationary joint probability density function of response displacement and velocity. This expression yields an exact joint probability density function for the case when n = 2.

3) For n = 1, all approximate methods yield agreeable results.

4) For higher values of n and ϵ^*, the Equivalent Non-linear Differential' equation method yields an agreeable results with analogue computer results. The agreement between Equivalent Non-linear Differential equation method and Equivalent linearisation technique deterioates as n increases. This is due to the fact that Equivalent linearisation method assumes a gaussian response, instead of the true non-gaussian response.

5) It is possible to measure the non-linear parameter, ϵ, from the measured mean square response and excitation power spectral density using modified equivalent differential equation method.

REFERENCES

1 Anon. Wind Effects on Buildings and Structures
Proc. of Conf. at NPL Teddington June 16-28 1963

2 Anon. Wind Effects on Buildings and Structures
Proc. of Int. Res. Sem. at Ottawa Sept.11-15 1967

3 Anon. Wind Effects on Building and Structures
Proc. of Symp at LUT, Loughbourgh April 2-4 1968

4 Anon. Wind Effects on Buildings and Structures
Proc. of Third Int. Conf. at Tokyo 1971

5 Anon. Vibration Problems in Industry
Int. Symp. at Keswick, England April 10-12 1973

6 Sachs P. 'Wind forces in engineering'
Pergamon Press 1972

7 Basu I. R. 'Response of Suspension Bridge to Strong Motion Earthquake'
M.Sc. Thesis C.I.T. Cranfield 1973

8 Wiegel R.L. Earthquake Engineering

9 Lyon R.H. 'On the vibration statistics of Randomly excited Hard spring Oscill.'
J. of ASA. Vol.32 no.6 1960

10 Crandall S.H. 'Random Vibration of Systems with Non-linear Restoring Forces'
Proc. Intern. Symp. Non-linear Oscill. Kiev Sept.1961

11 Stephens D.G. 'Experimental investigation of the effect of model scale on structural-joint damping'
NASA TN D - 4192 1967

12 Kirk C.L. 'Random vibration with non-linear damping'
Journal of Royal Aeronautical Society Nov.1973

13	Davenport	A.G.	'The response of Slender Line-like Structure to Gusty-wind' American Soc. of Civil Engineering Structural Div. PP.no 6610
14	Bleich Teller	F. L.W.	'Structural damping in suspension bridges' American Soc.of Civil Eng. Structural Division Paper No 2486
15	Lazan	B.J.	'Damping of materials and members in structural mechanics' 1968
16	Kimbell Lovell	A.L. D.E	'Internal Friction in Solids' Phys. Rev. 30, Second Series, 1927
17	Goodman, Lazan	L.E. B.J.	Material and Interface damping Shock and Vib. Handbook Vol.2 1961
18	Crandall Khabbaz Manning	S.H. G.R. J.E.	'Random vib. of an oscillator with non-linear damping' Journal of Acoustic Soc. of America Vol.36 July 1961
19	Pian, Hallowell	T.H.H. F.C.	'Structural damping in a simple built-up beam' Proc. First U.S. Nat.Cong. of Appl. Mech. ASME, New York 1952
20	Pian	T.H.H.	'Structural damping of simple built-up beam with rivited joints in bending' J.Appl.Mech. 24 35-38 (1957)
21	Klumpp, Goodman	J.H. L.E.	'Slip damping of press fit joint under linearity varying pressure' WADC TR 56-291 1956
22	Lazan, Brown Gannett Kimser Klumpp	B.J. J. A. P. J.	'Dynamic testing of material and structures with a new resonance vibration excitation control' Proc. of ASTM Vol.52 1952
23	Heckl	M.A.	New approachs to structural vibration analysis and control. (april 1962)
24	Goodman	L.E.	A review of progress in analysis of interfacial slip damping. Structural Damping.Ed. by Ruzicka J.
25	Tschebotarloff	G.P.	'Soil mechanics, foundations and earth structures' McGraw-Hill New York 1951

26	Mead, Mallik		Material damping under random excitation.Journal of Sound and Vib. (1976)
27	Lenning Mathocsen	P.C. R.B.	'Forced vibration of tall steel frame building' EESD Vol. 107-132 1972
28	Simpson	A.	'An improved displaced frequency method for estimation of dynamical characteristics of mechanical systems' J. Royal Aero. Soc. 70(666) June 1966
29	Warburton	G.B.	'The dynamical behaviour of structure' Pengamon Press 1964
30	Brammeier	G.F.	'A study of amplitude freq. plots with non-linear damping' Shock and vibration bulletin
31	Bendot Piersol	J.S. A.G.	Random data analysis and measurement procedure 1971
32	Beaucham	K.G.	'Signal processing using analogue to digital techniques' 1973
33	Cherry Brady	S. A.G	'Determination of structural dynamic properties by statistical analysis of random vibration'
34	Enochson Otnes	L.D. R.K.	'Programming and analysis of digital time series data' The shock of vibration information centre 1968
35	Shannon		A mathematical theory of communication •Bell Syst. Tech.J. 27 1968
36	Gabri Wallace	B.S. R.	'Computer control random testing system'
37	Pickering Kline	R.C. D.	A load feedback controlled hydraulic loading system,RAE TR 68190 1968
38	Thayer	W.J.	'Transfer function for Moog Servovalves' Technical Bulletin No. 103

39	Tow	J.	'A step - by - step active filter design, IEEE Spectrum Dec.1969
40	Raven	F.H.	'Automatic control engineering' McGraw-Hill and Co.
41	Guillon	M.	'Hydraulic Servo Systems: Analysis and design' Butterworths London
42	James, Nichols Phillips	H.M. N.B. R.S.	'Theory of Servomechanisms'
43	Walters	R.	'Hydraulic and Electrohydraulic Servo systems ILIFFE Book Ltd.
44	Takahashi	T.	'Control and Dynamic Systems'
45	Crandall	S.H.	'Perturbation techniques for random vibration of non-linear systems' J.Acoust.Soc.Amer.35.1700-1705 1963
46	Crandall,	S.H.	'Random excitation of non-linear system'. Random vibration, Vol.2 MIT Press, Cambridge; Mass.1963
47	Crandall and Khabbaz Manning	S.H. G.R. J.E.	'Random vibration of an oscillator with non-linear damping' Jour. A.S.A., Vol.36 No.7 1965
48	Khabbaz	G.R.	'Power spectral density of the response of a non-linear system to random excitation' Jour. A.S.A., Vol.38 No.5 1965
49	Stoker	J.J.	'Non-linear vibration' Interscience New York 1950
50	Tung Penzien Horonjeff	C.C. J. R.	'The effect of runway unevenness on the dynamic response of supersonic transports' NASA Report CR-119 1964
51	Krylor Bogoliubov	N. N.	'Introduction to non-linear mechanics' 1943

52 Caughey T.K. 'Equivalent linearisation techniques' Jour.Acoust.Soc.Amer. 35.1706-1711 1903

53 Foster E.T. 'Semilinear Random Vibration in discrete systems' J.Applied Mech.5 560-564 1968

54 Iwan W.D. Yang I. 'Application of statistical linearisation techniques to non-linear multi-degree-of-freedom systems' J.Appl.Mech.39, 545-550 1972

55 Caughey T.K. 'Derivation and application of the Fokker-Planck equation to discrete non-linear dynamic systems subjected to white random excitation' Jour.A.S.A. Vol.35,No.11 1963

56 Caughey T.K. 'On the response of a class of non-linear oscillator to stochastic excitation' Proc.Colloq.Interm.du Centre.Nat.Rech Sci.No.148 1964

57 Marklinger U.J. 'Control system described by Gaussian processes' Ph.D. Thesis Cambridge 1963

58 Caughey T.K. 'Non-linear theory of random vibration'

59 Unlenbeck G.E. 'On the theory of Brownian Motion: Selected papers on noise and stochastic processes' Edited by Nelson Wax, Dover Pub.Inc. New York

60 Kirk C.L. 'Application of the Fokker-Planck equation to random vibration of non-linear systems' Cranfield Report Aero No.20 1974

61 Crede C.E. 'Failure resulting from vibration' Random Vibration II. pp 103-146 1963

62 Rice S.O. 'Mathematical analysis of random noise' Bell system Tech.Jour.24 1945

63 Robert J.B. 'Probability of first passage failure for lightly damped oscillator' Sounds ans Vibs.

64 Littlebury K.H. Non-linear stochastic system; the dynamic response of a stayed mast to wind turbulence

APPENDIX A

THEORETICAL FREQUENCY RESPONSE

SYSTEM DATA

Actuator stroke	= 10 in peak to peak
Actuator piston area (A)	= 1 in^2
Servovalve	Moog series 76
Hydraulic supply pressure	= 2000 psi
Hydraulic fluid	Shell Telex 33
Bulk modulus of the fluid	= 150 x 10^3 lb/in^2
Volume or the actuator (V_t)	= 9 in^3
Actuator attachment stiffness	= ∞
Generalised mass of the tower	= 1.2 lb in^{-1} s^2
Generalised stiffness	= 1555.2 lb/in
Fundamental frequency	= 36 rad/s
Spring stiffness	See figure A1
K_v	= 1.885 cis/mA
K_1	= 30 K_p mA/v
K_5	= 0.01 $^v/_{lb}$
β	= 0.005

The open loop transfer function (equation 4.15)

$$G(s) = \frac{G_{11}}{G_{22}}$$

and closed loop transfer function (equation 4.16)

$$G_c(s) = \frac{G_{11}}{G_{33}}$$

Maximum Force

The maximum force is determined by the maximum pressure difference P and the piston area A.

$Fm = A\ P = 1 \times 1000 = 1000$ lb

The compliance between the tower and the actuator does not have any effect on this.

Maximum Velocity

The maximum velocity is determined by the piston area and the maximum flow through the servovalve. The flow throught the servolvalve is proportional to the square root of the pressure drop across the valve. The characteristic equation of the actuator is

$$V = G_a \sqrt{\frac{1000 - F}{2}}$$

where V = velocity

G_a = actuator constant

F = force acting on the actuator

The variation of the velocity with the load is as shown in figure (A2).

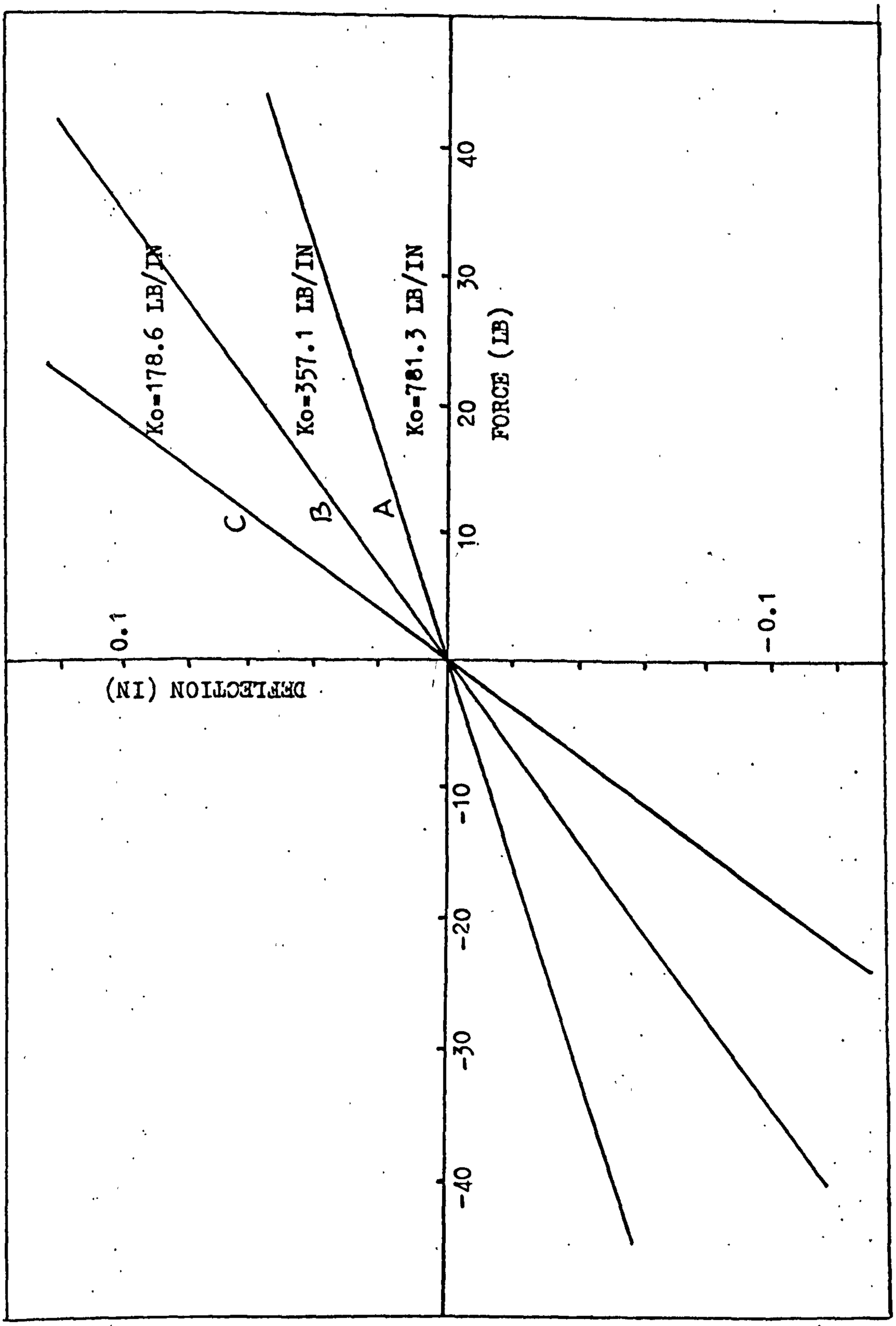

FIGURE A1 STIFFNESS OF VARIOUS SPRINGS

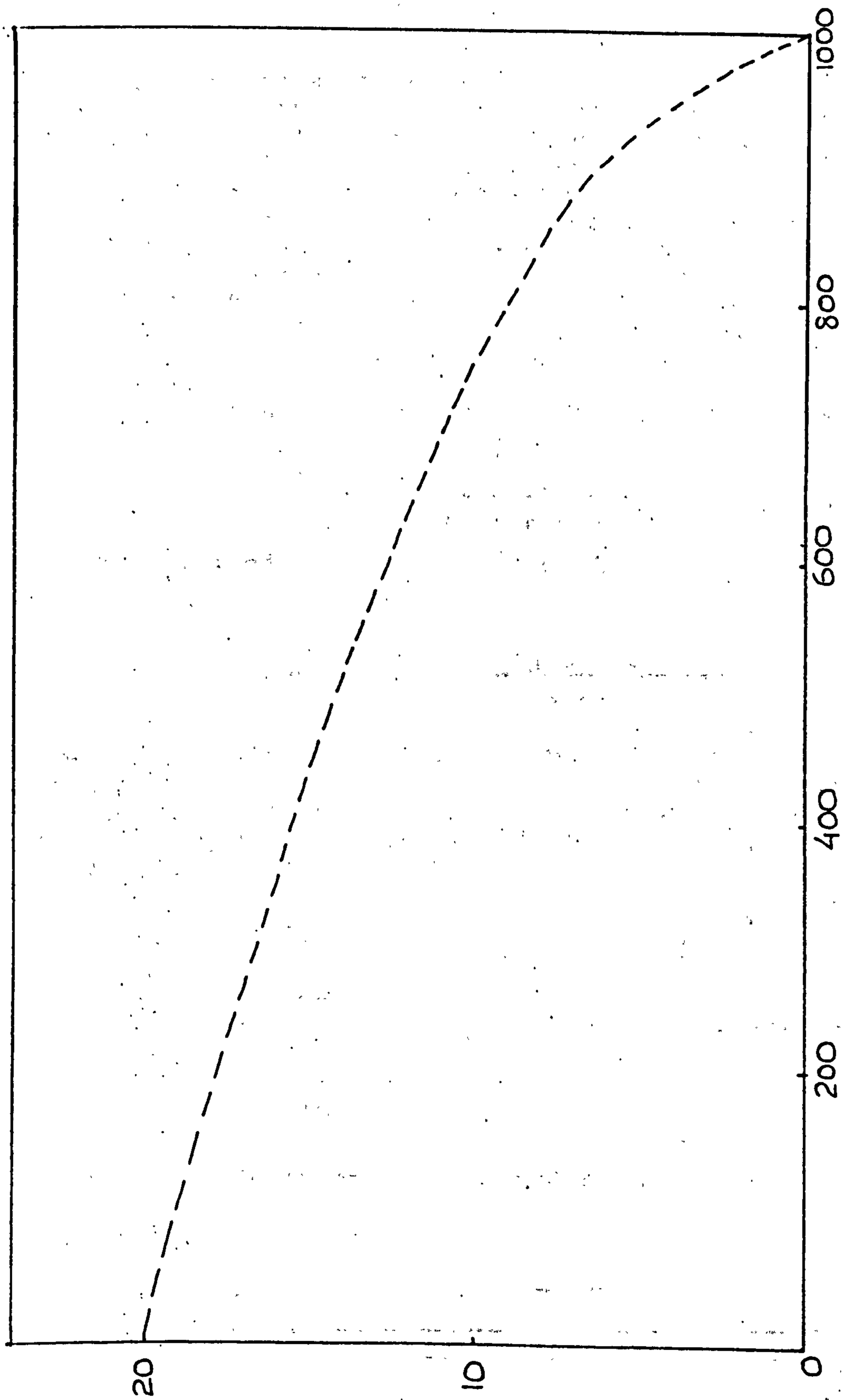

VARIATION OF VELOCITY WITH FORCE

FIGURE A2

APPENDIX B

FILTER

As seen in section (4), in order to maintain the force acting on the structure at constant level in the frequency range of interest a filter is required in the input section of the control system having a frequency response which is the reciprocal of that of the control system. Various commercially available notch filters were tried but they had too large a bandwidth compared with that required, and one could not alter one parameter of the filter without effecting the other. The filter used is the one shown in figure (B1). It is basically a bandpass filter and unity gain amplifier in parallel.

The transfer function of the bandpass filter is

$$\frac{V_2}{V_1} = \frac{c\ s}{\left[s^2 + a\ s + b\right]} \qquad \ldots(1)$$

and the combined transfer function is

$$\frac{V_3}{V_1} = \frac{\left[s^2 + (a + c)s + b\right]}{\left[s^2 + a\ s + b\right]} \qquad \ldots(2)$$

In ref.32 the elements values expressed in terms of the coefficients, a, b, c, are given for the realization of equation 1. This method - referred to as the operational amplifier biquard realization- uses resisters, capacitors and operational amplifiers.

$$R_1 = {}^1/a\ C_1 \qquad R_2 = {}^K/\sqrt{b\ C_2}$$

$$R_3 = {}^1/K\sqrt{b\ C_1} \qquad R_4 = {}^1/c\ \ C_1$$

$$R_5 = R_6 = 10\ K$$

$\therefore$ transfer function of the band pass filter

$$\frac{V_2}{V_1} = \frac{\frac{1}{R_4\ C_1}\ s}{\left[s^2 + \frac{1}{R_1\ C_1}\ s + \frac{R_6}{R_2\ R_3\ C_1\ C_2\ R_5}\right]}$$

$$= \frac{G(2\beta_f\omega_f)s}{[s^2 + (2\beta_f\omega_f)s + \omega_f^2]}$$

Therefore tuning can be achieved as follows:-

Resonant frequency ω_f by R_3

Bandwidth of the filter $(2\beta_f\omega_f)$ by R_1

and gain - G - by R_4

The values used in the circuit for f_f=5.75 Hz and gain of 3 are shown in table B1.

R_1	1.591 MΩ
R_2	27.6 KΩ
R_3	27.6 KΩ
R_4	0.796 MΩ
R_5	10 KΩ
R_6	10 KΩ
R_7	10 KΩ
R_8	10 KΩ
R_9	10 KΩ
R_{10}	10 KΩ
R_{11}	10 KΩ
C_1	1 μF
C_2	1 μF

TABLE B1. VALUES OF FILTER COMPONENTS FOR GAIN = 3 AND f_f = 5.75 Hz

For being able to tune to frequency between 5.6 and 5.9 Hz and change the gain, R_3 and R_4 are variable resistors. Table B2 gives the resistor values for various frequencies and gain. Figure B2 shows the frequency response of the filter.

FREQ(Hz)	R_1(MΩ)	R_2(KΩ)	R_3(MΩ)	R_4(MΩ)	GAIN(db)
5.6	1.591	27.6	29.26	0.796	3
5.75	1.591	27.6	27.60	0.796	3
5.90	1.591	27.6	26.36	0.796	3
5.75				1.59	2
5.75				3.18	1.5

TABLE B2. RESISTOR VALUES FOR VARIOUS FREQUENCIES AND GAIN

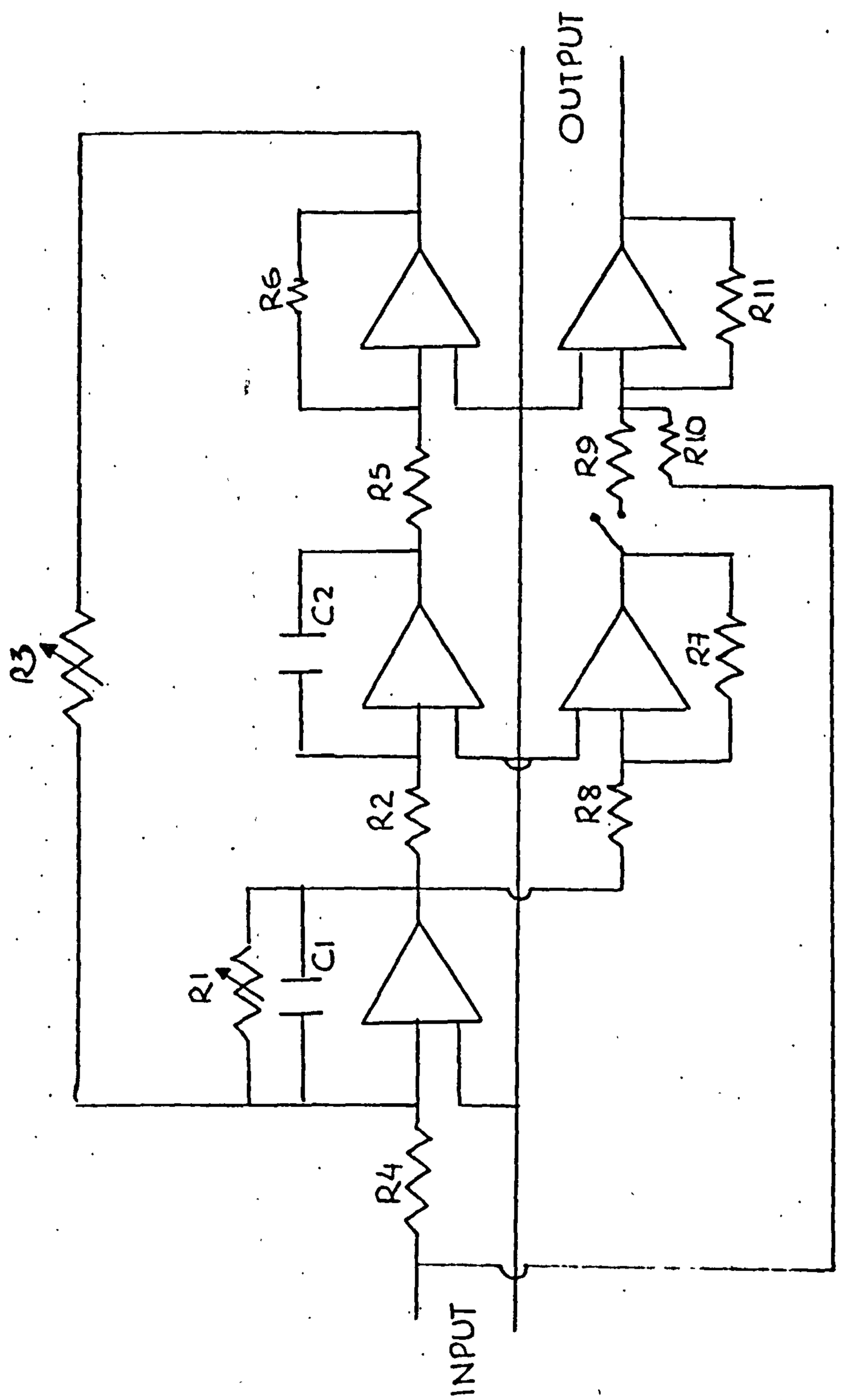

CIRCUIT DIAGRAM OF THE FILTER

FIGURE B1

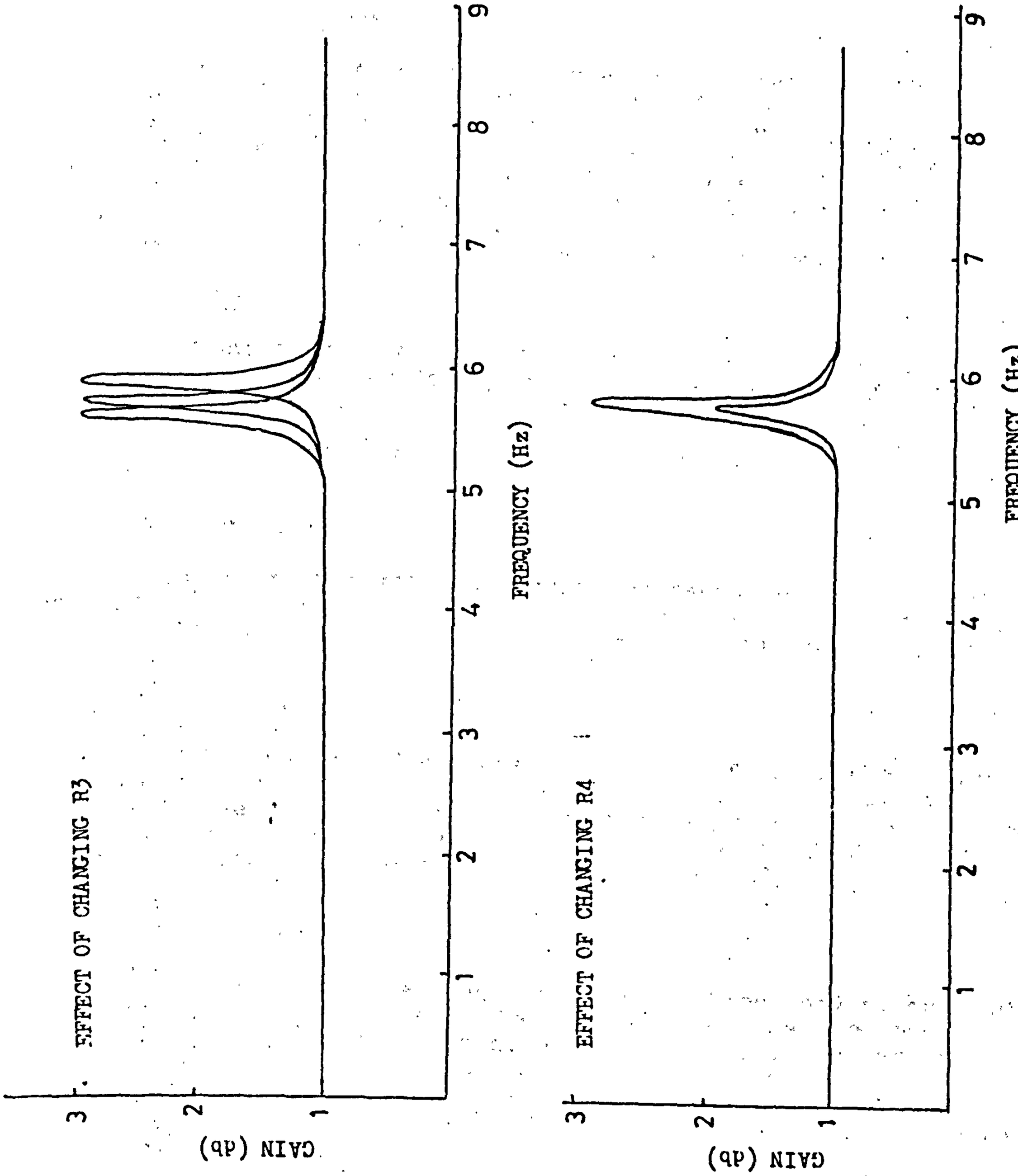
EFFECT OF CHANGING R3
GAIN (db)
FREQUENCY (Hz)
EFFECT OF CHANGING R4
GAIN (db)
FREQUENCY (Hz)

FIGURE B2

APPENDIX C

THE HYDRAULIC SYSTEM

The hydraulic system comprises of:-

1. Hydraulic Power Unit

The hydraulic power unit is a self contained free standing assembly having a tank capacity of 75 gallons. A fixed capacity internal gear pump with a continuous pressure rating of 2000 psi is motorised by a 25 hp T.E.F.C. Newman electric motor. All the equipment necessary for the control of pressure and temperature etc are included and assembled into the power unit. The oil is cooled with an air blast cooler which is motorised by a 0.5 hp motor.

2. Filters

A coarse strainer is fitted in the tank at the outlet to the pump. Higher grade filters of 150 microns capability at 98 % efficientcy are fitted immediately upstream of the servovalves. They have pressure switches to indicate when clogging has caused an appreciable drop of pressure across the filters.

3. Accumulators

The hydro-pneumatic accumulators used are of one quart capacity. They are fitted immediately upstream of the servovalves so as to smooth out line shocks and pressure surges caused by valve operation.

4. Servovalves

A moog series 27 servovalve having a flow rate of 5gpm at a pressure drop of 1000 psi was used in each loading channel. The servovalve has a nozzle-flapper pliot stage and a conventional four way second stage. The flow is proportional to the input signal whose polarity determine the direction of flow through the valve.

5. Actuators

The actuators are ones with low friction, having maximum pressure rating of 2000 psi. The annulus area has a permanent connection to the working pressure of the system. The areas of the actuator are such that the rod and annulus areas are equal and therefore the rod area is exactly half the full bore area. By this means a control of pressure in the full bore area

operating against the constant pressure in annulus area, an equal performance of force in both tension and compression can be provided. The stroke of the actuator is ± 5 inches.

6. Hydraulic Fluid

The fluid used is Shell-Telex 33.

APPENDIX D

ELECTRICAL SYSTEM

The electrical system comprises of:-

1. Electronic Control Unit

A complete set of electronic control equipment for the separate operation of three channels is mounted in a single free standing vertical cabinet. A start and safety panel provides a control of the power unit and indicates system failures. Push buttons are provided for starting and stopping the electric motor and loading and unloading the pump relief valve. Monitoring of the system static and dynamic performance is made using a double beam oscilliscope and digital voltmeter.

2. Three Team Controller (KSU 569)

This unit is an error amplifier, with separate proportional, integral and derivative gain controls. The proportional gain can be varied between 0 and 1.

3. DC Power Amplifier (KTU 5)

This is a current drive amplifier for the electro-hydraulic servovalve. The gain of the amplifier is 33 mA/v.

4. Load Cell (FL17)

This is a strain gauge load cell with a maximum rating of 1000 lb. The excitation is 12 volts d.c. and the load is measured with sensitivity of 1.694 mv/v.

5. Bridge Amplifier (KTU 10)

This amplifier is used to convert the low level signal derived from the strain gauge into 10 volts levels for use in system control and instrumentation. The load cell and amplifier gives an output of 0.01 volt/lb.

APPENDIX E

SETTING UP THE ELECTRO HYDRAULIC SYSTEM

Trim and maintenance procedures are usually provided by the manufacturers of the servo system. As this information was not available with this system, a brief description is given as how to trim the system.

The first step in trimming a system is to check for proper phasing. After the system is properly installed, apply partial hydraulic power. This is best done by lowering supply pressure to setting which will barely start the load moving. This will protect the system in case of phase reversal. As at one stage in this investigation, the system had to be converted to displacement control, the following description will refer to it. When a positive voltage is applied at the input of the operational amplifier, A (Figure E1), a negative voltage is supplied to the servovalve, B. The servovalve supplies fluid at lower pressure to the head end of the actuator, C. The actuator ram retracts, moving the feedback transducer inwards. If this produces a positive voltage at D, the amplifier output will increase. If the system is turned on in this condition, the actuator ram would go hard over as soon as the system is switched on. If a phase reversal is made at D, the system will become stable.

Gain

If gain is too high, the system will go unstable and oscillate at the system natural frequency. The best way to adjust it is to start with gain control at minimum. Increase hydraulic pressure to the rated value and then increase the amplifier gain slowly until the system starts to oscillate. Then lower the amplifier gain half way. This is the best gain setting for most systems.

Dither

The dither adjustment allows the system to be trimmed so that the valve spool moves at the dither frequency but at such lcw amplitude that the load does not respond to it. This reduces the valve deadband with no detrimental effects on the load.

Valve and Amplifier Null

Once the gain and dither has been set, valve and amplifier can be nulled. With the amplifier turned on, the hydraulic turned off and the command signal turned off, adjust the amplifier balance control until the output of the amplifier reads zero. Then with every thing turned on and system regulating a force, turn the servovalve null adjustment (mechanical) until the amplifier output again

reads zero. This means that with a single rod actuator the servovalve has been mechanically offset slightly, to produce more fluid pressure on the rod end of the actuator. The electrical system operates at zero null. The advantage of this arrangement is when one considers that electrical drift of amplifier and transducer generally is proportional to the current or voltage output of the device. If the output is zero, drift is zero.

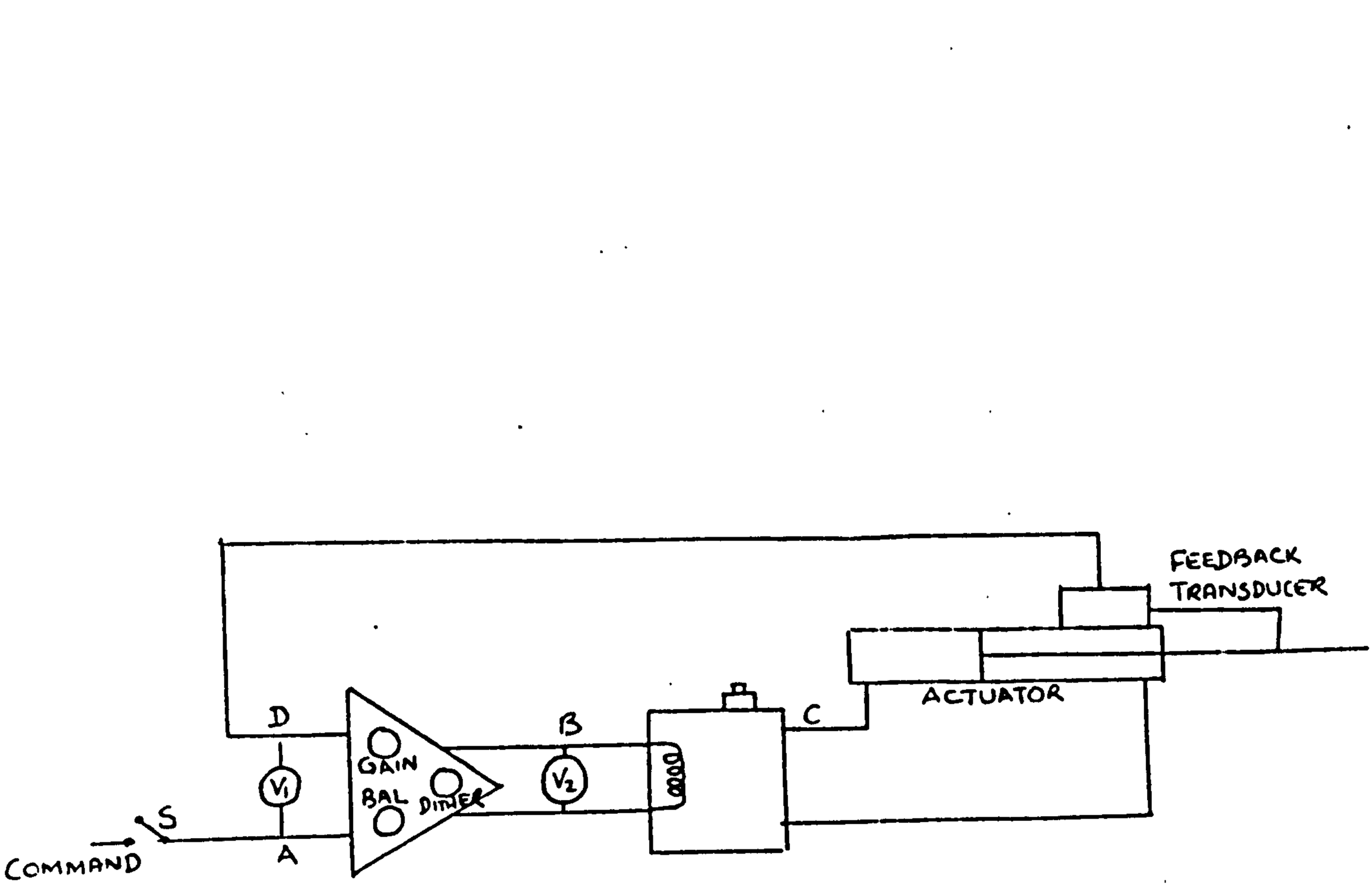

TRIMMING OF THE ELECTROHYRAULIC SYSTEM

FIGURE E1

APPENDIX F

SPACE FRAME PROGRAM

In order to calculate the stresses in the members of the tower, and hence the parameters C and ϵ, a finite element program was developed. In the finite element approach, the actual structure is represented by a system of idealised beam elements which are connected at the nodes. The tower was represented mathematically by 64 discrete nodes, placed at elements nodal points. The properties of each finite element such as the moment of inertia, length, area etc, were calculated from structural drawing and provided as input data.

The program generates the stiffness matrix for each structural element. Each matrix is first generated in its own local coordinates system. Transformation matrix is computed and applied to obtain the stiffness coefficient components of each element in a global coordinate system. The stiffness matrix is transformed from one coordinate system to another as follows

$$\left[K_{ij}\right] = \left[T_{pi}\right]^T \left[K_{pq}\right] \left[T_{qj}\right]$$

While T_{pi} is the transformation relating displacement in the original system to the displacements in the generalised coordinates in the new system and i,j,p, and q, are row and column indices.

Once the stiffness matrix for the element has been generated and transformed into global coordinates, it is merged into the stiffness matrix of the complete structure. The merging operation is basically a process of matrix addition in which corresponding stiffness coefficient from each structural element connecting at a given node are combined to obtain the stiffness properties of the structural model at that node. After merging, the boundary conditions for the node are imposed and matrix reduction performed. Fixed boundary conditions are imposed on complete stiffness matrix by deleting the rows and columns associated with the degrees of freedom at fixed points on the structure. A pin joint can be introduced by reducing the appropriate rotational freedom prior to merging.

Other ways of reducing the size of stiffness matrix is to eliminate those degrees of freedom which are subjected to zero inertia loading. These degrees of freedom can be eliminated from force deflection relation by process of matrix reduction. If the force deformation matrix equation can be partitioned as follows

$$\begin{bmatrix} K_{uu} & K_{ul} \\ K_{lu} & K_{ll} \end{bmatrix} \begin{Bmatrix} q_u \\ q_l \end{Bmatrix} = \begin{Bmatrix} 0 \\ F_l \end{Bmatrix}$$

where q_u are displacements of unloaded nodes, and q_l and F_l are displacement and forces at the loaded nodes. The reduced stiffness matrix becomes

$$[K]_R = [T]^T [K] [T] = [K_{ll} - K_{lu}K_{uu}^{-1}K_{ll}]$$

The dimensions of the reduced stiffness matrix are R rows and R columns smaller than the original matrix, where R is equal to the number of unloaded degree of freedom.

After assembling the stiffness matrix of the elements, the resulting system of equation relating forces and displacement at the nodes of the structure are solved for unknown displacements. Finally corresponding displacements are substituted back into the stiffness relation of each element and element stresses are computed. A general purpose computer program at Lloyds was used to compute the natural frequencies and mode shapes of the tower. For each normal mode $\phi_i(X)$, there corresponds and external load system which when applied to the tower will cause it to deform in its ith mode shape with the amplitude of unity. For the ith mode this loading is given by the following inertia forces

$$F_j = m_j \omega_i^2 \phi_i(Y_j)$$

or

$$\{F\} = [m] \omega_i^2 \{\phi\}$$

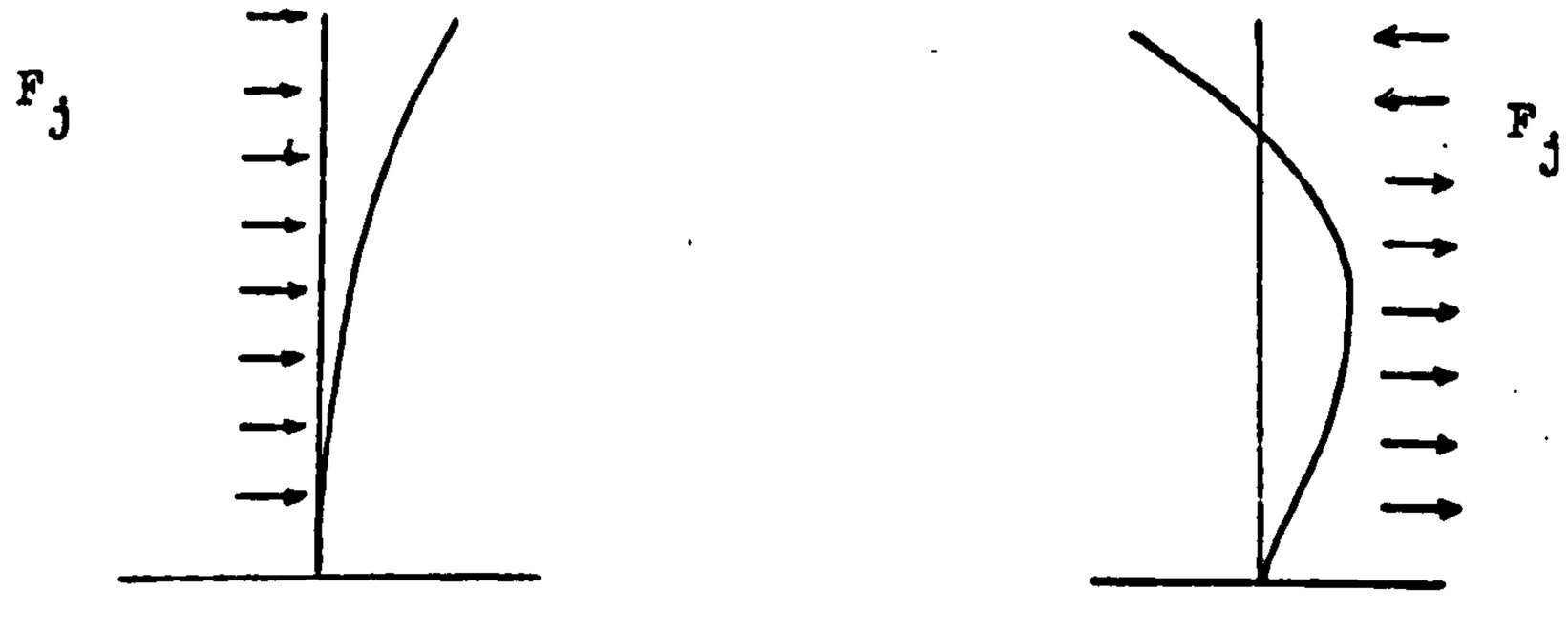

FIGURE 1

The application of these loading should deflect the structure in its corresponding mode shape. The deflected normalised mode shape of the two loading are shown in Fig.(2) and it is seen that they agree with the original mode shapes of the tower.

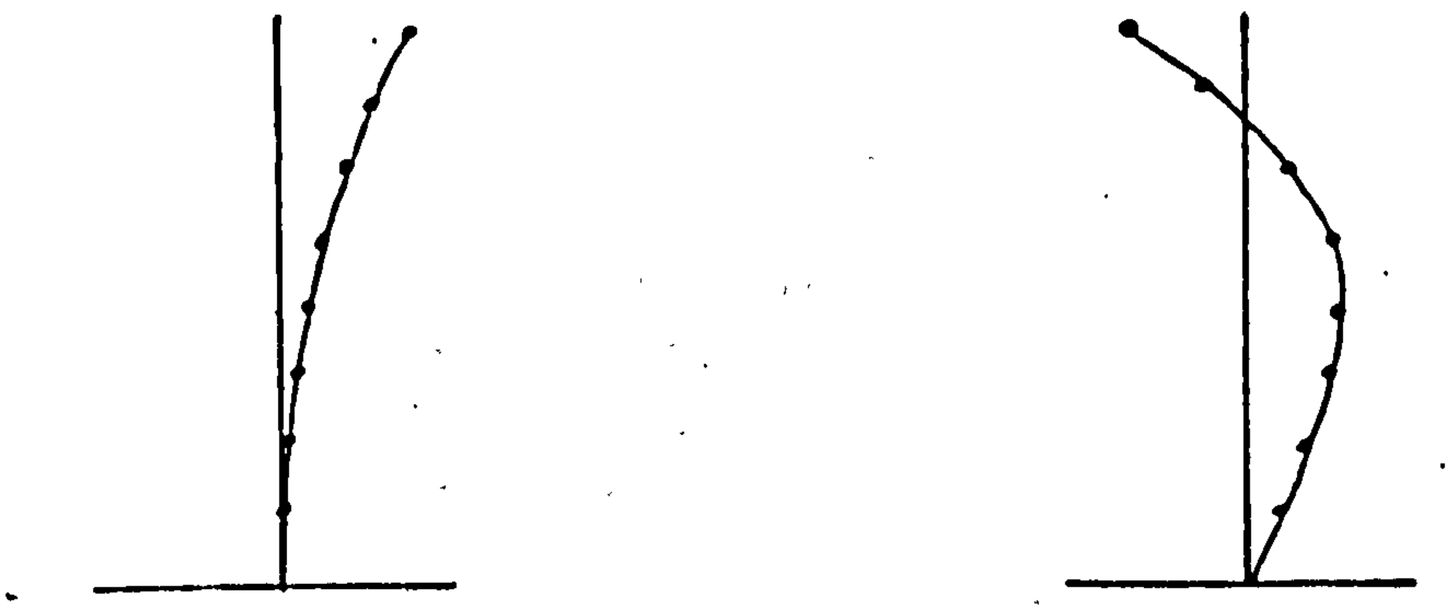

FIGURE 2

These inertia forces are function of modal displacements and not of spatial derivates. Using these inertia forces, the corresponding member stresses are computed and summed to yield C and ϵ for the ith mode.

Prior to calculating these constants, force - deflection characteristics of finite element model were compared with those of the actual tower and a good agreement was obtained between the two as shown in Fig(3).

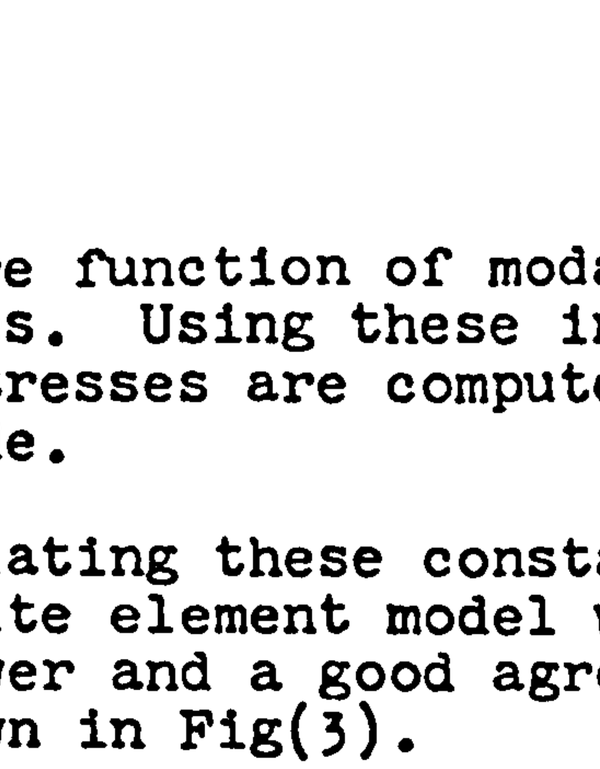

FIGURE 3

FLOW DIAGRAM OF FINITE ELEMENT PROGRAM

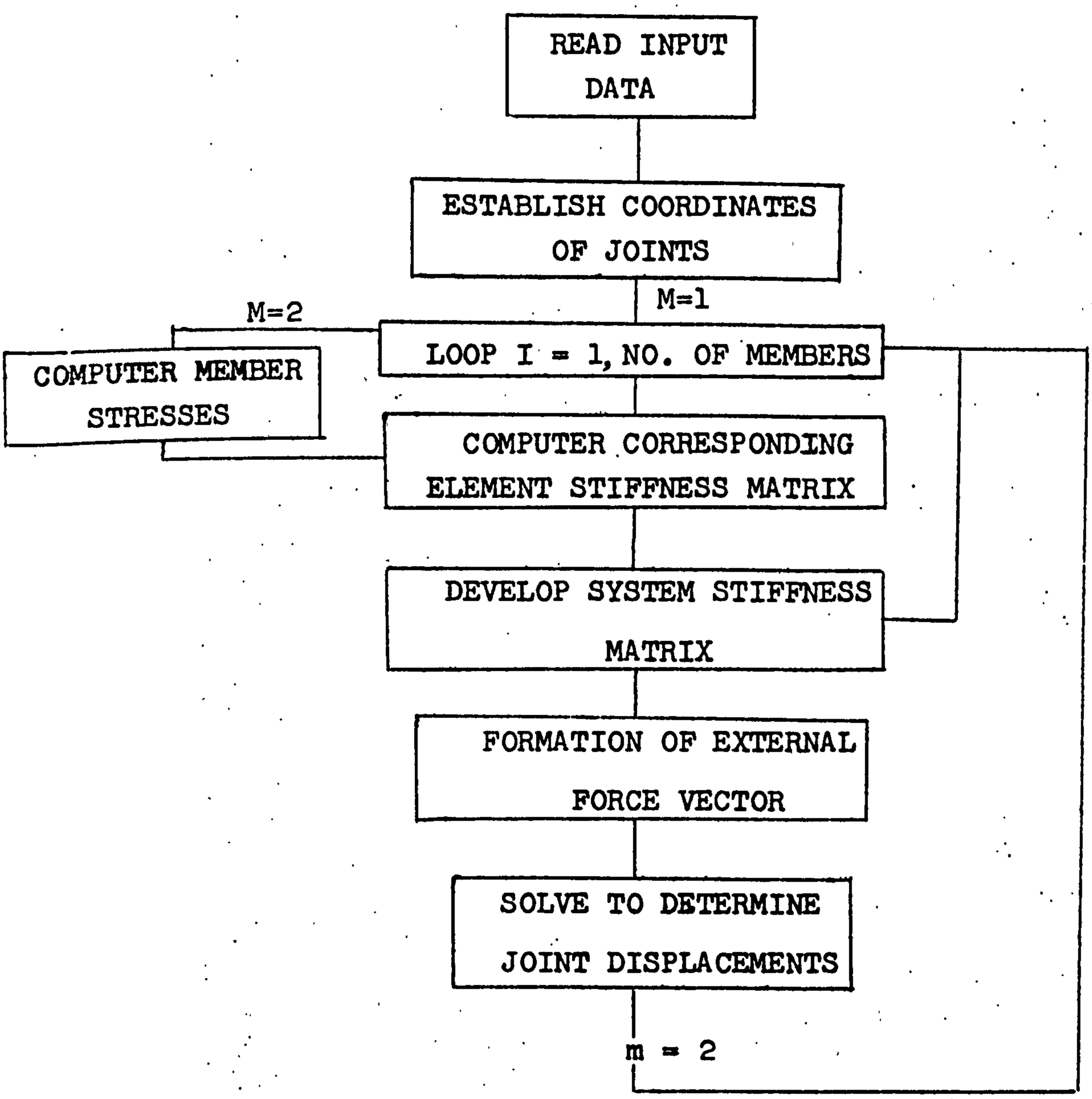

FINITE ELEMENT PROGRAM

In order to calculate the stresses in the members and hence determine the material damping constants C and ϵ, the following input data is required:

NP NO OF STRUCTURES TO BE ANALYSISED
M NO. OF MEMBERS
NJ NO. OF JOINTS
NBW HALF BANDWIDTH
E MODULUS OF ELASTICITY
NF NO. OF FORCES
NB NO OF CONSTRAINED JOINTS
IXT,IYT,IZT,IXR,IYR,IZR ARE DEGREE OF FREEDOM AT EACH JOINT
FOR CONSTRAINED JOINTS THEY ARE SET TO 1, OTHERWISE 0
J,K ARE ENDS OF MEMBER
QA CROSS-SECTIONAL AREA OF MEMBER
RO MASS DENSITY OF THE MATERIAL
X
Y ARE PRINCIPAL AXES
Z
XI TORSION CONSTANT
YI PRINCIPAL MOMENT OF INERTIA ABOUT Y AXIS
ZI PRINCIPAL MOMENT OF INERTIA ABOUT Z AXIS
SI ANGLE OF ROLL
ISI 0 FOR INCLINED MEMBERS
1 FOR VERTICAL MEMBERS

```
      PROGRAM(D10A)
      INPUT1=CR0
      OUTPUT2=LP0
      TRACE 2
      END
      MASTER DYNAMICS
      DIMENSION  X(6)
      COMMON1/GAB1/ NE,NJ,NBU,NB,NCH,E,NF,NDF,NSZF,NBC(5),NFIX(5),
     1R1(264),ESTIFM(12,12),SK(264,97),X(45),Y(45),Z(45),NOP(92,2)
      COMMON/GAB2/ KKK,KK,JDATA(4),IDATA(5),II(2),FDATA(6),DDATA(5)
      CALL USEFILE(3,2HED,12HSUBFILE MK1,0,1)
      CALL USEFILE(5,2HED,12HSUBFILE MK2,0,1)
      NL=1
      NCH=2
      NDF=6
      READ(1,99)NP
   99   FORMAT(I1)
      DO 425 IZ=1,NP
      READ(1,100)KODE,NE,NJ,NBU,E,FREQ,NF,NB
  100 FORMAT(A1,3I4,2F10.3,3I4)
      WRITE(2,91)
   91 FORMAT(//1H1,34X,14HSTRUCTURE DATA,// 5X,7HNUMBERS,
     16X,6HJOINTS,6X,3HNBU,/X,6HE(KS1),9X,11HFREQ(RAD/S),5X,
     22HNF,7X,2HNB/)
      WRITE(2,400)NE,NJ,NBU,E,FREQ,NF,NB
  400 FORMAT(I10,I12,I11,2F15.2,I11,I9)
      NSZF=NJ*NDF
      WRITE(2,92)
   92 FORMAT(//49X,10HJOINT DATA,//2X,5HJOINT/,1X,6HNUMBER,6X,
     13HIXT,6X,3HIYT,6X,3HIZT,6X,12HX-COORD,(IN),4X,12HY-COORD,(IN),
     26X,12HZ-COORD,(IN)/)
      DO 201  I=1,NJ
      READ(1,101)KODE,J,IXT,IYT,IZT,XCOOR,YCOOR,ZCOOR
  101 FORMAT(A1,4I4,3F10.3)
      WRITE(2,401)J,IXT,IYT,IZT,XCOOR,YCOOR,ZCOOR
  401 FORMAT(I4,I11,2I9,F16.2,F18.2,F17.2)
      X(J)=XCOOR
      Y(J)=YCOOR
      Z(J)=ZCOOR
  201 CONTINUE
      DO 203 I=1,NB
  203 READ(1,205)NBC(I),NFIX(I)
  205 FORMAT(2I9)
      DO 225 JJJ=1,NL
      FF=FREQ*FREQ
          KKK=1
          KK=1
          MM=2
          NQ=1
          KEY=JJJ
          IF(JJJ.EQ.1)WRITE(2,90)
   90 FORMAT(///39X,11HMEMBER DATA//,2X,6HMEMBER,19X,4HAREA,
     17X,6H   XI   ,11X,2HYI,10X,2HZI,
     2/ 2X,6HNUMBER,6X,1HJ,6X,1HK,4X,7H(IN**2),5X,7H(IN**4)
     37X,7H(IN**4),5X,7H(IN**4),6X,2HSI,7X,3HISI/)
          CALL FORMK(MM,KEY)
          NEB=NJ*NDF
 3001 DO 231 I=1,NEB
  231 R1(I)=0.0
```

```
      IF(KEY.EQ.1)WRITE(2,93)
   93 FORMAT(///40X,9HLOAD DATA //,27X,5HJOINT,
     13X,4HJXYZ,3X,11HFORCE(KIPS)/)
      DO 210 L=1,NF
      IF(KEY-1)354,353,354
  353 READ(1,140)KODE,J,R(1),R(2),R(3),R(4),R(5),R(6)
       JDATA(1)=KODE
      JDATA(2)=J
      FDATA(1)=R(1)
      FDATA(2)=R(2)
      FDATA(3)=R(3)
      FDATA(4)=R(4)
      FDATA(5)=R(5)
      FDATA(6)=R(6)
      CALL PUTARRAY(3,KK,JDATA)
      CALL PUTARRAY(3,KK,FDATA)
      WRITE(2,406)J,R(1),R(2),R(3)
  406 FORMAT(I30,3F18.3)
      GOTO 355
  354 CALL GETARRAY(3,KK,JDATA)
      CALL GETARRAY(3,KK,FDATA)
      KODE=JDATA(1)
      J=JDATA(2)
      R(1)=FDATA(1)
      R(2)=FDATA(2)
      R(3)=FDATA(3)
      R(4)=FDATA(4)
      R(5)=FDATA(5)
      R(6)=FDATA(6)
  140 FORMAT(A1,I9,6F0.0)
  355 DO 250 K=1,6
      IC=(J-1)*6+K
  250 R1(IC)=R1(IC)+R(K)
  210 CONTINUE
   25 WRITE(2,28)
   28 FORMAT(1H1,//30X,23H*** LUMPED MASS METHOD ***)
   34 CONTINUE
      WRITE(2,94)
   94 FORMAT(///34X,21HJOINT DEFLECTIONS(IN),//3X,5HJOINT,7X,6HNUMBER,
     110X,12HX-DEFLECTION,10X,12HY-DEFLECTION,10X,12HZ-DEFLECTION/)
      CALL SOLVE
      DO 418 I=1,NJ
      J=(I-1)*6+1
      WRITE(2,420)I,R1(J),R1(J+1),R1(J+2)
  420 FORMAT(I12,E24.5,2E22.5)
  418 CONTINUE
      KKK=1
      MM=1
      WRITE(2,35)
   35 FORMAT(////,45X,18HMEMBER END ACTIONS,
     1/,30X,5HJ-END,40X,5HK-END,
     2/,5X,6HMEMBER,6X,13HX-FORCE(KIPS),6X,13HSTRESS(KIPS/IN2),
     37X,13HX-FORCE(KIPS),6X,13HSTRESS(KIPS/IN2)/)
      CALL STRUSS(MM,KEY)
  500 CONTINUE
  225 CONTINUE
  425 CONTINUE
       CALL FREEFILE (3)
       CALL FREEFILE (5)
      STOP
      END
      SUBROUTINE FORMK(MM,KEY)
      COMMON/BAB1/ NE,NJ,NBW,NB,NCH,E,FF,NDF,NSZF,IBC(5),NFIX(5),
     1R1(264),ESTIFM(12,12),SK(264,47),X(45),Y(45),Z(45),NOP(92,2)
      NBAND=NBW
      DO 300 N=1,NSZF
```

```
      DO 300 N=1,MBAND
  300 SK(M,N)=0.0
      DO 400 M=1,NE
      CALL STRUSS(NM1,KEY)
      DO 350 JJ=1,NCN
      NROWB=(NOP(M,JJ)-1)*NDF
      DO 350 J=1,NDF
      NROWB=NROWB+1
      I=(JJ-1)*NDF+J
      DO 330 KK=1,NCN
      NCOLB=(NOP(M,KK)-1)*NDF
      DO 320 K=1,NDF
      L=(KK-1)*NDF+K
      NCOL=NCOLB+K+1-NROWB
      IF (NCOL) 320,320,310
  310 SK(NROWB,NCOL)=SK(NROWB,NCOL)+ESTIFM(I,L)
  320 CONTINUE
  330 CONTINUE
  350 CONTINUE
  400 CONTINUE
      DO 500 N=1,NB
      NX=10**(NDF-1)
      I=NBC(N)
      NROWB=(I-1)*NDF
      DO 420 M=1,NDF
      NROWB=NROWB+1
      ICON=NFIX(N)/NX
      IF (ICON) 450,450,420
  420 SK(NROWB,1)=1.0
      DO 430 J=2,MBAND
      SK(NROWB,J)=0.0
      NR=NROWB+1-J
      IF (NR) 430,430,425
  425 SK(NR,J)=0.0
  430 CONTINUE
      NFIX(N)=NFIX(N)-NX*ICON
  450 NX=NX/10
  460 CONTINUE
  500 CONTINUE
      RETURN
      END
      SUBROUTINE SOLVE
      COMMON/DAB1/ NE,NJ,NBW,NB,NCN,E,FF,NDF,NSZF,NBC(5),NFIX(5),
     1R1(264),ESTIFM(12,12),SK(264,47),X(45),Y(45),Z(45),NOP(92,2)
      MBAND=NBW
      DO 300 N=1,NSZF
      I=N
      DO 290 L=2,MBAND
      I=I+1
      IF (SK(N,L)) 240,290,240
  240 C=SK(N,L)/SK(N,1)
      J=0
      DO 270 K=L,MBAND
      J=J+1
      IF(SK(N,K)) 260,270,260
  260 SK(I,J)=SK(I,J)-C*SK(N,K)
  270 CONTINUE
  280 SK(I,L)=C
      R1(I)=R1(I)-C*R1(N)
  290 CONTINUE
  300 R1(N)=R1(N)/SK(N,1)
      N=NSZF
  350 N=N-1
      IF(N) 500,500,360
  360 L=N
      DO 400 K=2,MBAND
```

```
      L=L+1
      IF (SK(N,K)) 370,400,370
  370 R1(N)=R1(N)-SK(N,K)*R1(L)
  400 CONTINUE
      GO TO 350
  500 RETURN
      END
      SUBROUTINE STRUSS(NN,KEY)
      DIMENSION BS(12,12),B(12,12),DEF(12),DEFE(12),T(12,12)
      DIMENSION PS(12),P(12)
      COMMON/GAB1/ NE,NJ,NBM,NB,NCM,E,FF,IDF, ISZF,MBC(5),NFIX(5),
     1R1(264),ESTIFM(12,12),SK(264,47),X(45),Y(45),Z(45),NOP(92,2)
       COMMON/GAB2/ KKK,KK,JDATA(4),MDATA(5),MJ(2),FDATA(6),SDATA(5)
      DATA KODEC/5HABCDE/
      NEIG=3.0
      RO=0.283
       G=E/2.5
      SE=40.
      AJM=0.7
      GAM=6.0
       NMM=1
      PI=3.1415925/180.
       IF(MM-2)0,17,0
      DO 15 IJK=1,NE
      IF(MEV-1)4,200,4
  200 IF(MM-2)4,3,4
    3 READ(1,103)KODE,I,J,K
        MDATA(1)=KODE
      MDATA(2)=I
      MDATA(3)=J
      MDATA(4)=K
      NOP(I,1)=J
      NOP(I,2)=K
       CALL PUTARRAY(5,KKK,MDATA)
  403 FORMAT(I6,I9,I7,I8,F12.4,F15.3,2F12.3,I )
      GO TO 5
    4 CALL GETARRAY(5,KKK,MDATA)
      KODE=MDATA(1)
      I=MDATA(2)
      J=MDATA(3)
      K=MDATA(4)
      ISI=MDATA(5)
  103 FORMAT(A1,I4,I7,I3,I4,F10.4,F10.0,3F1 .4,I4)
    5 NOJ=J
      NOK=K
      SL=SQRT((X(K)-X(J))**2+(Y(K)-Y(J))**2+(Z(K)-Z(I))**2)
      CX=(X(K)-X(J))/SL
      CY=(Y(K)-Y(J))/SL
      CZ=(Z(K)-Z(J))/SL
      DO 3001 LIA=1,5
      KIA=1
      CALL COMP(KIA,KODE,1,KODEC,LIA)
      IF(KIA-1)0,3002,0
 3001 CONTINUE
 3002 GO TO (201,202,203,204,205),LIA
  201 OA=0.434
      W=RO*OA
      YI=0.001
      ZI=0.001
      XI=0.005
      SI=0.
      GO TO 3003
  202 OA=1.187
      ISI=1
      YI=0.703
      ZI=0.703
```

```
      XI=0.024
      U=R0*0A
      SI=0.0
      GO TO 3003
203   0A=0.809
      ISI=1
      U=R0*0A
      YI=0.394
      ZI=0.394
      XI=0.009
      SI=0.0
       GO TO 3003
204   0A=1.562
      U=R0*0A
      YI=0.305
      ZI=0.305
      XI=0.031
       SI=0.
      GO TO 3003
205   0A=.621
      U=R0*0A
      YI=0.179
      ZI=0.179
      XI=0.007
      ISI=1
      SI=0.0
3003  CONTINUE
      IF(NN-2)18,0,18
      WRITE(2,403)I,J,K,XI,YI,ZI,SI,ISI
      WEIG=WEIG+U*SL
      IF(I.EQ.132)WRITE(2,505)WEIG
505   FORMAT(1X,25HTOTAL STRUCTURAL WEIGHT =,E15.4,2X,34L15)
18    CONTINUE
      U=U*SL/386000.
      SK0=FF*U/2.
      SK1=2.*E*YI/SL
      SK2=2.*E*ZI/SL
      SK3=3.*SK1/SL
      SK4=3.*SK2/SL
      SK5=2.*SK3/SL
      SK6=2.*SK4/SL
      SK7=G*XI/SL
       SK8=E*0A/SL
      DO 7 I=1,12
      DO 7 J=1,12
7     B(I,J)=0.0
      IF(NN.EQ.3)FF=0.0
8     B(1,1)=SK8-SK0
      B(1,7)=-SK8
      B(7,7)=SK8-SK0
      B(2,2)=SK6-SK0
      B(3,3)=SK5-SK0
      B(4,4)=SK7-SK0
      B(5,5)=2.*SK1-SK0
      B(6,6)=2.*SK2-SK0
      B(8,8)=SK6-SK0
      B(9,9)=SK5-SK0
      B(10,10)=SK7-SK0
      B(11,11)=2.*SK1-SK0
      B(12,12)=2.*SK2-SK0
      B(2,6)=SK4
      B(2,8)=-SK6
      B(2,12)=SK4
      B(3,5)=-SK3
      B(3,9)=-SK5
      B(3,11)=-SK3
```

```
      B(4,10)=-SK?
      B(5,9)=SK3
       B(5,1)=SK1
       B(6,8)=-SK4
      B(6,12)=SK2
      B(3,12)=-SK4
      B(9,11)=SK3
   30 CONTINUE
      DO 91 I=1,12
      DO 91 J=1,12
91      T(I,J)=0.
      IF(SI.EQ.0) GO TO 600
      IF(SI.EQ.90)GO TO 601
      GO TO 603
600   CS=1.
      SN=0.
      GO TO 602
601   CS=0.
      SN=1.
      GO TO 602
603   SZ=SI*D1
      SN=SIN(SZ)
      CS=COS(SZ)
602   CONTINUE
      IF(ISI.EQ.0) GO TO 64
      T3=SQRT(CX**2+CY**2)
      T(1,1)=CX
      T(1,2)=CY
      T(1,3)=CZ
      T(2,1)=(-CX*CZ*SN-CY*CS)/T3
      T(2,2)=(-CY*CZ*SN+CX*CS)/T3
      T(2,3)=T3*SN
      T(3,1)=(-CX*CZ*CS+CY*SN)/T3
      T(3,2)=(-CY*CZ*CS-CX*SN)/T3
      T(3,3)=T3*CS
      GO TO 63
   64 T3=SQRT(CX**2+CZ**2)
      T(1,1)=CX
      T(1,2)=CY
      T(1,3)=CZ
      T(2,1)=(-CX*CY*CS-CZ*SN)/T3
      T(2,2)=T3*CS
      T(2,3)=(-CY*CZ*CS+CX*SN)/T3
      T(3,1)=(CX*CY*SN-CZ*CS)/T3
      T(3,2)=-T3*SN
      T(3,3)=(CY*CZ*SN+CX*CS)/T3
   63 DO 62 K=3,9,3
      DO 62 I=1,3
      DO 62 J=1,3
      IK=I+K
      JK=J+K
   62 T(IK,JK)=T(I,J)
      IF(MM-1)31,32,31
   31 DO 40 I=1,12
      DO 40 K=1,12
      SUM=0.0
      DO 45 J=1,12
   45 SUM=SUM+T(J,I)*B(J,K)
      BS(I,K)=SUM
   40 CONTINUE
      DO 50 I=1,12
      DO 50 K=1,12
      SUM=0.0
      DO 55 J=1,12
   55 SUM=SUM + BS(I,J)*T(J,K)
      B(I,K)=SUM
```

```
      ESTIFM(I,K)=B(I,K)
   50 CONTINUE
      GO TO 15
   32 DO 213 K=1,6
      IC=(NOJ-1)*6+K
      ICC=(NOK-1)*6+K
      DEF(K)=R1(IC)
      DEF(6+K)=R1(ICC)
  213      CONTINUE
      DO 214 I2=1,12
      SUM=0.0
      DO 215 I3=1,12
  215 SUM=SUM+T(I2,I3)*DEF(I3)
      DEFE(I2)=SUM
  214 CONTINUE
      DO 211 J=1,12,6
      SUM=0.0
      DO 212 K=1,12
  212 SUM=SUM+B(J,K)*DEFE(K)
      P(J)=SUM
      PS(J)=SUM/QA
  211 CONTINUE
      VOL=QA*SL
      SUM1=SUM1+(PS(1)/SE)**2*VOL
      SUM2=SUM2+(PS(1)/SE)**3*VOL
      WRITE(2,991)IJK,P(1),PS(1),P(7),PS(7)
  991  FORMAT(I9,2X,E17.3,E23.4,E17.3,E23.4)
      IF(IJK.EQ.NE)GO TO 999
      GO TO 15
  999 XTOP=R1(1)
      FREQR=37.
      C=AJM*SUM1/(3.142*FREQR*XTOP**2)
      ESP=AJM*GAM*SUM2/(2.*1.77257*FREQR**7*XTOP**3*0.35451)
      WRITE(2,989)C,ESP
  989 FORMAT(1X,4HC = ,E12.4,10X,6HESP = ,E12.4)
   15 CONTINUE
  520 CONTINUE
  510 CONTINUE
    2 RETURN
      END
      FINISH
****
```

MEMBER END ACTIONS

MEMBER	J-END X-FORCE(KIPS)	J-END STRESS(KIPS/INS)	K-END X-FORCE(KIPS)	K-END STRESS(KIPS/INS)
1	0.236E-02	0.1514E-02	-0.236E-02	-0.1514E-02
2	-0.153E 00	-0.9797E-01	0.153E 00	0.9797E-01
3	0.810E-02	0.5188E-02	-0.810E-02	-0.5188E-02
4	0.242E 00	0.1552E 00	-0.242E 00	-0.1552E 00
5	-0.666E 00	-0.1534E 01	0.666E 00	0.1534E 01
6	-0.129E-01	-0.2973E-01	0.129E-01	0.2973E-01
7	0.414E 00	0.9536E 00	-0.414E 00	-0.9536E 00
8	-0.155E-01	-0.3565E-01	0.155E-01	0.3565E-01
9	0.495E-02	0.7974E-02	-0.495E-02	-0.7974E-02
10	-0.320E 00	-0.5154E 00	0.320E 00	0.5154E 00
11	0.704E-01	0.1134E 00	-0.704E-01	-0.1134E 00
12	0.443E 00	0.7135E 00	-0.443E 00	-0.7135E 00
13	0.666E 00	0.1072E 01	-0.666E 00	-0.1072E 01
14	-0.333E 00	-0.5368E 00	0.333E 00	0.5368E 00
15	-0.866E 00	-0.1395E 01	0.866E 00	0.1395E 01
16	0.418E 00	0.6730E 00	-0.418E 00	-0.6730E 00
17	-0.513E 00	-0.1182E 01	0.513E 00	0.1182E 01
18	0.754E-02	0.1738E-01	-0.754E-02	-0.1738E-01
19	0.639E 00	0.1473E 01	-0.639E 00	-0.1473E 01
20	0.219E-01	0.5056E-01	-0.219E-01	-0.5056E-01
21	0.120E 01	0.1478E 01	-0.120E 01	-0.1478E 01
22	-0.861E 00	-0.1064E 01	0.861E 00	0.1064E 01
23	-0.111E 01	-0.1369E 01	0.111E 01	0.1369E 01
24	0.700E 00	0.8658E 00	-0.700E 00	-0.8658E 00
25	-0.296E-01	-0.6823E-01	0.296E-01	0.6823E-01
26	-0.534E 00	-0.1230E 01	0.534E 00	0.1230E 01
27	-0.682E-03	-0.1571E-02	0.682E-03	0.1571E-02
28	0.658E 00	0.1517E 01	-0.658E 00	-0.1517E 01
29	0.115E 01	0.1426E 01	-0.115E 01	-0.1426E 01
30	0.160E 01	0.1975E 01	-0.160E 01	-0.1975E 01
31	-0.111E 01	-0.1367E 01	0.111E 01	0.1367E 01
32	-0.155E 01	-0.1914E 01	0.155E 01	0.1914E 01
33	0.324E-01	0.7460E-01	-0.324E-01	-0.7460E-01
34	-0.682E 00	-0.1570E 01	0.682E 00	0.1570E 01
35	-0.223E-02	-0.5142E-02	0.223E-02	0.5142E-02

36	0.517E 00	0.1192E 01	-0.517E 00	-0.1192E 01
37	0.163E 01	0.2014E 01	-0.163E 01	-0.2014E 01
38	0.190E 01	0.2347E 01	-0.190E 01	-0.2347E 01
39	-0.154E 01	-0.1904E 01	0.154E 01	0.1904E 01
40	-0.196E 01	-0.2425E 01	0.196E 01	0.2425E 01
41	-0.610E 00	-0.1406E 01	0.610E 00	0.1406E 01
42	-0.162E-01	-0.3725E-01	0.162E-01	0.3725E-01
43	0.606E 00	0.1397E 01	-0.606E 00	-0.1397E 01
44	-0.132E-01	-0.3045E-01	0.132E-01	0.3045E-01
45	-0.159E-01	-0.1019E-01	0.159E-01	0.1019E-01
46	0.287E-02	0.1839E-02	-0.287E-02	-0.1839E-02
47	0.255E-01	0.1630E-01	-0.255E-01	-0.1630E-01
48	0.362E-02	0.2315E-02	-0.362E-02	-0.2315E-02
49	-0.240E 01	-0.2963E 01	0.240E 01	0.2963E 01
50	0.190E 01	0.2347E 01	-0.190E 01	-0.2347E 01
51	0.235E 01	0.2899E 01	-0.235E 01	-0.2899E 01
52	-0.188E 01	-0.2319E 01	0.188E 01	0.2319E 01
53	0.631E 00	0.1453E 01	-0.631E 00	-0.1453E 01
54	0.280E-01	0.6450E-01	-0.280E-01	-0.6450E-01
55	-0.594E 00	-0.1369E 01	0.594E 00	0.1369E 01
56	-0.245E-01	-0.5652E-01	0.245E-01	0.5652E-01
57	-0.269E 01	-0.3327E 01	0.269E 01	0.3327E 01
58	0.237E 01	0.2932E 01	-0.237E 01	-0.2932E 01
59	0.270E 01	0.3336E 01	-0.270E 01	-0.3336E 01
60	-0.242E 01	-0.2991E 01	0.242E 01	0.2991E 01
61	0.634E 00	0.1460E 01	-0.634E 00	-0.1460E 01
62	-0.135E-01	-0.3105E-01	0.135E-01	0.3105E-01
63	-0.574E 00	-0.1323E 01	0.574E 00	0.1323E 01
64	0.970E-02	0.2234E-01	-0.970E-02	-0.2234E-01
65	0.317E 01	-0.2668E 01	0.317E 01	0.2668E 01
66	0.268E 01	0.2260E 01	-0.268E 01	-0.2260E 01
67	0.321E 01	0.2708E 01	-0.321E 01	-0.2708E 01
68	-0.268E 01	-0.2258E 01	0.268E 01	0.2258E 01
69	0.556E 00	0.1281E 01	-0.556E 00	-0.1281E 01
70	0.109E-01	0.2519E-01	-0.109E-01	-0.2519E-01
71	0.631E 00	-0.1454E 01	0.631E 00	0.1454E 01
72	-0.683E-02	-0.1574E-01	0.683E-02	0.1574E-01
73	-0.348E 01	-0.2935E 01	0.348E 01	0.2935E 01
74	0.323E 01	0.2723E 01	-0.323E 01	-0.2723E 01
75	0.345E 01	0.2907E 01	-0.345E 01	-0.2907E 01

76	-0.318E 01	-0.2677E 01	0.318E 01	0.2677E 01
77	0.578E 00	0.1332E 01	-0.578E 00	-0.1332E 01
78	-0.136E-01	-0.3126E-01	0.136E-01	0.3126E-01
79	-0.601E 00	-0.1386E 01	0.601E 00	0.1386E 01
80	0.951E-02	0.2192E-01	-0.951E-02	-0.2192E-01
81	-0.400E 01	-0.3368E 01	0.400E 01	0.3368E 01
82	0.341E 01	0.2874E 01	-0.341E 01	-0.2874E 01
83	0.397E 01	0.3344E 01	-0.397E 01	-0.3344E 01
84	-0.345E 01	-0.2907E 01	0.345E 01	0.2907E 01
85	-0.423E-01	-0.9756E-01	0.423E-01	0.9756E-01
86	0.629E 00	0.1449E 01	-0.629E 00	-0.1449E 01
87	0.457E-01	0.1053E 00	-0.457E-01	-0.1053E 00
88	-0.534E 00	-0.1231E 01	0.534E 00	0.1231E 01
89	-0.461E-01	-0.2949E-01	0.461E-01	0.2949E-01
90	-0.282E-01	-0.1806E-01	0.282E-01	0.1806E-01
91	0.417E-01	0.2669E-01	-0.417E-01	-0.2669E-01
92	0.314E-01	-0.2008E-01	0.314E-01	0.2008E-01
93	0.401E 01	0.3378E 01	-0.401E 01	-0.3378E 01
94	0.422E 01	0.3553E 01	-0.422E 01	-0.3553E 01
95	-0.404E 01	-0.3400E 01	0.404E 01	0.3400E 01
96	-0.423E 01	-0.3565E 01	0.423E 01	0.3565E 01
97	0.609E 00	0.1404E 01	-0.609E 00	-0.1404E 01
98	0.303E-01	0.6993E-01	-0.303E-01	-0.6993E-01
99	-0.559E 00	-0.1287E 01	0.559E 00	0.1287E 01
100	-0.208E-01	-0.4803E-01	0.208E-01	0.4803E-01
101	-0.479E 01	-0.4039E 01	0.479E 01	0.4039E 01
102	0.423E 01	0.3565E 01	-0.423E 01	-0.3565E 01
103	0.482E 01	0.4061E 01	-0.482E 01	-0.4061E 01
104	-0.423E 01	-0.3566E 01	0.423E 01	0.3566E 01
105	0.584E 00	0.1345E 01	-0.584E 00	-0.1345E 01
106	0.779E-02	0.1796E-01	-0.779E-02	-0.1796E-01
107	-0.610E 00	-0.1407E 01	0.610E 00	0.1407E 01
108	-0.183E-01	-0.4219E-01	0.183E-01	0.4219E-01
109	-0.504E 01	-0.4245E 01	0.504E 01	0.4245E 01
110	0.484E 01	0.4077E 01	-0.484E 01	-0.4077E 01
111	0.502E 01	0.4233E 01	-0.502E 01	-0.4233E 01
112	-0.483E 01	-0.4067E 01	0.483E 01	0.4067E 01
113	0.311E-01	0.7170E-01	-0.311E-01	-0.7170E-01
114	0.602E 00	0.1388E 01	-0.602E 00	-0.1388E 01
115	-0.201E-01	-0.4635E-01	0.201E-01	0.4635E-01

116	-0.608E 00	-0.1402E 01	0.608E 00	0.1402E 01
117	-0.500E 01	-0.4216E 01	0.500E 01	0.4216E 01
118	-0.563E 01	-0.4746E 01	0.563E 01	0.4746E 01
119	0.500E 01	0.4216E 01	-0.500E 01	-0.4216E 01
120	0.563E 01	0.4746E 01	-0.563E 01	-0.4746E 01
121	0.205E-01	-0.4729E-01	0.205E-01	0.4729E-01
122	0.603E 00	0.1390E 01	-0.603E 00	-0.1390E 01
123	0.977E-02	0.2252E-01	-0.977E-02	-0.2252E-01
124	-0.593E 00	-0.1366E 01	0.593E 00	0.1366E 01
125	-0.562E 01	-0.4737E 01	0.562E 01	0.4737E 01
126	-0.578E 01	-0.4873E 01	0.578E 01	0.4873E 01
127	0.561E 01	0.4726E 01	-0.561E 01	-0.4726E 01
128	0.579E 01	0.4877E 01	-0.579E 01	-0.4877E 01
129	0.490E-01	0.1129E 00	-0.490E-01	-0.1129E 00
130	0.577E 00	-0.1330E 01	0.577E 00	0.1330E 01
131	0.390E-01	-0.8994E-01	0.390E-01	0.8994E-01
132	0.579E 00	0.1334E 01	-0.579E 00	-0.1334E 01

C 0.1692E 00 ESP = 0.2729E-13

APPENDIX G

4.1 Analogue Computer Simulation

4.2 Transfer of Equations into Computer Variables

The non-linear equations of motion given in section 5 were solved using Applied Dynamic AD 256 analogue computer. Before setting up the analogue computer circuit for solving such differential equations, it is necessary to determine whether time and amplitude scaling is required to maintain the magnitudes and frequencies of the systems in acceptable limits.

4.3 Time Scaling

To decrease the period of motion, the frequencies of the simulated system can be increased by a factor of 10 or 100 of AD 256 by pressing a single button. This increases the gain of all the integrators by 10 or 100 respectively. It should be noted that this time scaling does not effect the actual motion of the system but merely decreases the time required to study the motion.

Amplitude Scaling Using Normalised Variables

This method of scaling is essentially the same as the scale factor method except that the scale factors are not evaluated. Each system variable is divided by its estimated maximum value to give a set of variables with maximum unity. These normalised variables can be related directly to computer amplifier outputs measured in computer units.

Consider a system of variable X with maximum value X_m. The normalised variable is (X/X_m) and this is used as the computer variables. The value of the system variable X can be obtained by multiplying the measured output value of the computer variable in computer units by X_m. To convert a set of system equations to computer equations replace the system variable X by the normalised variable (X/X_m) multiplied by X_m

$$\text{i.e.} \quad X = (X/X_m)\, X_m$$

4.4 Equation in Computer Variables

The non-linear equation of (5.44) could be rewritten as follows:-

$$\left[\ddot{X}/\ddot{X}_m\right] \ddot{X}_m = - \gamma \left(1+\epsilon \left|\dot{X}/\dot{X}_m\right|^{n}_{\cdot}{}^{n}_{X_m}\right) (\dot{X}/\dot{X}_m) \dot{X}_m$$

$$- \omega^2 \left(\frac{X}{X_m}\right) X_m + \left(\frac{N(t)}{N_m}\right) N_m$$

Dividing both sides by $\ddot{X}_m$ yields

$$\left(\frac{\ddot{X}}{\ddot{X}_m}\right) = - \gamma \left(1+\epsilon \left|\frac{X}{X_m}\right|^{n}_{\cdot}{}^{n}_{X_m}\right) \left(\frac{\dot{X}}{\dot{X}_m}\right) \left(\frac{\dot{X}_m}{\dot{X}_m}\right)$$

$$- \omega^2 \left(\frac{X}{X_m}\right) \left(\frac{X_m}{\dot{X}_m}\right) + \frac{N_m}{\dot{X}_m} \left(\frac{N(t)}{N_m}\right)$$

The circuit representing this equation of motion is shown in figure 1.

A pseudo random noise signal was used here and was generated on the analogue computer using the circuit shown in figure (2). For the mean square transfer function and probability density measurement circuit see Ref.(54). Figure (3) shows the force and narrow band response of the simulated system. The mean square response of the system was calculated for various values of force input levels and are shown in figure 5 . Since analogue circuits are prone to electrical noise, drifts and amplifier saturation, the investigation of the non-linearity was limited to velcoity square. The system was later simulated on digital computer as it is free of such errors. The results obtained on the analogue computer supplied the results for testing the digital simulation.

Measurement of RMS of random signal.

The rms value of a random signal is defined mathematically as

$$\sqrt{E(X^2)} = \sqrt{\frac{1}{T} \int_0^T X^2(t)dt}$$

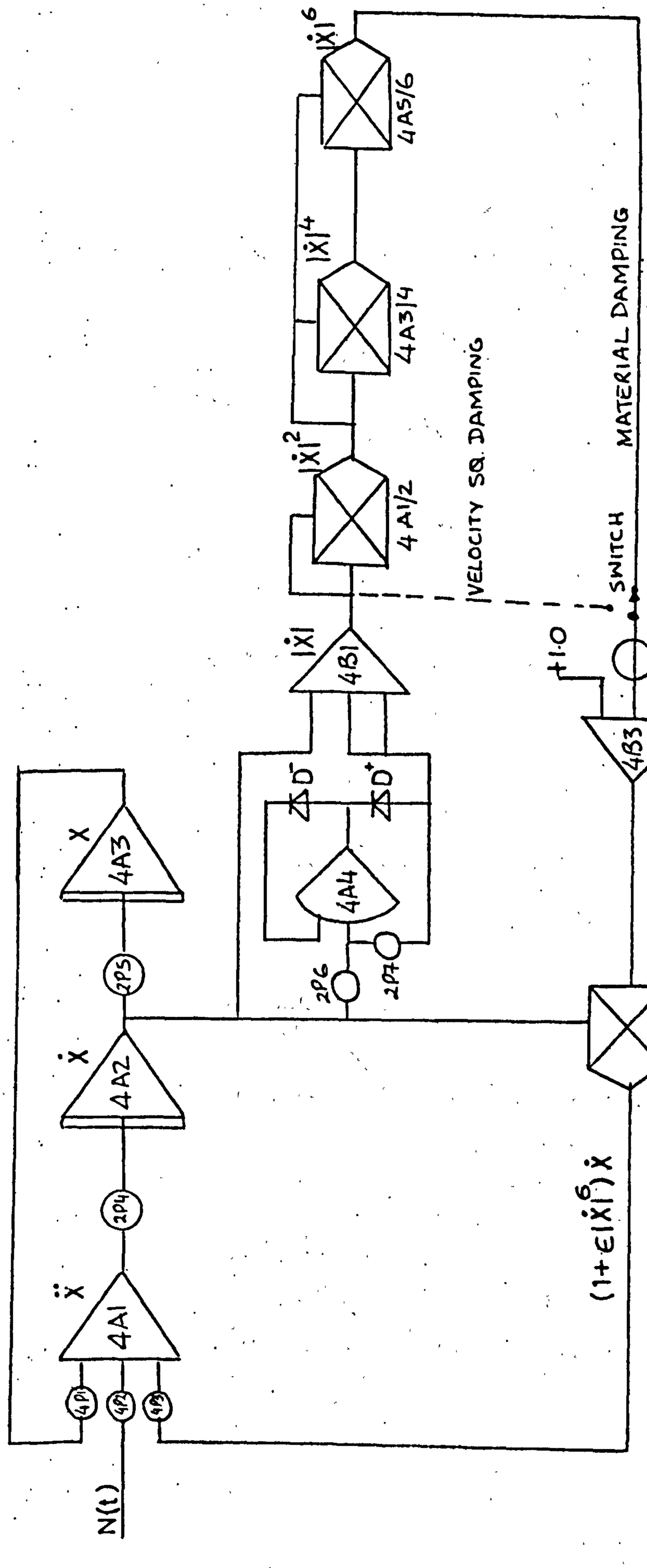

CIRCUIT DIAGRAM FOR NONLINEAR MATERIAL DAMPING

FIGURE G1

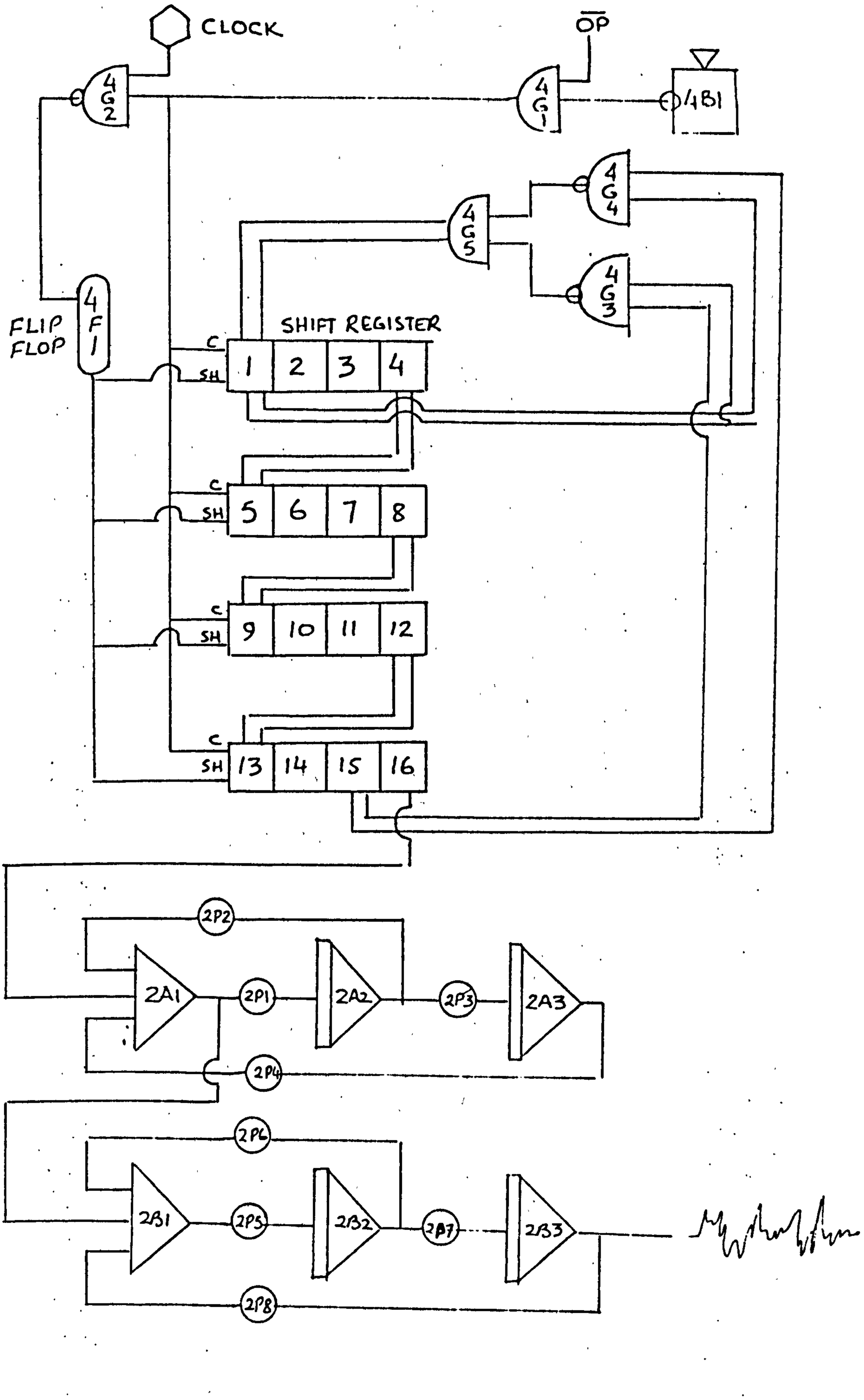

CIRCUIT FOR GENERATING PSEUDO RANDOM NOISE

FIGURE G2

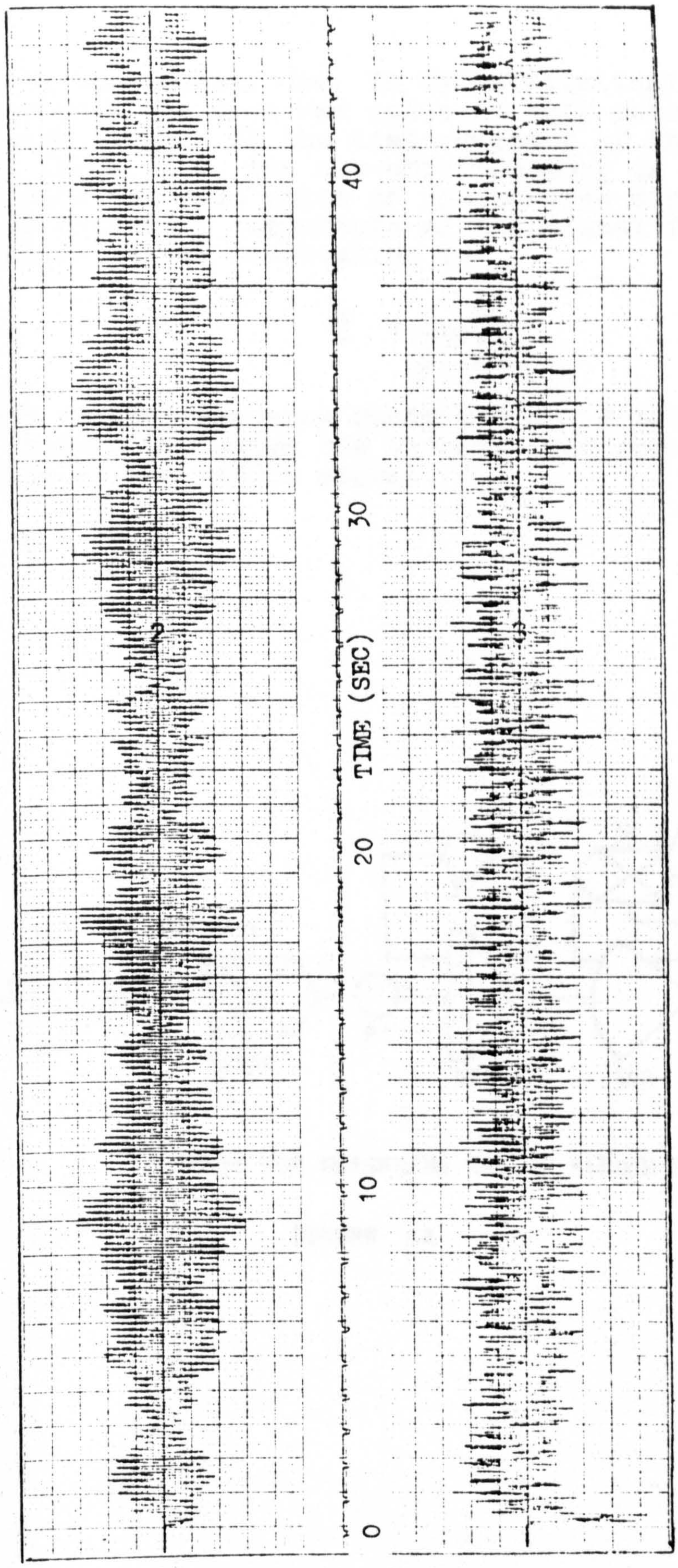

FIGURE G3
FORCE AND RESPONSE TIME HISTORIES

where T is the averaging time. In the statistically varying random signal the true rms value is only obtained if T is infinitely large. If the time constant of the RC-averager is very large, i.e. the cut-off frequency is very low it passes only the mean value of the squared signal and the very low frequency components of the signal fluctuations. The measure of rms fluctuation is

$$\hat{\epsilon} = \frac{1}{\sqrt{2\Delta\omega T}}$$

where $\Delta\omega$ is the frequency bandwidth and T is the averaging time. Figure (G4) shows the circuit used for measuring the rms value of the random signal.

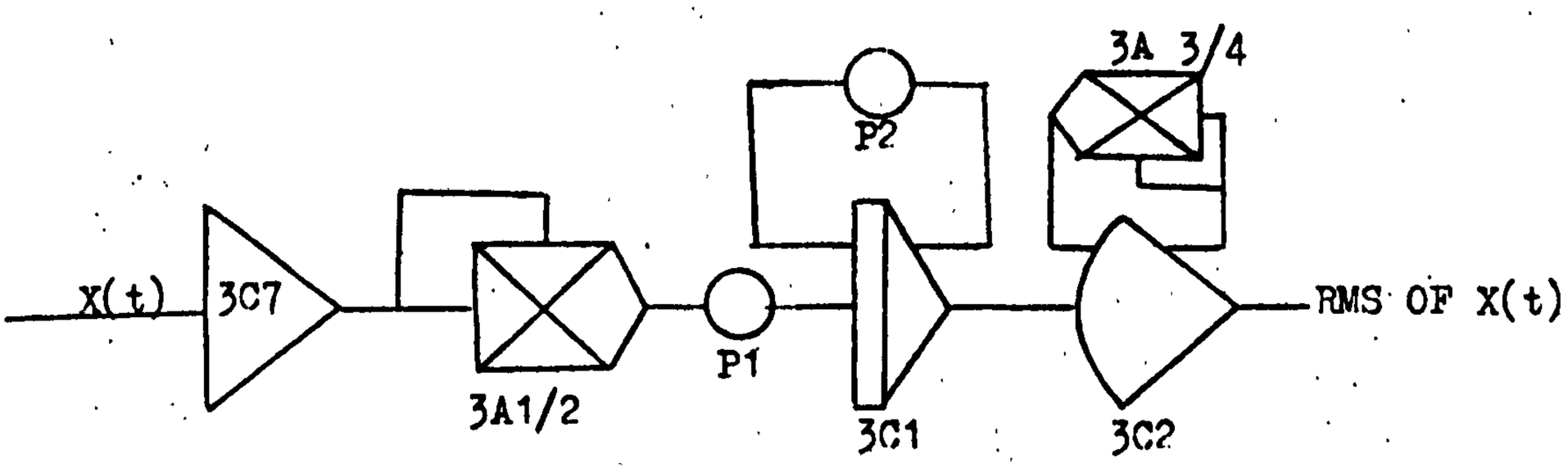

CIRCUIT FOR MEASURING RMS OF RANDOM SIGNAL

FIGURE G4

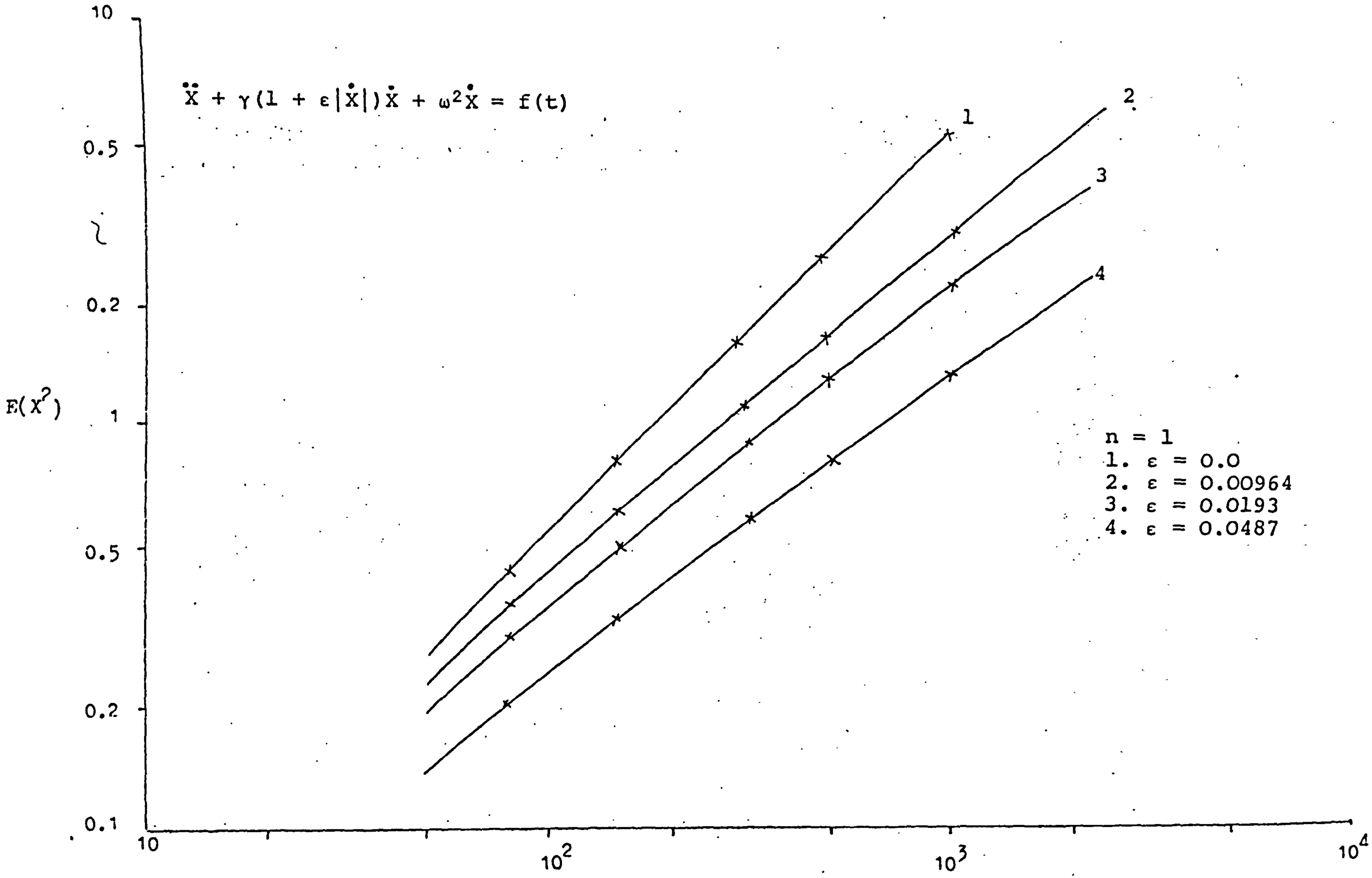

MEAN SQUARE RESPONSE VERSUS PSD OF EXCITATION

FIGURE G5

ANALOGUE SIMULATION ON DIGITAL COMPUTER

As the analogue computer used in this study became obsolete the simulation of the nonlinear system was carried out on digital computer.

Initially SLAM: Simulation Language for Analogue Modeling was used for simulating the nonlinear system on the ICL machine. As the time required for simulation was long (hence expensive), the simulation was carried out on a mini computer. This required the simulation program to be written in assembler. The general listing and the typical output from the program is given below.

GENERAL LISTING (XRLP) 31/03/78

```
1       DOC SOURCE-MFAL
2       #NAME=GABRI
3               JPU START
4       #MAC=S2WD
5               JSI IS2WD
6       ←
7       #MAC=GMA
8               *3461
9       ←
10      #MAC=ASK,F
11              JSI IASK
12              +F
13      ←
14      #MAC=TYPE,F
15              JSI ITYPE
16              +F
17      ←
18      #MAC=PUT,F,G
19              JSI IPUT
20              +F
21              +G
22      ←
23      #MAC=TAKE,F,G
24              JSI ITAKE
25              +F
26              +G
27      ←
28      #MAC=FLNG
29              *2150
30      ←
31      #MAC=NL
32              JSI INI
33      ←
34      #MAC=HEADING
35              JSI IHFADING
36      ←
37      #MAC=DATAOUT
38              JSI IDATAOUT
39      ←
40      #MAC=DEBUG
41              JSI IDFBUG
42      ←
43      #MAC=FLGT,F
44              *2305
45              +F
46      ←
47      #MAC=FLST,F
48              *3425
49              +F
50      ←
51      #MAC=FLAD,F
52              *2765
53              +F
54      ←
55      #MAC=FLSB,F
56              *2767
57              +F
```

```
58      ←
59      #MAC=FLMY,F
60              *2625
61              +F
62      ←
63      #MAC=FLDV,F
64              *2506
65              +F
66      ←
67      #MAC=DERST,F,G
68              *2305           (FLGT
69              +F
70              JSI IPUT
71              +&A1
72              +G
73      ←
74      #MAC=ICST,F,G
75              *2305           (FLGT
76              +F
77              JSI IPUT
78              +&A3
79              +G
80      ←
81      #MAC=INTGT,F,G
82              JSI ITAKE
83              +&A2
84              +G
85              *3425           (FLST
86              +F
87      ←
88      #MAC=FLTINT,F
89              *2305           (FLGT
90              +F
91              *3550           (FLIX
92              +WL1
93              GET WL1+1
94      ←
95      #MAC=JUMP,F,G,H
96              JPN F
97              JPZ G
98              JPU H
99      ←
100     #MAC=INTFLT,F
101             STO WL1+1
102             CLA
103             STO WL1
104             *3521           (FLLT
105             +WL1
106             *3425           (FLST
107             +F
108     ←
109     #MAC=FLLT,F
110             *3521
111             +F
112     ←
113             IS2WD=T
114             +&S2WD
115             IASK=T
116             +&ASK
```

```
117             IPRINT=T
118             +&PRINT
119             IFRAN=T
120             +&FRAN
121             ITYPE=T
122             +&TYPE
123             IPUT=T
124             +&PUT
125             ITAKE=T
126             +&TAKE
127             INL=T
128             +&NL
129             IHEADING=T
130             +&HEADING
131             IDATAOUT=T
132             +&DATAOUT
133             IDEBUG=T
134             +&DEBUG
135             ITEXTIO=T
136             +&TEXTIO
137             IPERIN=T
138             +&PERIN
139             IPEROUT=T
140             +&PEROUT
141             ISETUP=T
142             +&SETUP
143             ISEGINT=T
144             +&SEGINT
145             IRKFS=T
146             +&RKFS
147             II4=T
148             +&I4
149             II5=T
150             +&I5
151             II6=T
152             +&I6
153             IGROUT=T
154             +&GROUT
155             ISCALE=T
156             +&SCALE
157             &RANDOM=T
158             +0
159             +0
160             ILOG=T
161             +&LOG
162             IEXP=T
163             +&EXP
164             AW1=T    (100
165             *062001
166             *121407
167             AW2=T      (1000
168             *076375
169             *036412
170             XNOR=T
171             T=T+2
172             #TEXT
173     XNOR←
174             YNOR=T
175             T=T+2
```

```
176                 #TEXT
177       YNOR←
178                 ANOR=T
179                 T=T+2
180                 #TEXT
181       ANOR←
182                 GNOR=T
183                 T=T+2
184                 #TEXT
185       GNOR←
186                 ILAST=T
187                 +0
188                 LOCA=T
189                 +&FOF
190                 LOCR=T
191                 +&FOG
192                 LOCC=T
193                 +120000
194                 LOCD=T
195                 +050207
196                 LOCE=T
197                 +0
198                 NOP=T
199                 T=T+2
200                 #TEXT
201       NOP←
202                 LN=T
203                 T=T+2
204                 LCO=T
205                 T=T+300
206                 AL1=T
207                 T=T+2
208                 AL2=T
209                 T=T+2
210                 LCL=T
211                 T=T+2
212                 RATIO=T
213                 T=T+2
214                 NMS=T
215                 T=T+2
216                 #TEXT
217       NMS←
218                 WL1=T
219                 T=T+2
220                 WL2=T
221                 T=T+2
222                 WL3=T
223                 T=T+2
224                 WL4=T
225                 T=T+2
226                 ISQT=T
227                 +&SQT
228                 IRAISE=T
229                 +&RAISE
230                 IFLAB=T
231                 +&FLAB
232                 PI=T        (PI=3.142
233                 *062207
234                 *176402
```

```
235             C1=T            (2
236             *040000
237             *000402
238             C2=T            (628.4
239             *047214
240             *146412
241             C3=T            (1
242             *040000
243             *000401
244             C4=T            (6
245             *060000
246             *000403
247             C5=T            (0
248             *000000
249             *000000
250             C6=T              (0.01
251             *050753
252             *103372
253             C7=T              (6.284
254             *062213
255             *042403
256             C8=T              (1024
257             *040000
258             *000413
259             C9=T            (0.5
260             *040000
261             *000400
262             C10=T             (1025
263             *040020
264             *000413
265             C11=T             (1023
266             *077740
267             *000412
268             C12=T             (5
269             *050000
270             *000403
271             C13=T             (50331642
272             *060000
273             *000432
274             C14=T             (8388607
275             *040000
276             *00043O
277             C15=T    (1.87
278             +0
279             +0
280             C16=T          (SD=0.00215
281             +0
282             +0
283             C17=T          (AFOR=0.196
284             +0
285             +0
286             C18=T
287             +0
288             +0
289             C19=T
290             +0
291             +0
292             C20=T
293             +0
```

```
294             +0
295             N1=T
296             T=T+2
297             N2=T
298             T=T+2
299             ND=T
300             T=T+2
301             CINT=T
302             T=T+2
303             NUMB=T
304             T=T+2
305             ONE=T       (1
306             *040000
307             *000401
308             DU=T        (INTEGER SEED
309             *123456
310             DL=T
311             *123456
312             BU=T          (1953125
313             *000035
314             BL=T
315             *146545
316             CU=T
317             +0
318             CL=T
319             +0
320             CONST=T         (4(0430.5
321             *077777
322             *177426
323             SD=T
324                 T=T+2
325                 #TEXT
326         SD←
327                 ESPN=T
328                 T=T+2
329                 #TEXT
330         ESPN←
331                 ESP=T
332                 T=T+2
333                 #TEXT
334         ESP←
335                 PO=T
336                 T=T+2
337                 #TEXT
338         PO←
339                 WPSD=T
340                 T=T+2
341                 #TEXT
342         WPSD←
343                 TERM=T
344                 T=T+2
345                 #TEXT
346         TERM←
347                 KU=T
348                 T=T+2
349                 #TEXT
350         KU←
351                 AMP=T
352                 T=T+2
```

```
353             #TEXT
354     AMP←
355             NLEVEL=T
356             T=T+2
357             #TEXT
358     NLEVEL←
359             MESSAGE=T
360             #TEXT
361     SIMULATION OF SDOF SYSTEM WITH NON-LINEAR DAMPING←
362             NU=T
363             T=T+2
364             CON=T
365             T=T+2
366             D=T
367             T=T+2
368             #TEXT
369     D←
370             AFOR=T
371             T=T+2
372             #TEXT
373     AFOR←
374             WFFR=T
375             T=T+2
376             #TEXT
377     WFFR←
378             XIC=T
379             T=T+2
380             #TEXT
381     XIC←
382             YIC=T
383             T=T+2
384             #TEXT
385     YIC←
386             M=T
387             T=T+2
388             W=T
389             T=T+2
390             BW2=T
391             T=T+2
392             BMAX=T
393             T=T+2
394             #TEXT
395     BMAX←
396             J1=T
397             T=T+2
398             #TEXT
399     J1←
400             IJK=T
401             T=T+2
402             NPOINT=T
403             T=T+2
404             JPC=T
405             T=T+2
406             JT=T
407             T=T+2
408             IPOINT=T
409             T=T+2
410             BY=T
411             T=T+2
```

```
412                 #TEXT
413       BY←
414                 BX=T
415                 T=T+2
416                 #TEXT
417       BX←
418                 IK=T
419                 T=T+2
420                 XS=T
421                 T=T+2
422                 BFORCEA=T
423                 T=T+2
424                 XV=T
425                 T=T+2
426                 #TEXT
427       XV←
428                 Y=T
429                 T=T+2
430                 #TEXT
431       Y←
432                 X=T
433                 T=T+2
434                 #TEXT
435       X←
436                 AU=T
437                 T=T+2
438                 AV=T
439                 T=T+2
440                 YDOT=T
441                 T=T+2
442                 #TEXT
443       YDOT←
444                 BB=T
445                 T=T+2
446                 N=T
447                 T=T+2
448                 R=T
449                 T=T+2
450                 KFR=T
451                 T=T+300
452                 BM=T
453                 T=T+2
454                 #TEXT
455       BM←
456                 RF=T
457                 T=T+2
458                 #TEXT
459       RF←
460                 RX=T
461                 T=T+2
462                 #TEXT
463       RX←
464                 XLIN=T
465                 T=T+2
466                 #TEXT
467       XLIN←
468                 X4=T
469                 T=T+2
470                 #TEXT
```

```
471     X4←
472             KUR=T
473             T=T+2
474             #TEXT
475     KUR←
476             AB=T
477             T=T+4
478             JK=T
479             T=T+2
480             IS=T
481             T=T+2
482             SW=T
483             T=T+2
484             GFORCEA=T
485             T=T+2
486             #TEXT
487     GFORCE←
488             LR=T
489             T=T+2
490             SM=T
491             T=T+2
492             J=T
493             +0
494             U=T
495             +0
496             I=T
497             +0
498             K=T
499             +0
500             DEBUG
501     L10=T
502     START=T
503             S2WD            (SET 2WORD
504             GET /*1
505             CLA
506             STO DU
507             GET /1
508             STO DL
509             STI ITEXTIO     (TEXT O/P
510             SWB
511             (SET SWB TO 0   FOR VDU INPUT
512             (           SET SWB TO 2 FOR FAST PAPER READER
513             STI IPERIN      (T/T  I/P
514             GET /1
515             STI IPEROUT       (LPT O/P
516             GET /0
517             STI II4         (TABULAR O/P
518             NL
519             JSI IPRINT
520             +MESSAGE
521             NL
522             GET /0
523             STI IPEROUT     (LPT O/P
524     L20=T
525             ASK,SD
526             NL
527             ASK,ESPN
528             NL
529             ASK,PO
```

```
530             NL
531             ASK,WPSD
532             NL
533             ASK,TERM
534             NL
535             ASK,KU
536             NL
537             ASK,NLEVEL
538             NL
539             ASK,AFOR
540             NL
541             ASK,ESP
542             NL
543             (------ SET UP TERM
544             FLGT,C19
545             FLST,TERM       (TERM=C19
546             (---- SET UP NLEVEL
547             FLGT,TERM
548             FLDV,C6
549             FLMY,C1
550             FLST,NUMB       (NUMB=TERM*2/C6
551             FLGT,C1
552             FLDV,C12
553             FLST,WL1        (WL1=2/5
554             FLGT,NUMB
555             FLSB,C3
556             FLST,CINT       (CINT=(NUMB-1)
557             JSI ILOG
558             FLMY,WL1
559             JSI IEXP
560             FLMY,C15
561             FLSB,C1
562             FLST,NLEVEL     (NLEVEL=1.87(NUMB-1)**2/5
563             FLGT,C5         (ZEROISE AB
564             PUT,AB./1
565             PUT,AB./2
566             FLTINT.NLEVEL           (ZEROISE KFR
567             STO I
568             FLGT,C5
569     LA6=T
570             PUT,KFR,I
571             DEC I
572             JPU LA6
573             FLTINT.NLEVEL       (ZEROISE LCO
574             STO I
575             FLGT,C5
576     LA16=T
577             PUT,LCO,I
578             DEC I
579             JPU LA16
580     L30=T
581             FLGT,C5
582             FLST,RF         (RF=0
583             FLGT,C5
584             FLST,NU         (NU=0
585             FLGT,AW2
586             FLST,WPSD
587             FLGT,C1
588             FLST,KU
```

```
589                FLGT,C20
590                FLST,P0          (P0=C20
591                FLGT,C17
592                FLST,AFOR        (AFOR=0.196
593                FLGT,C16
594                FLST,Sn          (Sn=0.00215
595                FLGT,C5
596                FLST,A1.1
597                FLGT,C5
598                FLST,A12
599                FLGT,C5
600                FLST,NnP
601                FLGT,C5
602                FLST,NMS
603                FLGT,C5
604                FLST,RATIO
605                FLGT,C2
606                FLMY,WPSD
607                JSI ISQT
608                FLST,D           (D=SQRT(628.4*WPSD)
609                FLGT,C4
610                FLST,WFFR        (WFFR=6
611           L35=T
612                FLGT,C5
613                FLST,XIC         (XIC=0
614                FLGT,C5
615                FLST,YIC         (YIC=0
616           L40=T
617                FLGT,C6
618                FLDV,C1
619                FLST,&CI         (CI=0.005
620                FLGT,C3
621                FLST,&SC         (SC=1
622                FLGT,C1
623                FLST,KII
624                FLGT,C3
625                FLST,IS
626                ICST,YIC,/1      (A3(1)=YIC
627                ICST,XIC,/2      (A3(2)=XIC
628           L45=T
629                FLGT,C5
630                FLST,M           (M=0
631           L50=T
632                     FLGT,C1
633                     FLST,&NI    (NI=2
634                     FLGT,C7
635                     FLMY,WFFR
636                     FLST,W      (W=6.284*WFFR
637                     FLGT,C1
638                     FLMY,Sn
639                     FLMY,W
640                     FLST,BW2    (BW2=2*Sn*W
641                     FLGT,C5
642                     FLST,BMAX   (BMAX=0
643                     FLGT,C5
644                     FLST,J1     (J1=0
645                     FLGT,C5
646                     FLST,IJK    (IJK=0
647                     FLGT,C5
```

```
648             FLST,X4          (X4=0
649             FLGT,C5
650             FLST,KUR         (KUR=0
651             FLGT,WPSD
652             FLMY,PI
653             FLDV,C1
654             FLDV,SD
655             FLST,WI2
656             FLGT,W
657             FLMY,W
658             FLMY,W
659             FLST,WI1
660             FLGT,WI2
661             FLDV,WI1
662             JSI ISQT
663             FLST,XIIN
664             FLGT,XIIN
665             FLMY,AFOR
666             FLST,XIIN
667             ( --------CALCULATE ESP FROM ESPN----------------
668             FLGT,W
669             FLMY,XIIN
670             JSI ILOG
671             FLMY,PO
672             JSI IEXP
673             FLST,WI1
674             FLGT,ESPN
675             FLDV,WI1
676             FLST,ESP
677             (---- IF ESPN IS USED IN INPUT, SET ESP=/ HERE
678             FLGT,XIIN
679             FLMY,C1
680             FLMY,C1
681             FLST,AMP
682             FLGT,AMP
683             FLMY,C1
684             FLDV,NIEVEL
685             FLST,CON         (CON=2*AMP/NLEVEL
686     L60=T
687             FLGT,CR
688             FLST,NPOINT      (NPOINT=1024
689             FLGT,C3
690             FLST,JPC         (JPC=1
691             FLGT,C5
692             FLST,JT          (JT=0
693             FLGT,CR
694             FLST,IPOINT      (IPOINT=0
695             FLGT,C5
696             FLST,BY          (BY=0
697     L70=T
698             FLGT,C5
699             FLST,BX          (BX=0
700             FLGT,C3
701             FLST,IK          (IK=1
702     L80=T
703              GET /1
704             STI IPFROUT       (LPT O/P
705             (-------- SET UP FOG
706             GET LOCD
```

```
707             ADD LOCE
708             STO T+3
709             GET LOCC
710             ADD LOCB
711             +0
712             TYPE,XTC
713             NL
714             TYPE,YTC
715             NL
716             TYPE,SD
717             NL
718             TYPE,WFFR
719             NL
720     L90=T
721             TYPE,AFOR
722             NL
723             TYPE,ESP
724             NL
725             TYPE,ESPN
726             NL
727             TYPE,WDSD
728             NL
729             TYPE,PD
730             NL
731             TYPE,&CI
732             NL
733             TYPE,&SC
734             NL
735             TYPE,TERM
736             NL
737             TYPE,D
738             NL
739             TYPE,AMP
740             NL
741     L110=T
742             TYPE,NIEVEL
743             NL
744             TYPE,KU
745             NL
746             GET LOCD
747             ADD LOCE
748             STO T+3
749             GET LOCC
750             ADD LOCA
751             +0
752             NL
753             JSI ISEGINT    (SEGMENT INITIALISATION
754             JSI ISETUP       (SETUP J1.RF,WDSD,XV,KUR
755             (              SETUP NMS,ESPN
756             +6
757             +J1
758             +RF
759             +WPSD
760             +XV
761             +KUR
762             +NMS
763             HEADING         (O/P HEADING
764             NL
765             JSI ISETUP    (SETUP XLIN,RX,BMAX,RV,BX
```

```
825             FLGT,AFOR
826             FLMY,GFORCE
827             FLAD,AU
828             FLST,AU         (AU=AU+AFOR*GFORCE
829             FLGT,AU
830             FLST,YDOT       (YDOT=AU
831     L200=T
832             DERST,YDOT,/1   (A1(1)=YDOT
833             DERST,Y,/2      (A1(2)=Y
834             GTI 116
835             JUMP,L160,L210,L210     (IF(16),160,210,210
836     L210=T
837             FLGT,XIIN
838             FLMY,C1
839             FLMY,C1
840             FLST,WI1
841             FLGT,X
842             FLDV,WI1
843             FLST,XNOR
844             FLGT,Y
845             FLDV,WI1
846             FLDV,W
847             FLST,YNOR
848             FLGT,YDOT
849             FLDV,WI1
850             FLDV,W
851             FLDV,W
852             FLST,ANOR
853             FLGT,GFORCE
854             FLDV,D
855             FLDV,C1
856             FLDV,C1
857             FLST,GNOR
858             JPS &DACOUT
859             +XNOR
860             +1
861             JPS &DACOUT
862             +YNOR
863             +2
864             JPS &DACOUT
865             +ANOR
866             +3
867             JPS &DACOUT
868             +GNOR
869             +4
870             GET /-1
871             STIII5
872             FLGT,X
873             FLSB,BMAX
874             FLST,BR         (BB=X-BMAX
875             FLGT,BR
876             GMA
877             JUMP,L240,L240,L230     (IF(BB),240,240,230
878     L230=T
879             FLGT,X
880             FLST,BMAX       (BMAX=X
881     L240=T
882             FLGT,X
883             FLDV,CON
```

```
884             FLST,WI2
885             FLGT,NIEVEL
886             FLDV,C1
887             FLAD,WI2
888             FLAD,C3
889             FLST,WI2
890             FLTINT,WL2
891             INTFLT,N          (N=FITR(X/CON+NLEVEL/2+1-0.5)
892     L245=T
893             FLGT,X
894             JSI IFIAB
895             FLSB,AMP
896             GMA
897             JUMP,L270,L250,L250       (IF(FAB(X)-AMP),270,250,250
898     L250=T
899             FLGT,X
900             FLSB,AMP
901             GMA
902             JUMP,L310,L260,L260       (IF(X-AMP),310,260,260
903     L260=T
904             FLTINT,N
905             SUB /1
906             INTFLT,N          (N=N-1
907             JPU L310                  (G=310
908     L270=T
909             FLGT,X
910             FLDV,CON
911             FLST,WI2
912             FLTINT,WL2
913             INTFLT,WL2
914             FLGT,WI2
915             FLMY,CON
916             FLSB,X
917             FLNG
918             GMA
919             JUMP,L310,L280,L310       (IF(X-FITR(X/CON),310,280,310
920     L280=T
921             GET ILAST
922             ADD /1
923             STO ILAST
924             AND /*1
925             JPZ L300
926             JPU L310
927     L300=T
928             FLTINT,N
929             SUB /1
930             INTFLT,N          (N=N-1
931     L310=T
932             FLTINT,N
933             STO WL2
934             TAKE,KFR,WL2
935             FLAD,C3
936             PUT,KFR,WL2       (KFR(N)=KFR(N)+1
937     L311=T
938             FLGT,X
939             FLST,AL2
940     L312=T
941             FLGT,AI2
942             FLSB,AI1
```

```
943             GMA
944             JUMP,L318,L318,L313
945     L313=T
946             FLGT,AI2
947             FLDV,CON
948             FLST,WI2
949             FLGT,NIEVEL
950             FLDV,C1
951             FLAD,WI2
952             FLAD,C3
953             FLST,WI2
954             FLTINT. WL2
955             INTFLT,N2
956             FLGT,AI1
957             FLDV,CON
958             FLST,WI2
959             FLGT,NIEVEL
960             FLDV,C1
961             FLAD,WL2
962             FLAD,C3
963             FLST,WI2
964             FLTINT.WL2
965             INTFLT.N1
966             FLGT,N2
967             FLSB,N1
968             FLST,ND
969             GMA
970             JUMP,L318,L318,L315
971     L315=T
972             FLTINT.ND
973             STO I
974     L314=T
975             FLTINT.N1
976             ADD I
977              STO J
978             TAKE,LCO,J
979             FLAD,C3
980             PUT,LCO,J
981             DEC I
982             JPU L314
983     L318=T
984             FLGT,AI2
985             FLST,AI1
986             FLGT,X
987             FLMY,X
988             FLAD,XS
989             FLST,XS          (XS=XS+X↑2
990             FLGT,X
991             FLMY,X
992             FLMY,X
993             FLMY,X
994             FLAD,X4
995             FLST,X4      (X4=X4+X**4
996     L320=T
997             FLGT,GFORCE
998             FLMY,GFORCE
999             FLAD,BFORCEA
1000            FLST,BFORCEA          (BFORCEA+GFORCE↑2
1001    L330=T
```

```
1002            FLGT,J1
1003            FLAD,C3
1004            FLST,J1         (J1=J1+1
1005            FLGT,IJK
1006            GMA
1007            JUMP,L340,L340,L390         (IF(IJK),340,340,390
1008    L340=T
1009            FLGT,XS
1010            FLDV,J1
1011            JSI ISQT
1012            FLST,RX                     (RX=FSQT(XS/J1)
1013            FLDV,XI IN
1014            FLST,RATIO
1015            FLMY,RATIO
1016            FLST,NMS        (NMS=(RX/XI IN)**2
1017            FLGT,BFORCEA
1018            FLDV,J1
1019            JSI ISQT
1020            FLST,RF             (RF=FSQT(BFORCEA/J1)
1021    L350=T
1022            FLGT,&TIME
1023            FLSB,C3
1024            GMA
1025            JUMP,L380,L360,L360     (IF(TIME-1),380,360,380
1026    L360=T
1027            FLGT,XS
1028            FLMY,XS
1029            FLST,WL1
1030            FLGT,X4
1031            FLDV,WL1
1032            FLMY,J1
1033            FLST,KUR        (KUR=<X**4>/<X**2>**2
1034            FLGT,XS
1035            FLDV,J1
1036            FLST,XV                 (XV=XS/J1
1037            FLGT,XV
1038            PUT,AB,/2                   (AR(2)=XV
1039            TAKE,AR,/2
1040            FLMY,IK
1041            FLST,WL2
1042            TAKE,AR,/1
1043            FLST,WL3
1044            FLGT,IK
1045            FLSB,C3
1046            FLMY,WL3
1047            FLSB,WL2
1048            FLNG
1049            FLST,BY             (BY=IK*AB(2)-(IK-1)*AB(1)
1050    L370=T
1051            FLGT,BY
1052            JSI  ISQT
1053            FLST,BX             (BX=FSQT(BY)
1054            TAKE,AR,/2
1055            PUT,AB,/1           (AB(1)=AB(2)
1056            FLGT,IK
1057            FLAD,C3
1058            FLST,IK         (IK=IK+1
1059            JPU L390
1060    L380=T
```

```
1061            FLGT,C18
1062            GMA
1063            JUMP,L390,L390,L381     (IF C18=0 NO OUTPUT AT THIS PO
1064    L381=T
1065            JSI ISETUP
1066            +6
1067            +J1
1068            +RF
1069            +WPSD
1070            +XV
1071            +KUR
1072            +NMS
1073            DATAOUT
1074            NL
1075            JSI ISETUP
1076            +6
1077            +XLIN
1078            +RX
1079            +BMAX
1080            +BY
1081            +BX
1082            +NOP
1083            DATAOUT
1084            NL                      (OUT J1,RF,WPSD,XV,RX,BM,BY,BX
1085    L390=T
1086            FLTINT,IJK
1087            ADD /1
1088            INTFLT,IJK      (IJK=IJK+1
1089            FLGT,J1
1090            FLSB,C10
1091            GMA
1092            JUMP,L410,L410,L400     (IF(J1-1025),410,410,400
1093    L400=T
1094            FLGT,IJK
1095            FLSB,CR
1096            GMA
1097            JUMP,L430,L420,L430     (IF(IJK-1024),430,420,430
1098    L410=T
1099            FLGT,IJK
1100            FLSB,C11
1101            GMA
1102            JUMP,L430,L420,L430     (IF(IJK-1023),430,420,430
1103    L420=T
1104            FLGT,C5
1105            FLST,IJK                (IJK=0
1106            FLGT,C5
1107            FLST,JPC                (JPC=0
1108    L430=T
1109            FLGT,&TIME
1110            FLSB,TERM
1111            GMA
1112            JUMP,L130,L440,L440     (IF(TIME-TERM),130,440,440
1113    L440=T
1114            (--- IF C18=0 OUTPUT IS PRODUCED
1115            FLGT,C18
1116            GMA
1117            JUMP,L441,L441,L442
1118    L441=T
1119            JSI ISETUP
```

```
1120                +6
1121                +J1
1122                +RF
1123                +WPSD
1124                +XV
1125                +KUR
1126                +NMS
1127                DATAOUT
1128                NL
1129                JSI ISFTUP
1130                +6
1131                +XLIN
1132                +RX
1133                +BMAX
1134                +BY
1135                +BX
1136                +NOP
1137                DATAOUT
1138                NL
1139          L442=T
1140                FLTINT,NLEVEL
1141                STO I
1142          LA1=T
1143                TAKE,KFR,I
1144                FLDV,CON
1145                FLDV,J1
1146                FLMY,XIIN
1147                PUT,KFR,I
1148                DEC I
1149                JPU LA1
1150                FLGT,NLEVEL
1151                FLDV,C1
1152                FLSB,C3
1153                FLST,LN                 (LN=NLEVEL/2-1
1154                FLTINT,NLEVEL
1155                STO I
1156          LA11=T
1157                TAKE,LCO,I
1158                FLDV,CON
1159                FLDV,NOP
1160                FLDV,WFFR
1161                FLST,WL1
1162                FLGT,LN
1163                FLMY,C1
1164                FLAD,C3
1165                FLDV,C1
1166                FLMY,CON
1167                FLDV,XLIN
1168                FLST,WI2
1169                FLMY,WL2
1170                FLDV,C1
1171             JSI IEXP
1172                FLMY,WI1
1173                PUT,LCO,I
1174                FLGT,LN
1175                FLSB,C3
1176                FLST,LN
1177                GMA
1178                JPN LA18
```

```
1179            DEC I
1180            JPU LA11
1181    LA18=T
1182    L450=T
1183            GET /0                          (No TEXT ON O/P
1184            STI ITFXTIO
1185            FLTINT,NLEVEL
1186            STO J
1187            GET /1
1188            STO I
1189    LA4=T
1190            GET /5
1191            STO K
1192    LA2=T
1193            TAKE,KFR,I
1194            FLST,WI2
1195            TYPE,WI2
1196            INC I
1197            DEC K
1198            JPU LA2
1199            NL
1200            GET J
1201            SUB /5
1202            STO J
1203            JPZ LA3
1204            JPU LA4
1205    LA3=T
1206            NL  (F I=0,5,NLEVEL;T KFR(I+1),KFR(I+2),KFR(I+3),KFR(I+
1207            TYPE,NOP
1208            NL
1209            GET /0
1210            STI ITFXTIO
1211            FLTINT,NLEVEL
1212            STO J
1213            GET /1
1214            STO I
1215    LA14=T
1216            GET /5
1217            STO K
1218    LA12=T
1219            TAKE,LC0,I
1220            FLST,WI2
1221            TYPE,WI2
1222            INC I
1223            DEC K
1224            JPU LA12
1225            NL
1226            GET J
1227            SUB /5
1228            STO J
1229            JPZ LA13
1230            JPU LA14
1231    LA13=T
1232            NL
1233    L460=T
1234            JPU L10         (G 10
1235            (-------------------------------------------------------
1236    L1180=T
1237            FLGT,IS
```

```
1238            GMA
1239            JUMP,L1240,L1240,L1190  (IF(IS),1240,1240,1190
1240    L1100=T
1241            FLGT,D
1242            GMA
1243            JUMP,L1250,L1250,L1200 (IF(D),1250,L1250,L1200
1244    L1200=T
1245            FLGT,C5
1246            FLST,SM         (SM=0
1247    L1210=T
1248              GET /12
1249              STO I
1250    LA5=T
1251            JPS AUXSR         (F I=1,12:D 1240/1300
1252            DEC I
1253            JPU LA5
1254    L1220=T
1255            FLGT,SM
1256            FLSB,C13
1257            FLMY,D
1258            FLDV,C14
1259            FLAD,M
1260            FLST,GFORCEA   (GFORCE=M+(D*(SM-503316))/8388607
1261    L1230=T
1262            JPU L140        (G 140
1263    L1240=T
1264            HLT             (QUIT
1265    L1250=T
1266            HLT             (QUIT
1267    (-------------------------------------------------------
1268            LKJ
1269            FRAN=T
1270            &FRAN=T         (RANDOM NUMBER GENERATOR
1271            +0
1272            GET DL
1273            MPY
1274            +BL
1275            STO CU          (DL*BL
1276            SWP
1277            STO CL
1278            GET DL
1279            MPY
1280            +BU
1281            SWP
1282            ADD CU
1283            STO CU
1284            GET DU
1285            MPY
1286            +BL
1287            SWP
1288            ADD CU
1289            STO CU
1290            GET /9
1291            DLL
1292            +CU
1293            DRL
1294            +CU
1295            GET CU
1296             STO DU
```

```
1297            GET CL
1298            STO DL
1299            FLLT,C11
1300            GMA
1301            JPZ T+2
1302            JPU LA7
1303            FLGT,ONE
1304    LA7=T
1305            FLDV,CONST      (4194303.5
1306            FLSB,ONE
1307            FLST,&RANDOM
1308            JPU FRAN-1
1309    (-------------------------------------------------------
1310            LKJ
1311            AUXSR=T
1312            +0
1313    L1260=T
1314            JSI IFRAN
1315            FLAD,C3
1316            FLMY,C9
1317            FLMY,C14
1318            FLST,LR         (LR=0.5*(FRAN(0)+1)*8338607
1319    L1280=T
1320            FLGT,LR
1321            GMA
1322            JUMP,L1290,L1290,L1300   (IF(LR)1290,1290,1300
1323    L1290=T
1324            FLGT,C3
1325            FLST,LR          (LR=1
1326    L1300=T
1327            FLGT,SM
1328            FLAD,LR
1329            FLST,SM         (SM=SM+LR
1330            JPU AUXSR-1
1331    #END
1332    #FIN
```

TYPICAL OUTPUT FROM DIGITAL SIMULATION PROGRAM

XIC= 0.00000
YIC= 0.00000
SD= .00500
WFFR= 6.00000
AFOR= .19600
ESF= .00000
ESFN= .10000
WPSD= 1000.00000
FO= 6.00000
CI= .00500
SC= 1.00000
TERM= 1024.20020
D= 792.71680
AMP= 1.89806
NLEVEL= 100.00000
KU= 2.00000

TIME	J1	RF	WPSD	XV	KUR	NMS
0.00000	1.00000	38.51738	1000.00000	0.00000	0.00000	4.44120
0.00000	.47452	1.00000	0.00000	0.00000	0.00000	0.00000
40.95605	8192.00000	787.39307	1000.00000	.11012	2.25765	.48905
40.95605	.47452	.33184	.81648	.11012	.33184	0.00000
81.95605	1.63840 E 04	787.51514	1000.00000	.14296	2.26541	.63489
81.95605	.47452	.37809	.98881	.17579	.41928	0.00000
122.95605	2.45760 E 04	792.28003	1000.00000	.14991	2.30892	.66577
122.95605	.47452	.38718	1.03036	.16381	.40474	0.00000
163.95605	3.27680 E 04	790.66724	1000.00000	.14093	2.38049	.62589
163.95605	.47452	.37540	1.03036	.11399	.33762	0.00000
204.95605	4.09600 E 04	793.77637	1000.00000	.13879	2.39999	.61641
204.95605	.47452	.37255	1.03036	.13026	.36091	0.00000
245.95605	4.91520 E 04	794.37402	1000.00000	.13809	2.38181	.61330
245.95605	.47452	.37161	1.03036	.13459	.36687	0.00000
286.95605	5.73440 E 04	796.14966	1000.00000	.13691	2.37242	.60804
286.95605	.47452	.37001	1.03036	.12981	.36029	0.00000
327.95605	6.55360 E 04	795.18335	1000.00000	.13047	2.43447	.57943

327.95605	.47452	.36120	1.03036	.08537	.29218	0.00000
368.95605	7.37280 E 04	795.95166	1000.00000	.12396	2.51563	.55054
368.95605	.47452	.35208	1.03036	.07193	.26819	0.00000
409.95605	8.19200 E 04	793.75439	1000.00000	.12311	2.49371	.54676
409.95605	.47452	.35087	1.03036	.11543	.33975	0.00000
450.95605	9.01120 E 04	793.06323	1000.00000	.12513	2.46493	.55574
450.95605	.47452	.35374	1.03036	.14535	.38125	0.00000
491.95605	9.83040 E 04	792.90137	1000.00000	.12594	2.45030	.55934
491.95605	.47452	.35489	1.03036	.13488	.36727	0.00000
532.44482	1.06496 E 05	793.72266	1000.00000	.12773	2.41235	.56727
532.44482	.47452	.35739	1.03036	.14913	.38617	0.00000
572.44482	1.14688 E 05	794.32642	1000.00000	.12849	2.40562	.57067
572.44482	.47452	.35846	1.03036	.13846	.37210	0.00000
612.44482	1.22880 E 05	794.64917	1000.00000	.12837	2.40599	.57011
612.44482	.47452	.35829	1.03036	.12661	.35582	0.00000
652.44482	1.31072 E 05	795.13037	1000.00000	.13008	2.41690	.57773
652.44482	.47452	.36067	1.03036	.15581	.39473	0.00000
692.44482	1.39264 E 05	794.47827	1000.00000	.12842	2.42922	.57036
692.44482	.47452	.35836	1.03036	.10187	.31917	0.00000
732.44482	1.47456 E 05	794.21069	1000.00000	.12995	2.42969	.57713
732.44482	.47452	.36049	1.03036	.15589	.39483	0.00000
772.44482	1.55648 E 05	794.41040	1000.00000	.13037	2.42995	.57901
772.44482	.47452	.36107	1.03036	.13799	.37147	0.00000
812.44482	1.63840 E 05	794.83594	1000.00000	.13092	2.42919	.58145
812.44482	.47452	.36183	1.03036	.14133	.37593	0.00000
852.44482	1.72032 E 05	794.15039	1000.00000	.13120	2.43808	.58268
852.44482	.47452	.36221	1.03036	.13675	.36980	0.00000
892.44482	1.80224 E 05	794.39746	1000.00000	.13178	2.43523	.58527
892.44482	.47452	.36302	1.03036	.14404	.37953	0.00000

932.44482	1.88416 E 05	794.21118	1000.00000	.13054	2.44979	.57974
932.44482	.47452	.36130	1.03036	.10313	.32114	0.00000
972.44482	1.96608 E 05	793.89966	1000.00000	.13280	2.43617	.58979
972.44482	.47452	.36442	1.03036	.18485	.42994	0.00000
1012.44482	2.04800 E 05	793.62109	1000.00000	.13332	2.43012	.59211
1012.44482	.47452	.36513	1.03036	.14585	.38190	0.00000

0.00000	0.00000	0.00000	0.00000	0.00000	
0.00000	0.00000	0.00000	0.00000	0.00000	
0.00000	0.00000	0.00000	0.00000	0.00000	
0.00000	0.00000	0.00000	0.00000	0.00000	
.00006	.00012	.00060	.00157	.00308	
.00754	.01478	.02630	.03879	.05737	
.07776	.10153	.13368	.14394	.17507	
.17998	.22085	.25753	.27937	.30796	
.33565	.35309	.37402	.39706	.42922	
.43724	.46029	.46734	.46789	.46983	NORMALISED
.47917	.47223	.46282	.46155	.44104	PROBABILITY
.42940	.40195	.38060	.34965	.33402	DENSITY
.30314	.28667	.25216	.22894	.19636	FUNCTION
.16843	.14689	.12807	.10418	.07957	
.05966	.04253	.02491	.01418	.00730	
.00392	.00097	.00012	0.00000	0.00000	
0.00000	0.00000	0.00000	0.00000	0.00000	
0.00000	0.00000	0.00000	0.00000	0.00000	
0.00000	0.00000	0.00000	0.00000	0.00000	
0.00000	0.00000	0.00000	0.00000	0.00000	
0.00000	0.00000	0.00000	0.00000	0.00000	
0.00000	0.00000	0.00000	0.00000	0.00000	
0.00000	0.00000	0.00000	0.00000	0.00000	
0.00000	0.00000	0.00000	0.00000	0.00000	
.00237	.00198	.01326	.01819	.03923	
.07215	.12677	.19683	.26190	.33905	
.41873	.51130	.58489	.63540	.69404	
.73373	.77716	.81687	.84989	.87707	
.90413	.92062	.93769	.95364	.96910	NORMALISED
.97952	.98812	.99573	.99816	.99867	LEVEL CROSSING
.99962	.99508	.99259	.98375	.96927	RATE
.95761	.94051	.91805	.90079	.87906	
.85131	.81228	.77881	.73253	.68247	
.63686	.58935	.51402	.43767	.35699	
.27048	.18925	.11803	.07723	.03804	
.01399	.00166	0.00000	0.00000	0.00000	
0.00000	0.00000	0.00000	0.00000	0.00000	
0.00000	0.00000	0.00000	0.00000	0.00000	
0.00000	0.00000	0.00000	0.00000	0.00000	
0.00000	0.00000	0.00000	0.00000	0.00000	

APPENDIX H

The solution of the Fokker-Planck equation yields a joint probability density function as

$$p(X\dot{X}) = C\ EXP\left[-\frac{\gamma}{\pi S_o}\left(\left(\frac{\dot{X}^2+\omega_o^2X^2}{2}\right)+\frac{2\epsilon_o}{(n+2)}\left(\frac{\dot{X}^2+\omega_o^2X^2}{2}\right)^{\frac{n+2}{2}}\right)\right] \quad (1)$$

where C is a normalising constant obtained from

$$\int_{-\infty}^{\infty} P\,(X\dot{X})dXd\dot{X} = 1 \quad (2)$$

Substituting equation (1) in (2) yields

$$1 = \int_{-\infty}^{\infty}\int_{\infty}^{\infty} C\ e^{-\frac{\gamma}{\pi S_o}\left[\left(\frac{\dot{X}^2+\omega_o^2X^2}{2}\right)+\left(\frac{2\epsilon_o}{(n+2)}\right)\left(\frac{\dot{X}^2+\omega_o^2X^2}{2}\right)^{\frac{n+2}{2}}\right]} dXd\dot{X} \quad (3)$$

Let $\omega_o X = Y$

$\dot{X} = Z$

$\therefore\ dXd\dot{X} = \omega_o dydZ$

$$1 = \frac{1}{\omega_o}\int_{-\infty}^{\infty}\int_{-\infty}^{-\infty} C\ e^{-\frac{\gamma}{\pi S_o}\left[\left(\frac{Z^2+Y^2}{2}\right)+\left(\frac{2\epsilon_o}{(n+2)}\right)\left(\frac{Z^2+Y^2}{2}\right)^{\frac{n+2}{2}}\right]} dYdZ \quad (4)$$

Let $Z = r\,Sin\,(\theta)$

$Y = r\,Cos\,(\theta)$

$dYdZ = r\,d\theta\,dr$

$$\therefore\ 1 = \frac{C}{\omega_o}\int_0^{2\pi} d\theta \int_0^{\infty} r\ e^{-\frac{\gamma}{\pi S_o}\left(\left(\frac{r^2}{2}\right)+\left(\frac{\epsilon_o}{(n+2)}\right)\left(r^2/_2\right)^{\frac{n+2}{2}}\right)} dr$$

$$= \frac{2\pi}{\omega_o} C \int_o^{\infty} r\ e^{-\frac{\gamma}{\pi S_o}\left(\left(r^2/_2\right)+\left(\frac{2\epsilon_o}{(n+2)}\right)\left(\gamma^2/_2\right)^{\frac{n+2}{2}}\right)} dr$$

$$\therefore\ C = \frac{\omega_o}{2\pi}\int_o^{\infty} r\ e^{-\frac{\gamma}{\pi S_o}\left(\left(r^2/_2\right)+\left(\frac{2\epsilon_o}{(n+2)}\right)\left(r^2/_2\right)^{\frac{n+2}{2}}\right)} dr \quad (5)$$

The statistical moments are given by

$$E(X^m) = \int_{-\infty}^{\infty}\int_{-\infty}^{\infty} X^m p(X\dot{X})\,dX\,d\dot{X} \qquad (6)$$

$$= C \int_{-\infty}^{\infty}\int_{\infty}^{\infty} X^m e^{-\frac{\gamma}{\pi S_o}\left(\left(\frac{\dot{X}^2+\omega_e^2X^2}{2}\right)+\frac{2\epsilon_o}{(n+2)}\left(\frac{\dot{X}^2+\omega_e^2X^2}{2}\right)^{\frac{n+2}{2}}\right)} dX\,d\dot{X}$$

Introducing change of variables yields

$$E(X^m) = \frac{2\pi C}{\omega_o^3}\int_0^{2\pi} \mathrm{Cos}^m\theta\,d\theta \int_0^{\infty} r^{m+1} e^{-\frac{\gamma}{\pi S_o}\left((r^2/2)+\frac{2\epsilon_o}{(n+2)}(r^2/2)^{\frac{n+2}{2}}\right)} dr \qquad (7)$$

Substituting the value of C from (5) yields

$$E(X^m) = \frac{1}{\omega_e^2}\frac{\int_0^{2\pi}\mathrm{Cos}^m\theta\,d\theta\int_0^{\infty} r^{m+1} e^{-\frac{\gamma}{\pi S_o}\left((r^2/2)+\frac{2\epsilon_o}{(n+2)}(r^2/2)^{\frac{n+2}{2}}\right)}dr}{\int_0^{\infty} r\,e^{\frac{-\gamma}{\pi}\left((r^2/2)+\left(\frac{2\epsilon_o}{n+2}\right)(r^2/2)^{\frac{n+2}{2}}\right)}dr}$$

$$= \frac{4}{\omega_o^2}\frac{\int_0^{\frac{\pi}{2}}\mathrm{Cos}^m\theta\,d\theta\int_0^{\infty} r^{m+1} e^{-\frac{\gamma}{\pi S_o}\left((r^2/2)+\frac{2\epsilon_o}{(n+2)}(r^2/2)^{\frac{n+2}{2}}\right)}dr}{\int_0^{\infty} re^{-\gamma/\pi S_o\left((r^2/2)+\frac{2\epsilon_o}{(n+2)}(r^2/2)^{\frac{n+2}{2}}\right)}dr}$$

let $\int_0^{\pi/2}\mathrm{Cos}^m\theta\,d\theta = I_m$

$$\therefore\quad E(X^m) = \frac{\frac{4}{\omega_o^2}I_m\int_0^{\infty} r^{m+1}e^{-\frac{\gamma}{\pi S_o}\left((r^2/2)+\frac{2\epsilon_o}{(n+2)}(r^2/2)^{\frac{n+2}{2}}\right)}dr}{\int_0^{\infty} r\;e^{-\frac{\gamma}{\pi S_o}\left((r^2/2)+\frac{2\epsilon_o}{(n+2)}(r^2/2)^{\frac{n+2}{2}}\right)}dr} \qquad (8)$$

The probability density function is converted to non-dimensional variables as follows

$$P(X\dot{X}) = C\, e^{\frac{-\gamma}{\pi S_o}\left[\left(\frac{\dot{X}^2+\omega_o^2X^2}{2}\right) + \frac{2\epsilon_o}{(n+2)}\left(\frac{\dot{X}^2+\omega_o^2X^2}{2}\right)^{\frac{n+2}{2}}\right]} \tag{8}$$

Since $\frac{\gamma}{\pi S_o} = 1/\dot{\delta}_o^2$

$$P(X\dot{X}) = C\, e^{-\left[\frac{1}{2}\left(\left(\frac{\dot{X}}{\sigma_o}\right)^2+\left(\frac{X}{\sigma_o}\right)^2\right)+\frac{2\epsilon_o}{(n+2)}\dot{\sigma}_o^n\left(\frac{1}{2}\left(\left(\frac{X}{\sigma_o}\right)^2+\left(\frac{X}{\sigma_o}\right)^2\right)\right)^{\frac{n+2}{2}}\right]} \tag{9}$$

Substituting the expression for ϵ_o yields

$$P(X\dot{X}) = C\, e^{-\left[\frac{1}{2}\left(\left(\frac{\dot{X}}{\sigma_o}\right)^2+\left(\frac{X}{\sigma_o}\right)^2\right)+\alpha_n\,\epsilon_n^*\left(\frac{1}{2}\left(\left(\frac{\dot{X}}{\sigma_o}\right)^2+\left(\frac{X}{\sigma_o}\right)^2\right)\right)^{\frac{n+2}{2}}\right]} \tag{10}$$

Where $$\alpha_n = \frac{2^{\frac{n+6}{2}}}{(n+2)\,\pi} I_{n+2}$$

and $$\epsilon_n^* = \epsilon\, \sigma_o^n \omega_o^n$$

$C = \dfrac{1}{\int_{-\infty}^{\infty}\int_{-\infty}^{\infty} P(X_1\dot{X})\, dX d\dot{X}}$ is a normalised factor

Let $\left(\frac{X}{\sigma_o}\right) = Y$

$\left(\frac{\dot{X}}{\dot{\sigma}_o}\right) = Z$

$dX d\dot{X} = dY dz\, \sigma_o\, \dot{\sigma}_o$

$$C = \frac{1}{\sigma_o\dot{\sigma}_o\int_{-\infty}^{\infty}\int_{-\infty}^{\infty} e^{-\left[\left(\frac{Y^2+z^2}{2}\right)+\alpha_n\epsilon_n'\left(\frac{Y^2+Z^2}{2}\right)^{\frac{n+2}{2}}\right]} dy dz}$$

Transforming into polar coordinates yields

$$(Y = r \text{ Sin } \theta,\ Z = r \text{ Cos } \theta)$$

$$C = \frac{1}{2\pi \ \dot{\delta}_o \delta_o \int_o^{\infty} r e^{-\left((r^2/2) + \alpha_n \epsilon_n^{*} (r^2/2)^{\frac{n+2}{2}}\right)} dr}$$

$$\therefore \quad P(Y,Z) = \sigma_o \dot{\sigma}_o \ P(X\dot{X})$$

$$P(YZ) = \frac{1}{2\pi} \quad \frac{e^{-\left[\frac{1}{2}(Y^2+z^2)+\alpha_n \epsilon_n^{*}\left(\frac{Y^2+z^2}{2}\right)^{\frac{n+2}{2}}\right]}}{\int_o^{\infty} r e^{-\left[(r^2/2)+\alpha_n \epsilon_n^{*}(r^2/2)^{\frac{n+2}{2}}\right]} dr} \qquad (11)$$

For n=2, the mean square response becomes

$$E(Y^2) = \frac{1}{2} \ \frac{\int_o^{\infty} r^3 \text{EXP}\left[-\left(r^2/2 + \frac{\alpha_2 \epsilon^{*}_2 r^4}{4}\right)\right] dr}{\int_o^{\infty} r \text{ EXP}\left[-\left(r^2/2 + \frac{\alpha_2 \epsilon^{*}_2}{4} r^4\right)\right] dr}$$

Let $a = \frac{1}{2}$

$$b = \frac{\alpha_2 \epsilon^{*}_2}{4}$$

$$\therefore \quad E(Y^2) = \frac{1}{2} \ \frac{\int_o^{\infty} r^3 \text{ EXP}\left[-\left(ar^2 + br^4\right)\right] dr}{\int_o^{\infty} r \text{ EXP}\left[-\left(ar^2 + br^4\right)\right] dr}$$

writting $a r^2 + b r^4$ as $\left(\sqrt{b}\, r^2 + \frac{a}{2\sqrt{2}}\right)^2 - \frac{a^2}{4b}$

and substituting

$$\sqrt{b} \quad r^2 + \frac{a}{\alpha\sqrt{b}} = \theta \qquad rdr = \frac{d\theta}{2\sqrt{b}}$$

yields $$E(Y^2) = \frac{1}{2} \frac{\frac{1}{2\sqrt{b}} \int_{\frac{a}{2\sqrt{b}}}^{\infty} (\theta - \frac{a}{2\sqrt{b}}) \, EXP\left[-\frac{a^2}{4b}\right] EXP\left[-\theta^2\right] d\theta}{\frac{1}{2\sqrt{b}} \int_{\frac{a}{2\sqrt{b}}}^{\infty} EXP\left[-\frac{a^2}{4b}\right] EXP\left[-\theta^2\right] d\theta}$$

$$\frac{2}{\sqrt{\pi}} \int_0^X e^{-u^2} du = erf(X)$$

$$\frac{2}{\sqrt{\pi}} \int_q^{\infty} e^{-u^2} du = \frac{2}{\sqrt{\pi}} \left[\int_0^{\infty} e^{-u^2} du - \int_0^q e^{-u^2} du \right]$$

$$= 1 - \frac{2}{\sqrt{\pi}} \int_0^q e^{-u^2} du$$

$$= 1 - erf(q) = erfc(q)$$

$$\frac{1}{\sqrt{b}} \int_{\frac{a}{2\sqrt{b}}}^{\infty} \theta \, e^{-\theta^2} d\theta - \frac{a}{2b} \int_{\frac{a}{2\sqrt{b}}}^{\infty} e^{-\theta^2} d\theta$$

$$\therefore E(Y^2) = \frac{1}{2} \frac{\frac{1}{2\sqrt{b}} \int_{\frac{a}{2\sqrt{b}}}^{\infty} \theta \, e^{-\theta^2} d\theta - \frac{a}{2b} \int_{\frac{a}{2\sqrt{b}}}^{\infty} e^{-\theta^2} d\theta}{\frac{\sqrt{\pi}}{2} erfc\left(\frac{a}{2\sqrt{b}}\right)}$$

$$= \frac{1}{2} \frac{\frac{1}{\sqrt{b\pi}} \int_{\frac{a}{2\sqrt{b}}}^{\infty} \theta \, e^{-\theta^2} d\theta - \frac{a}{2b} \frac{\sqrt{\pi}}{2} erfc\left(\frac{a}{2\sqrt{b}}\right)}{\frac{\sqrt{\pi}}{2} erfc\left(\frac{a}{2\sqrt{b}}\right)}$$

$$\therefore E(Y^2) = \frac{\frac{1}{2\sqrt{b\pi}} EXP\left[-\frac{a^2}{4b}\right] - \frac{a}{4b} erfc\left(\frac{a}{2\sqrt{b}}\right)}{erfc\left(\frac{a}{2\sqrt{b}}\right)}$$

$$\frac{a^2}{4b} = \frac{4}{4 \alpha_2 \epsilon_2^*} = \frac{1}{\alpha_2 \epsilon_2^*}$$

$$\frac{a}{2\sqrt{b}} = \frac{1}{2\sqrt{\alpha_2 \epsilon_2^*}}$$

$$\frac{a}{4b} = \frac{1}{2\alpha_2 \epsilon_2^*}$$

$$E(Y^2) = \frac{EXP\left[\frac{1}{\alpha_2 \epsilon_2^*}\right]}{\sqrt{\pi \alpha_2 \epsilon_2^*} erfc\left(\frac{1}{2\sqrt{\epsilon_2^* \alpha_2}}\right)} - \frac{1}{2\alpha_2 \epsilon_2^*}$$

LEVEL CROSSING RATIO USING MODIFIED EQUIVALENT NON-LINEAR DIFFERENTIAL EQUATION METHOD (MENL).

The level crossing rate

$$\nu^{+}_{NLM} = \int_{o}^{\infty} \dot{X} P(a,\dot{X}) d\dot{X}$$

$$= \int_{o}^{\infty} \dot{X} C EXP\left[- \frac{2\beta}{(n+2)\pi S_o} \left(\frac{\dot{X}^2+\omega_o^2 X^2}{2}\right)^{\frac{n+2}{2}} \right] d\dot{X}$$

where $$C = \frac{1}{\int_{-\infty}^{\infty}\int_{-\infty}^{\infty} P(X\dot{X}) dX d\dot{X}}$$

$$= \frac{1}{\int_{-\infty}^{\infty}\int_{-\infty}^{\infty} EXP\left[- \frac{2\beta}{(n+2)\pi S_o} \left(\frac{\dot{X}^2+\omega_o^2 X^2}{2}\right)^{\frac{n+2}{2}} \right] dx d\dot{x}}$$

Let $\dot{X} = Y$

$\omega_o X = Z$

$$\therefore \quad C = \frac{}{\int_{-\infty}^{\infty}\int_{-\infty}^{\infty} EXP\left[- \frac{2\beta}{(n+2)\pi S_o} \left(\frac{Y^2+Z^2}{2}\right)^{\frac{n+2}{2}} \right] \frac{dY dZ}{\omega}}$$

Using polar co-ordinates yields

$$\nu^{+}_{NLM} = \frac{\omega_o}{2\pi} \frac{\int_{o}^{\infty} \dot{X}\, EXP\left[- \frac{2\beta}{(n+2)\pi S_o} \left(\frac{\dot{X}^2+\omega_o^2 X}{2}\right)^{\frac{n+2}{2}} \right] d\dot{X}}{\int_{o}^{\infty} r\, EXP\left[- \frac{2\beta}{(n+2)\pi S_o} \left(r/2\right)^{\frac{n+2}{2}} \right] dr}$$

$$\text{Let} \quad \left(\frac{2\beta}{(n+2)\pi S_o}\right)^{\frac{2}{n+2}} \left(\frac{\dot{X}^2 + \omega_c^2 a^2}{2}\right) = T$$

$$\therefore \quad \dot{X}d\dot{X} = \frac{dT}{\left(\frac{2\beta}{(n+2)\pi S_o}\right)^{\frac{2}{n+2}}}$$

$$\therefore \quad \nu^+_{NLM} = \frac{\omega_o}{2\pi} \frac{\int_A^\infty \text{EXP}\left[-T^{\frac{n+2}{2}}\right] dT}{\int_o^\infty r\ \text{EXP}\left[-\frac{2\beta}{(n+2)\pi S_o}\left(\frac{r^2}{2}\right)^{\frac{n+2}{2}}\right] dr}$$

$$\text{where} \quad A = \left(\frac{2\beta}{(n+2)\pi S_o}\right)^{\frac{2}{n+2}} \frac{\omega_o^2 a^2}{2}$$

For Linear system

$$\nu_L^+ = \frac{\omega_o}{2\pi} e^{-\frac{a^2}{2\sigma_o}}$$

$$\therefore \quad \frac{\nu^+_{NLM}}{\nu^+_L} = e^{\frac{\lambda^2}{2}} \frac{\int_A^\infty \text{EXP}\left[-T^{\frac{n+2}{2}}\right] dT}{\int_o^\infty r\ \text{EXP}\left[-\frac{2\beta}{(n+2)\pi S_o}(r^2/2)^{\frac{n+2}{2}}\right] dr}$$

In the non-dimensional form it becomes

$$\frac{\nu^+_{NLM}}{\nu^+_L} = e^{\frac{\lambda^2}{2}} \frac{\int_o^\infty Y\ \text{EXP}\left[-\frac{2\beta}{(n+2)}\left(\frac{Y^2+\eta^2}{2}\right)^{\frac{n+2}{2}}\right] dY}{\int_o^\infty r\ \text{EXP}\left[-\frac{2\beta}{(n+2)}(r^2/2)^{\frac{n+2}{2}}\right] dr}$$

APPENDIX I

TORQUE - TENSION CHARACTERISTICS

Since the interface pressure at the joint is an important parameter influencing the damping produced by the joint, it wasthought desirable to obtain some idea of the variation in the bolt tension for a given value of tighting torque. Figure (I1) shows the apparatus used in studying the torque-tension behaviour of the nut and bolt assemblies. Figure (I2) shows the tension versus torque curve measured with this apparatus. The curve shown pertain to $\frac{1}{2}$ inch stainless steel bolt with washers under bolt head and nut. The torque was measured with a torque wrench, with which the nuts were tightened on the full scale structure. The torque wrench has a range of 30-300 lbft and could be set accurately to 10 lbft.

Figure (I2) shows the torque tension characteristics to the first tightening of a new nut and new bolt, each one pertain to a different nut and bolt assembly. Different behaviour may be expected if nuts are loosened and retightened a number of times. Figure (I3) shows a typical result obtained for the fourth tightening. It is evident that the curves of figure (I3) have smaller slopes than those of figure (I2) and that less tension is obtaines for a given torque during the fouth tightening than during the first. The effect of tension obtained with a given torque, with the number of times a nut is tightened is shown in figure (I4). From figure (I4) it is evident that there is a considerable spread in the tension data for a given torque. It also appears that this spread decreases with increasing numbers of tightening. From the visible scoring of the washers produced by turning the nut, it can be summarised that a part of the applied torque is used to seal the nut during retightening thus leaving less torque to produce less tension in the bolt.

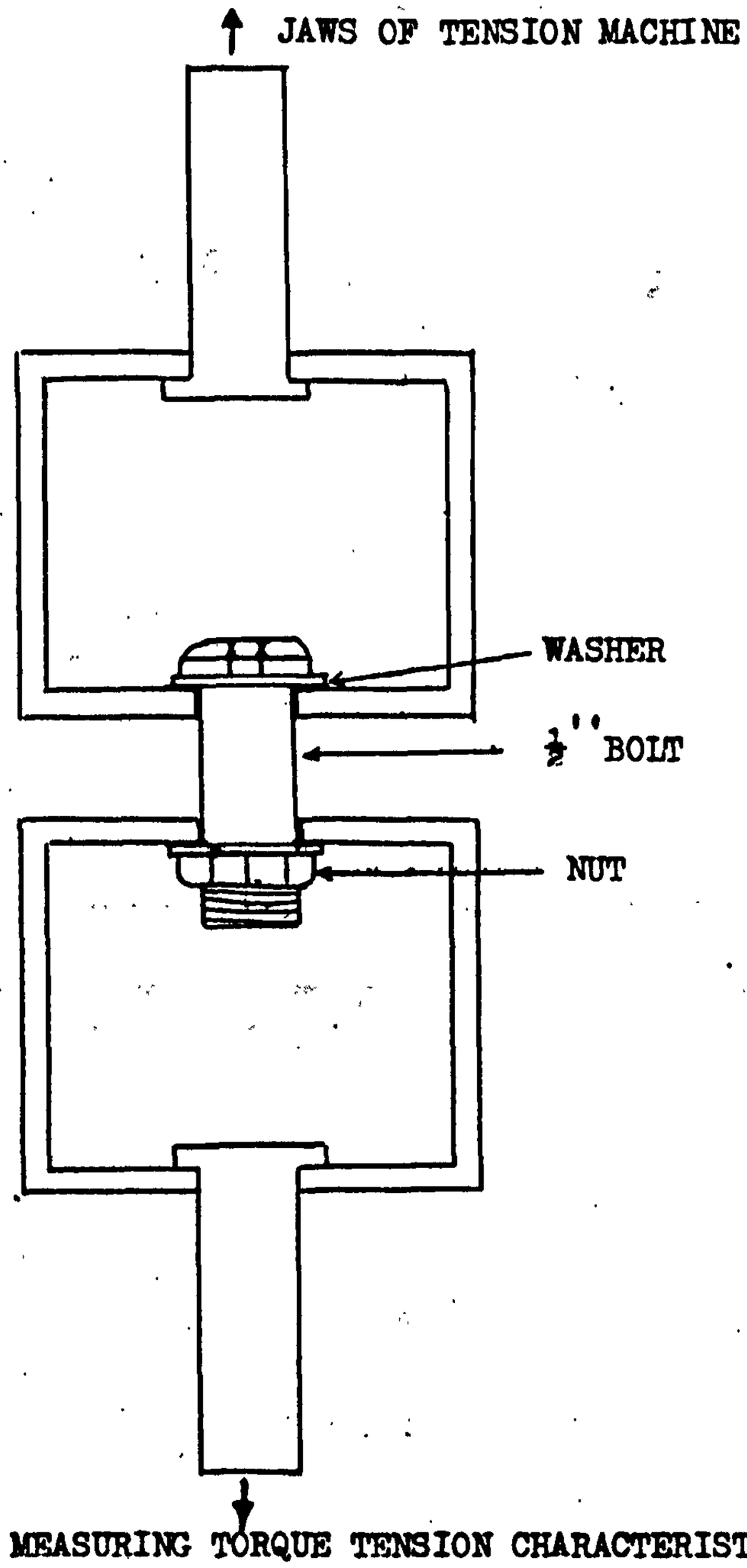

ASSEMBLY FOR MEASURING TORQUE TENSION CHARACTERISTICS

FIGURE I1

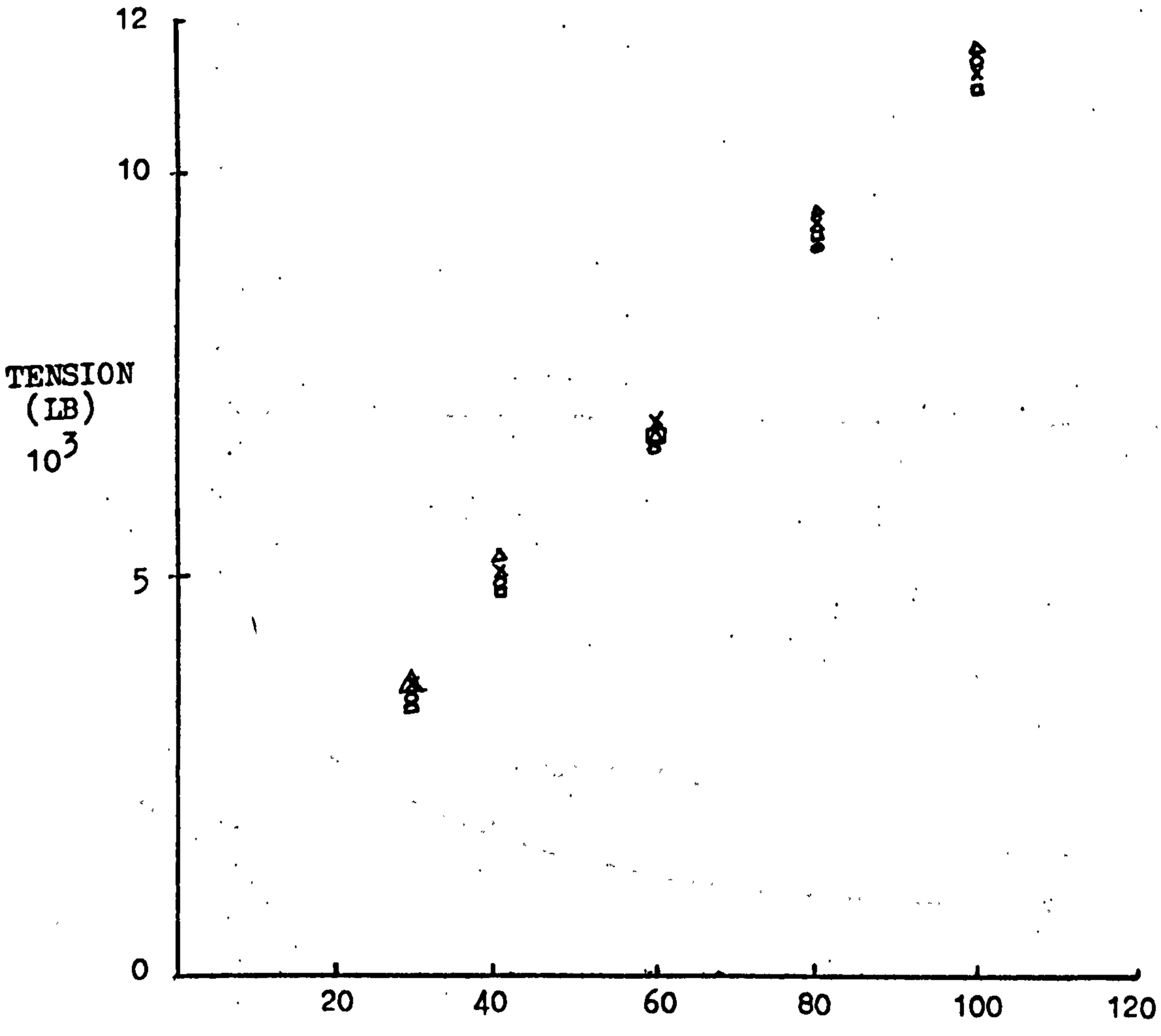

INITIAL TIGHTENING
FIGURE I2

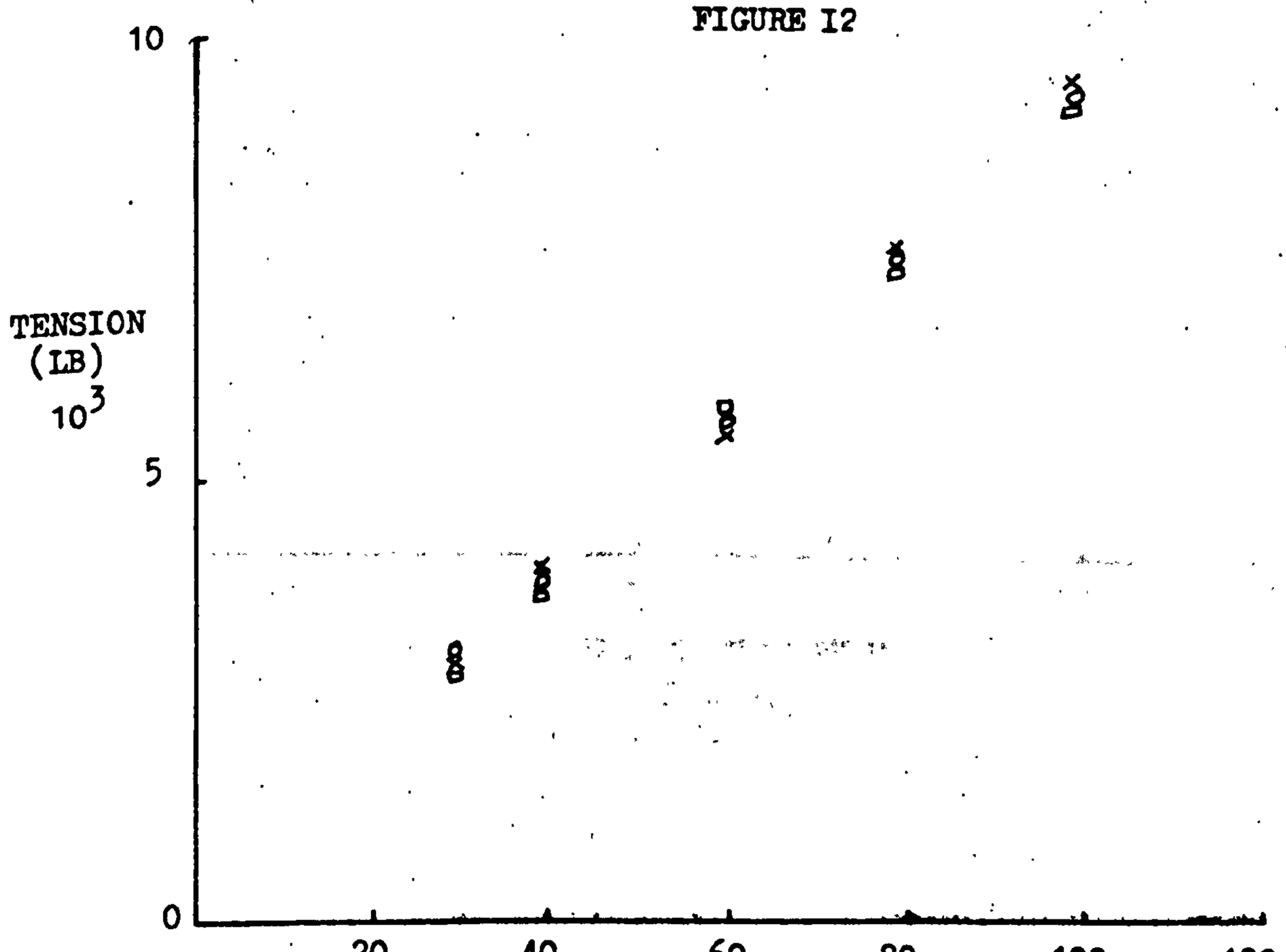

FOURTH TIGHTENING
FIGURE I3

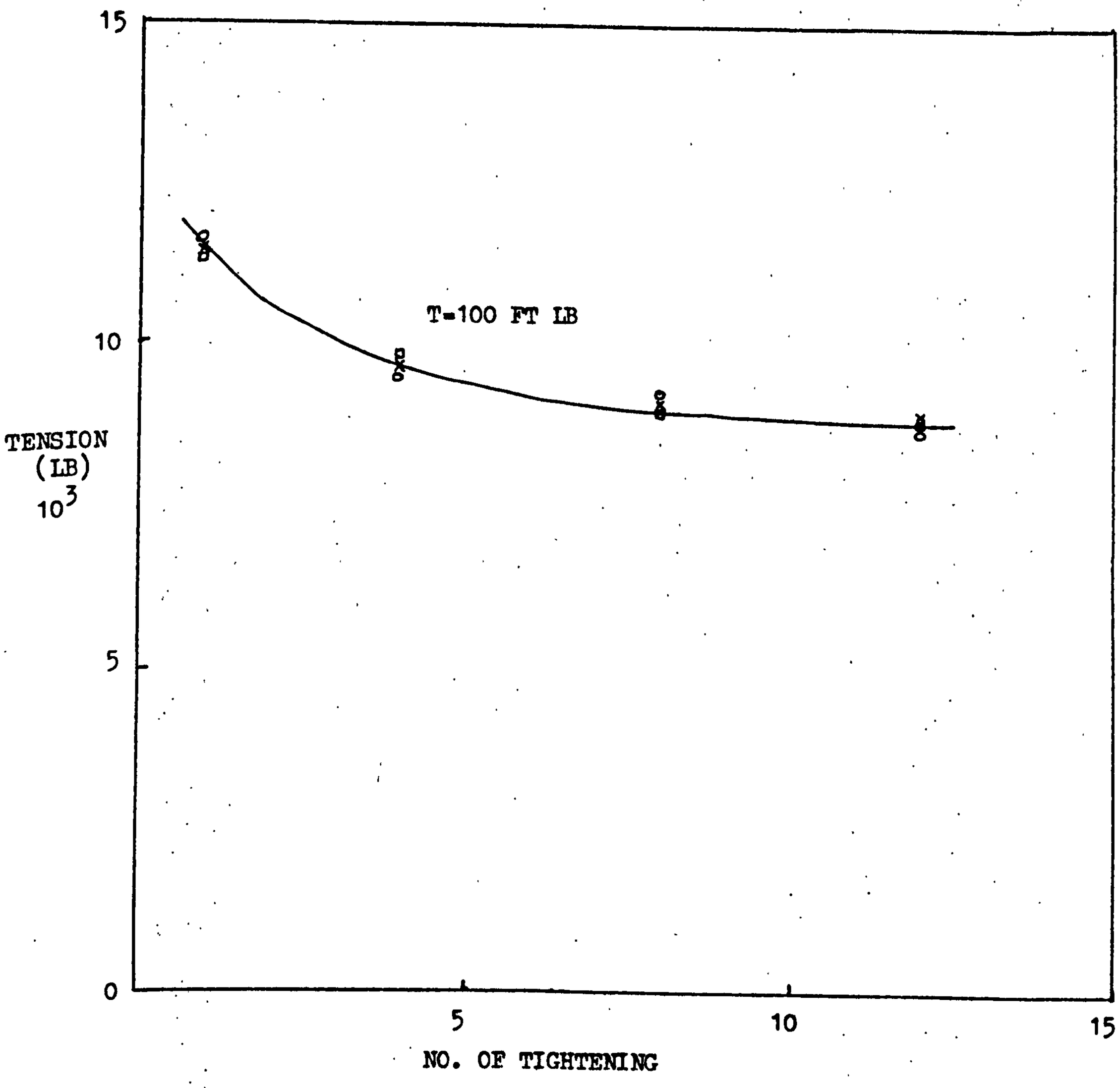

FIGURE I4

APPENDIX J

Tower shape structures, such as television towers, tall chimneys, floodlighting towers etc. are a very special form of civil engineering structures. These structures are susceptible to random loading to wind and earthquakes. In order to study the non-linear behaviour in such structures under random loading, a full scale, 30 feet high and $2\frac{1}{4}$ feet square, self supporting floodlighting tower was used in this investigation so that the factor affecting the non-linear damping could be varied and measured. The tower was erected on a massive concrete foundation so that the ground effects are minimised. Details of the tower and foundation are shown in figures (J1 and J2). Static deflection in the case of free vibration tests is provided by shear pin assembly as shown in figure (J3).

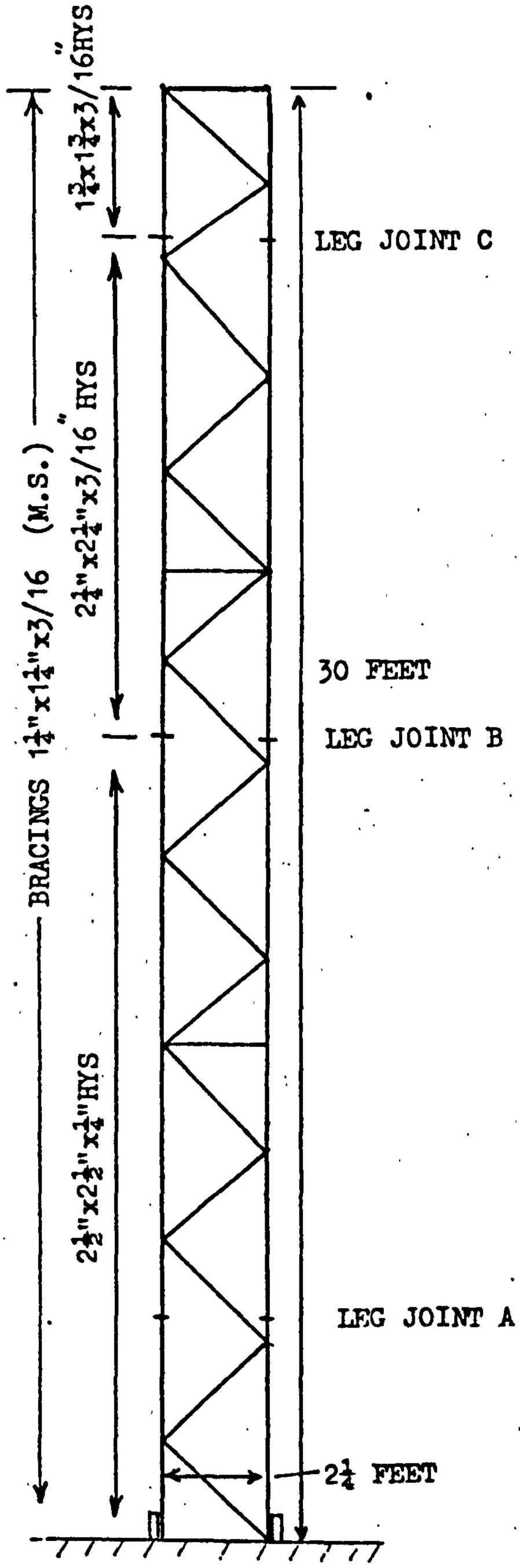

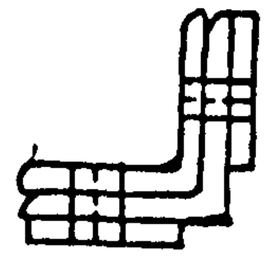

DETAIL OF LEG JOINT A

1 of 2¼x2¼x3/16 BOSOM ANGLE
2 of 2"x¼" HYS COVER PLATES
20 of ½" HYS BOLTS

1) All material – mild steel to B.S. 4360 Grade 43A
2) All high yield steel B.S. 4360 Grade 50B
3) All bolts of H.Y.S. & to B.S. 916
4) All bolts ½" Dia.
5) All welds to B.S. 2642

DETAILS OF THE LATTICE SELF SUPPORTING TOWER

FIGURE J1

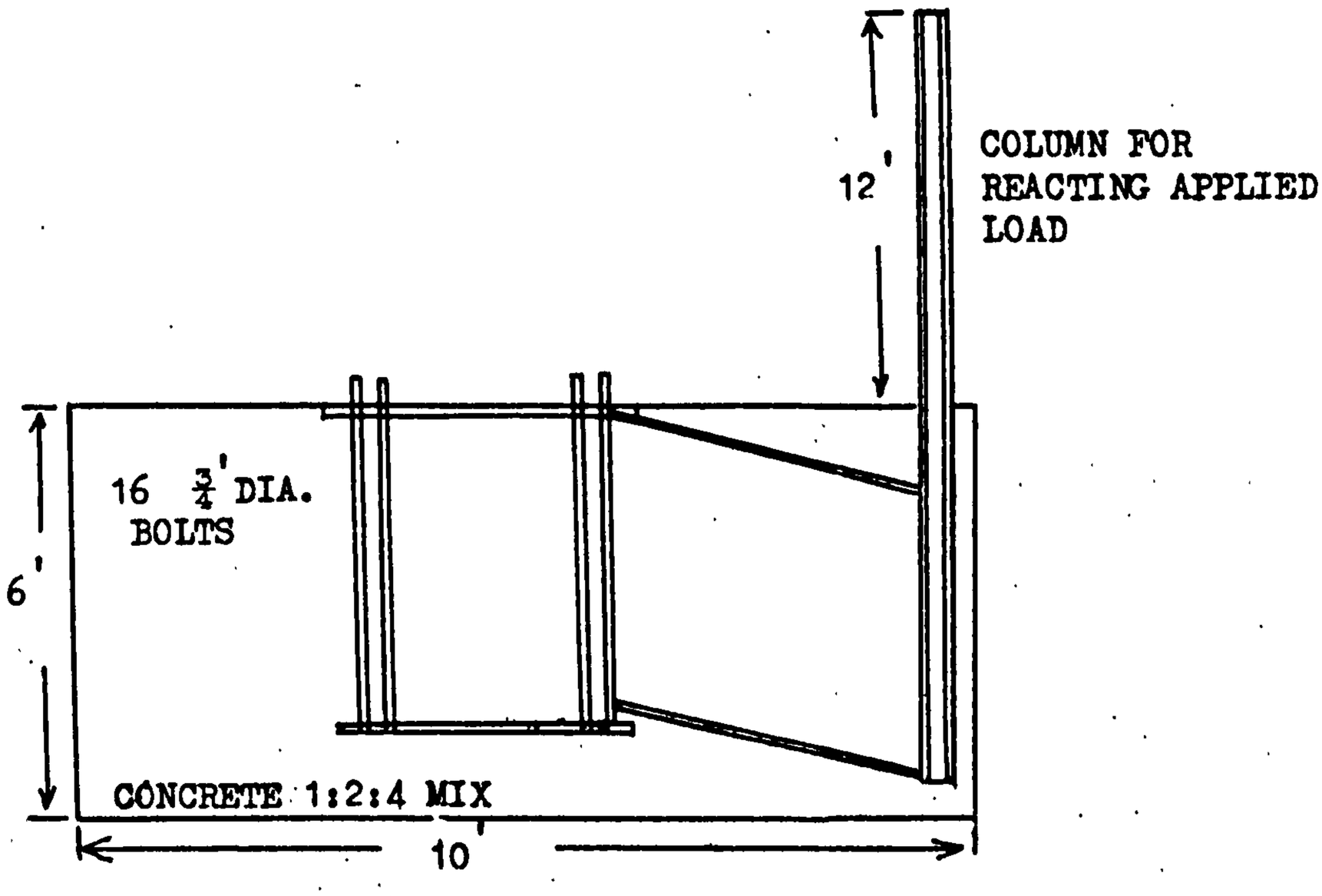

FIGURE J2a

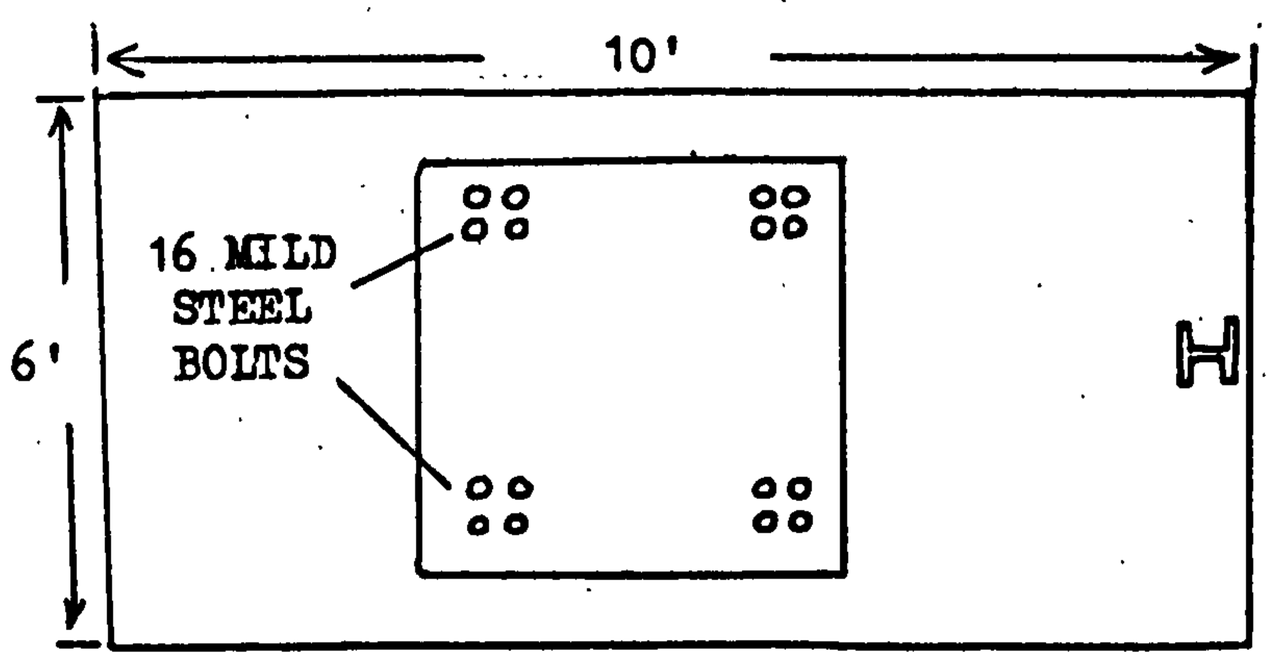

FIGURE J2b

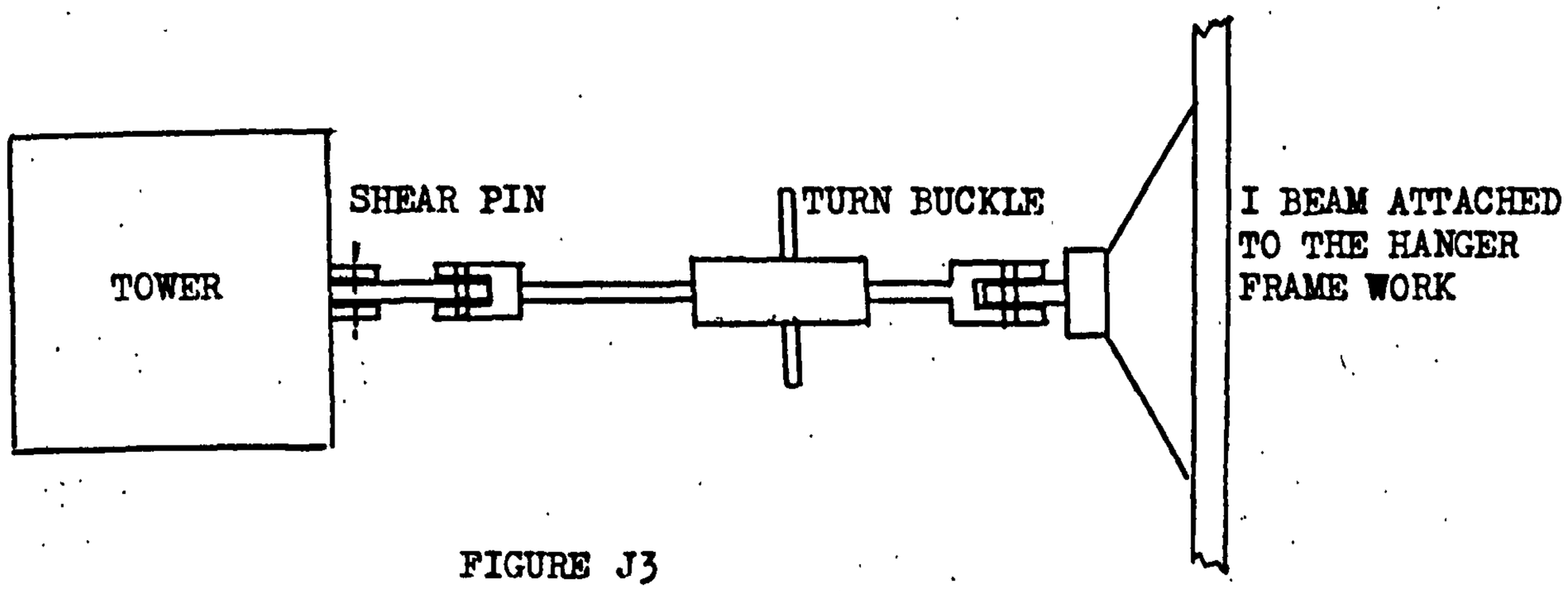
TOWER
SHEAR PIN
TURN BUCKLE
I BEAM ATTACHED
TO THE HANGER
FRAME WORK

FIGURE J3

APPENDIX K

CALIBRATION OF DC-LVDT DISPLACEMENT TRANSDUCER

A LVDT transducer is a self-contained measuring system combining the reliable characteristics of the 'Linear Variable Differential Transformer' with compact solid state circuitry. It produces a DC output in direct proportion to a linear motion of its moveable core. In the central position the DC output is zero. The DC output is positive when the core is moved from zero position in one direction and negative when the core is moved in the opposite direction. It has infinite resonition.

The transducer has a range of ± 1.0 inch with scale factor of 7.7 volts/inch for 24 volts excitation. The dynamic range of the transducer is 0-35 Hz. This is well above the dynamic range of the hydraulic excitation system. In order the transducer could be directly used with the other instrumentation, the excitation voltage was reduced to 17.3 volts so that scale factor of 5.0 volts/inch was obtained. The transducer was calibibrated using precision spacer blocks and output voltage for a given displacement were plotted as shown in Figure (K1).

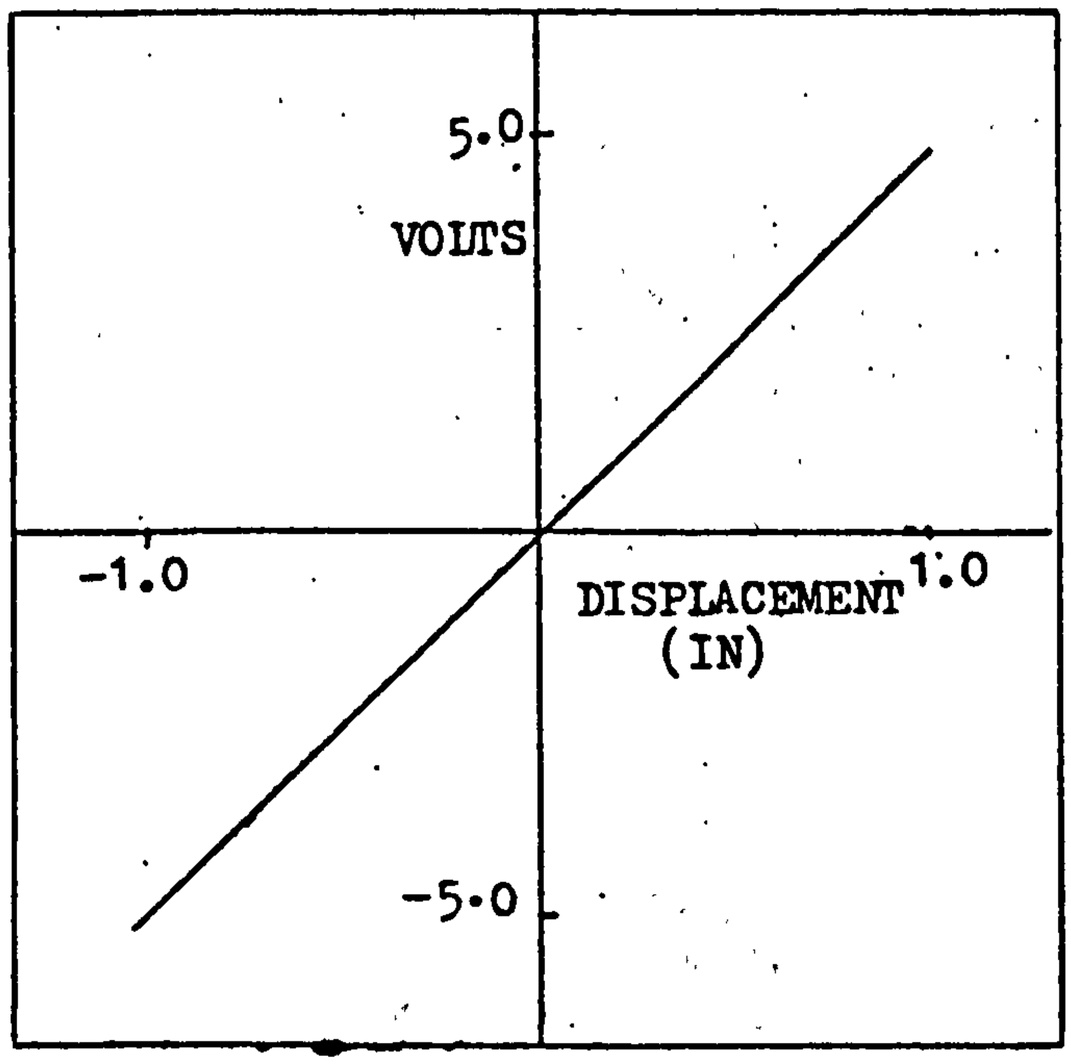

CALIBRATION CURVE FOR DISPLACEMENT TRANSDUCER

FIGURE K1

2. Calibration of Strain Gauges

In order to measure the maximum stresses in the tower during vibration tests, the strain gauges were fixed to the tower as shown in figure K2 . The main disadvantage from an experimental point of view on the use of strain gauges is that,

a) Gauges cannot be moved to another location once they have been cemented.

b) They are capable to giving a measure of average stress over the gauge length and thus comparatively intensive to localised variations.

Wire strain gauges were used and they were coupled to form a wheatstone bridge as shown in figure K3

The output signal from the bridge, if all four resistances change is given by

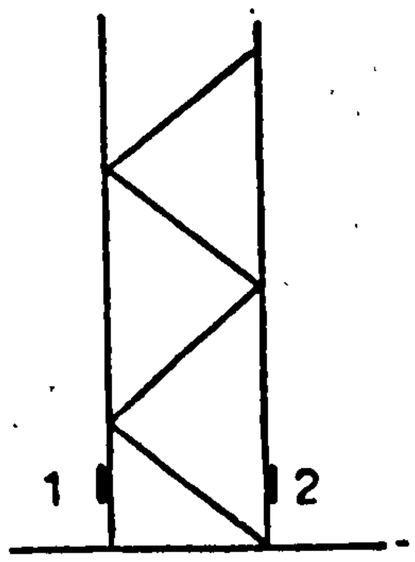

FIGURE K2

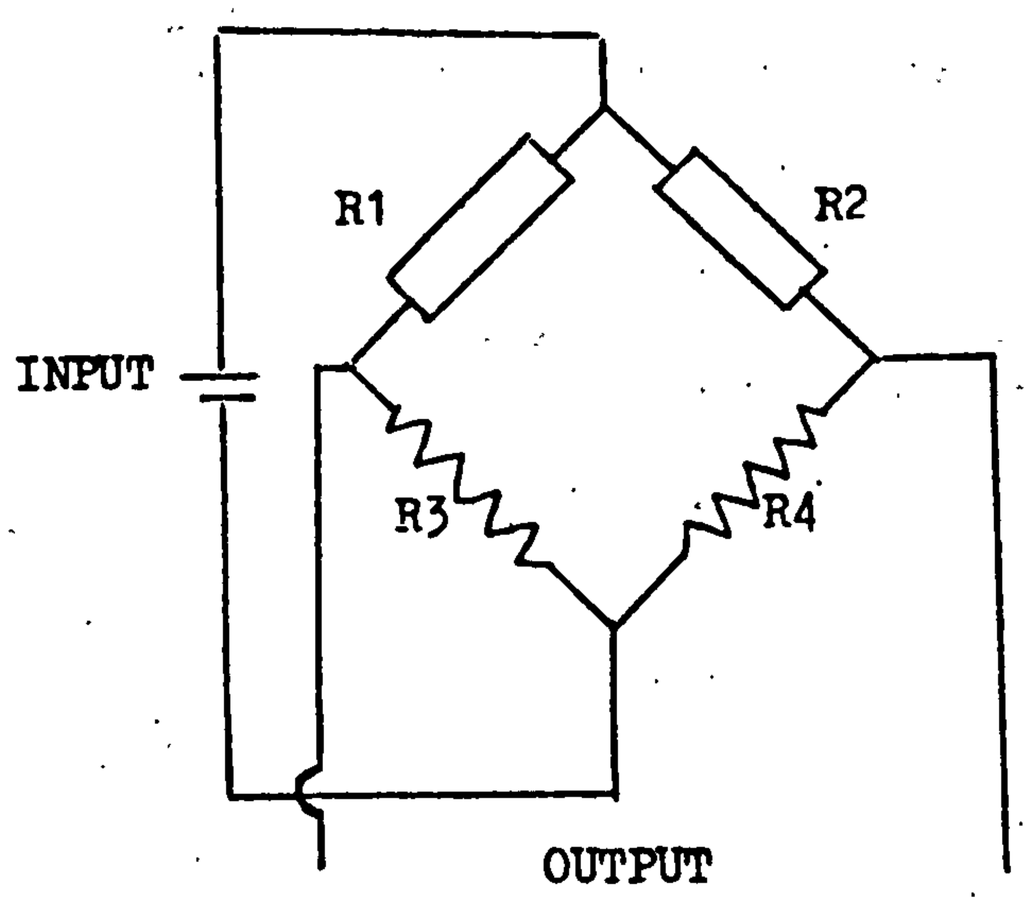

FIGURE K3

$$E_o = \frac{ER_G}{4(R+R_G)} \left(\frac{\Delta R_1}{R_1} - \frac{\Delta R_2}{R_2} + \frac{\Delta R_3}{R_3} - \frac{\Delta R_4}{R_4}\right) \quad (1)$$

Where all four gauges have a nominal resistance R. In the present set up only two resistance, namely R1 and R2 were allowed to change. Hence the output of the bridge becomes

$$E_o = \frac{E\ R_G}{4(R+R_G)} \left(\frac{\Delta R_1}{R_1} - \frac{\Delta R_2}{R_2}\right) \quad (2)$$

Since R_1 measures tension and R_2 measures compression with an experimental accuracy, the change can be taken to be equal, hence

$$\frac{\Delta R_1}{R_1} = -\frac{\Delta R_2}{R_2} \quad (3)$$

$$\therefore \quad E_o = \frac{ER_G}{4(R+R_4)} \frac{2\Delta R}{R_1}$$

$$= \frac{ER_G}{2(R+R_G)} \frac{\Delta R}{R_1} \quad (4)$$

The Gauge factor, which is defined as change in gauge resistance divided by change in gauge length (strain) is given by

$$F = \left(\frac{\Delta R}{R}\right) / \left(\frac{\Delta L}{L}\right) = \frac{\Delta R}{R} / \theta \quad (5)$$

where θ = strain.

It is measure of the resistance change for a given strain, an index of strain sensitivity of the gauge.

Substituting (5) and (4) yields

$$E_o = \frac{EF\theta R_G}{2(R+R_G)} = \frac{EF\theta}{2(1+R/R_G)} \qquad (6)$$

As the resistance of the measuring instrument is large compared with gauge resistance

$$E_o = \frac{EF\theta}{2}$$

Thus the output is proportional to the supply voltage (E), gauge factor (F) and strain (θ).

$$\therefore \quad \theta = \frac{2E_o}{EF}$$

Strain gauges used were of type PC-10 of gauge length 10mm, resistance of 120 Ω and gauge factor of 2.08. The input voltage was 4 volts and the amplifier gain was 1000.

$$\therefore \quad \theta = \frac{E_o}{4000}$$

$$\therefore \text{ Stress} = \theta * \text{Modulus of Elasticity of the steel}$$

$$= 30 \times 10^6 \times \theta$$

$$\text{stress} = 7500\ E_o \ \text{lb/in}^2$$

Thus one volt output from the strain gauge amplifier $= 7500\ \text{lb/in}^2$

Calibration of Accelerometers

ACB, variable mutual inductance accelerometers type J223, were used in conjunction with carrier amplifier type SE 423, to provide a voltage proportional to acceleration. The frequency range of the accelerometers was 0 to 200 Hz with maximum normal range of measurement of $\pm$6g. The block diagram below shows the setup for calibrating the accelerometers.

The accelerometer was initially set so that it produced no output and the amplifier zero set to zero. The accelerometer was then rotated in earths gravitational field to give +1g, and the amplifier gain set to give maximum output. It was then rotated in the opposite direction to give -1g and the output measured. The amplifier gain was then set such that $\pm$1g produced 0.33 volts, so that maximum of $\pm$6g could be recorded on the FM tape recorder without any further alteration.

APPENDIX L

PROGRAMS USED FOR CALCULATING THE VARIOUS STATISTICAL PROPERTIES OF THE NONLINEAR DYNAMICAL SYSTEM

```
      LIBRARY(SUBGROUPFSCE)
C     ***********************************************
C     ENL - EQUIVALENT NONLINEAR DIFFERENTIAL EQ. METHOD
C     EL. - EQUIVALENT LINEARISATION METHOD
C     MENL  - MODIFIED ENL
C     ***********************************************
C
C     EX21 - MEAN SQ. RESPONSE USING ENL
C     EX22 - MEAN SQ. RESPONSE USING MENL
C     EX23 - MEAN SQ.  RESPONSE USING EL
C
C     ***********************************************
      LIBRARY(SUBGROUPNAGF)
      PROGRAM(D10A)
      INPUT 1=CRO
      OUTPUT 2=LPO
      COMPACT DATA
      COMPRESS INTEGER AND LOGICAL
      END
      MASTER MSRESPONSE
      DIMENSION A(10),REA(10),DIMA(10),DA(10),B(10)
      COMMON ESPN,ALPHA,N
      PI=3.142
      IND2=10
      IND1=10
      AL1=0.0
      BL1=2000.0
      ACC=0.001
      AL2=0.0
      BL2=2000.0
1     READ(1,2)N,ESPN
2     FORMAT(I0,2F0.0)
      IF(N.LT.0)GO TO 200
C     CALCULATE NORMALISED MEAN SQ. RESPONSE USING ENL
      X1=(N+3.)/2.
      X2=(N+4.)/2.
      IF1=0
      IF2=0
      G1=S14AAF(X1,IF1)
      G2=S14AAF(X2,IF2)
      AI=0.5*SQRT(PI)*G1/G2
      ALPHA=AI*8.0*2.0**(N/2.)/(PI*(N+2))
      EXTERNAL AA
      CALL F4INTSMP(AL1,BL1,AA,ACC,IND1,AREA1)
      EXTERNAL BB
      CALL F4INTSMP(AL2,BL2,BB,ACC,IND2,AREA2)
      XMSN=0.5*AREA1/AREA2
      EX21=XMSN
C     CALCULATE NORMALISED MEAN SQ. RESPONSE USING EL
      DO 9 I=1,10
      B(I)=0.0
9     A(I)=0.0
      A1=ESPN*2.**((N+2.)/2.)*G1/SQRT(PI)
      A(N+3)=A1
      A(3)=1.0
      A(1)=-1.0
      M=N+4
      DO 10 L=1,N+3
10    B(L)=A(M-L)
      NO=N+3
      IFAIL=0
      CALL C02ACF(B,NO,REA,DIMA,DA,IFAIL)
```

```
      J=0
      DO 11 I=1,NO-1
      IF(DIMA(I).NE.0.0)GO TO 11
      IF(REA(I).LE.0.0)GO TO 11
      IF(J.GE.1)GO TO 14
      J=1
       XL2=REA(I)
       GO TO 11

14    XL1=REA(I)
      IF(XL2.GT.XL1)XL2=XL1
11    ICON=I
      XMSNL=XL2**2
      EX23=XMSNL
C     CALCULATE NORMALISED MEAN SQ.RESPONSE USING APPROX
C     FNL
      IF(N.EQ.1)GO TO 4
      IF(N.EQ.6)GO TO 7
      IF(N.EQ.2)GO TO 8
      WRITE(2,23)
23    FORMAT(1X,22HN....CAN.ONLY.BE.1.2.6//)
      GO TO 50
4     A1=(1.2*ESPN/0.8032864)**2
      A(1)=A1
      A(2)=-1.0
      A(3)=2.0
      A(4)=-1.0
      IFAIL=0
      M=4
      CALL C02ACF(A,M,REA,DIMA,DA,IFAIL)
      J=0
      DO 20 I=1,M-1
      IF(DIMA(I).NE.0.0)GO TO 20
      IF(REA(I).LE.0.0)GO TO 20
      IF(J.GE.1)GO TO 21
      J=1
      XM2=REA(I)
      GO TO 20
21    XM1=REA(I)
      IF(XM2.GT.XM1)XM2=XM1
20    ICON=I
      EX22=XM2
      GO TO 50
7     A1=4.375*ESPN
      B1=0.228473
      A(1)=A1
      A(2)=0.0
      A(3)=0.0
      A(4)=B1
      A(5)=-B1
      IFAIL=0
      M=5
      CALL C02ACF(A,M,REA,DIMA,DA,IFAIL)
      J=0
      DO 120 I=1,M-1
      IF(DIMA(I).NE.0.0)GO TO 120
      IF(REA(I).LE.0.0)GO TO 120
      IF(J.GE.1)GO TO 121
      J=1
      XM2=REA(I)
      GO TO 120
121    XM1=REA(I)
      IF(XM2.GT.XM1)XM2=XM1
120   ICON=I
      EX22=XM2
      GO TO 50
```

```
8       A1=1.5*ESPN
        B1=0.636804
        A(1)=A1
         A(2)=B1
        A(3)=-B1
        IFAIL=0
        M=3
        CALL CO2ACF(A,M,REA,DIMA,DA,IFAIL)
        J=0
        DO 220 I=1,M-1
        IF(DIMA(I).NE.0.0)GO TO 220
        IF(REA(I).LE.0.0)GO TO 220
        IF(J.GE.1)GO TO 221
        J=1
        XM2=REA(I)
        GO TO 220
221      XM1=REA(I)
        IF(XM2.GT.XM1)XM2=XM1
220     ICON=I
        EX22=XM2
50      WRITE(2,3)N,ESPN,EX21,EX22,EX23
3       FORMAT(I3,3X,F8.4,4E16.4)
        GO TO 1
200     STOP OK
        END
        FUNCTION AA(R)
        COMMON ESPN,ALPHA,N
        A=R**2/2.0
        B=(N+2.)/2.
        C=A+ESPN*ALPHA*A**B
        AA=R**3*EXP(-C)
        RETURN
        END
        FUNCTION BB(P)
        COMMON ESPN,ALPHA,N
        A=P**2/2.0
        B=(N+2.)/2.
        C=A+ESPN*ALPHA*A**B
        BB=P*EXP(-C)

        RETURN
        END
        FINISH
```

```
      LIBRARY(SUBGROUPNAGF)
      LIBRARY(SUBGROUPFSCE)
      PROGRAM(D10E)
      INPUT 1=CR0
      OUTPUT 2=LP0
      END
      MASTER PROBDENSITY
      DIMENSION  A(10),REA(10),DIMA(10),DA(10)
      COMMON BETA,X4
      COMMON X,ALPHA,ESP,N
1      READ(1,2)N,I1,I2,I3,ESP,RAT
      WRITE(2,5)N,ESP,RAT
5     FORMAT(1X,2HN=,I4,3X,4HESP=,E16.4,2X,4HRAT=,E12.4//)
      IF(N.LT.0)GO TO 7
      X3=4./(N+2.)
      X4=2./(N+2.)
      X5=1./X4
      IF3=0
      IF4=0
       G3=S14AAF(X3,IF3)
      G4=S14AAF(X4,IF4)
      X6=(N+3.)/2.0
      X7=(N+4.)/2.0
      IF6=0
      IF7=0
      G6=S14AAF(X6,IF6)
      G7=S14AAF(X7,IF7)
      A1=G3*X5/G4
      B=X4**(N/(N+2.))
      C=4.*2.**(N/2.)*ESP*SQRT(3.142)*G6/(2.*3.142*G7)
      D=A1*B
      IF(N.EQ.1)GO TO 3
      IF(N.EQ.6)GO TO 4
      GO TO 7
3     A(1)=1.0
      A(2)=-3.*C
      A(3)=(3.*C**2-D**3)
      A(4)=-C**3
      GO TO 15
4      A1=0.6913677
      C=4.375*ESP
      A(1)=1.
      A(2)=-(4.*C+A1)
      A(3)=6.*C**2
      A(4)=-4.*C**3
      A(5)=C**4
      GO TO 8
15     M=4
      IFAIL=0
      CALL C02ACF(A,M,REA,DIMA,DA,IFAIL)
      GO TO 30
8     M=5
      IFAIL=0
      CALL C02ACF(A,M,REA,DIMA,DA,IFAIL)
30    J=0
      DO 20 I=1,N-1
      IF(DIMA(I).NE.0.0)GO TO 20
      IF(REA(I).LE.0.0)GO TO 20
      IF(J.GE.1)GO TO 21
      J=1
      XM2=REA(I)
```

```
      GO TO 20
21    XM1=REA(I)
      IF(XM2.GT.XM1)XM2=XM1
20     ICON=I
      BETA=XM2
      DO 10 JK=I1,I2,I3
        X=0.25*JK
      ACC=0.001
      LIMIT=2000
      IND=20
2     FORMAT(4I0,3F0.0)
      IF(N.LT.0)GO TO 7
      IF1=0
      IF2=0
      X1=(N+3.)/2.0
      X2=(N+4.)/2.0
      G1=S14AAF(X1,IF1)
      G2=S14AAF(X2,IF2)
      AI=0.5*SQRT(3.142)*G1/G2
      ALPHA=AI*8.*2.0**(N/2.)/(3.142*(N+2.))
      YL1=0.0
      YL2=LIMIT
      ACC1=ACC
      ACC2=ACC
      IND1=IND
      IND2=IND
      RL1=0.0
      RL2=LIMIT
      EXTERNAL AA
      CALL F4INTSHP(YL1,YL2,AA,ACC1,IND1,RES1)
      AREA1=RES1
      EXTERNAL BB
      CALL F4INTSHP(RL1,RL2,BB,ACC2,IND2,RES2)
      AREA2=RES2
      PX=AREA1/(3.142*AREA2)
      EXTERNAL CC
      A1=(N+2.)/2.0
      A2=A1*(BETA/A1)**(1./A1)
      IND3=IND
      ACC3=ACC
      AL1=0.0
      BL1=LIMIT
      CALL F4INTSHP(AL1,BL1,CC,ACC3,IND3,AREA3)
      PD=2.*A2*AREA3/(6.284*G4)
      PXG=RAT*EXP(-0.5*RAT**2*X**2)/SQRT(6.284)
      WRITE(2,13)X,PX,PXG,PD
13     FORMAT(F8.3,3X,4E12.4)
10    ICON=JK
      GO TO 1
7     STOP OK
      END
      FUNCTION AA(Y)
      COMMON BETA,X4
      COMMON X,ALPHA,ESP,N
      A1=(X**2+Y**2)/2.
      A2=ALPHA*ESP
      A3=(N+2.)/2.0
      A4=A1+A2*A1**A3
      AA=EXP(-A4)
      RETURN
      END
      FUNCTION BB(R)
      COMMON BETA,X4
      COMMON X,ALPHA,ESP,N
      B1=0.5*R**2
      B2=ALPHA*ESP
```

```
B3=(N+2.)/2.0
B4=B1+B2*B1**B3
BB=R*EXP(-B4)
RETURN
END
FUNCTION CC(Z)
COMMON BETA,X4
COMMON X,ALPHA,ESP,N
A=(X**2+Z**2)/2.0
B=X4*BETA
C=B*A**(1./X4)
CC=EXP(-C)
RETURN
END
FINISH
```

```
      LABEL (SUBROUPNAME)
      PROGRAM(D10A)
      INPUT 1=CR0
      OUTPUT 2=LP0
      COMPACT DATA
      COMPRESS INTEGER AND LOGICAL
      END
      MASTER LEVELCROSSING
      COMMON ALPHA,ESPN,N,ETA
    1 READ(1,2)N,ESPN,IS,IE,ID
    2 FORMAT(I0,F0.0,3I0)
      IF(N.LT.0)GO TO 7
      PI=3.142
      X1=(N+3.)/2.
      X2=(N+4.)/2.
      IF1=0
      IF2=0
      ACC=0.001
      AL1=0.0
      AL2=2000.
      G1=S14AAF(X1,IF1)
      G2=S14AAF(X2,IF2)
      AI=0.5*SQRT(PI)*G1/G2
      ALPHA=AI*8.0*2.0**(N/2)/(PI*(N*2.))
      DO 11 IJ=IS,IE,ID
      ETA=0.25*IJ
      IND1=10
      IND2=10
      EXTERNAL AA
      CALL F4INTSHP(AL1,AL2,AA,ACC,IND1,AREA1)
      EXTERNAL BB
      CALL F4INTSHP(AL1,AL2,BB,ACC,IND2,AREA2)
      AN=EXP(ETA**2/2.)
      R1=AN*AREA1/AREA2
      IF(N.EQ.2)GO TO 10
      R2=0.0
      R22=0.0
      GO TO 11
   10 AX=1./SQRT(3.0*ESPN)
      X3=(AX+0.25*ETA**2/AX)
      X4=AX
      CALL F4ERFN(X3,ERF1,ERFC1)
      CALL F4ERFN(X4,ERF2,ERFC2)
      R2=AN*ERFC1/ERFC2
      R22=AN*(1.-ERF1)/(1.0-ERF2)
   11 WRITE(2,5)N,ESPN,ETA,R1,R2,R22
    5 FORMAT(I3,1X,F7.4,1X,F7.4,1X,3E12.4)
      GO TO 1
    7 STOP OK
      END
      FUNCTION AA(Z)
      COMMON ALPHA,ESPN,N,ETA
      A=(Z**2+ETA**2)/2.
      B=ALPHA*ESPN
      C=(N+2.)/2.
      D=A+B*A**C
      AA=Z*EXP(-D)
      RETURN
      END
      FUNCTION BB(R)
      COMMON ALPHA,ESPN,N,ETA
      A=R**2/2.
      B=ALPHA*ESPN
      C=(N+2.)/2.
      D=A+B*A**C
      BB=R*EXP(-D)
      RETURN
      END
      FINISH
```

```
      LIBRARY(SUBGROUPNAGF)
C     PROGRAM TO CALCULATE PDF USING JPDF DERIVED
C     FROM MODIFIED EQUIVALENT NONLINEAR DIFFERENTIAL
C     EQUATION METHOD
C
      LIBRARY(SUBGROUPFSCL)
      PROGRAM(D10T)
      INPUT 1=CR0
      OUTPUT 2=LP0
      COMPACT DATA
      END
      MASTER PROBDENISTY
      DIMENSION A(10),REA(10),DIMA(10),DA(10)
      COMMON BETA,Y,X6
1     READ(1,2)N,ESPN
2     FORMAT(I0,F0.0)
      X1=4./(N+2.)
      X2=2./(N+2.)
      X3=1./X2
      IF1=0
      IF2=0
       G1=S14AAF(X1,IF1)
      G2=S14AAF(X2,IF2)
      X4=(N+3.)/2.0
      X5=(N+4.)/2.0
      IF4=0
      IF5=0
      G3=S14AAF(X4,IF4)
      G4=S14AAF(X5,IF5)
      A1=G1*X3/G2
      B=X2**(N/(N+2.))
      C=4.*2.**(N/2.)*ESPN*SQRT(3.142)*G3/(2.*3.1-2*G4)
      D=A1*B
      IF(N.EQ.1)GO TO 3
      IF(N.EQ.6)GO TO 4
      GO TO 7
3     A(1)=1.0
      A(2)=-3.*C
      A(3)=(3.*C**2-D**3)
      A(4)=-C**3
      GO TO 5
4     CONTINUE
      A(1)=1
      A(2)=-(4.*C+D**4)
      A(3)=6.*C**2
      A(4)=-4.*C**3
      A(5)=C**4
      GO TO 8
5     M=4
      IFAIL=0
      CALL C02ACF(A,M,REA,DIMA,DA,IFAIL)
      GO TO 30
8     M=5
      IFAIL=0
      CALL C02ACF(A,M,REA,DIMA,DA,IFAIL)
30    J=0
      DO 20 I=1,M-1
      IF(DIMA(I).NE.0.0)GO TO 20
      IF(REA(I).LE.0.0)GO TO 20
      IF(J.GE.1)GO TO 21
      J=1
      XM2=REA(I)
```

```
      GO TO 20
2     XM1=REA(I)
      IF(XM2.GT.XM1)MX2=XM1
2.1     ICON=1
      BETA=XM2
1.1   READ(1,11)NS,NE,ND
1     FORMAT(3I0)

      IF(NS.LT.0)GO TO 1
      DO 35 IY=NS,NE,ND
      Y=0.25*IY
      A1=(N+2.)/2.
      A2=A1*(BETA/A1)**(1./A1)
      X6=X2
      G6=G2
      EXTERNAL AA
      IND=10
      ACC=0.001
      AL1=0.0
       BL1=2000.0
      CALL F4INTSIP(AL1,BL1,AA,ACC,IND,AREA)
      PD=2*A2*AREA/(6.284*G0)
      WRITE(2,12)Y,PD,FSPN,BETA,N
12    FORMAT(1X,F8.3,2X,3E10.4,I5)
35    ICNT=IY
      GO TO 10
7     STOP OK
      END
      FUNCTION AA(Z)
      COMMON BETA,Y,X6
      A=(Y**2+Z**2)/2.0
      B=X6*BETA
      C=B*A**(1./X6)
      AA=EXP(-C)
      RETURN
      END
      FINISH
```

```
      LIBRARY(SUBGROUPNAGF)
      LIBRARY(SUBGROUPESSE)
      PROGRAM(D10E)
      INPUT 1=CR0
      OUTPUT 2=LP0
      END
      MASTER PROBDENSITY
      COMMON X,ALPHA,ESPN,N
    1  READ(1,2)N,I1,I2,I3,ESPN,RAT
      IF(N.LT.0)GO TO 7
      DO 10 JK=I1,I2,I3
        X=0.25*JK
      ACC=0.001
      LIMIT=2000
      IND=20
    2 FORMAT(4I0,3F0.0)
      IF(N.LT.0)GO TO 7
      IF1=0
      IF2=0
      X1=(N+3.)/2.0
      X2=(N+4.)/2.0
      G1=S14AAF(X1,IF1)
      G2=S14AAF(X2,IF2)
      AI=0.5*SQRT(3.142)**1/G2
      ALPHA=AI*8.*2.0**(N/2.)/(3.142*(N+2.))
      YL1=0.0
      YL2=LIMIT
      ACC1=ACC
      ACC2=ACC
      IND1=IND
      IND2=IND
      RL1=0.0
      RL2=LIMIT
      EXTERNAL AA
      CALL F4INTSHP(YL1,YL2,AA,ACC1,IND1,RES1)
      AREA1=RES1
      EXTERNAL BB
      CALL F4INTSHP(RL1,RL2,BB,ACC2,IND2,RES2)
      AREA2=RES2
      PX=AREA1/(3.142*AREA2)
      PXG=RAT*EXP(-0.5*RAT**2-X**2)/SQRT(6.284)
      WRITE(2,3)N,ESPN,X,PX,PXG,ALPHA
    3 FORMAT(I4,2X,F6.3,3X,F8.3,3X,4E12.4)
      ICON=JK
      GO TO 1
    7 STOP OK
      END
      FUNCTION AA(Y)
      COMMON X,ALPHA,ESPN,N
      A1=(X**2+Y**2)/2.
      A2=ALPHA*ESPN
      A3=(N+2.)/2.0
      A4=A1+A2*A1**A3
      AA=EXP(-A4)
      RETURN
      END
      FUNCTION BB(R)
      COMMON X,ALPHA,ESPN,N
      B1=0.5*R**2
      B2=ALPHA*ESPN
      B3=(N+2.)/2.0
      B4=B1+B2*B1**B3
      BB=R*EXP(-B4)
      RETURN
      END
      FINISH
```

TYPES OF FOUNDATION	PILED FOUNDATION OR SPREAD FOOTING ON STIFF SOIL AND ROCK	SPREAD FOOTING ON MEDIUM STIFF SOIL	SPREAD FOOTING ON SOFT SOIL
FACTOR	1	1.5	3

Approximate Logarithmic Decrement Factors (from Ref. 24)

TABLE 1.

NODE NUMBER	MEMBER MASS (LB)	ADDED MASS (COVER PLATE + BOLTS) (LB)	TOTAL MASS (LB)
1.4	16.275	25.2695	41.5445
5.8	8.65	3.15775	11.80775
9.12	9.3	3.15775	12.458
13.16	9.925	0.2	10.125
17.20	9.925	0.2	10.125
21.24	21.875	0.8	22.675
25.28	9.925	3.928	13.853
29.32	11.225	3.928	15.153
33.36	12.5	0.2	12.70
37.40	12.5	0.2	12.70
41.44	24.7	0.8	25.50
45.48	12.5	0.2	12.70
49.52	12.5	5.91425	18.41425
53.56	12.5	5.91425	18.41425
57.60	12.5	0.2	12.70
60.64	6.25	8.91	15.16

Mass Distribution as Computed from the Structural Drawing

TABLE 2.

Measured Non-linear Damping Coefficient (ϵ) for Various Values of Torque

TABLE 3.

FREQ = 5.49 Hz.

TORQUE	β_o	SLOPE $*10^2$	ϵ $(in^{-1}s)$
40	0.215/100	0.69	0.1096
50		0.47	0.0746
60		0.44	0.0698
70		0.39	0.0619
80		0.55	0.0564
90		0.37	0.0588
100		0.36	0.0572
110		0.33	0.0523
120		0.30	0.0476
140		0.27	0.0428

Random Vibration Testing

TABLE 4a.

TORQUE lb/ft	β_o X 100	ϵ FROM FREE VIB. TEST	P.S.D. lb^2/Hz	$E(X^2)$ in^2 $X10^2$
140	0.21	0.0521	23.87	0.0917
			82.49	0.268
			143.05	0.5434
			306.44	0.9905
			482.8	1.451
			670.1	1.851

Random Vibration Testing

TABLE 4b.

TORQUE lb/ft	β_o x 100	ϵ	P.S.D. W lb^2/Hz	$E(X^2)$ in^2 $X10^2$
90	0.195	0.0692	28.59	0.101
			91.23	0.291
			143.09	0.495
			329.07	1.120
			525.01	1.492
			654.68	1.932

K_o =357.1 lb/in ϕ=0.169 β=0.005 Gain=0.4 ϕ=0.169 β=0.005

Gain(K_p)	Case 1	Case 2
0.01	S	S
0.01	S	S
0.2	S	US
0.3	S	US
0.5	S	US

K_o	Case 1	Case 2
100	S	US
300	S	US
600	S	US
800	S	US
α	US	US

Gain=0.4 β=0.005 K_o=357.1 lb/in K_o=357.1 lb/in ϕ=0.169 Gain=0.4

ϕ	Case 1	Case 2
1.0	S	US
0.169	S	US
0.071	S	US
0.011	S	US

β	Case 1	Case 2
0.005	S	US
0.05	S	US
0.10	S	US

Stability Results

TABLE 5.

TABLE 6a

	$E(X^2)$ (IN^2)				
S_o	LINEAR	ENL	MENL	EL	ANALOGUE
10	0.5329E-01	0.4308E-1	0.4345E-1	0.4295E-1	0.4350
30	0.1599	0.1154	0.1166	0.1147	0.1160
50	0.2665	0.1801	0.182	0.1787	0.1795
70	0.3430	0.2402	0.2429	0.2381	0.2431
90	0.4796	0.2972	0.3005	0.2943	0.3015
200	1.066	0.5761	0.5825	0.5683	0.5830
400	2.132	1.006	1.017	0.9892	1.021
600	3.197	1.385	1.399	1.359	1.395
800	4.263	1.732	1.749	1.697	1.952
1000	5.329	2.057	2. 76	3.013	2.084
2000	10.66	3.480	3.510	3.395	3.530

Mean Square Displacement Response For Various Excitation Levels For $n = 1$, $\epsilon = 0.964E - 2$ $\omega_o = 37.704$ Rad/s $\beta_o = .0055$

TABLE 6b

	$E(X^2)$ (IN^2)			
S_o	ENL	MENL	EI,	ANALOGUE
0.1000E 02	0.2724E-01	0.2754E-01	0.2634E-01	0.275E 01
0.3000E 02	0.6484E-01	0.6548E-01	0.6353E-01	0.652E 01
0.5000E 02	0.9592E-01	0.9680E-01	0.9375E-01	0.965E 01
0.7000E 02	0.1237E 00	0.1248E 00	0.1207E 00	0.123E 00
0.9000E 02	0.1493E 00	0.1506E 00	0.1455E 00	0.145E 00
0.3000E 03	0.3613E 00	0.3636E 00	0.3505E 00	0.371E 00
0.5000E 03	0.5216E 00	0.5245E 00	0.5051E 00	0.532E 00
0.7000E 03	0.6629E 00	0.6663E 00	0.6412E 00	0.651E 00
0.9000E 03	0.7921E 00	0.7960E 00	0.7696E 00	0.801E 00
0.1000E 04	0.8533E 00	0.8573E 00	0.8245E 00	0.845E 00
0.2000E 04	0.1388E 01	0.1393E 01	0.1339E 01	0.140E 00
0.3000E 04	0.1840E 01	0.1847E 01	0.1774E 01	0.179E 01
0.4000E 04	0.2247E 01	0.2254E 01	0.2164E 01	0.217E 01

Mean Square Displacement Response For Various Excitation Levels.

For $n = 1$, $\epsilon = 0.1$, $\omega_o = 37.704$ Rad/s $\beta_o = 0.0055$

TABLE 6c

	$E(X^2)$ (IN^2)			
S_o	ENL	MENL	EL	ANALOGUE
10	.5329E -1	0.5329E -1	0.533E-1	0.533E 1
20	0.1065	0.1066E +0	0.107E 0	0.107E 0
50	0.2650	0.2662	0.265E 0	0.266E 0
100	0.5162	0.5286	0.516E 0	0.529E 0
200	0.9377	0.1009E +1	0.881E 0	0.995E 0
500	0.1732E +1	0.190E 1	0.145E 1	0.185E 1
700	0.2070E +1	0.221E 1	0.163E 1	0.217E 1
1000	0.2444E +1	0.2653E +1	0.183E 1	0.258E 1
2000	0.3270E 1	0.331E 1	0.229E 1	0.321E 1
4000	0.4066E 1	0.418E 1	0.279E 1	0.409E 1

Mean Square Displacement Response for Various Excitation Levels for

$n = 6, \epsilon = 1.0E\text{-}12 \quad \beta_o = 0.0055 \quad \omega_o = 37.704$ Rad/sec

TABLE 7a

Non-linear Parameter Extraction From Random Testing
(With Ref. to Fig.40a)

W_o LB^2/Hz	S_o $LB^2/RAD/S/in/S^2$	$E(X^2)$ (IN^2)	ϵ $(IN^{-1}S)$
23.87	.0729	$.917x10^{-3}$	.05722
82.49	.252	$.268x10^{-2}$	.1022
143.05	.4373	$.5434x10^{-2}$	.0263
306.05	.9368	$.9908x10^{-2}$	.05447
482.8	1.4759	$0.1451x10^{-1}$	.05959
670.1	2.048	$0.1851x10^{-1}$	.06884

$n = 1$

$\beta = 0.21 \times 10^{-2}$

$\omega_o = 37.95$ RAD/S from equ.(7.5)

$$\epsilon = \frac{24.514 S_o}{10^5 x \left[E(X^2)\right]^{3/2}} - \frac{0.01755}{\left[E(X^2)\right]^{1/2}}$$

From Free Vibration Tests

$\epsilon = .0521$

TABLE 7b

Non-linear Parameter Extraction From Random Testing
(With Ref. to FIG.40b)

W	S_o $LB^2/RAD/S/IN/S^2$	$E(X^2)$ (IN^2)	ϵ $(IN^{-1}S)$
28.59	0.0874	0.101×10^{-2}	.163
91.23	0.2788	0.291×10^{-2}	.1416
143.09	0.4374	0.495×10^{-2}	.08055
329.07	1.006	0.112×10^{-1}	.0572
525.01	1.6049	0.1492×10^{-1}	.08806
654.68	2.0014	0.1932×10^{-1}	.0698

$$n = 1$$

$$\beta = .195 \times 10^{-2}$$

$$\omega_n = 37.95 \quad RAD/S$$

$$\epsilon = \frac{26.507 S_o}{10^5 \left[E(X^2)\right]^{3/2}} - \frac{0.017755}{\left[E(X^2)\right]^{1/2}}$$

From Free Vibration Tests

$$\epsilon = .0692$$

TABLE 8a

n	ESPN ϵ^*	ENL $(\frac{\sigma}{\sigma_o})^2$	EL $(\%\sigma_o)^2$	MENL $(\%_{\sigma_o})^2$
1	0.1000	0.8716E 00	0.8704E 00	0.8773E 00
1	0.2000	0.7830E 00	0.7801E 00	0.7902E 00
1	0.3000	0.7165E 00	0.7123E 00	0.7239E 00
1	0.4000	0.6640E 00	0.6587E 00	0.6713E 00
1	0.5000	0.6212E 00	0.6151E 00	0.6281E 00
1	0.6000	0.5853E 00	0.5786E 00	0.5919E 00
1	0.7000	0.5546E 00	0.5475E 00	0.5608E 00
1	0.8000	0.5280E 00	0.5206E 00	0.5338E 00
1	0.9000	0.5046E 00	0.4969E 00	0.5101E 00
1	1.0000	0.4838E 00	0.4760E 00	0.4891E 00
1	1.2000	0.4484E 00	0.4404E 00	0.4532E 00
1	1.4000	0.4193E 00	0.4111E 00	0.4235E 00
1	1.6000	0.3947E 00	0.3865E 00	0.3986E 00
1	1.8000	0.3736E 00	0.3655E 00	0.3772E 00
1	2.0000	0.3553E 00	0.3472E 00	0.3585E 00

Normalised Mean Square Response For Various Values of ϵ^* and n = 1

TABLE 8b

Normalised Mean Square Response For Various Values of ϵ^* and n = 6.

n	ESPN ϵ^*	ENL $(\sigma/\sigma_o)^2$	EL $(\sigma/\sigma_o)^2$	MENL $(\sigma/\sigma_o)^2$
6	0.0100	0.8030E 00	0.7192E 00	
6	0.0010	0.9430E 00	0.9236E 00	
6	0.1000	0.5924E 00	0.4733E 00	
6	0.2000	0.5277E 00	0.4095E 00	0.5766E 00
6	0.3000	0.4910E 00	0.3753E 00	0.5338E 00
6	0.4000	0.4658E 00	0.3524E 00	0.5044E 00
6	0.5000	0.4467E 00	0.3354E 00	0.4822E 00
6	0.6000	0.4315E 00	0.3221E 00	0.4646E 00
6	0.7000	0.4188E 00	0.3111E 00	0.4501E 00
6	0.8000	0.4081E 00	0.3019E 00	0.4377E 00
6	0.9000	0.3988E 00	0.2940E 00	0.4270E 00
6	1.0000	0.3905E 00	0.2871E 00	0.4176E 00
6	1.2000	0.3765E 00	0.2754E 00	0.4017E 00
6	1.4000	0.3650E 00	0.2658E 00	0.3886E 00
6	1.6000	0.3552E 00	0.2578E 00	0.3775E 00
6	1.8000	0.3467E 00	0.2509E 00	0.3680E 00
6	2.0000	0.3392E 00	0.2449E 00	0.3596E 00
6	0.1500	0.5543E 00	0.4352E 00	
6	0.0500	0.6583E 00	0.5431E 00	

TABLE 8c

% Error using various approximate methods

n=1

ϵ^*	% ERROR USING MENL	% ERROR USING EL
0.1	0.653	-0.137
0.2	0.919	-0.37
0.3	1.032	-0.586
0.4	1.099	-0.798
0.5	1.11	-0.9819
0.6	1.12	-1.14
0.7	1.11	-1.28
0.8	1.09	-1.40
0.9	1.08	-1.52
1.0	1.09	-1.61
1.2	1.07	-1.78
1.4	1.00	-1.95
1.6	0.988	-2.0
1.8	0.96	-2.16
2.0	0.90	-2.22

n=6

ϵ^*	% ERROR USING MENL	% ERROR USING EL
0.2	9.26	-10.308
0.4	8.716	23.56
0.6	7.67	25.35
0.8	7.25	26.023
1.0	6.94	-26.47
1.2	6.69	-26.85
1.4	6.46	27.17
1.6	6.27	27.42
1.8	6.14	27.63
2.0	6.014	27.80

n	ϵ^*	$Y=(X/6_0)$	P.D.F. ENL	P.D.F. GAUSSIAN	P.D.F MENL
1	0.200	0.000	0.4400E 00	0.4508E 00	0.4068E 00
1	0.200	0.250	0.4248E 00	0.4332E 00	0.3985E 00
1	0.200	0.500	0.3815E 00	0.3843E 00	0.3721E 00
1	0.200	0.750	0.3176E 00	0.3148E 00	0.3265E 00
1	0.200	1.000	0.2441E 00	0.2381E 00	0.2641E 00
1	0.200	1.250	0.1724E 00	0.1662E 00	0.1928E 00
1	0.200	1.500	0.1113E 00	0.1072E 00	0.1242E 00
1	0.200	1.750	0.6539E-01	0.6378E-01	0.6891E-01
1	0.200	2.000	0.3477E-01	0.3505E-01	0.3213E-01
1	0.200	2.250	0.1664E-01	0.1778E-01	0.1227E-01
1	0.200	2.500	0.7137E-02	0.8331E-02	0.3747E-02
1	0.200	2.750	0.2727E-02	0.3604E-02	0.8896E-03
1	0.200	3.000	0.9233E-03	0.1439E-02	0.1617E-03
1	0.200	3.250	0.2757E-03	0.5306E-03	0.2163E-04
1	0.200	3.500	0.7218E-04	0.1806E-03	0.2089E-05
1	0.200	3.750	0.1649E-04	0.5677E-04	0.1418E-06
1	0.200	4.000	0.3268E-05	0.1647E-04	0.6596E-08

n	ϵ^*	$Y=(X/6_0)$	P.D.F. ENL	P.D.F. GAUSSIAN	P.D.F. MENL
1	1.000	0.000	0.5431E 00	0.5735E 00	0.5170E 00
1	1.000	0.250	0.5177E 00	0.5376E 00	0.4998E 00
1	1.000	0.500	0.4445E 00	0.4429E 00	0.4445E 00
1	1.000	0.750	0.3375E 00	0.3207E 00	0.3517E 00
1	1.000	1.000	0.2216E 00	0.2041E 00	0.2374E 00
1	1.000	1.250	0.1229E 00	0.1141E 00	0.1304E 00
1	1.000	1.500	0.5608E-01	0.5608E-01	0.5550E-01
1	1.000	1.750	0.2053E-01	0.2422E-01	0.1738E-01
1	1.000	2.000	0.5875E-02	0.9192E-02	0.3806E-02
1	1.000	2.250	0.1279E-02	0.3066E-02	0.5525E-03
1	1.000	2.500	0.2064E-03	0.8988E-03	0.5092E-04
1	1.000	2.750	0.2404E-04	0.2316E-03	0.2773E-05
1	1.000	3.000	0.1968E-05	0.5242E-04	0.8553E-07
1	1.000	3.250	0.1102E-06	0.1043E-04	0.1418E-08
1	1.000	3.500	0.4113E-08	0.1824E-05	0.1199E-10
1	1.000	3.750	0.9958E-10	0.2803E-06	0.4909E-13
1	1.000	4.000	0.1523E-11	0.3785E-07	0.9241E-16

TABLE 9a

NORMALISED PROBABILITY DENSITY FUNCTIONS

n	ϵ^*	$Y=(X/\sigma_0)$	P.D.F. ENL	P.D.F. GAUSSIAN	P.D.F. MENL
6	0.100	0.000	0.4704E 00	0.5183E 00	0.4047E 00
6	0.100	0.250	0.4541E 00	0.4916E 00	0.3992E 00
6	0.100	0.500	0.4080E 00	0.4197E 00	0.3821E 00
6	0.100	0.750	0.3393E 00	0.3224E 00	0.3512E 00
6	0.100	1.000	0.2577E 00	0.2229E 00	0.3013E 00
6	0.100	1.250	0.1726E 00	0.1386E 00	0.2230E 00
6	0.100	1.500	0.9359E-01	0.7760E-01	0.1154E 00
6	0.100	1.750	0.3376E-01	0.3909E-01	0.2454E-01
6	0.100	2.000	0.5309E-02	0.1772E-01	0.5787E-03
6	0.100	2.250	0.1556E-03	0.7228E-02	0.1300E-06
6	0.100	2.500	0.1732E-06	0.2653E-02	0.3772E-14
6	0.100	2.750	0.4576E-12	0.8764E-03	0.4458E-29
6	0.100	3.000	0.2977E-22	0.2605E-03	0.3396E-57
6	0.100	3.250	0.3629E-40	0.6968E-04	0.0000E 00
6	0.100	3.500	0.1584E-70	0.1677E-04	0.0000E 00
6	0.100	3.750	0.0000E 00	0.3633E-05	0.0000E 00
6	0.100	4.000	0.0000E 00	0.7081E-06	0.0000E 00

n	ϵ^*	$Y=(X/\sigma_0)$	P.D.F. ENL	P.D.F. GAUSSIAN	P.D.F. MENL
6	1.000	0.000	0.5577E 00	0.6384E 00	0.5060E 00
6	1.000	0.250	0.5346E 00	0.5893E 00	0.4951E 00
6	1.000	0.500	0.4684E 00	0.4635E 00	0.4608E 00
6	1.000	0.750	0.3668E 00	0.3107E 00	0.3950E 00
6	1.000	1.000	0.2378E 00	0.1774E 00	0.2787E 00
6	1.000	1.250	0.9990E-01	0.8634E-01	0.1098E 00
6	1.000	1.500	0.1330E-01	0.3580E-01	0.7234E-02
6	1.000	1.750	0.8664E-04	0.1265E-01	0.2303E-05
6	1.000	2.000	0.3879E-09	0.3809E-02	0.5586E-14
6	1.000	2.250	0.2050E-21	0.9771E-03	0.2061E-34
6	1.000	2.500	0.1322E-47	0.2136E-03	0.0000E 00
6	1.000	2.750	0.0000E 00	0.3979E-04	0.0000E 00
6	1.000	3.000	0.0000E 00	0.6315E-05	0.0000E 00
6	1.000	3.250	0.0000E 00	0.8541E-06	0.0000E 00
6	1.000	3.500	0.0000E 00	0.9843E-07	0.0000E 00
6	1.000	3.750	0.0000E 00	0.9666E-08	0.0000E 00
6	1.000	4.000	0.0000E 00	0.8088E-09	0.0000E 00

TABLE 9b

NORMALISED PROBABILITY DENSITY FUNCTIONS

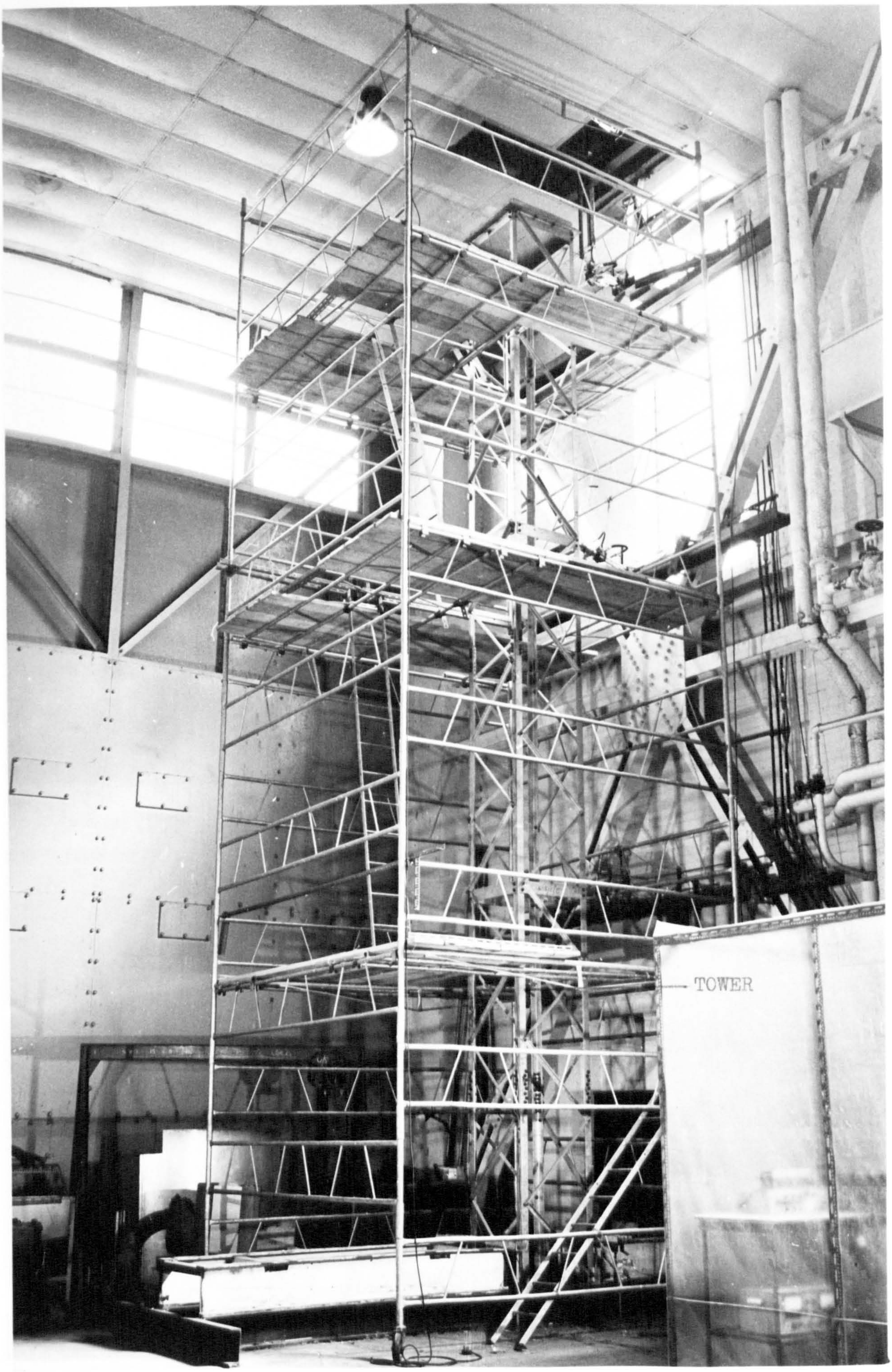

30 FOOT HIGH SELF SUPPORTING LATTICE TOWER
FIGURE 13

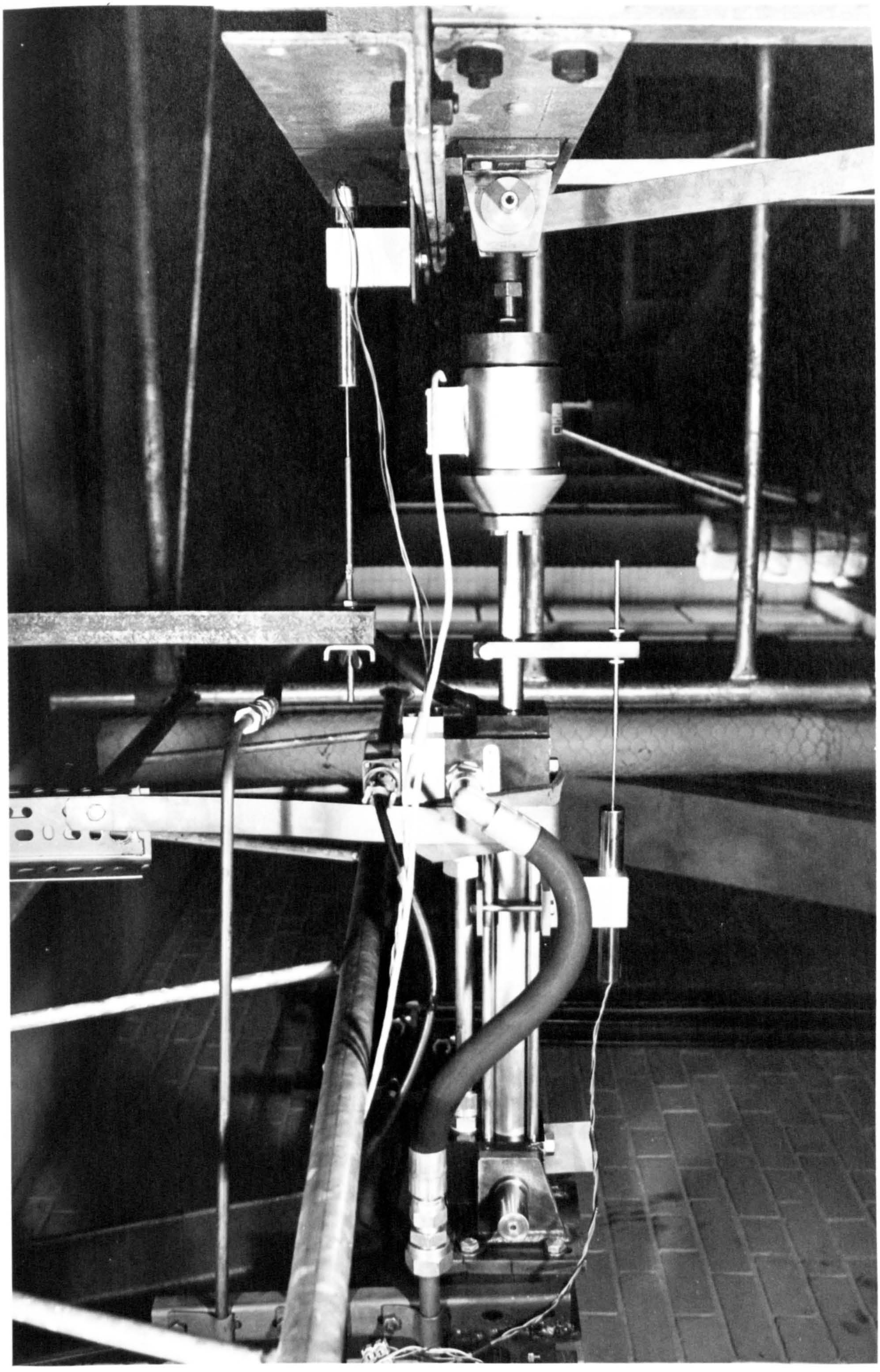

VIEW OF TOP ACTUATOR
FIGURE 14

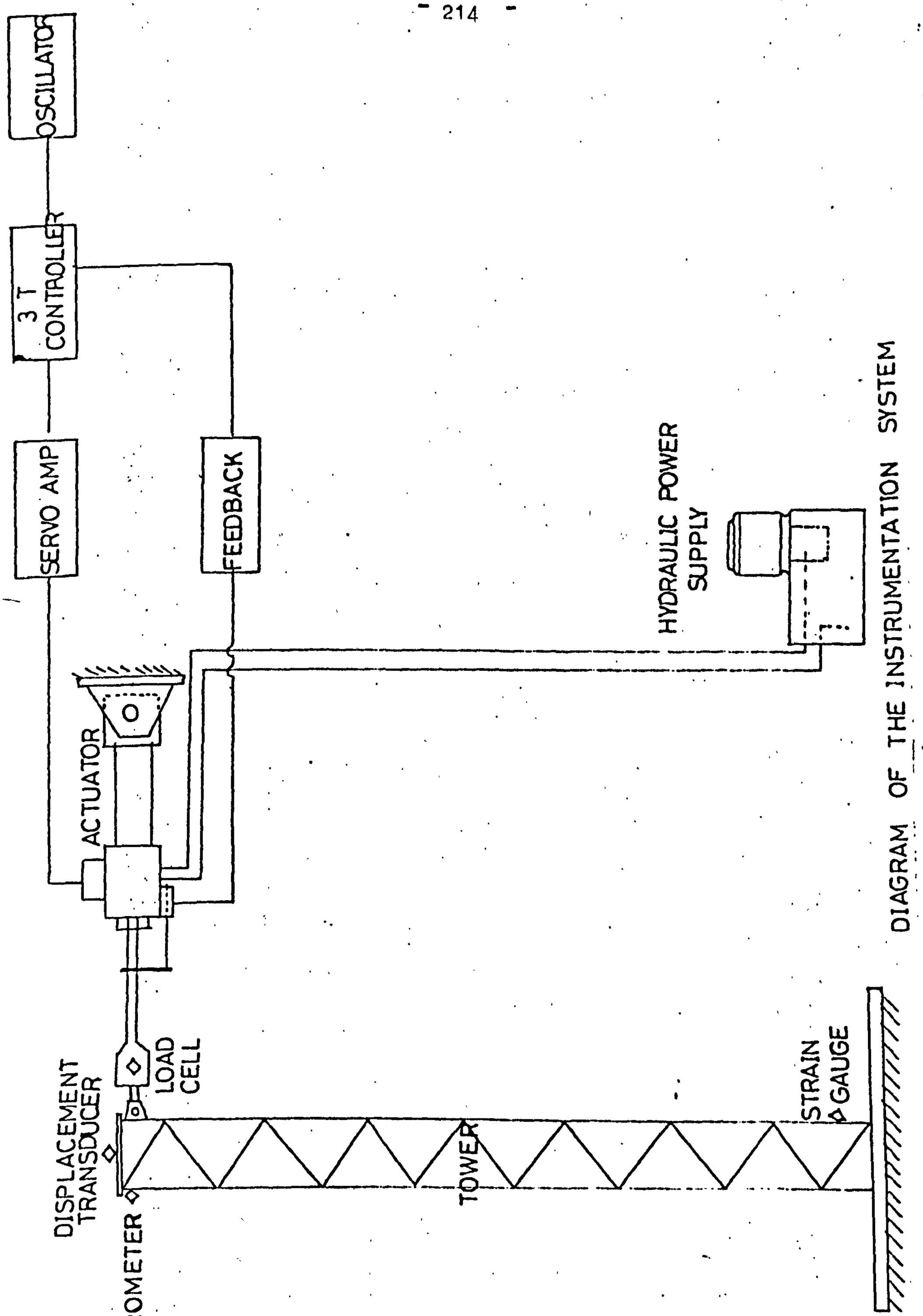

FIGURE 15

DIAGRAM OF THE INSTRUMENTATION SYSTEM

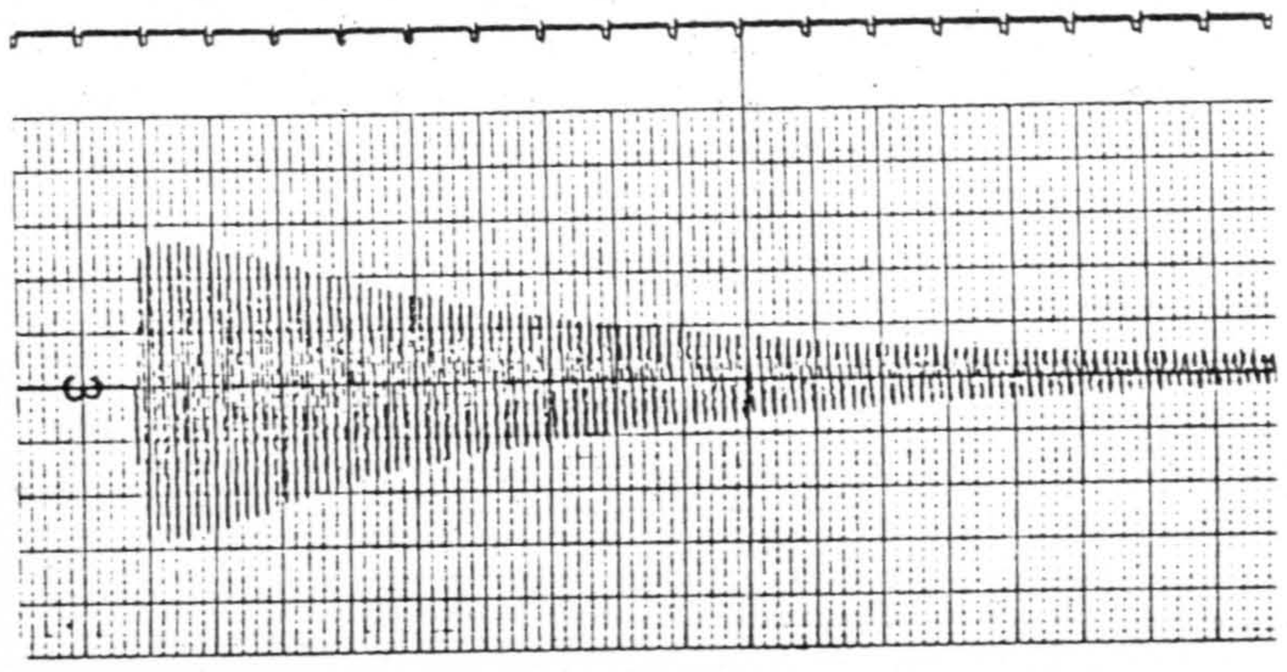

OSCILLATIONS IN LINE WITH INITIAL DISPLACEMENT X

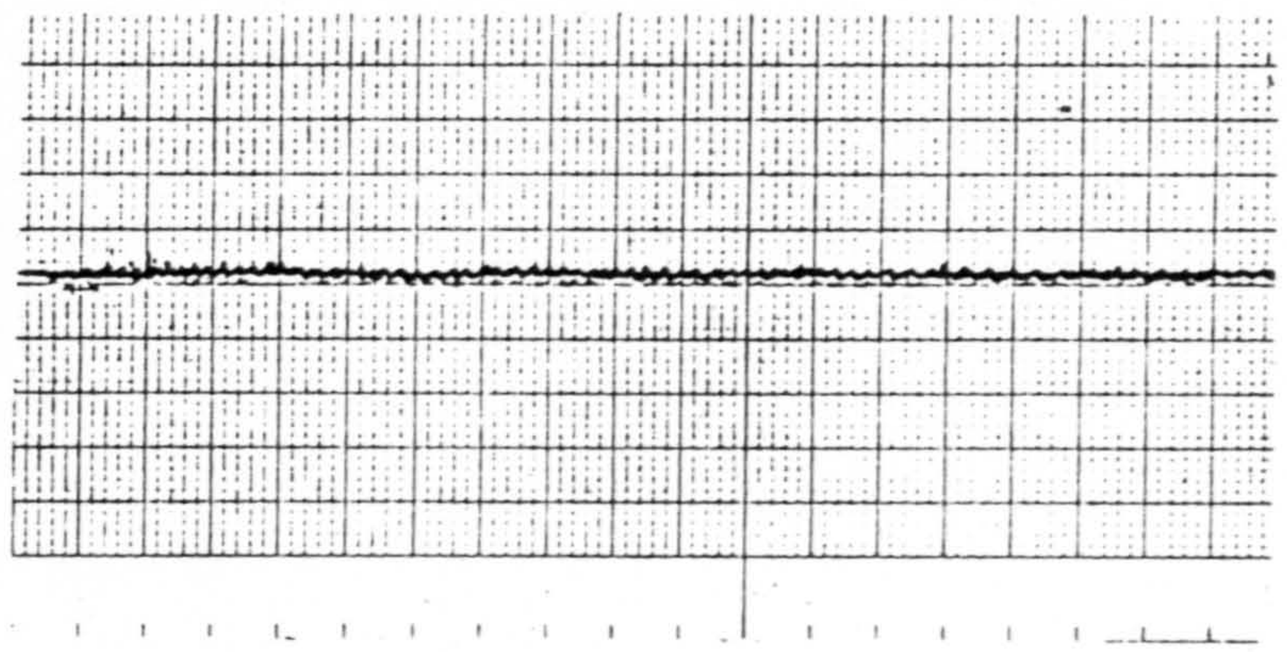

OSCILLATIONS IN ORTHOGONAL PLANE Y

FREE VIBRATION TIME HISTORIES
FIGURE 16

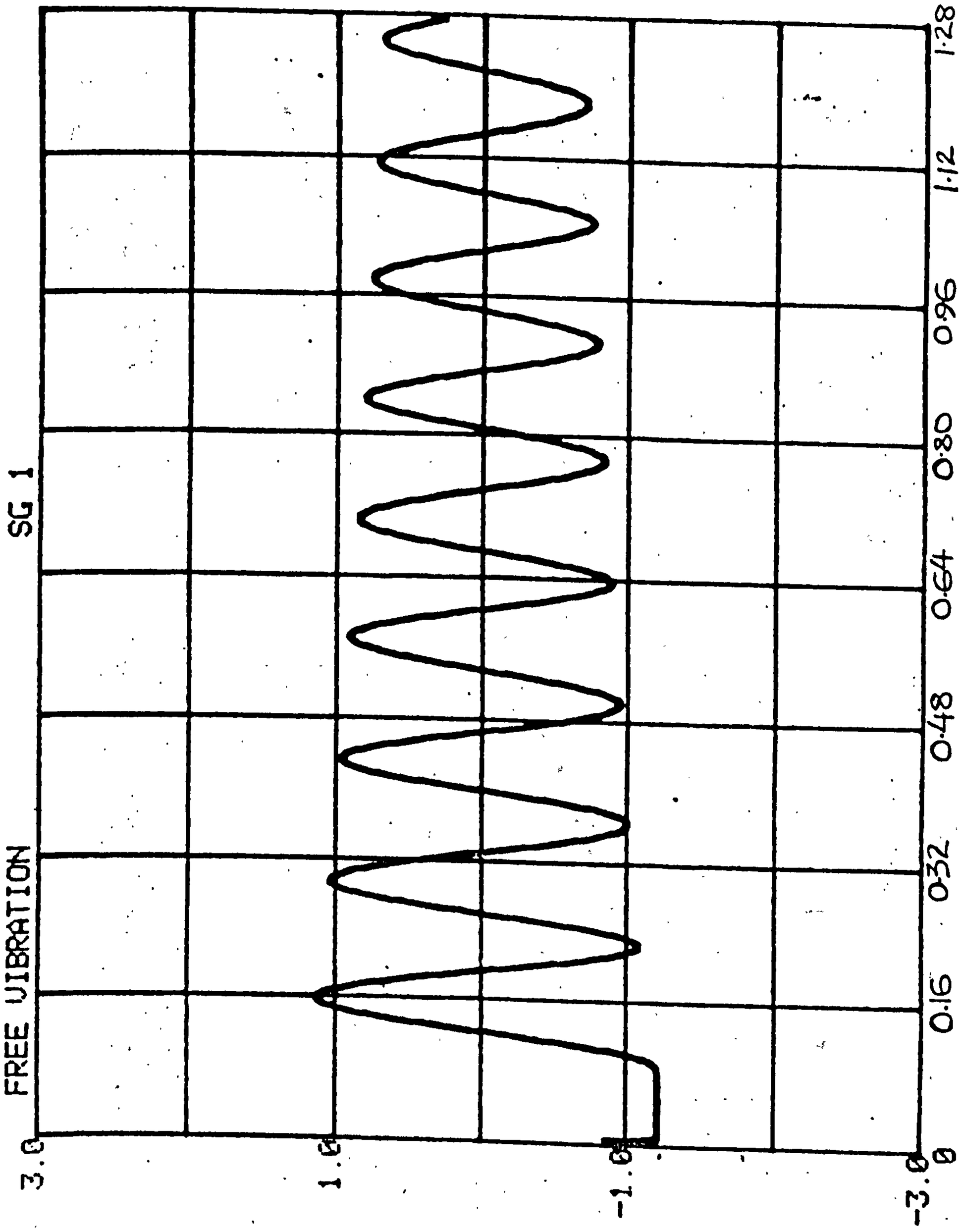

FREE VIBRATION TIME HISTORY
FIGURE 16b

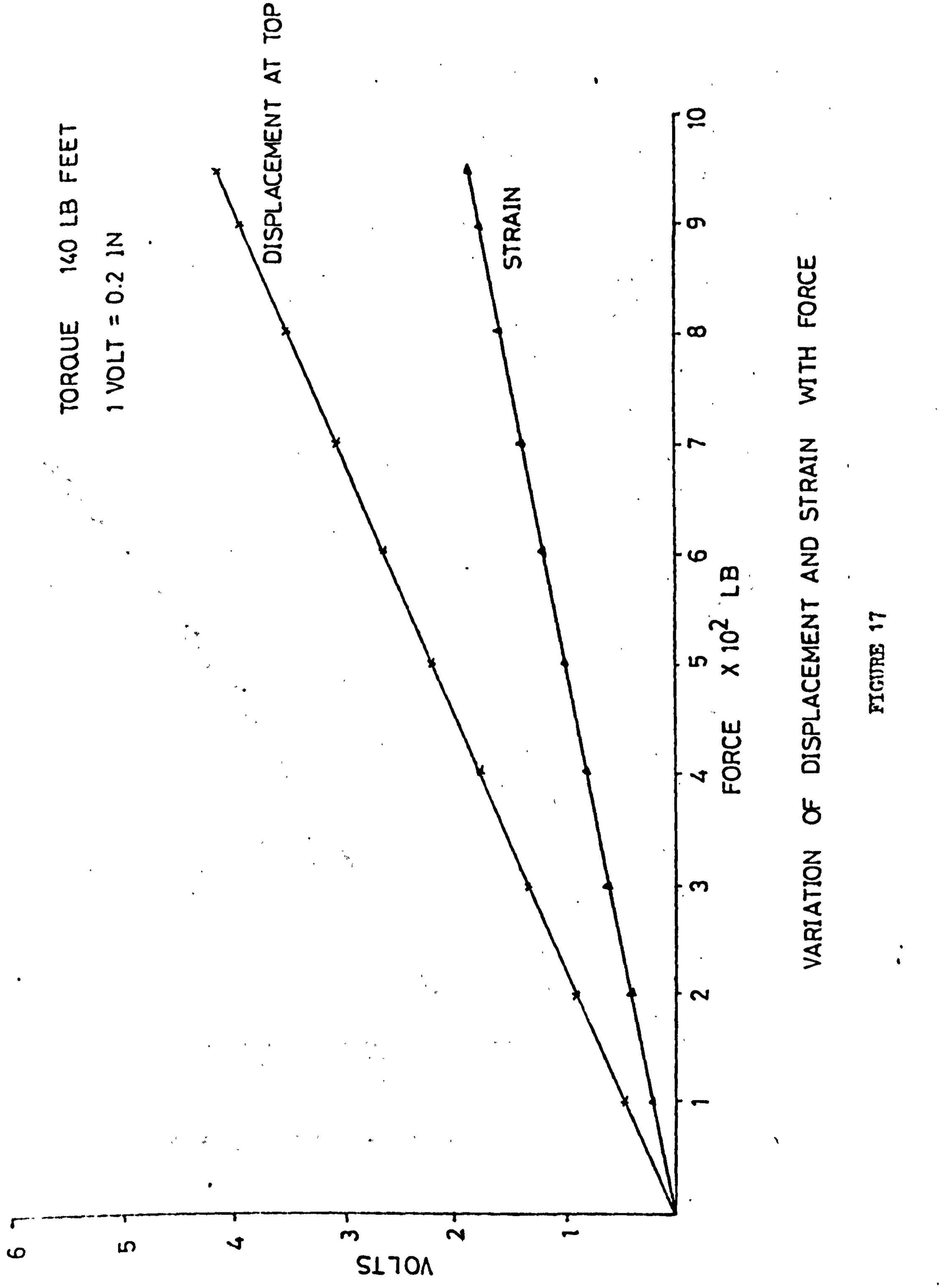

VARIATION OF DISPLACEMENT AND STRAIN WITH FORCE

FIGURE 17

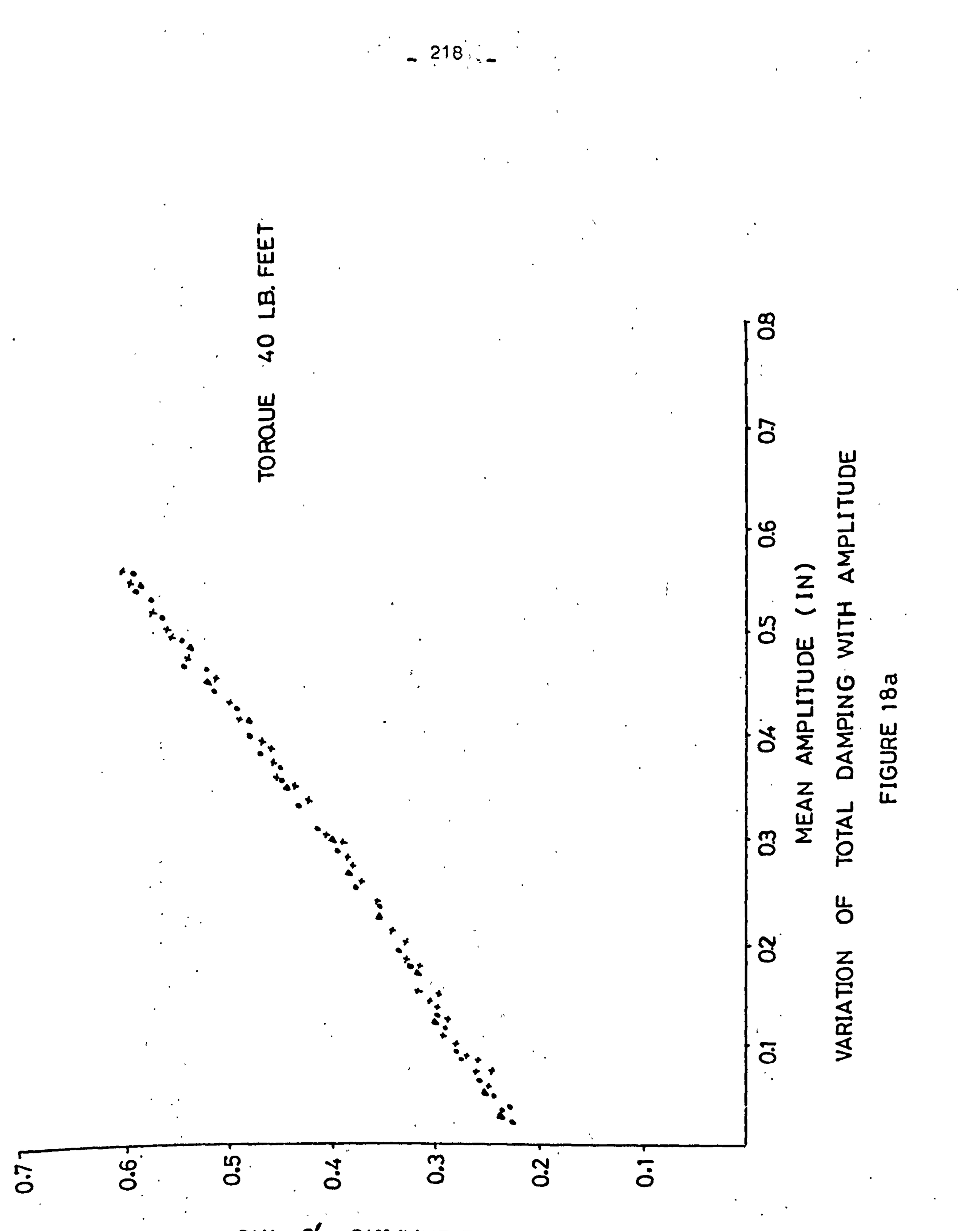
TOTAL DAMPING $\beta \times 10^2$
0.7
0.6
0.5
0.4
0.3
0.2
0.1
0.1
0.2
0.3
0.4
0.5
0.6
0.7
0.8
MEAN AMPLITUDE (IN)
VARIATION OF TOTAL DAMPING WITH AMPLITUDE
TORQUE 40 LB. FEET

FIGURE 18a

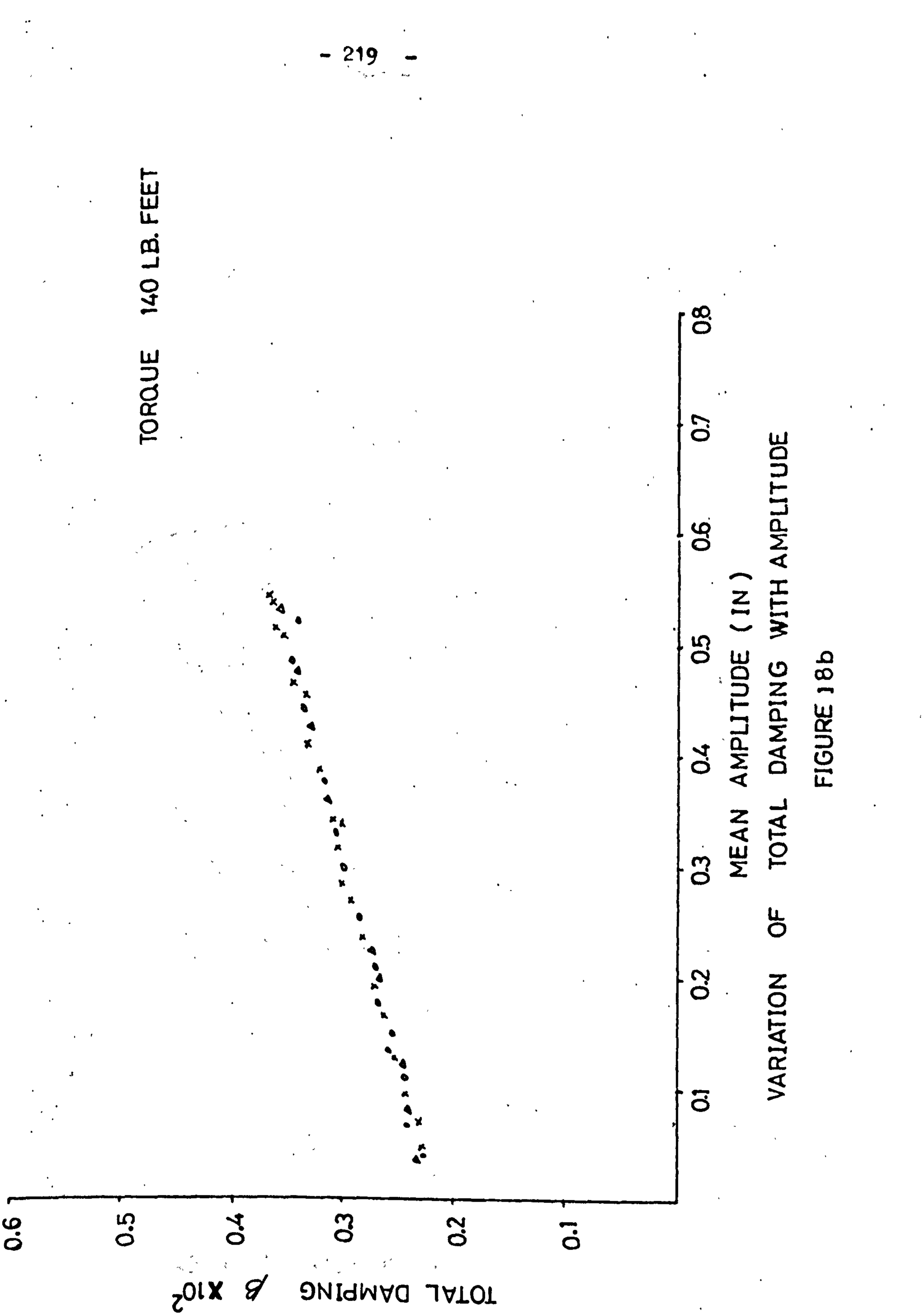

VARIATION OF TOTAL DAMPING WITH AMPLITUDE

FIGURE 18b

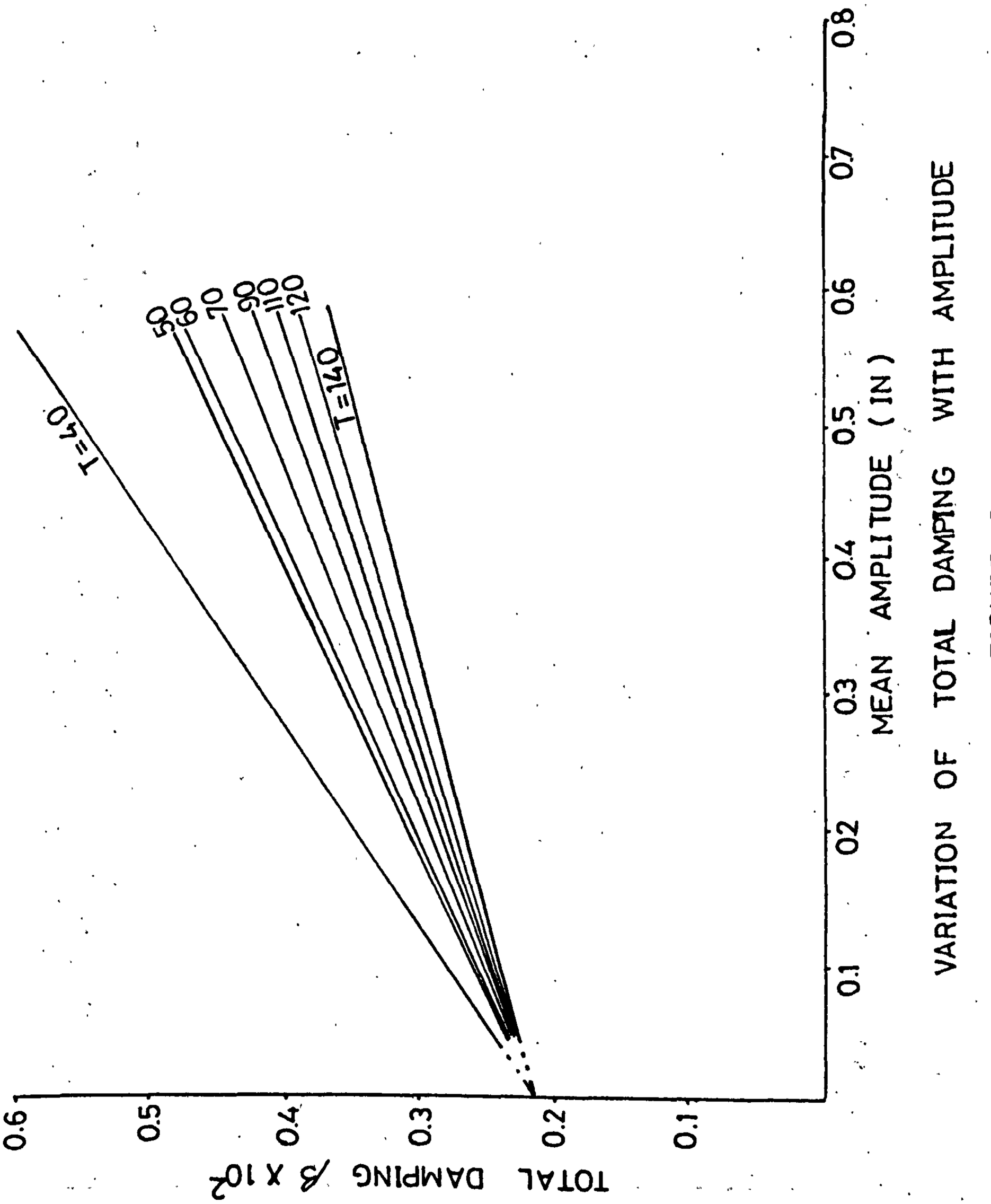

VARIATION OF TOTAL DAMPING WITH AMPLITUDE

FIGURE 18c

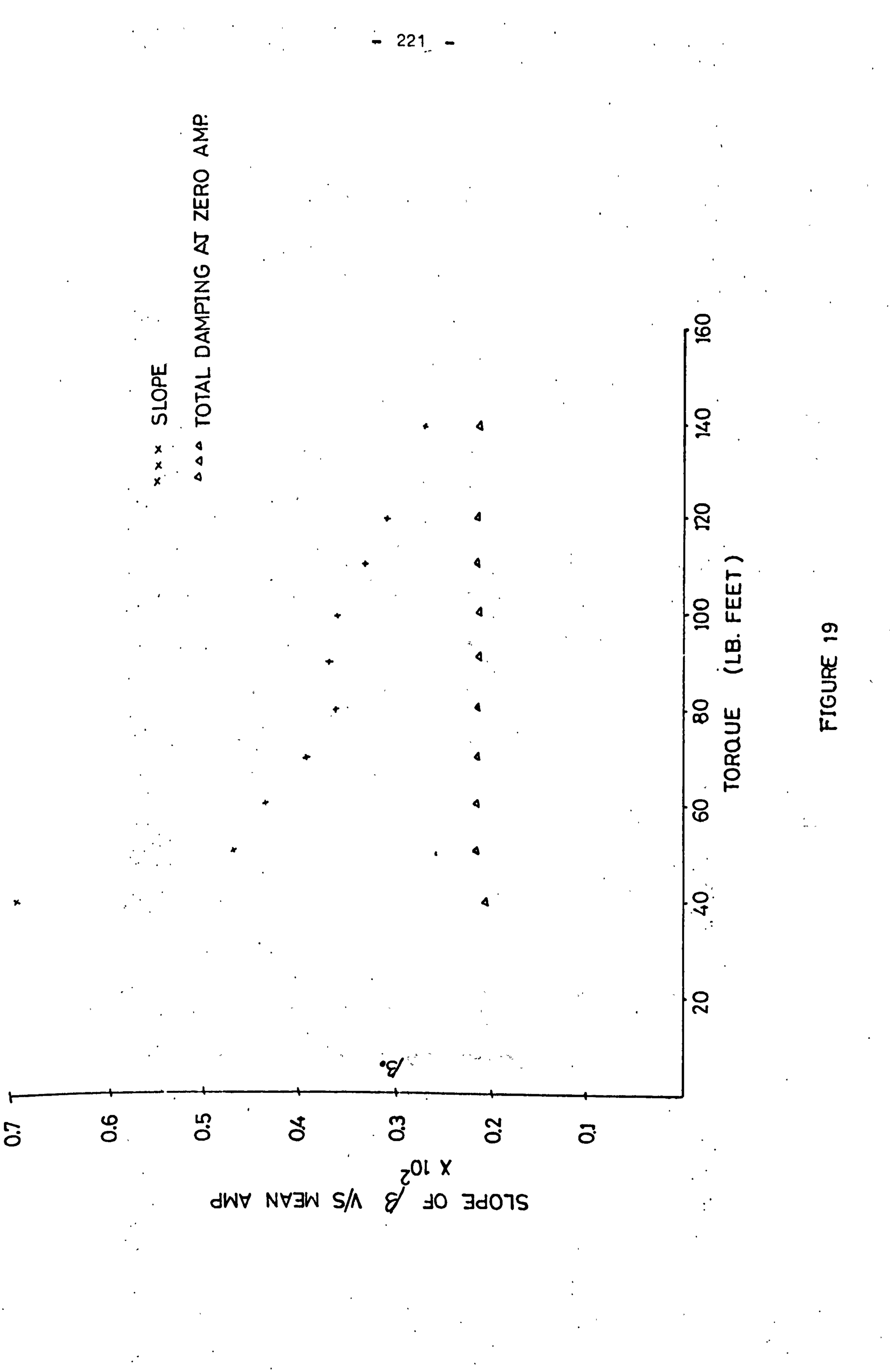
SLOPE OF β V/S MEAN AMP
X 10^2
β
0.7
0.6
0.5
0.4
0.3
0.2
0.1
TORQUE (LB. FEET)
20
40
60
80
100
120
140
160
× × × SLOPE
△ △ △ TOTAL DAMPING AT ZERO AMP.

FIGURE 19

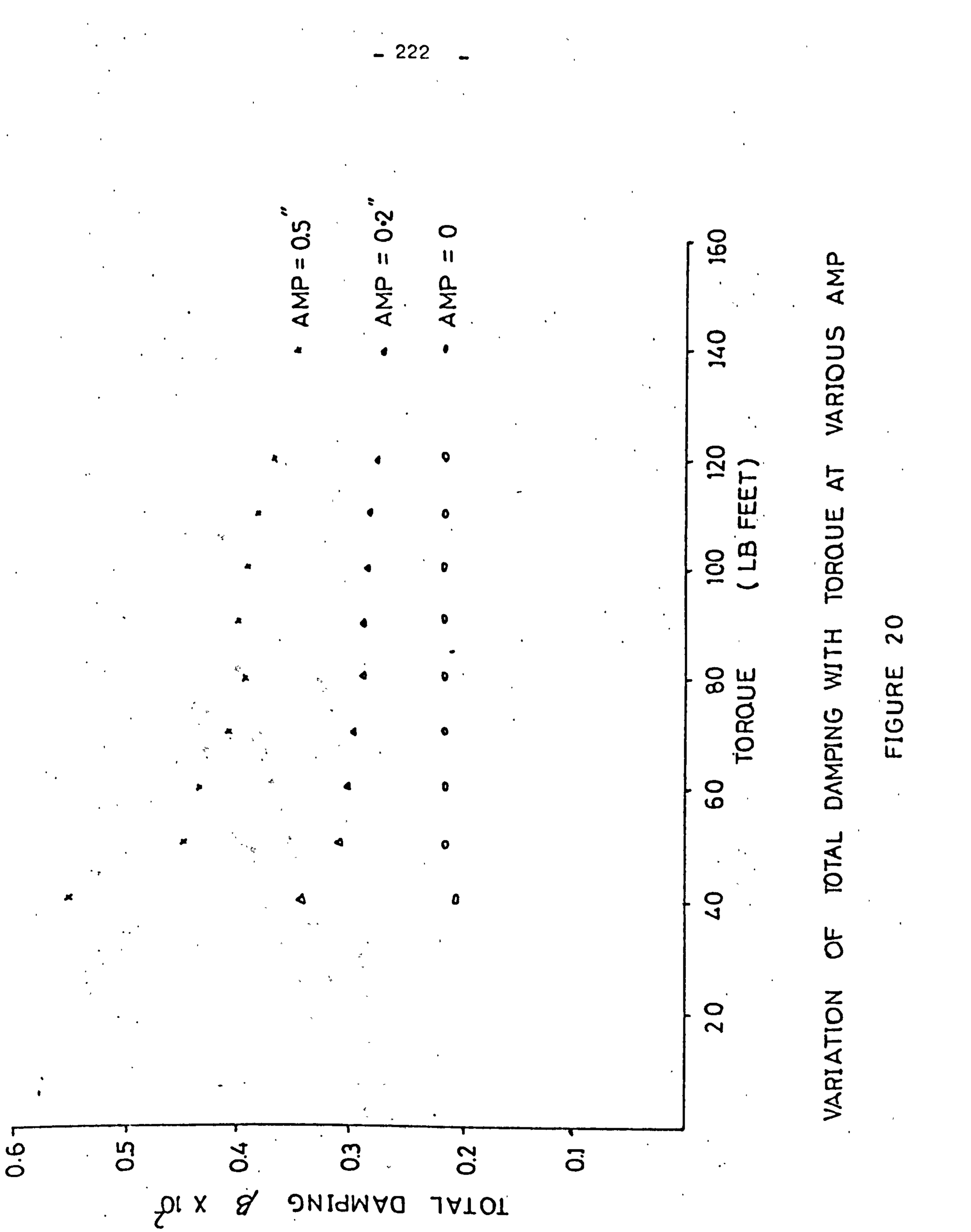
TOTAL DAMPING $\beta \times 10^2$
0.6
0.5
0.4
0.3
0.2
0.1
20
40
60
80
100
120
140
160
TORQUE (LB FEET)
VARIATION OF TOTAL DAMPING WITH TORQUE AT VARIOUS AMP
• AMP = 0.5"
• AMP = 0.2"
• AMP = 0

FIGURE 20

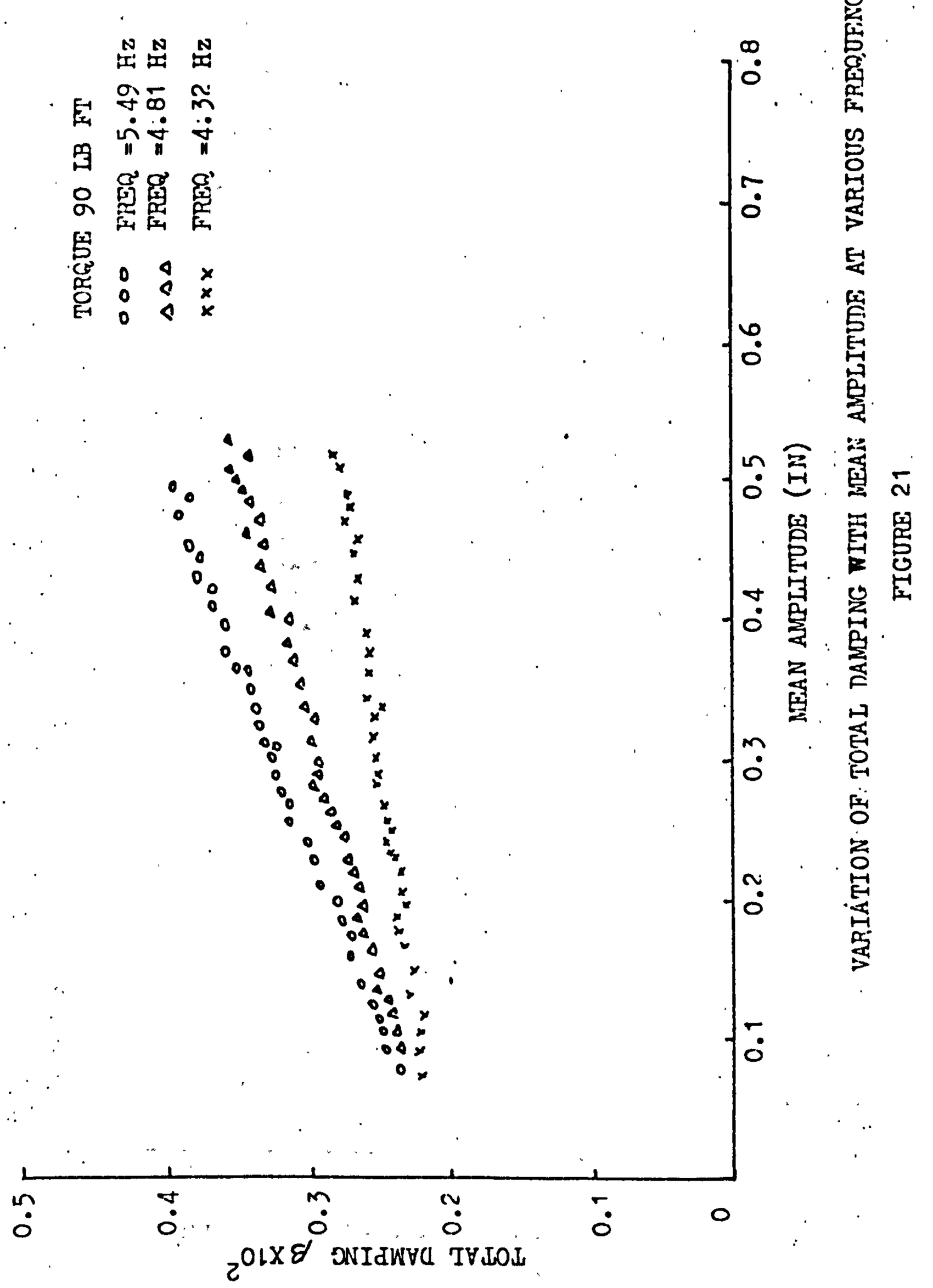

VARIATION OF TOTAL DAMPING WITH MEAN AMPLITUDE AT VARIOUS FREQUENCIES

FIGURE 21

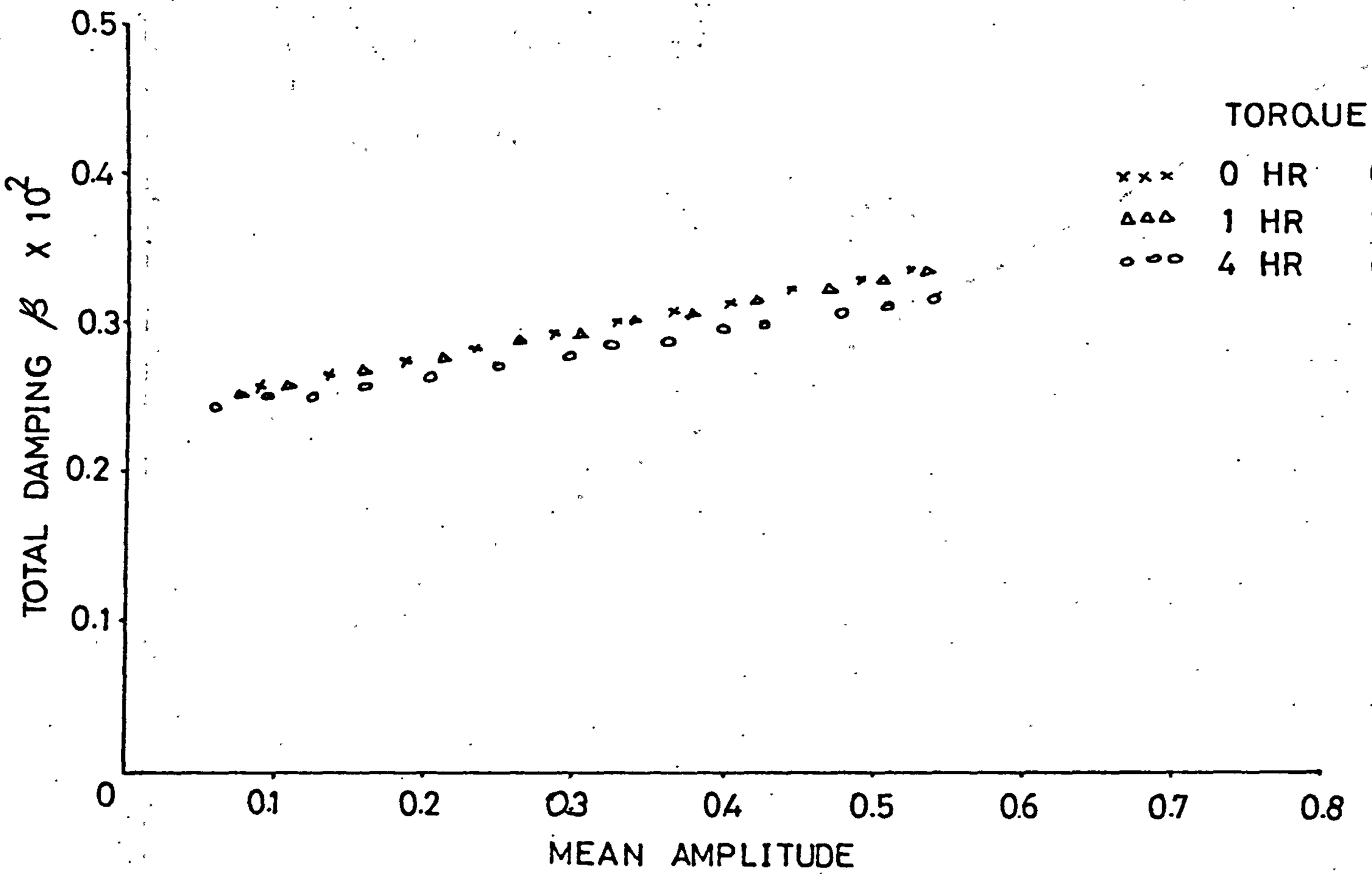

TIME EFFECT ON TOTAL DAMPING

FIGURE 22

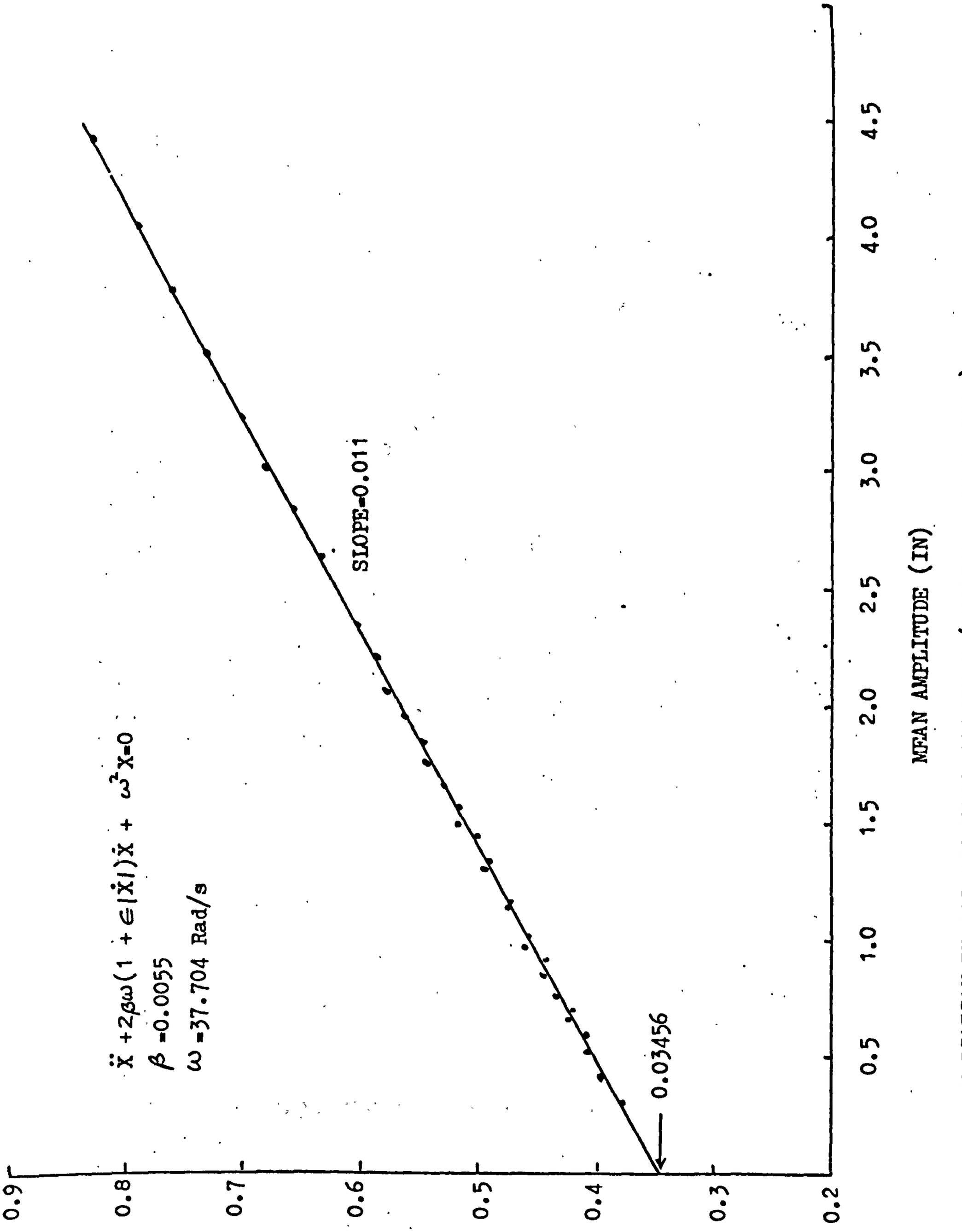

VARIATION IF LOG DEC WITH AMPLITUDE (DIGITAL SIMULATION)

FIGURE 23

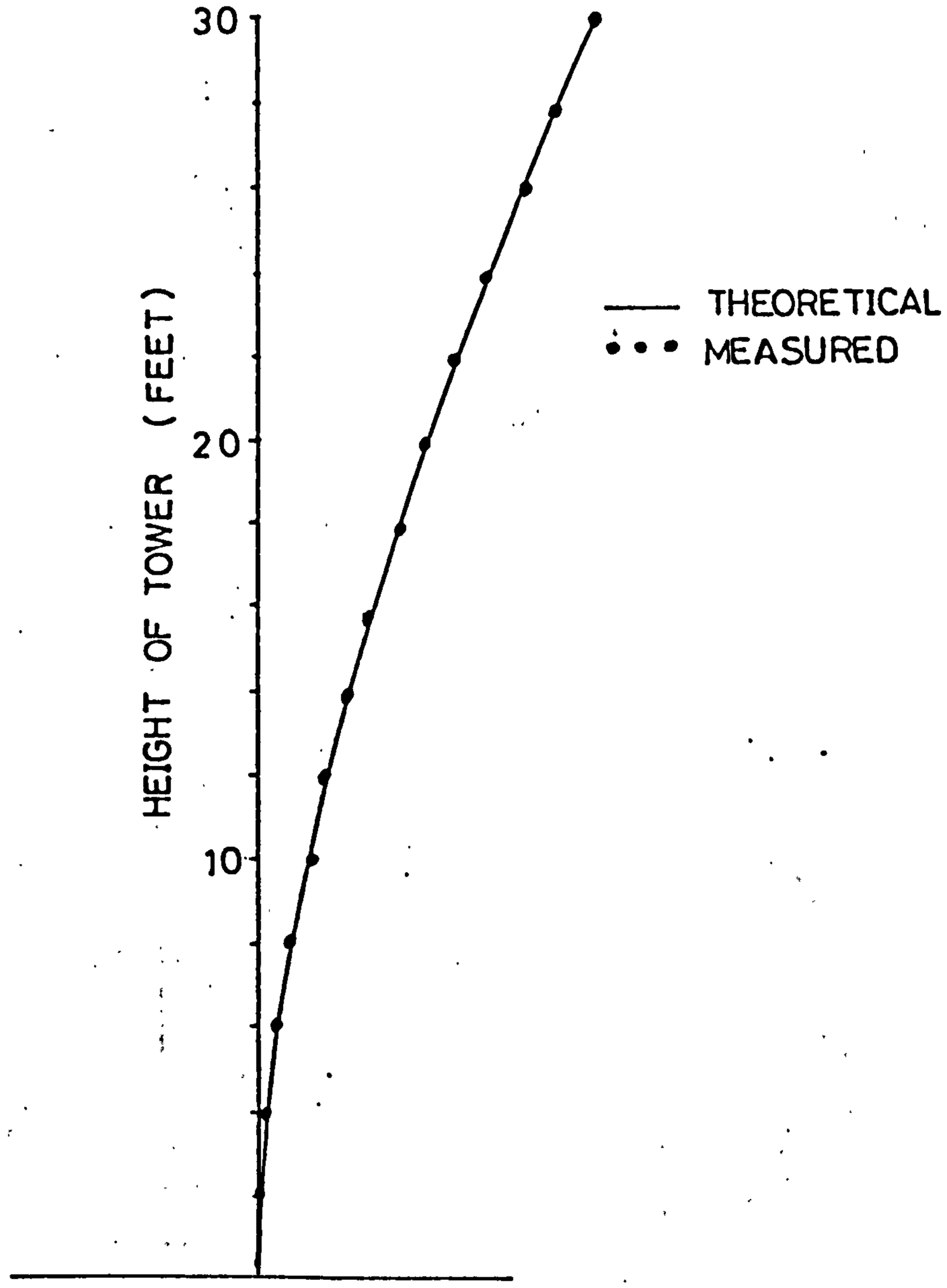

FUNDAMENTAL MODE SHAPE

FIGURE 24a

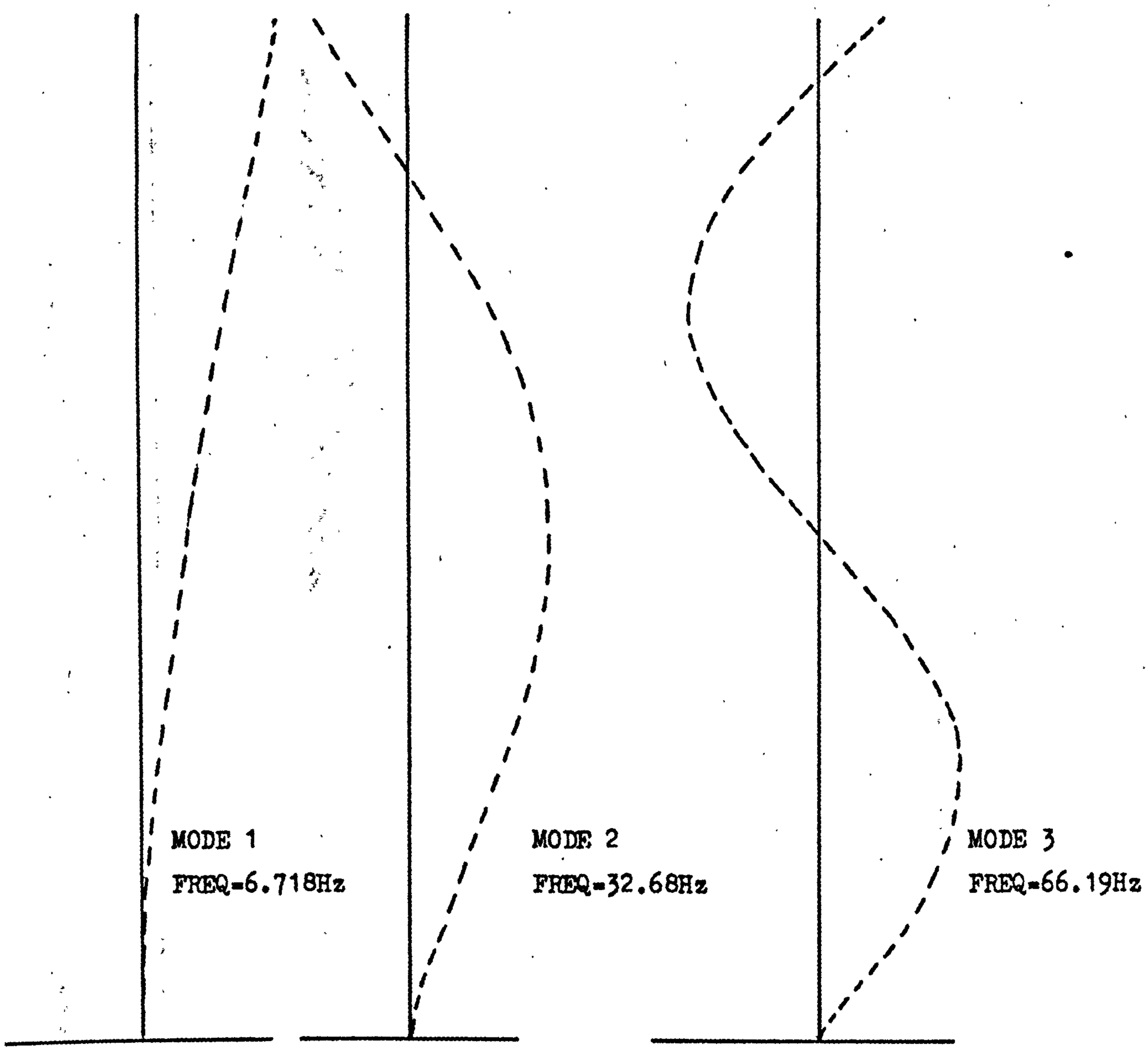

COMPUTED MODE SHAPES OF THE TOWER

FIGURE 24b

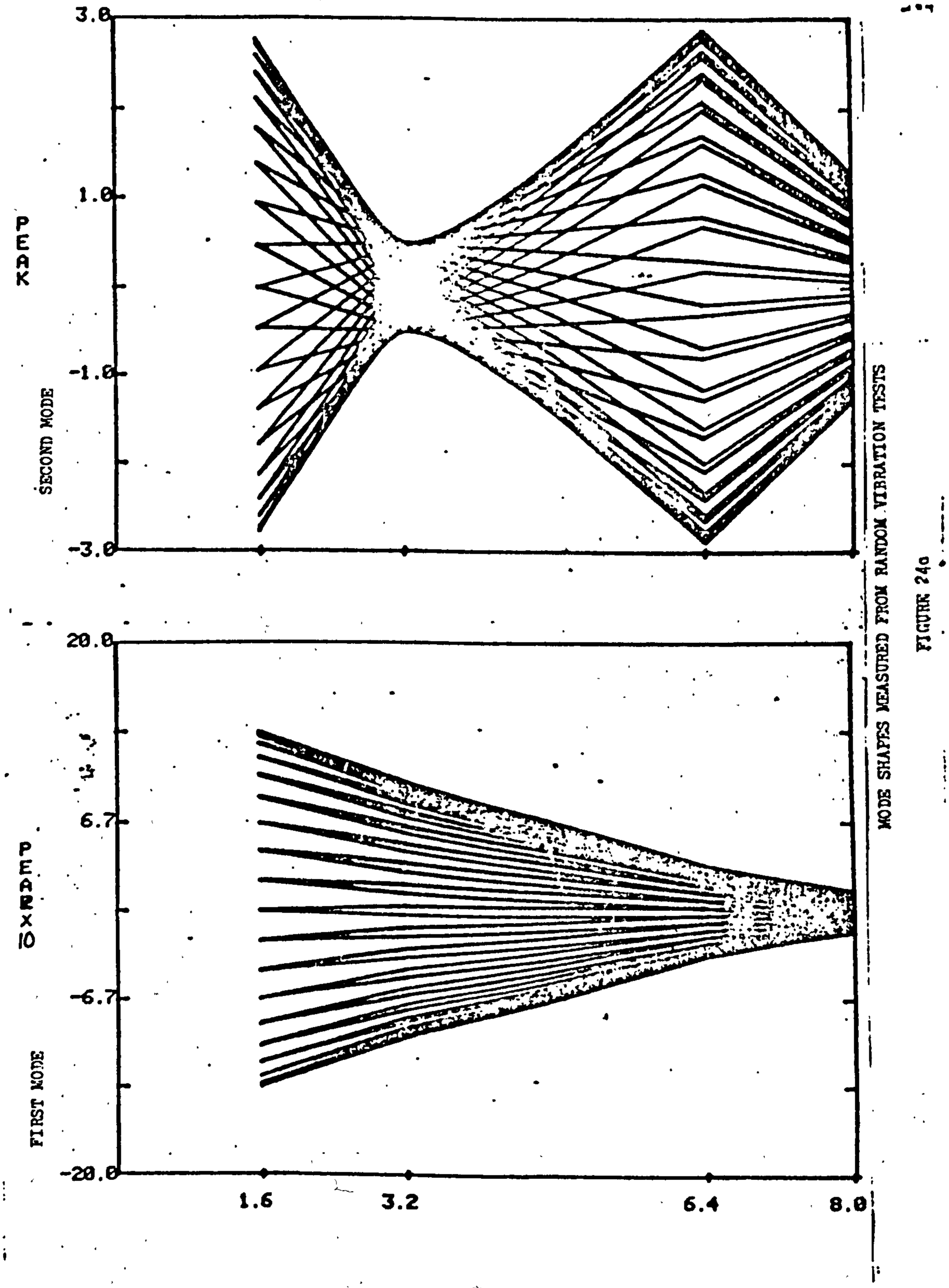

FIGURE 240 MODE SHAPES MEASURED FROM RANDOM VIBRATION TESTS

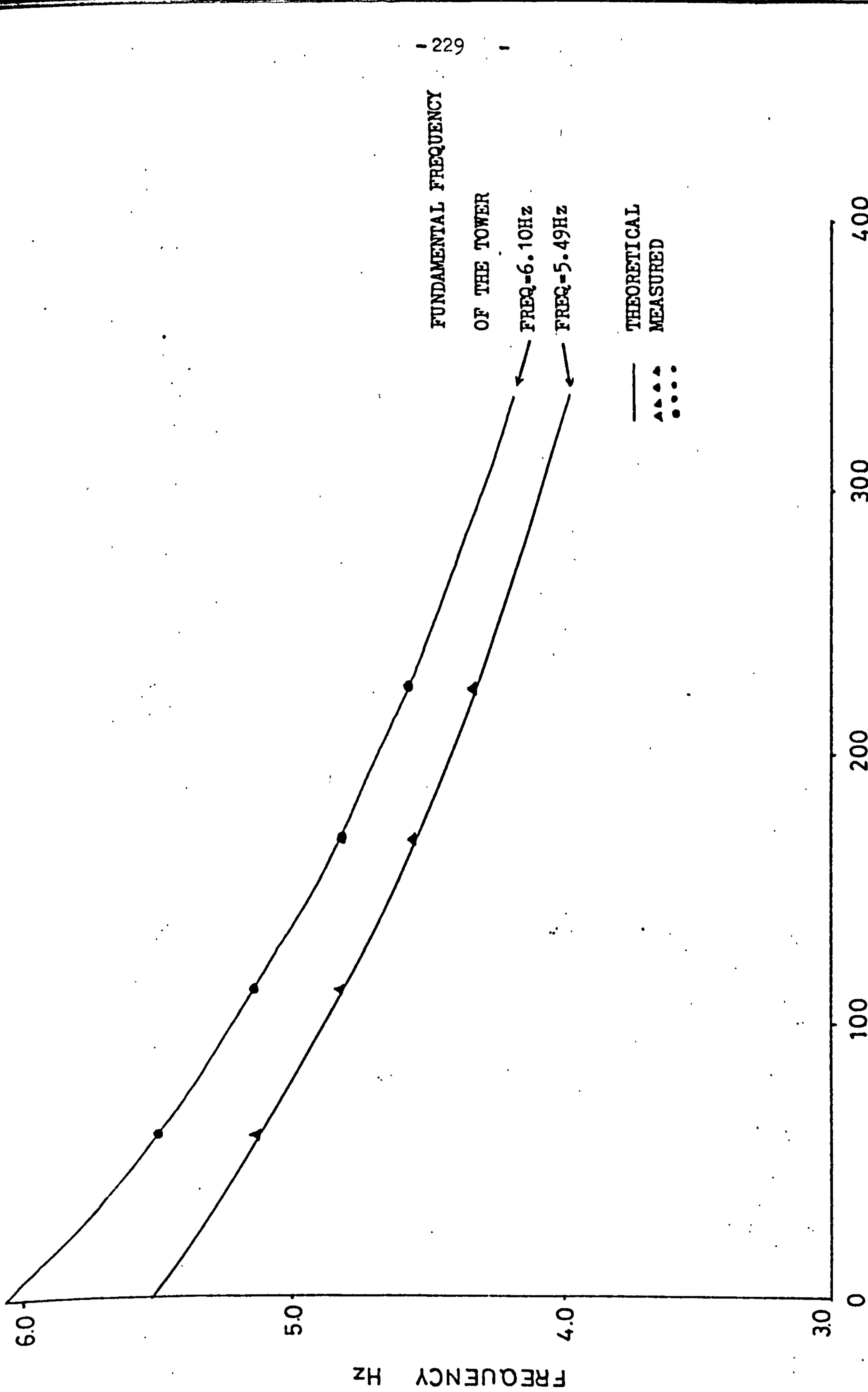
FUNDAMENTAL FREQUENCY
OF THE TOWER
FREQ=6.10Hz
FREQ=5.49Hz
THEORETICAL
MEASURED
400
300
200
100
0
MASS (LB)
ADDED
VARIATION OF FREQUENCY WITH ADDED MASS
6.0
5.0
4.0
3.0
FREQUENCY Hz

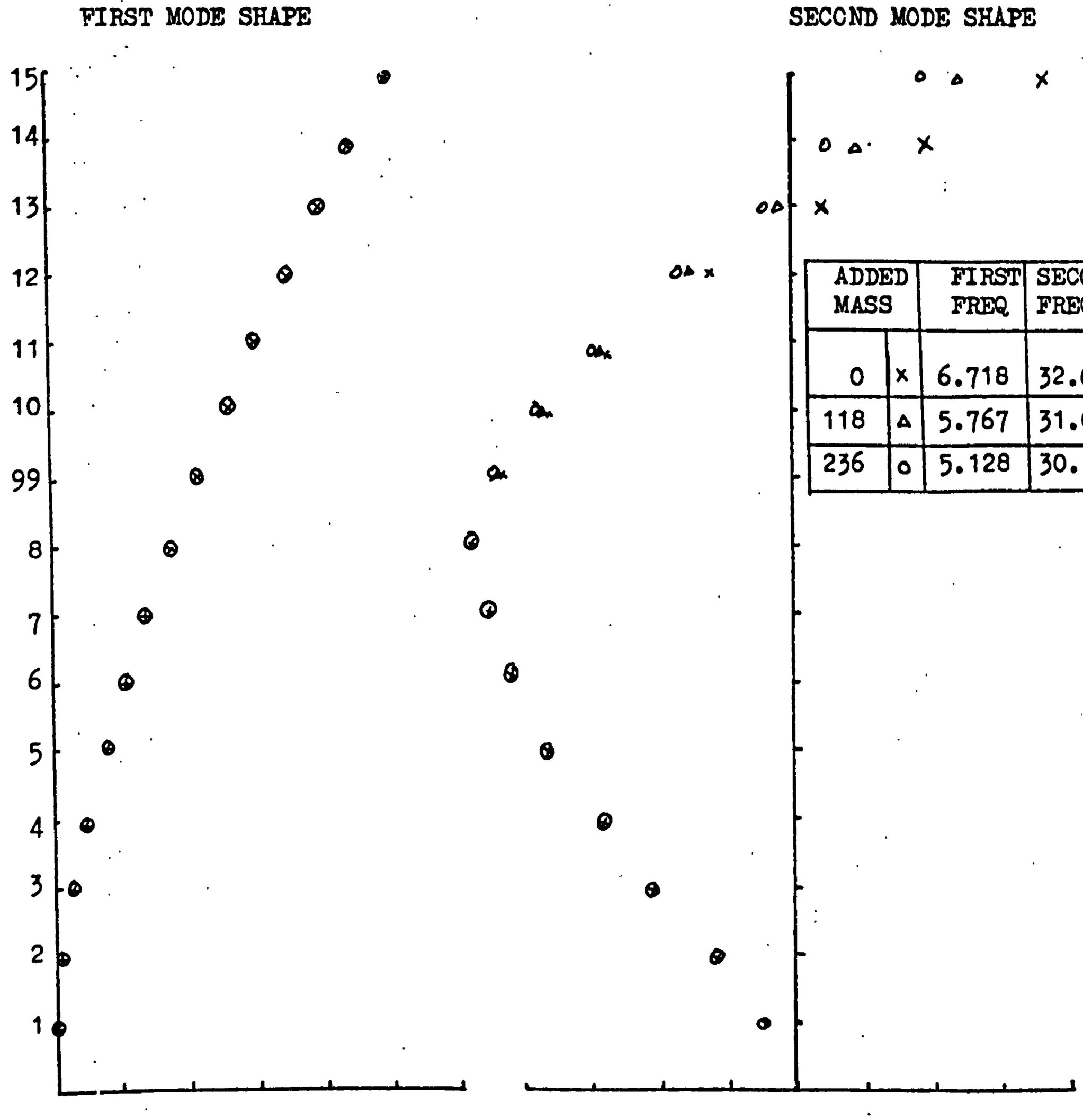

EFFECT OF ADDED MASS ON MODE SHAPE
(FINITE ELEMENT PROGRAM)

FIGURE 26

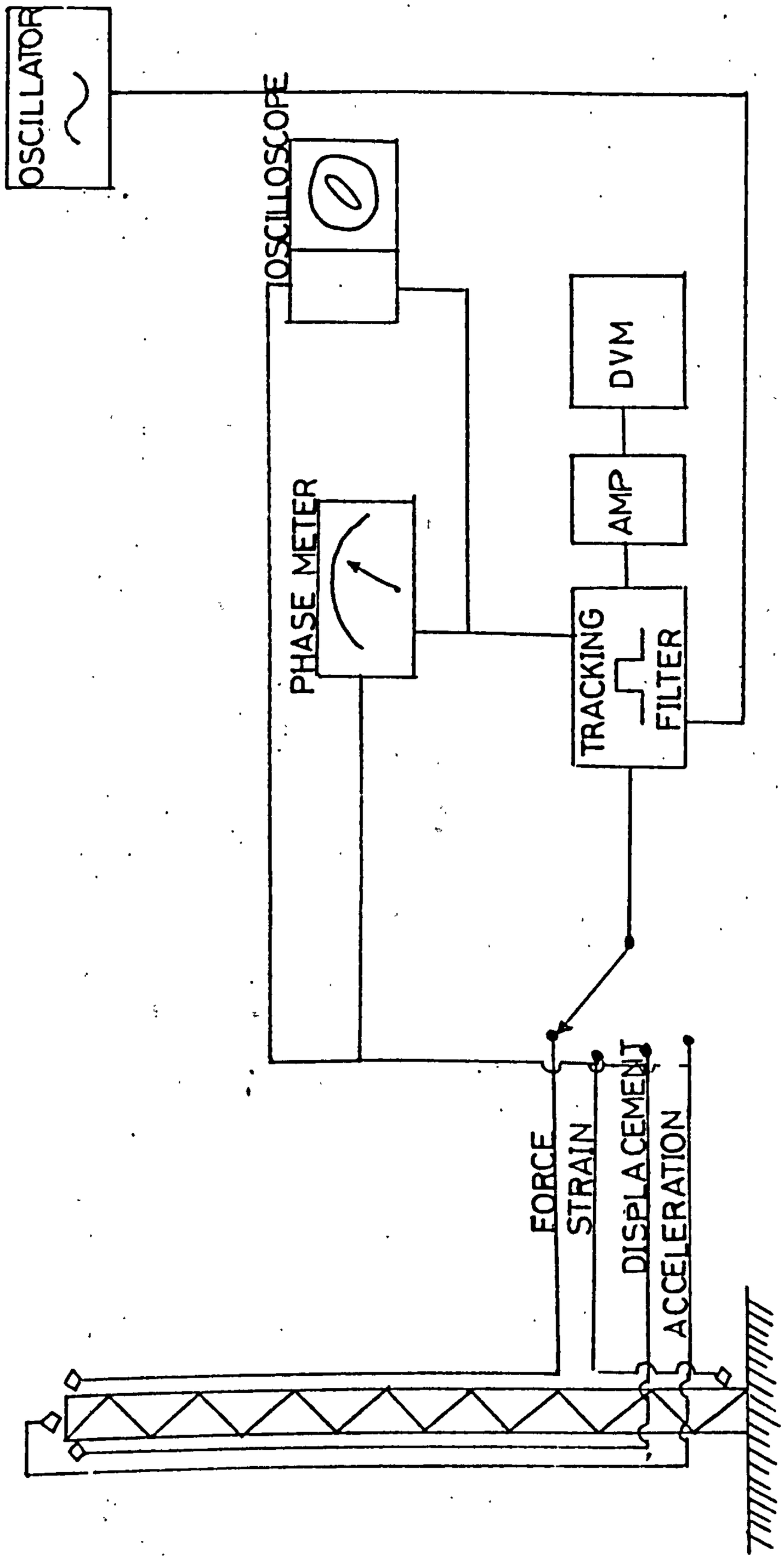

SET UP TO MEASURE FREQUENCY RESPONSE FUNCTION

FIGURE 27a

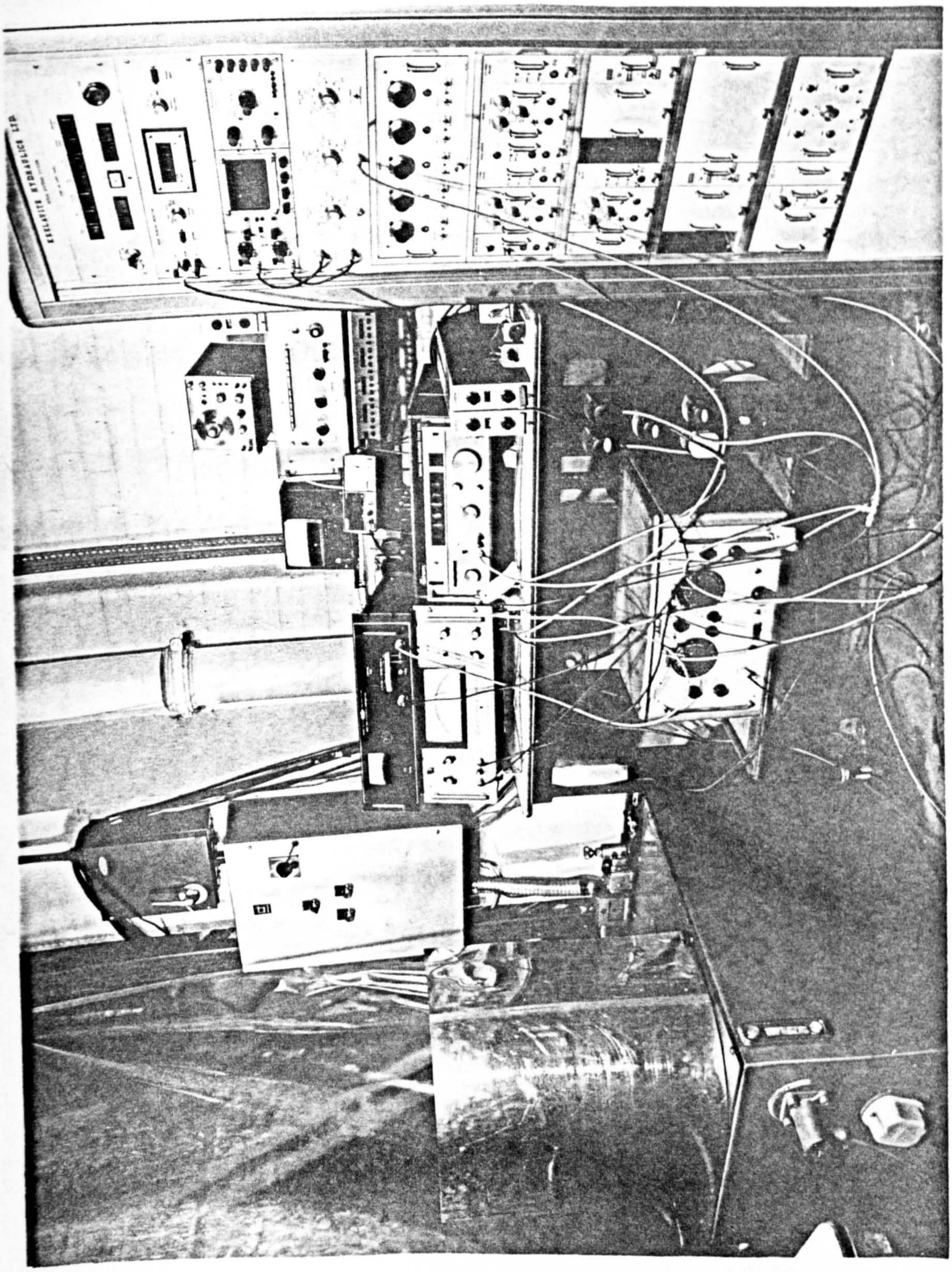

FIGURE 27b SET UP TO MEASURE FREQUENCY RESPONSE FUNCTION

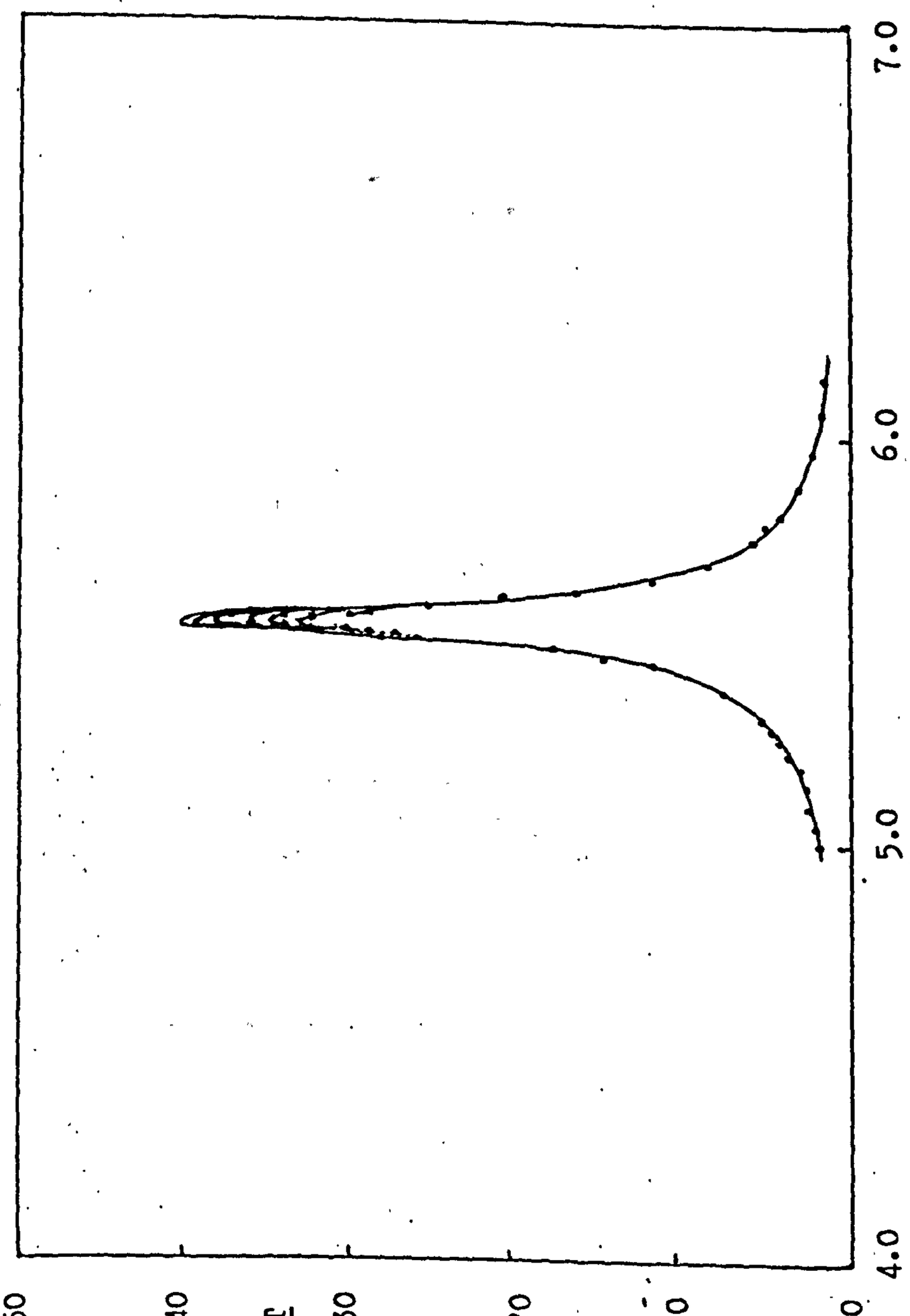
STEADY STATE RESONANCE TESTS (FREQUENCY RESPONSE FUNCTIONS)
DISPLACEMENT / FORCE (X 10^{-3})
50
40
30
20
10
0
4.0
5.0
6.0
7.0
FREQUENCY (Hz)

FIGURE 28a

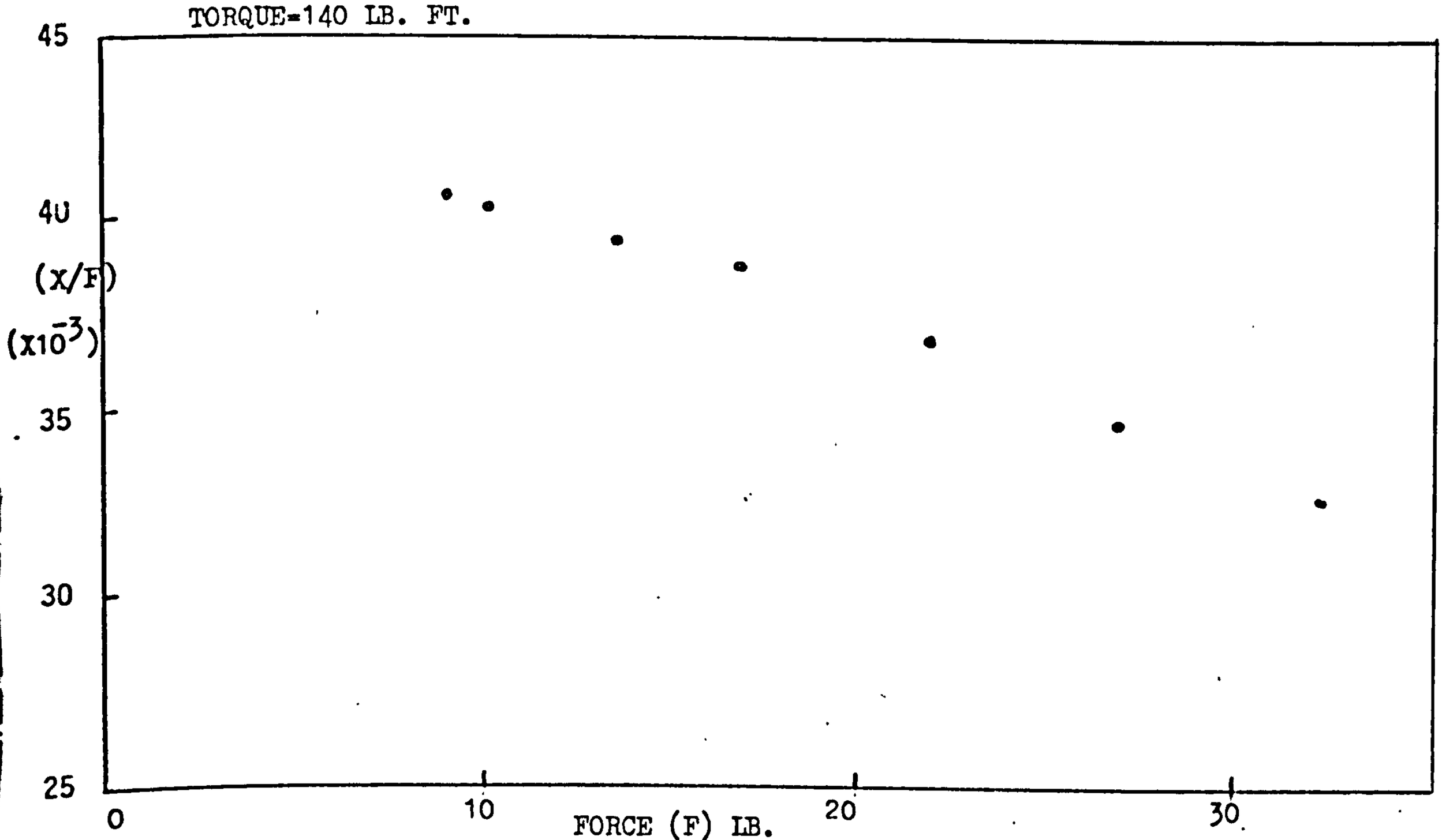

VARIATION OF (X/F) AT RESONANCE WITH APPLIED FORCE

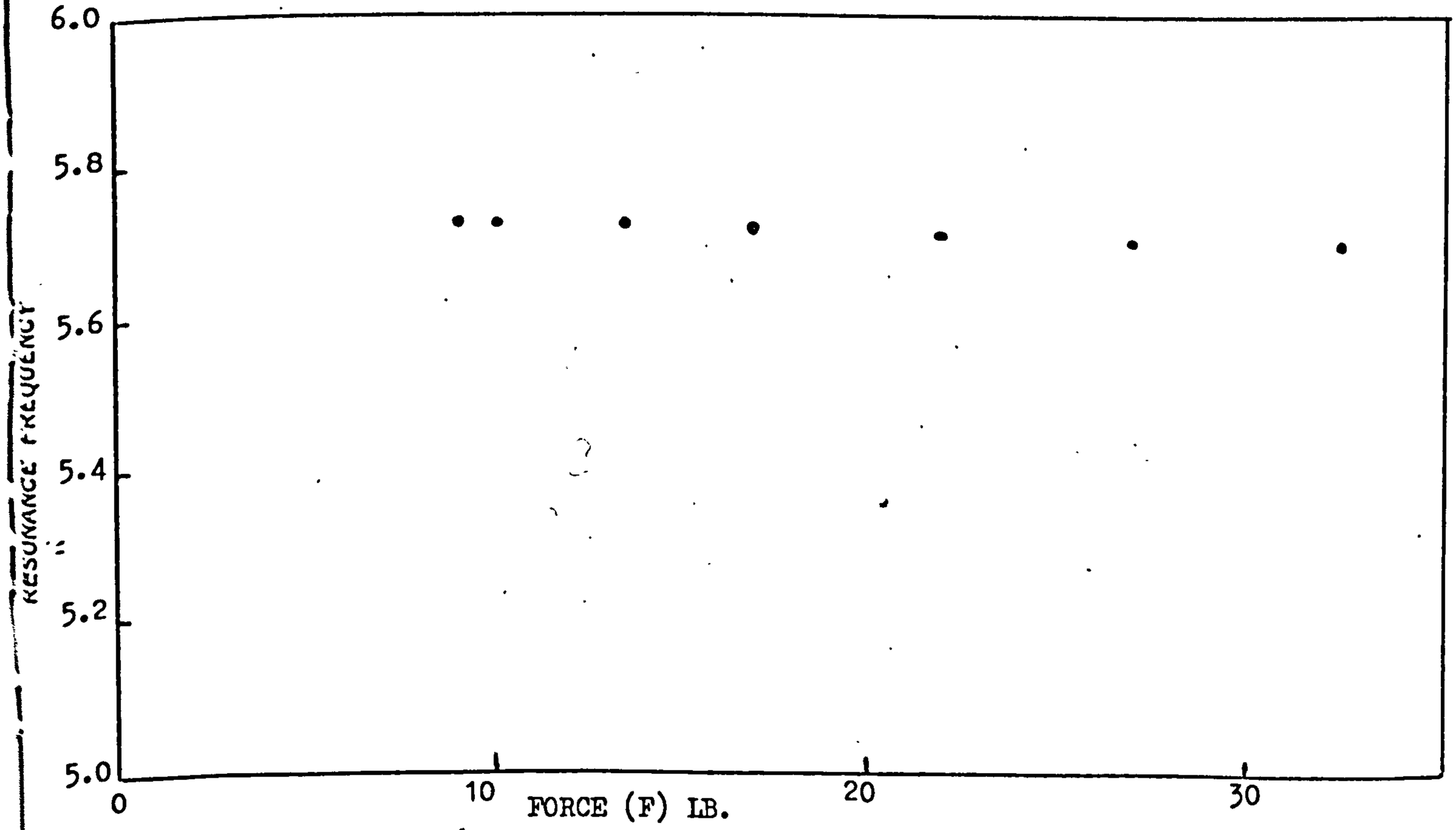

VARIATION OF RESONANCE FREQUENCY WITH APPLIED FORCE

FIGURE 28b

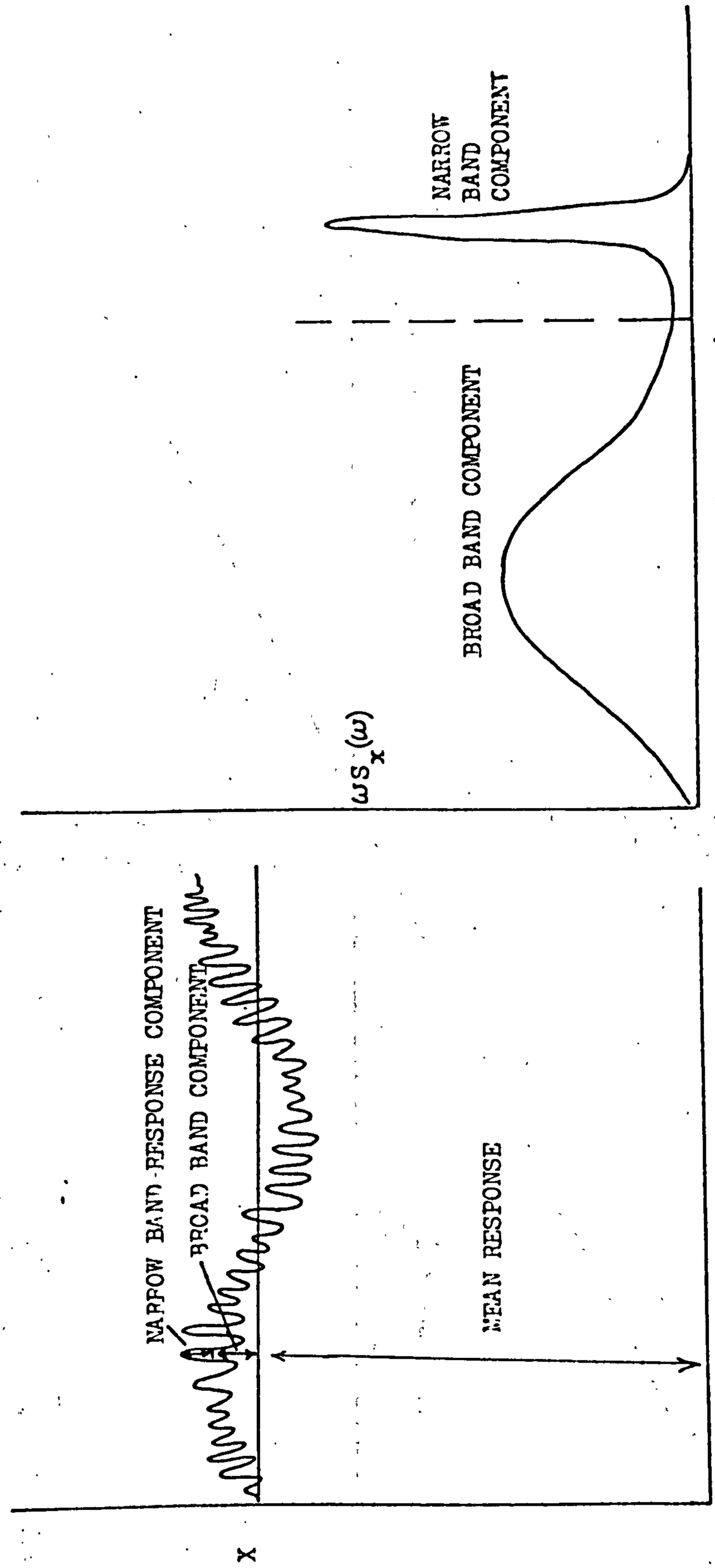
NARROW BAND COMPONENT
BROAD BAND COMPONENT
$\omega S_x(\omega)$
FREQUENCY (LOG. SCALE)
(b)
LOADING
NARROW BAND RESPONSE COMPONENT
BROAD BAND COMPONENT
MEAN RESPONSE
TIME
(a)
RESPONSE TO WIND
FIGURE 29
x

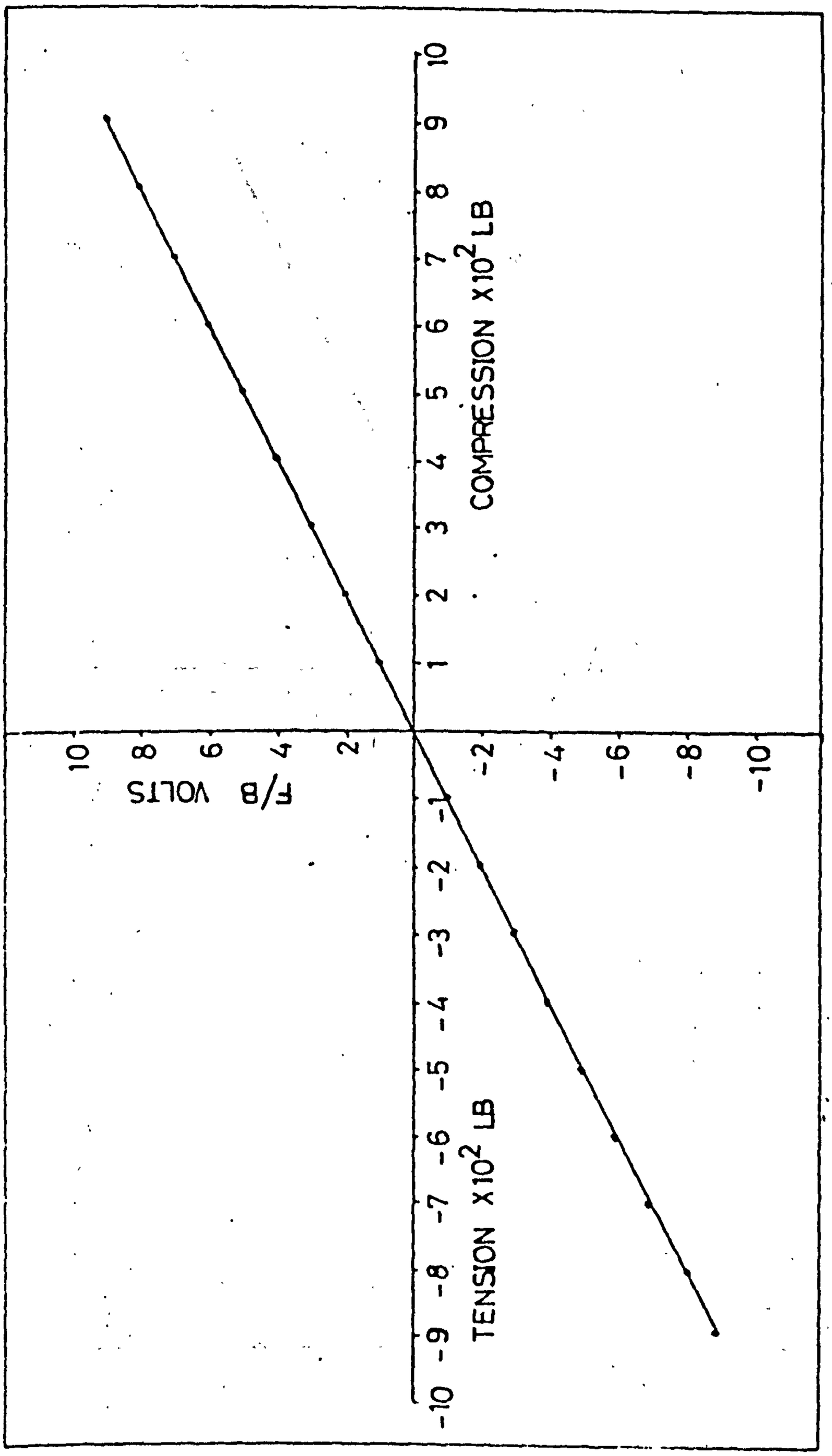

CALIBRATION OF THE LOADCAD CELL

FIGURE 30a

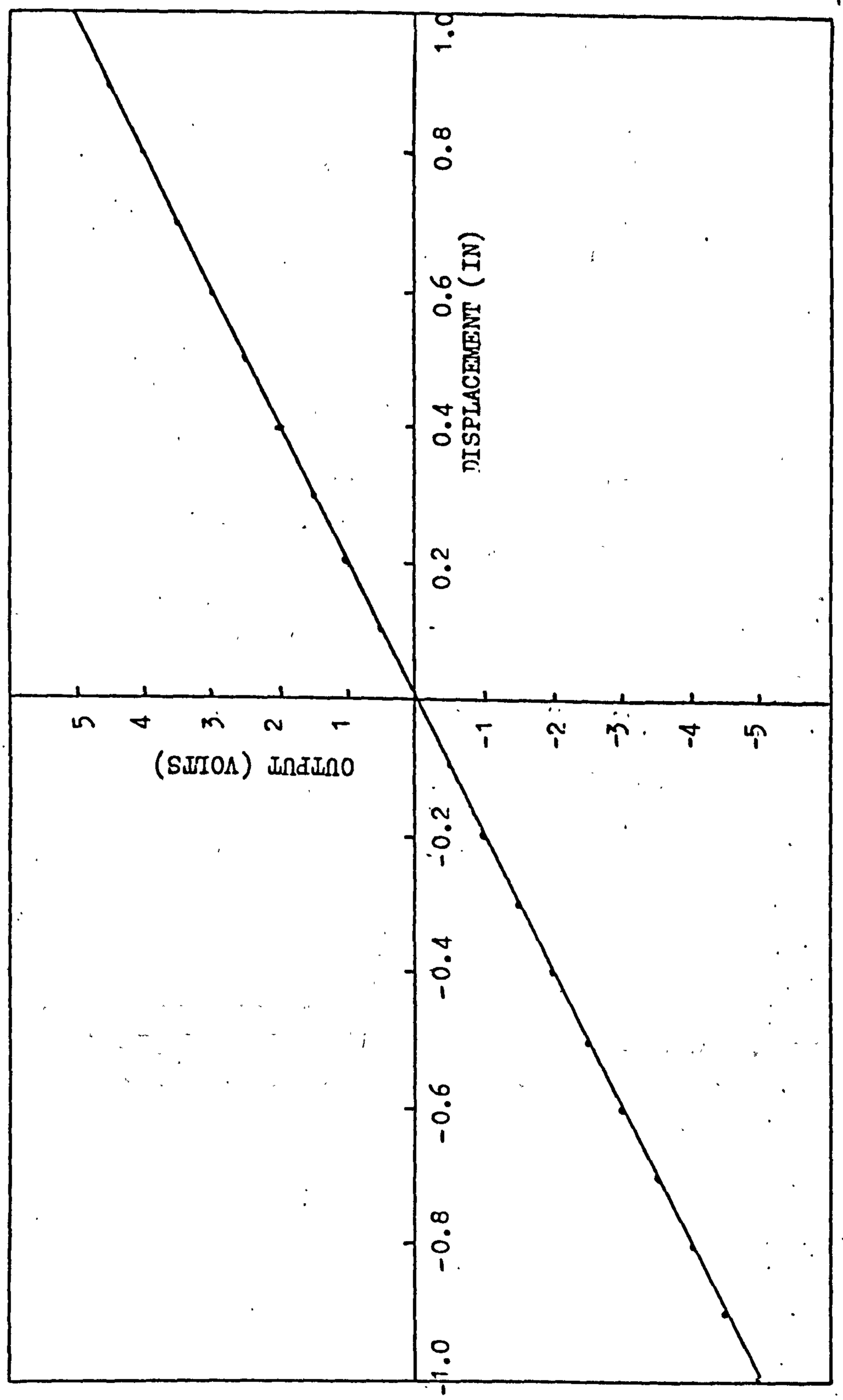

CALIBRATION OF DISPLACEMENT TRANSDUCER

FIGURE 30b

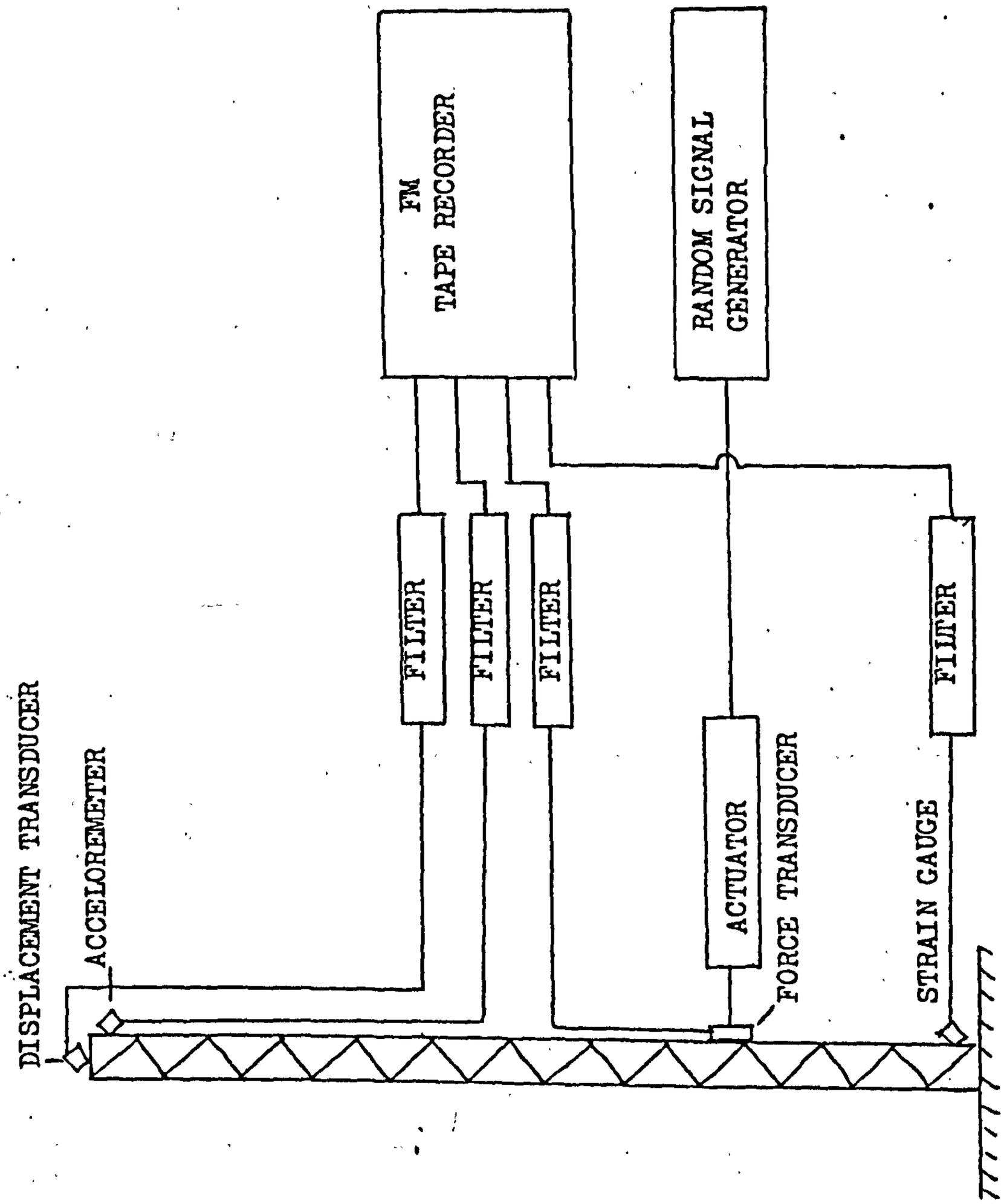

SET UP FOR RANDOM TESTING

FIGURE 31a

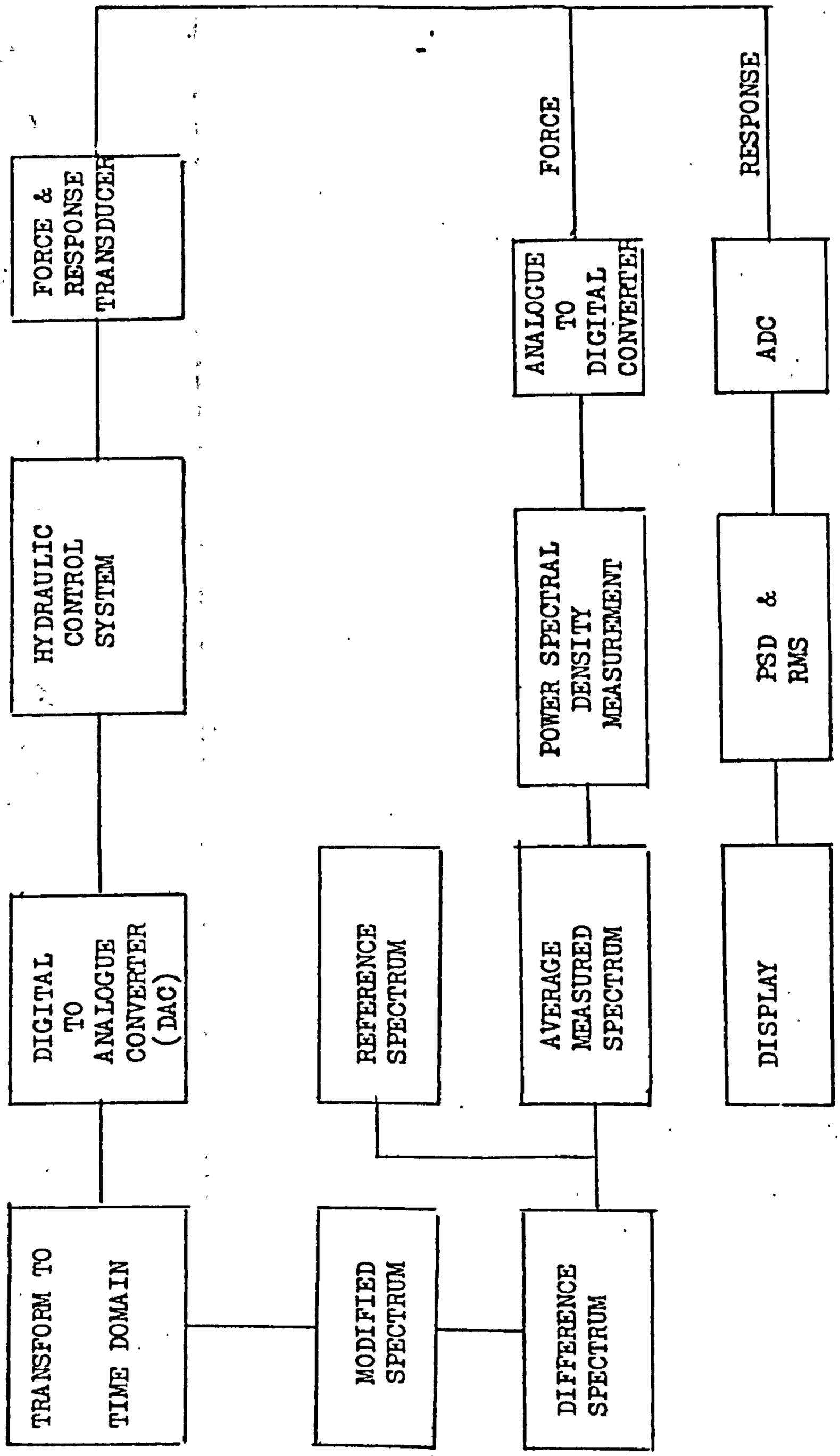

FIGURE 31b

RANDOM VIBRATION CONTROL AND MEASUREMENT SYSTEM

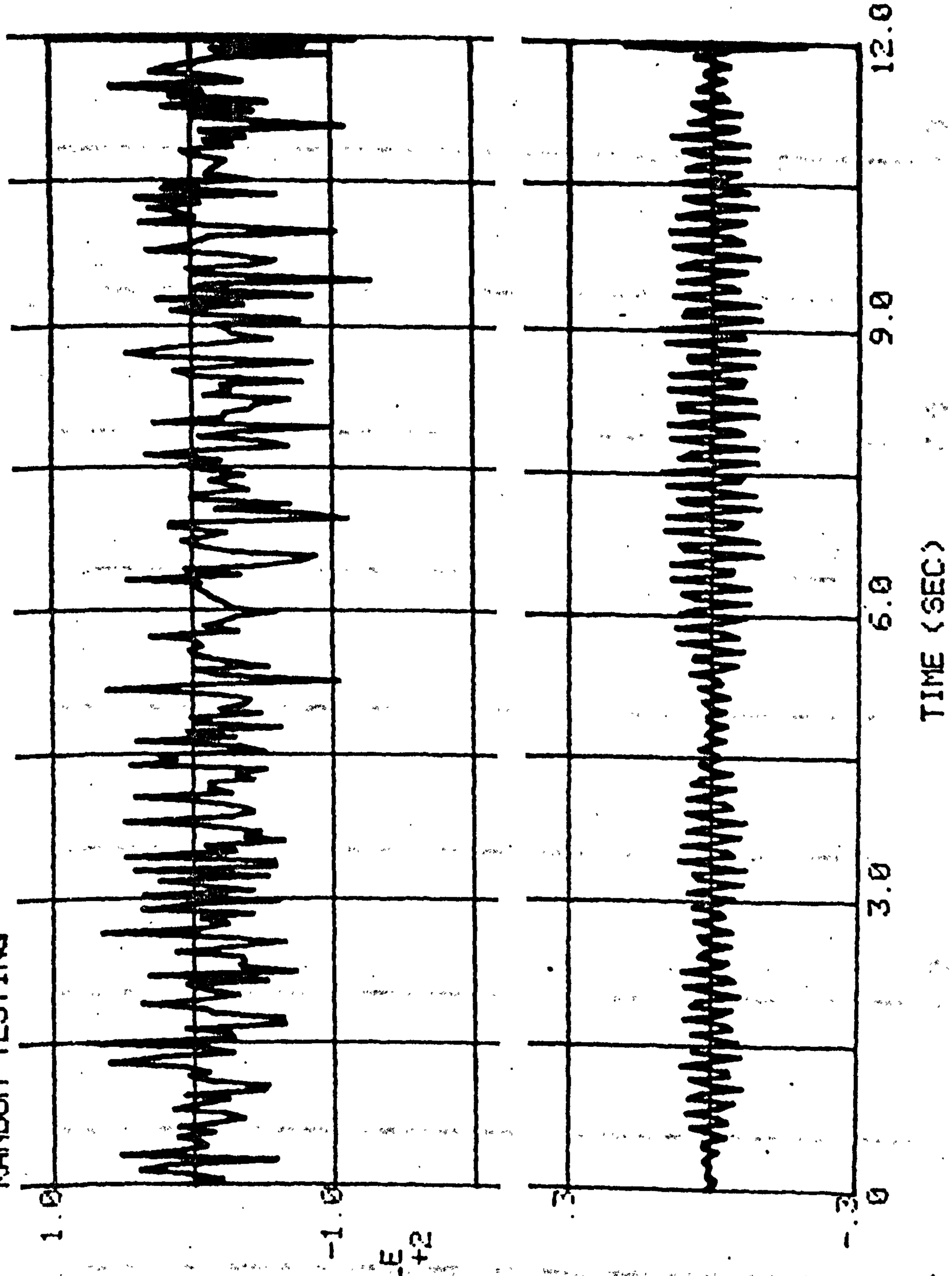

FIGURE 32

MEASURED FORCE AND RESPONSE TIME HISTORIES

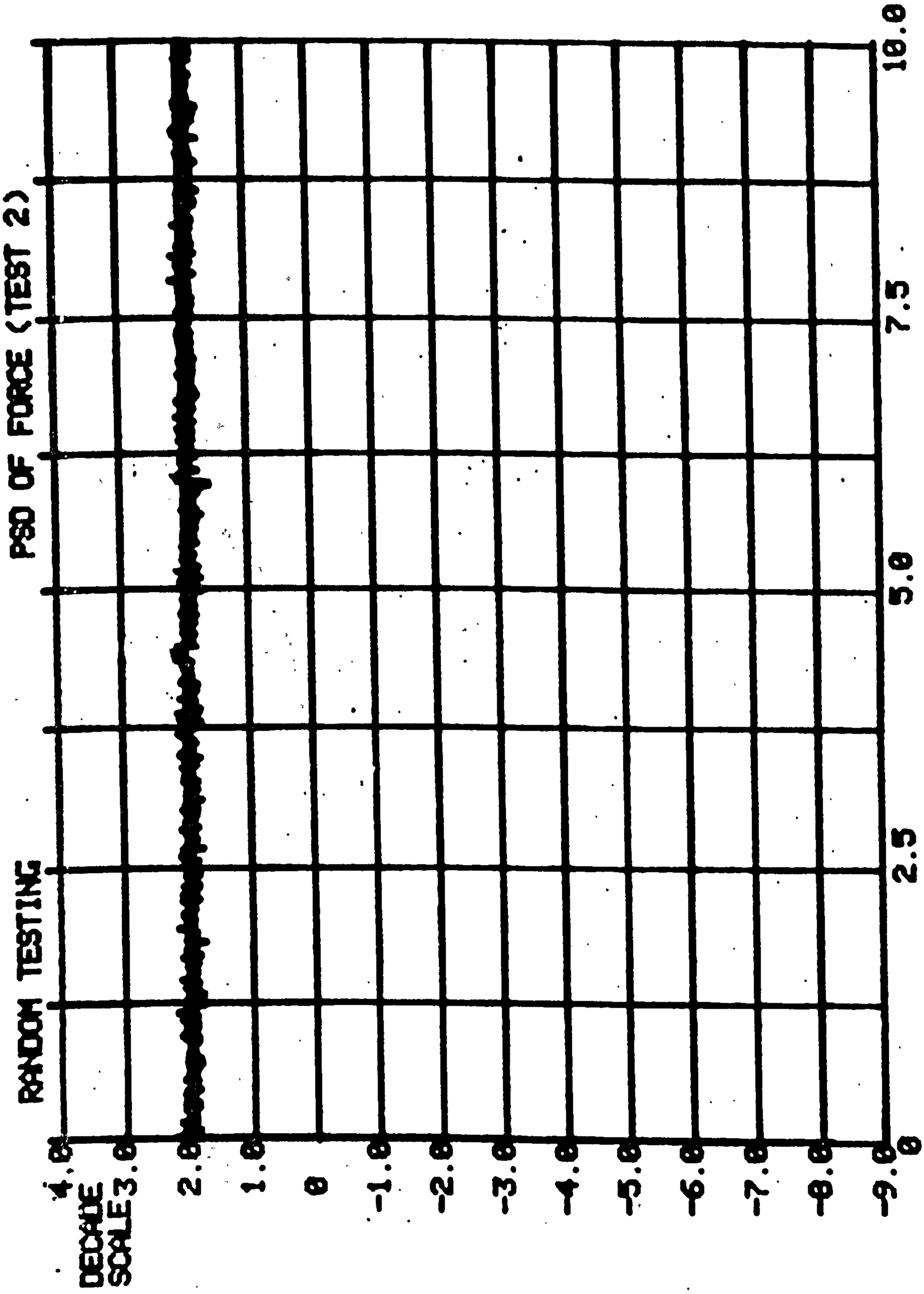

PSD OF FORCE
FIGURE 33a

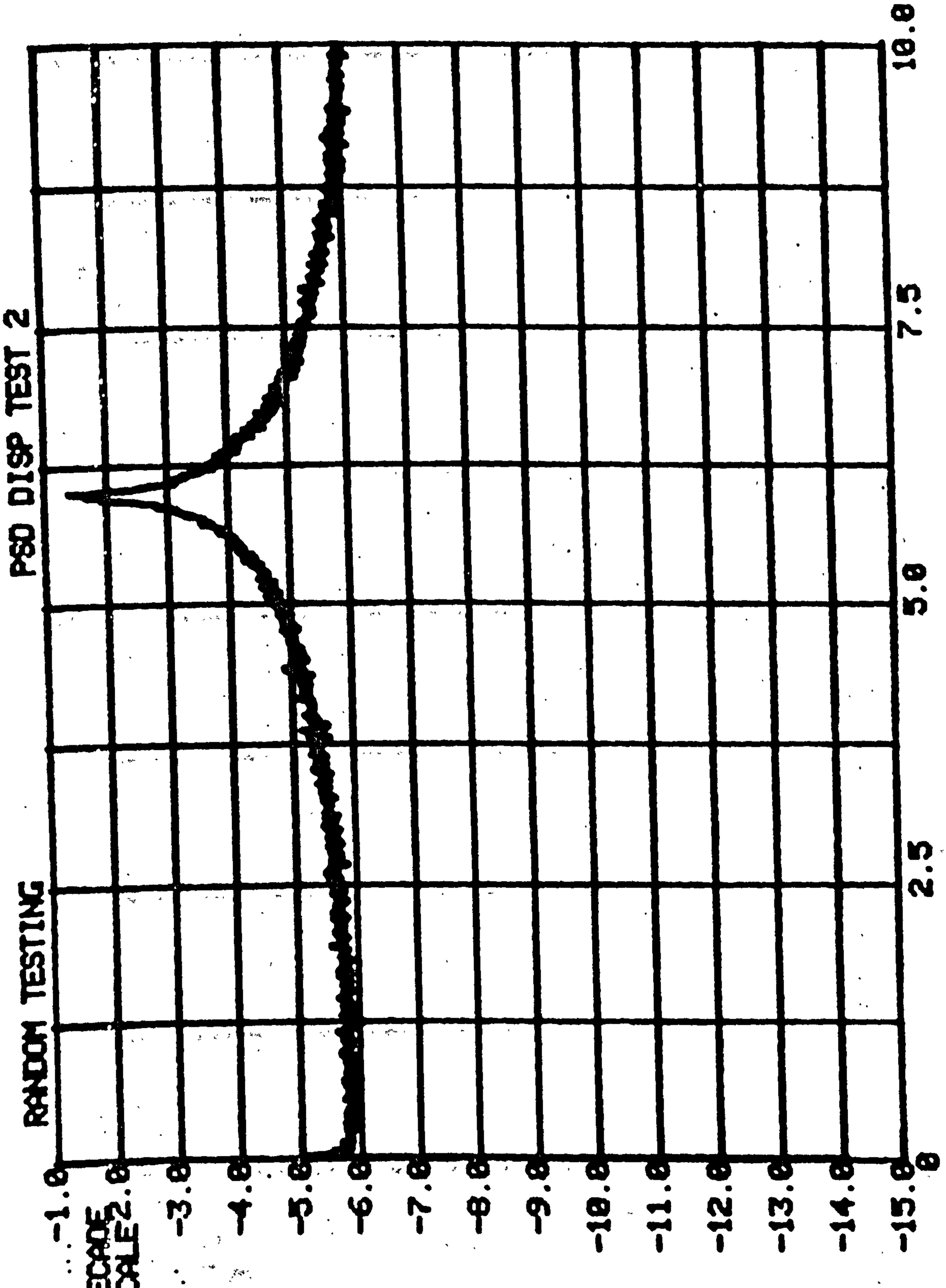

PSD FO DISPLACEMENT
FIGURE 33b

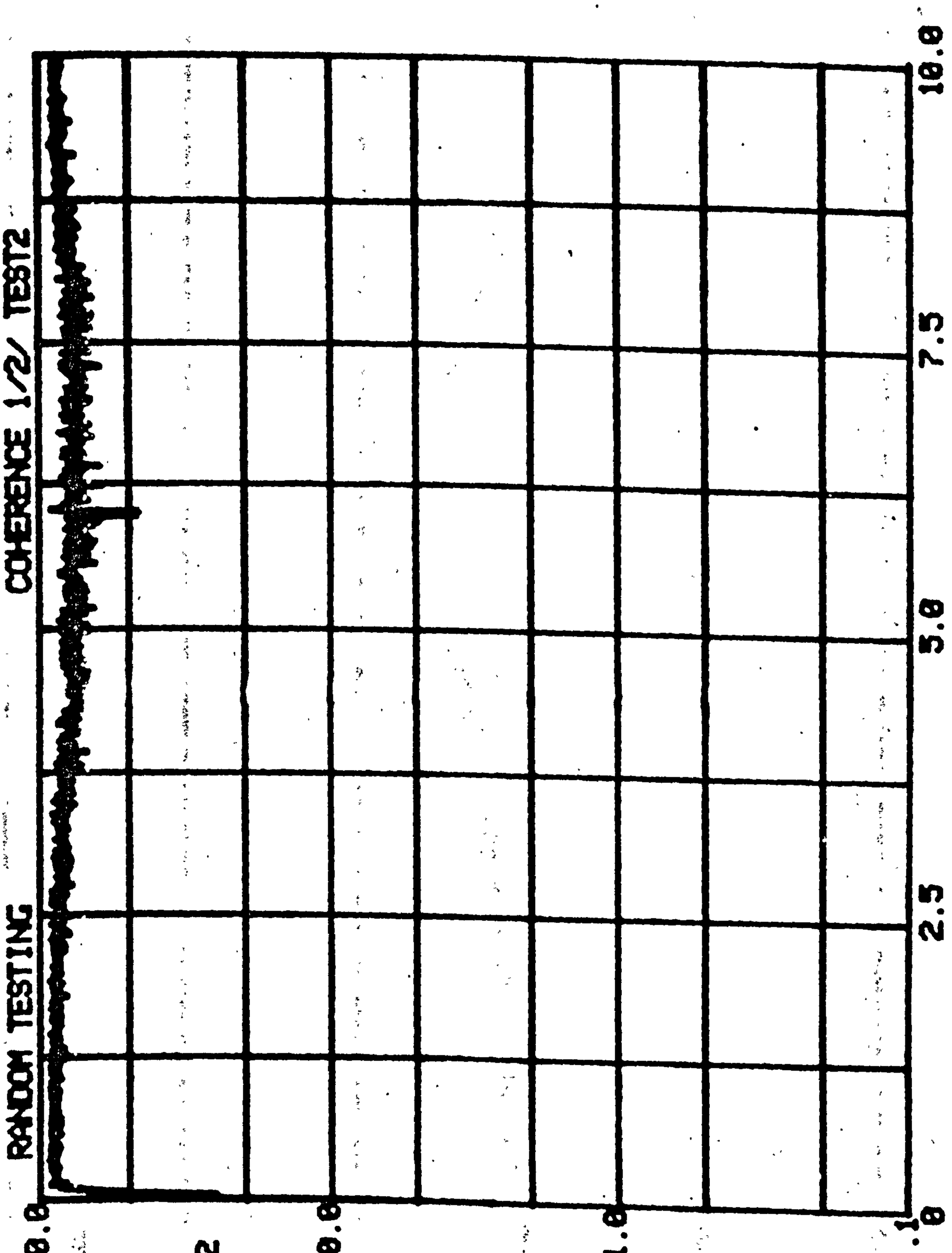

COHERENCE

FIGURE 34

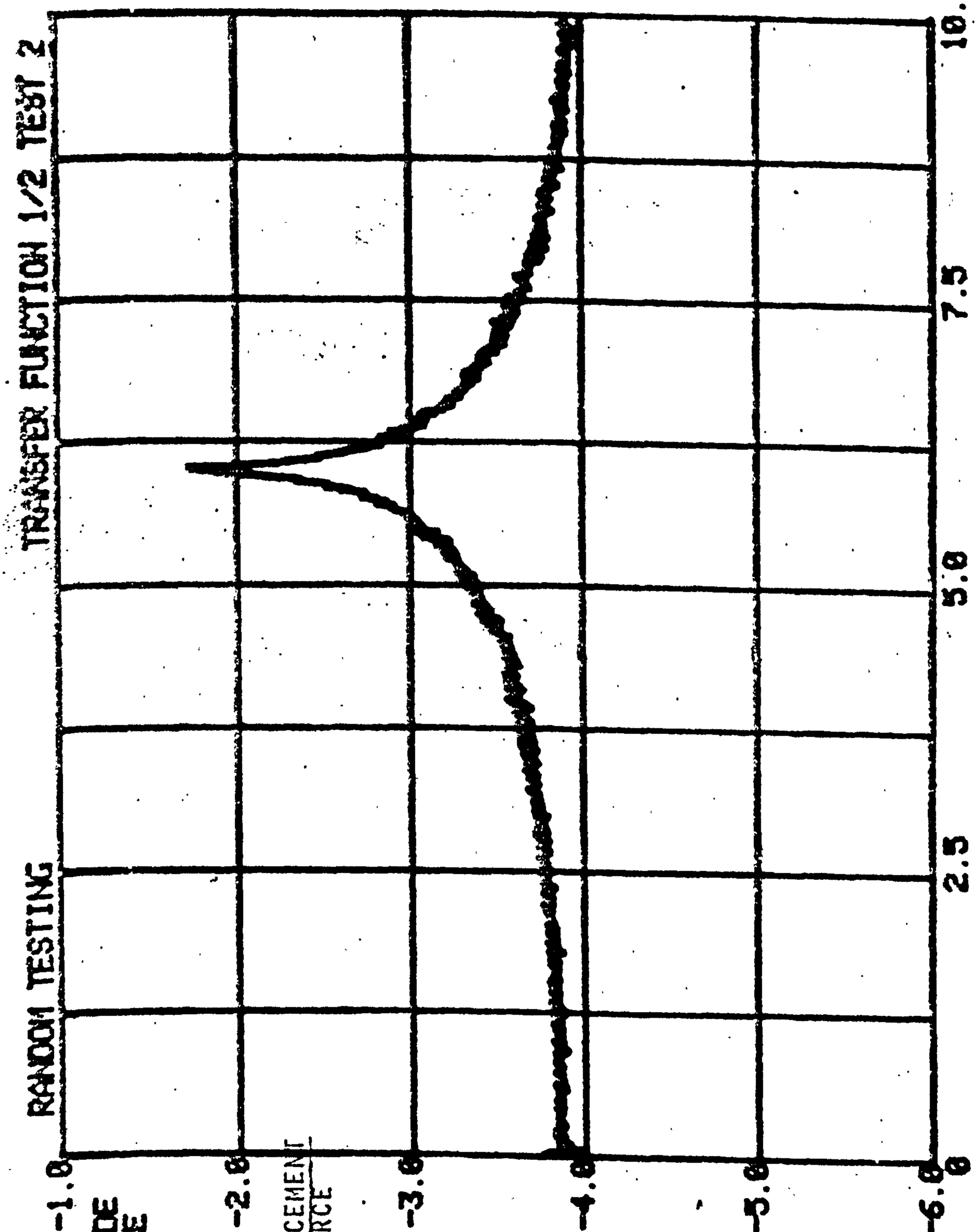

TRANSFER FUNCTION MEASURED FROM RANDOM TESTING

FIGURE 35

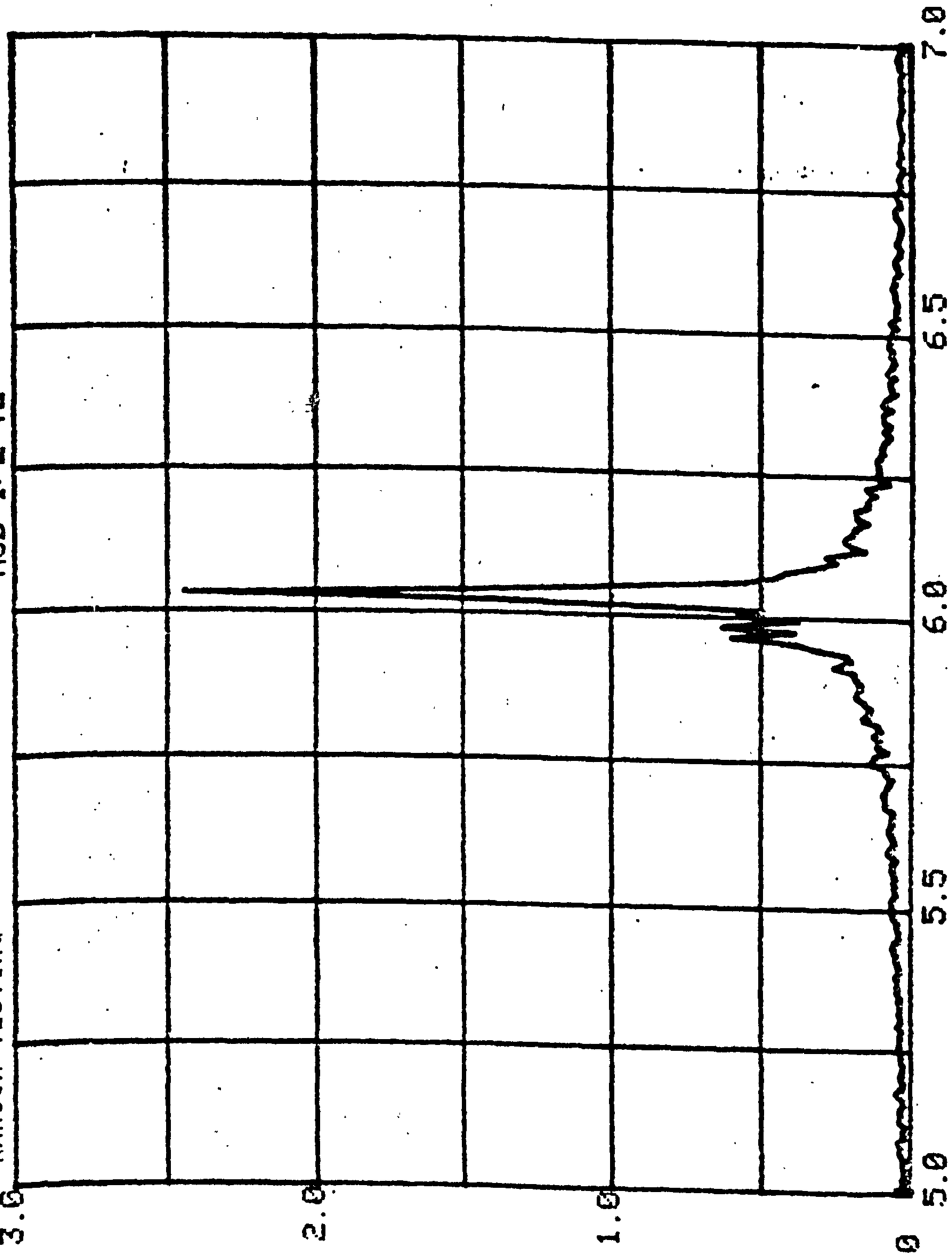

MODULUS OF TRANSFER FUNCTION

FIGURE 36

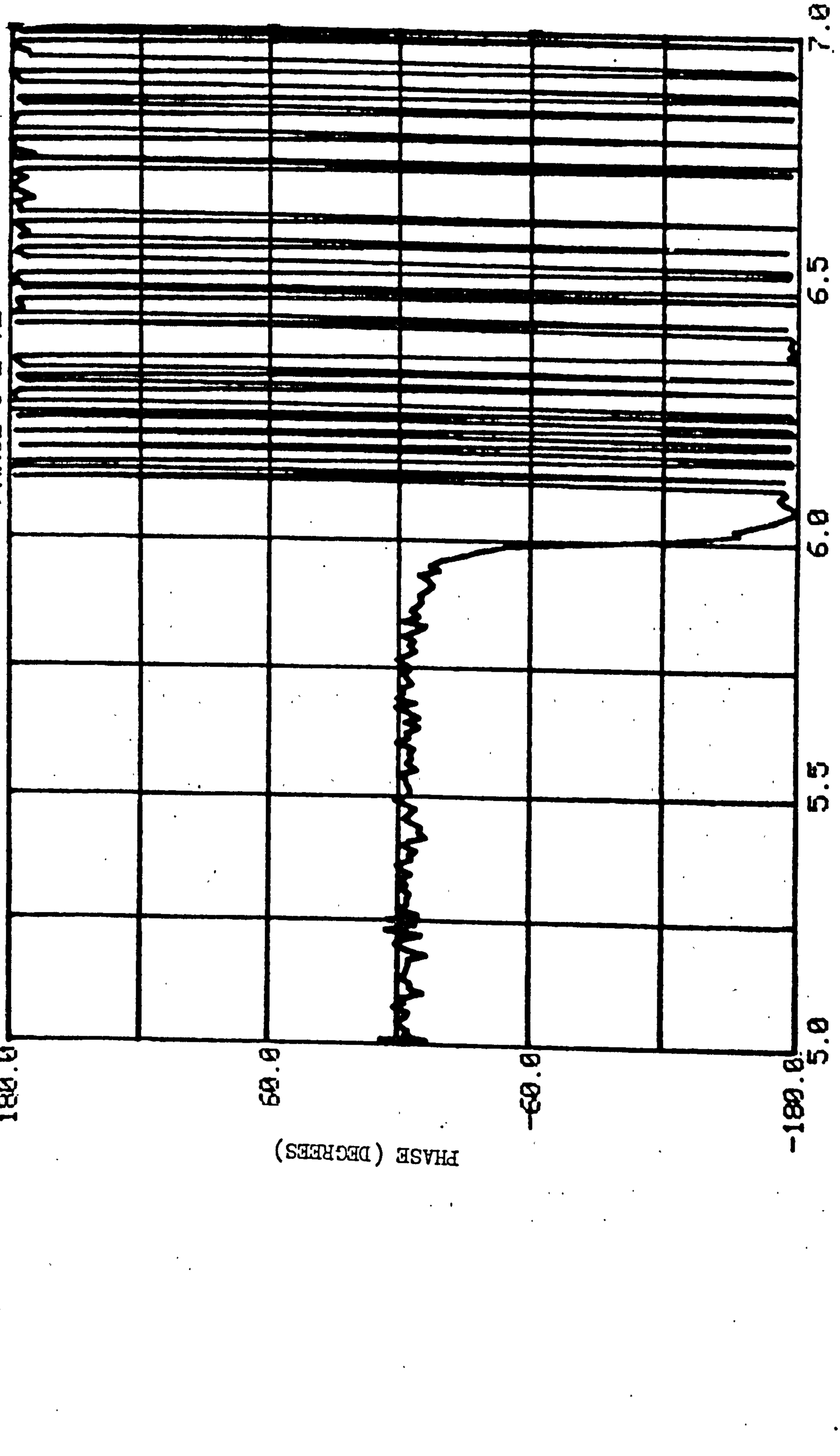

FIGURE 37
PHASE BETWEEN DISP AND FORCE

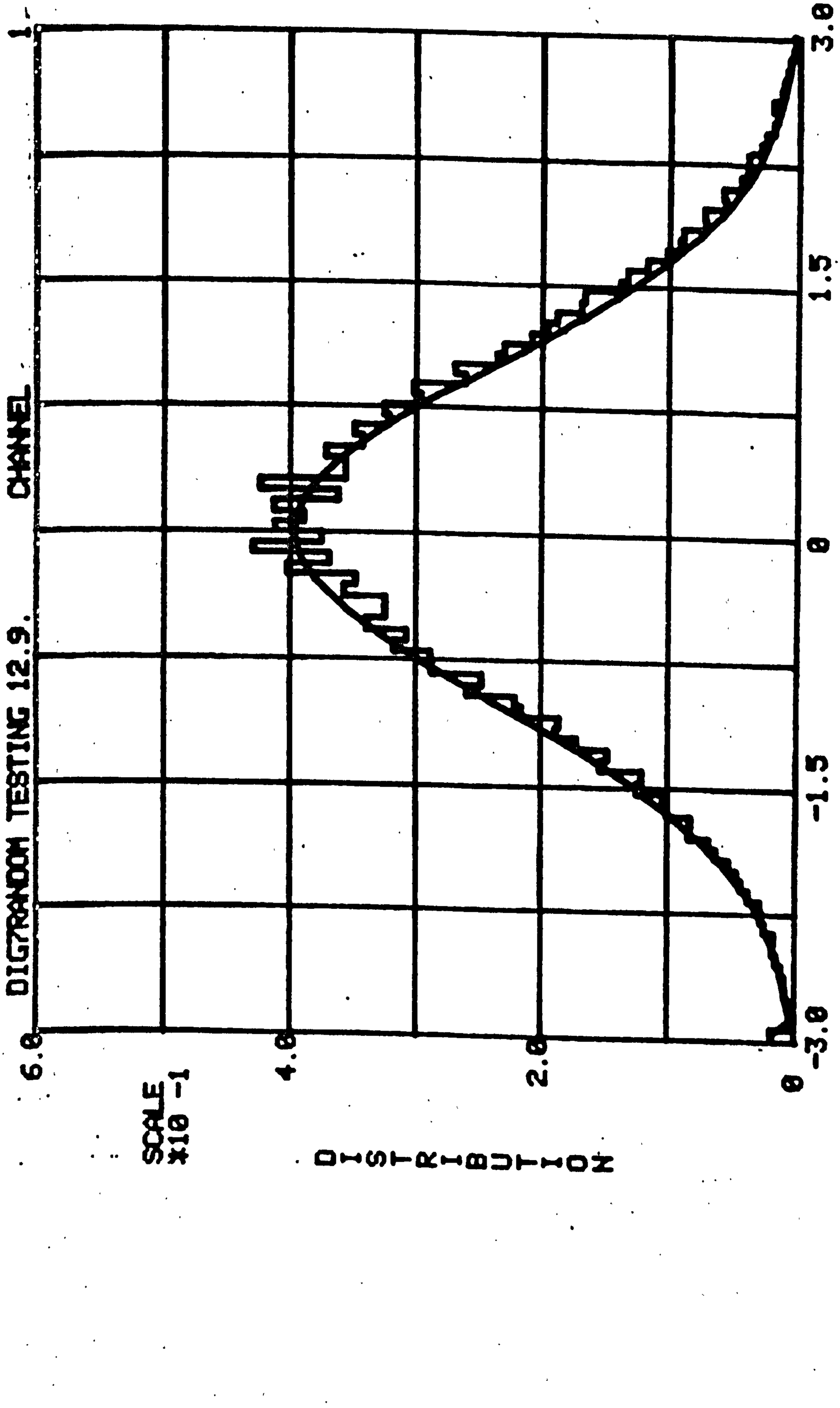

PROBABILITY DENSITY FUNCTION OF FORCE
FIGURE 38a

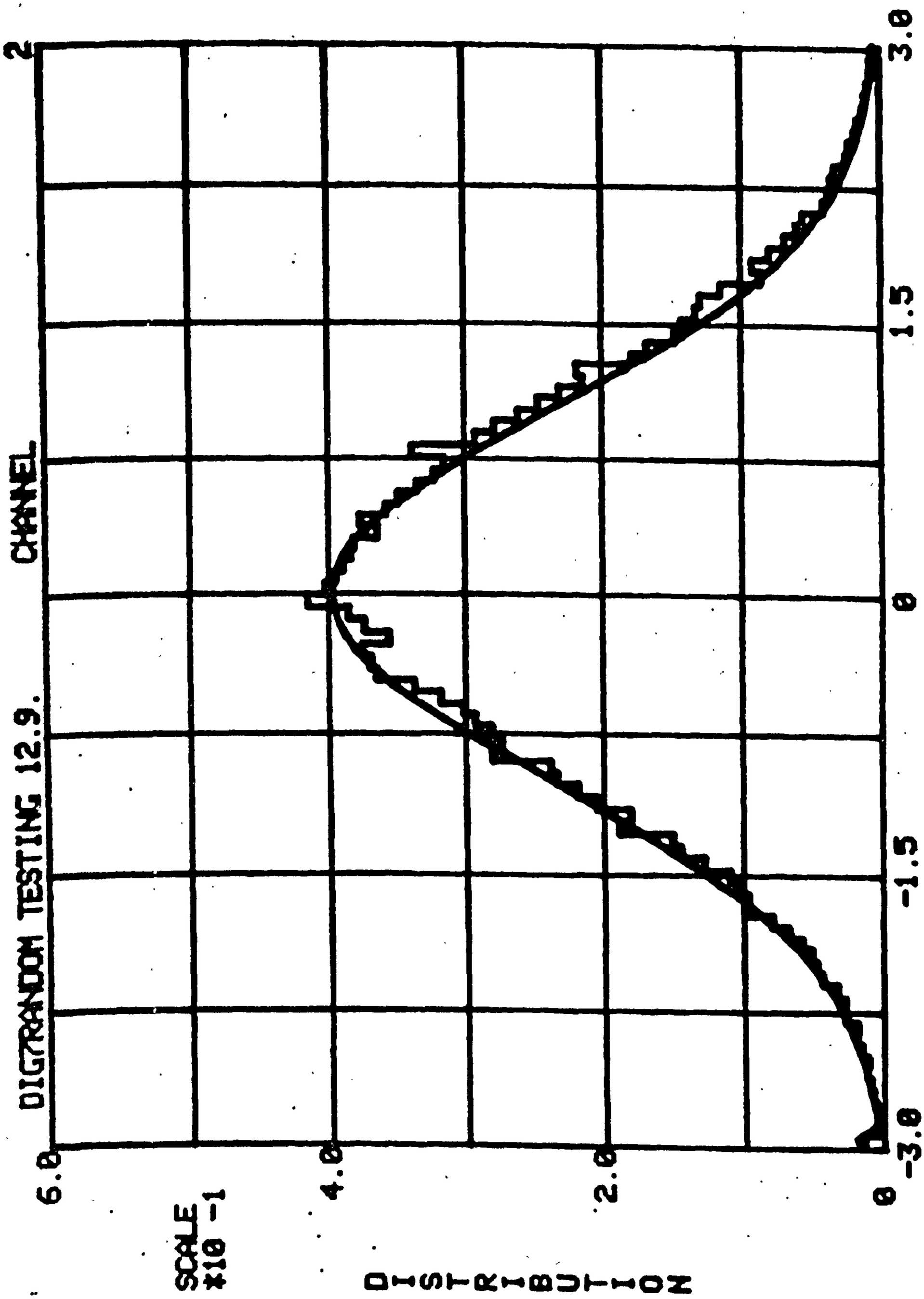

PROBABILITY DENSITY FUNCTION OF DISPLACEMENT

FIGURE 38b

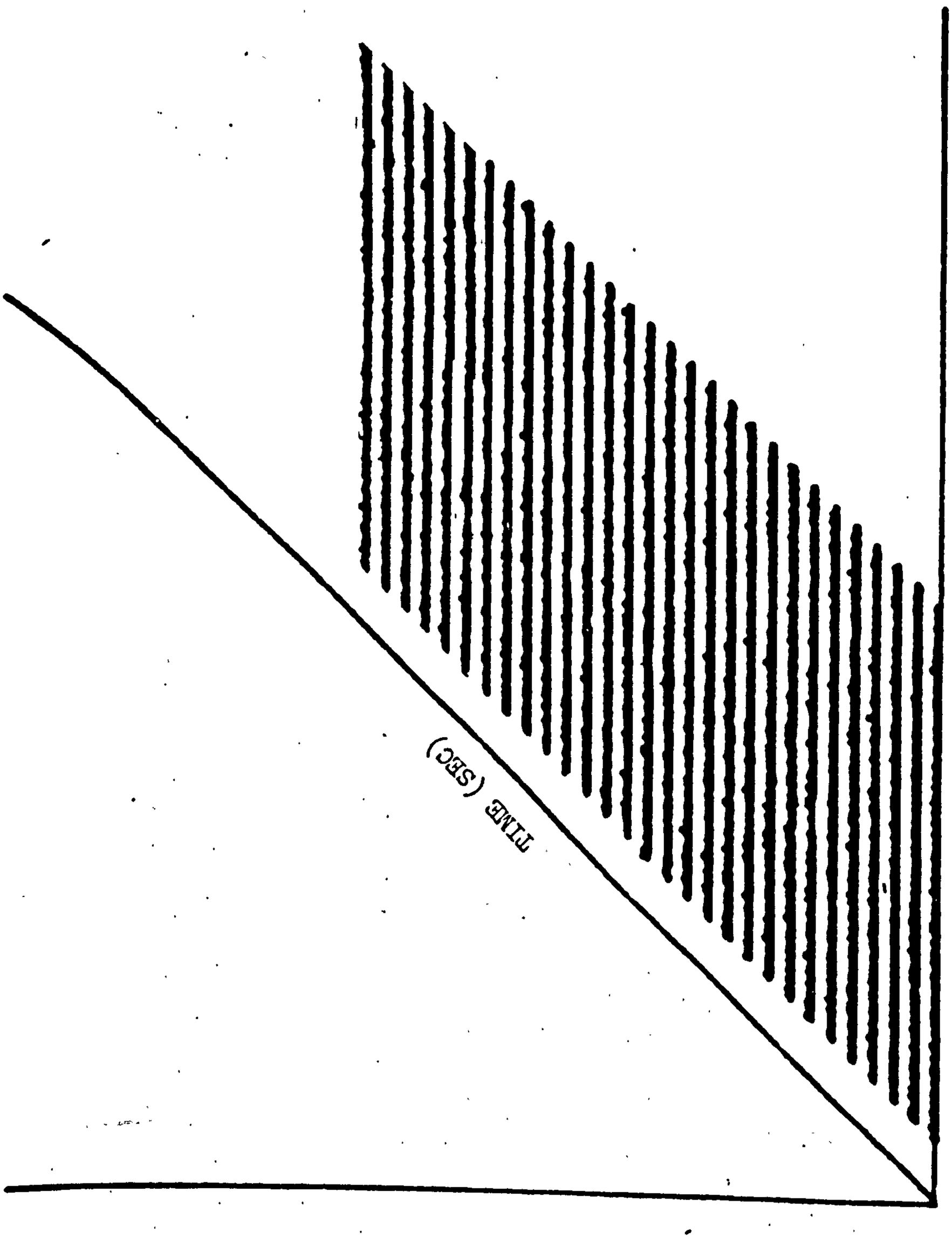
POWER SPECTRAL DENSITY OF FORCE
FIGURE 39a
FREQUENCY (HZ)
9.5
0
TIME (SEC)
LB^2/Hz

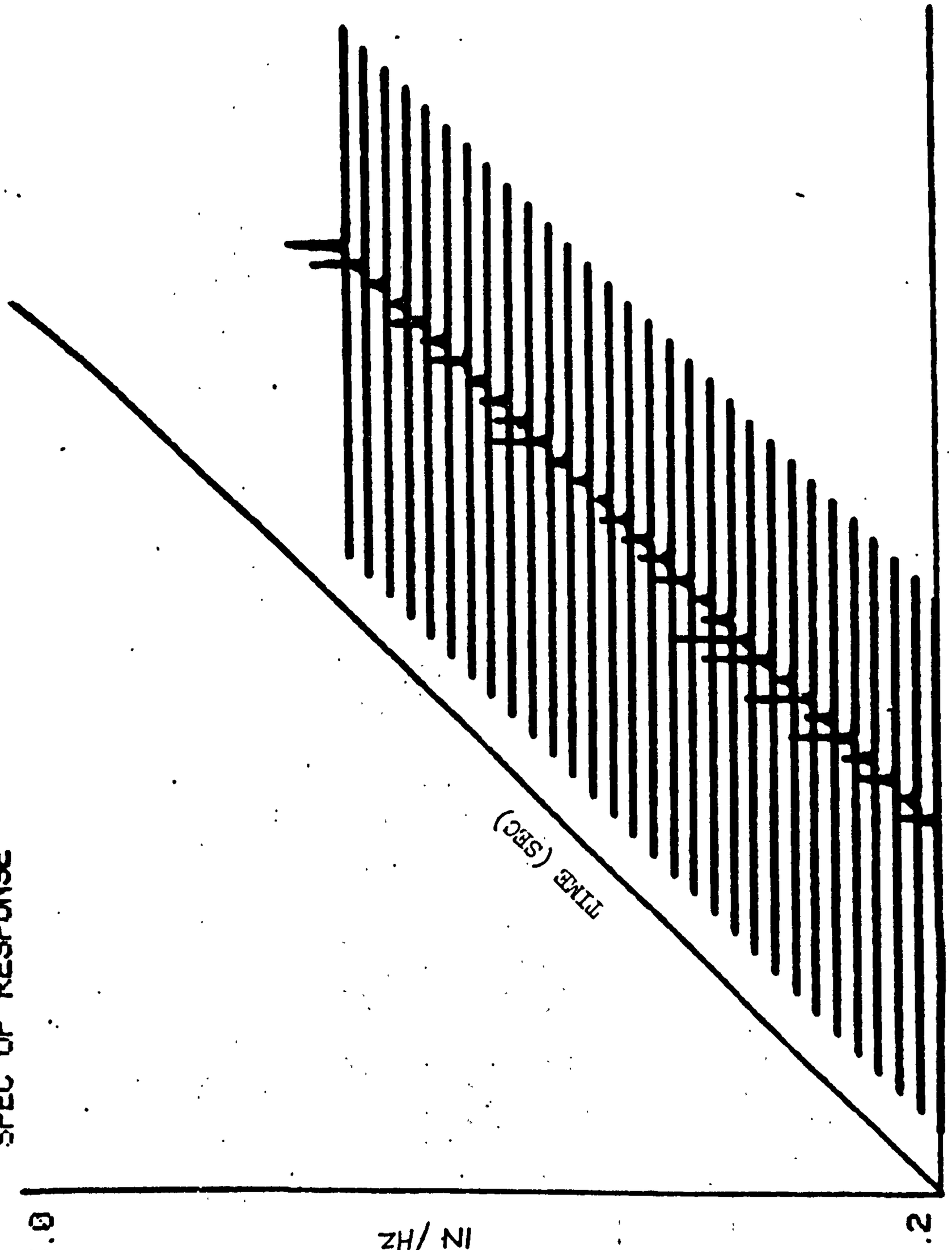

POWER SPECTRAL DENSITY OF DISPLACEMENT

FIGURE 39b

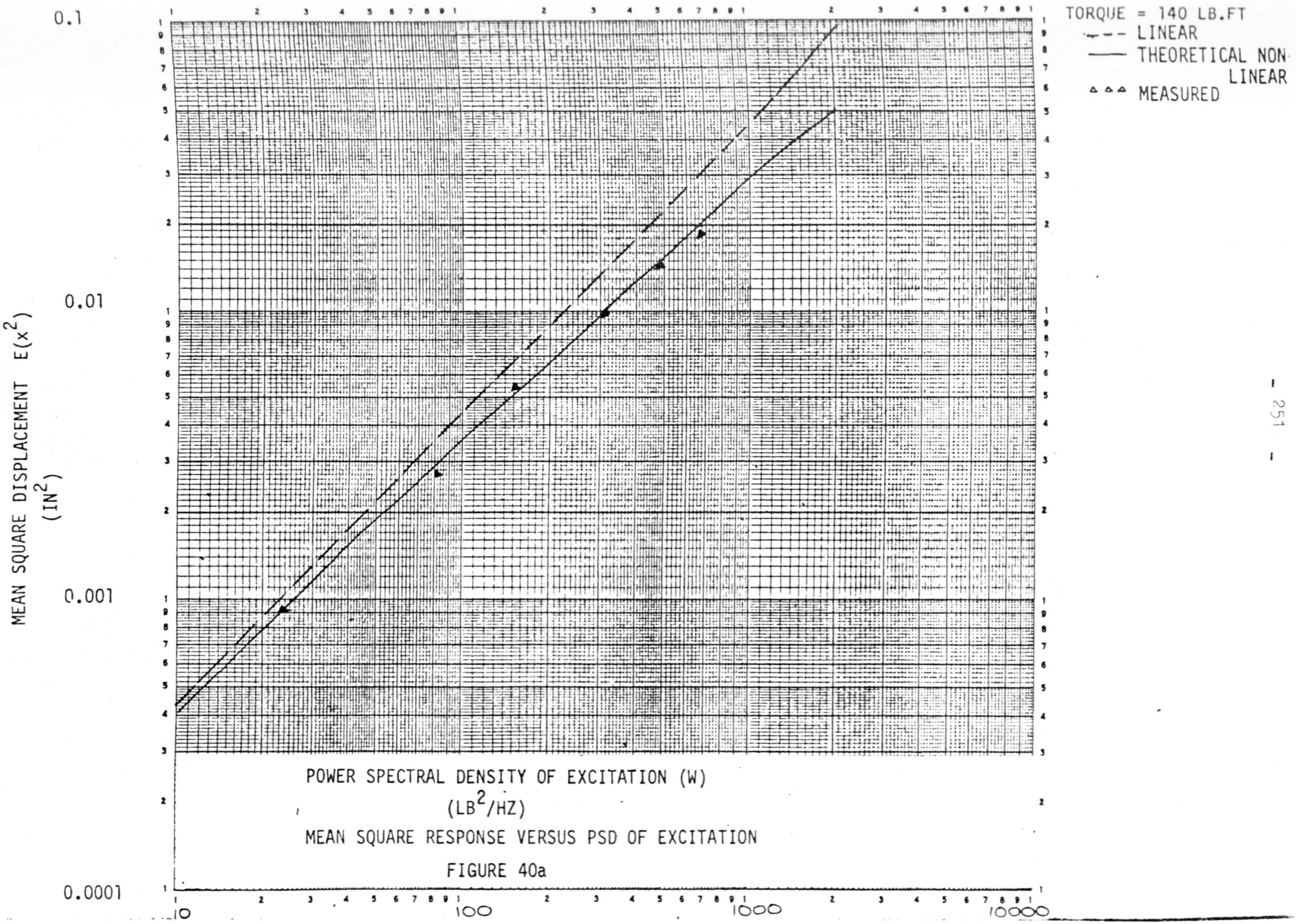

MEAN SQUARE RESPONSE VERSUS PSD OF EXCITATION

FIGURE 40a

TORQUE = 90 LB.FT.
--- LINEAR
——— THEORETICAL
ΔΔΔ MEASURED

MEAN SQUARE DISPLACEMENT $E(x^2)$ (IN^2)

0.1
0.01
0.001
0.0001

10 100 1000 10000

POWER SPECTRAL DENSITY OF EXCITATION (W)
(LB^2/HZ)

MEAN SQUARE RESPONSE VERSUS PSD OF EXCITATION

FIGURE 40b

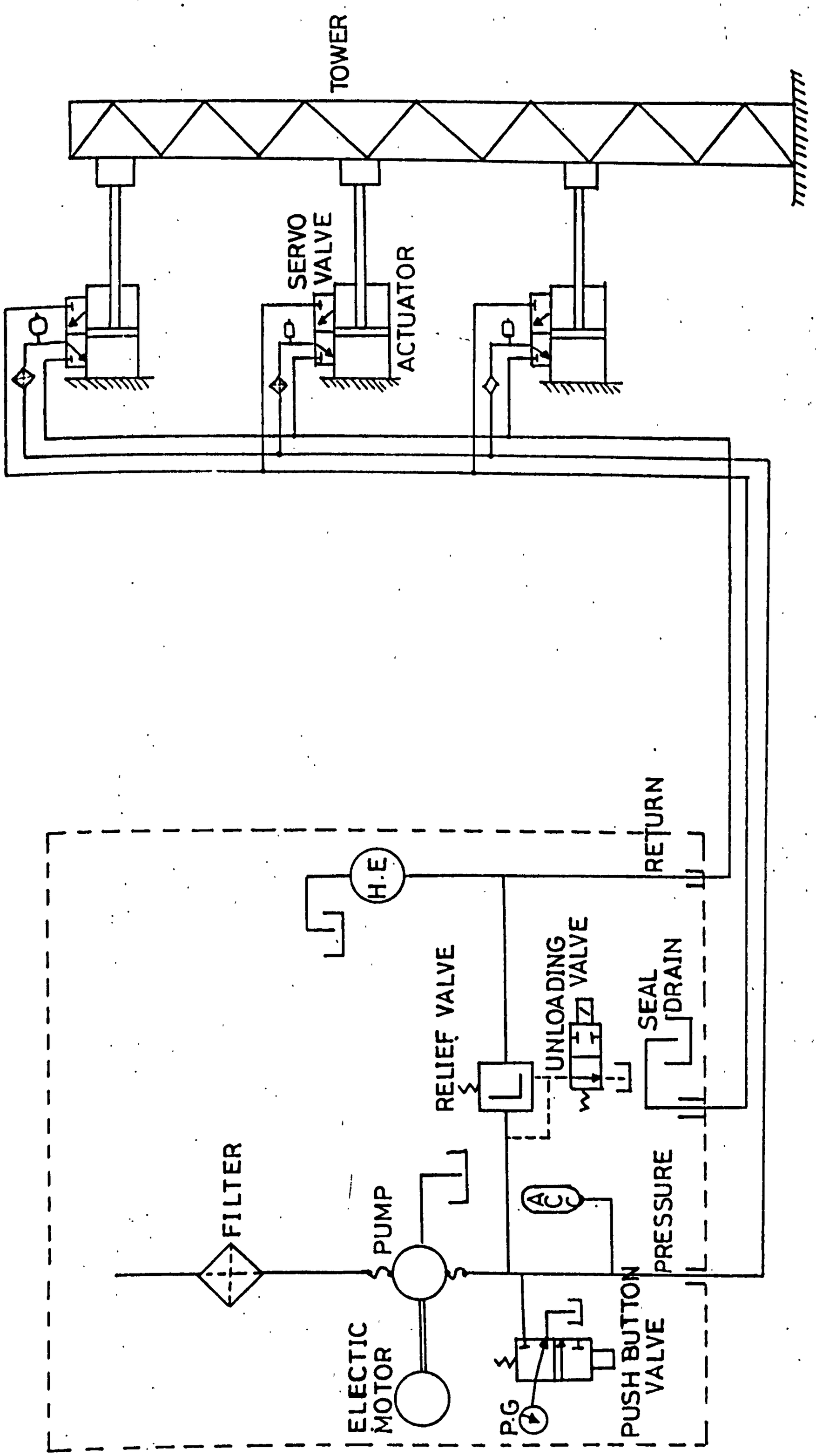

FIGURE 41

SCHEMATIC DIAGRAM OF HYDRAULIC SYSTEM

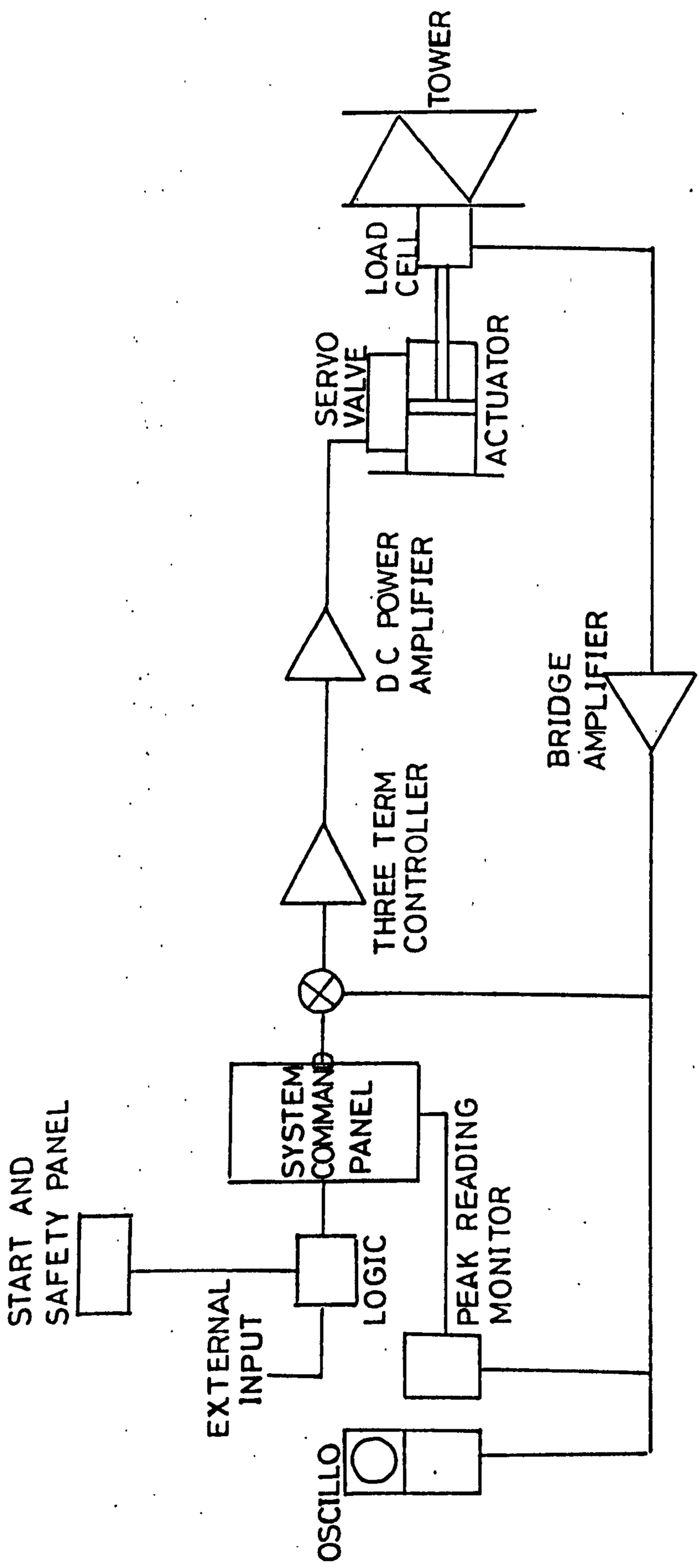

SCHEMATIC DIAGRAM OF ELECTRICAL SYSTEM

FIGURE 42

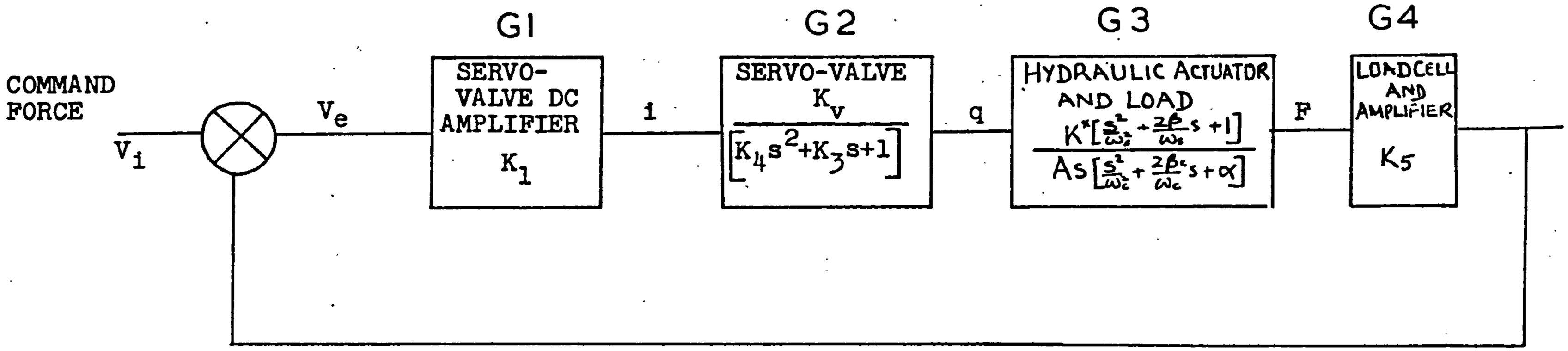

BLOCK DIAGRAM OF CONTROL SYSTEM

FIGURE 43

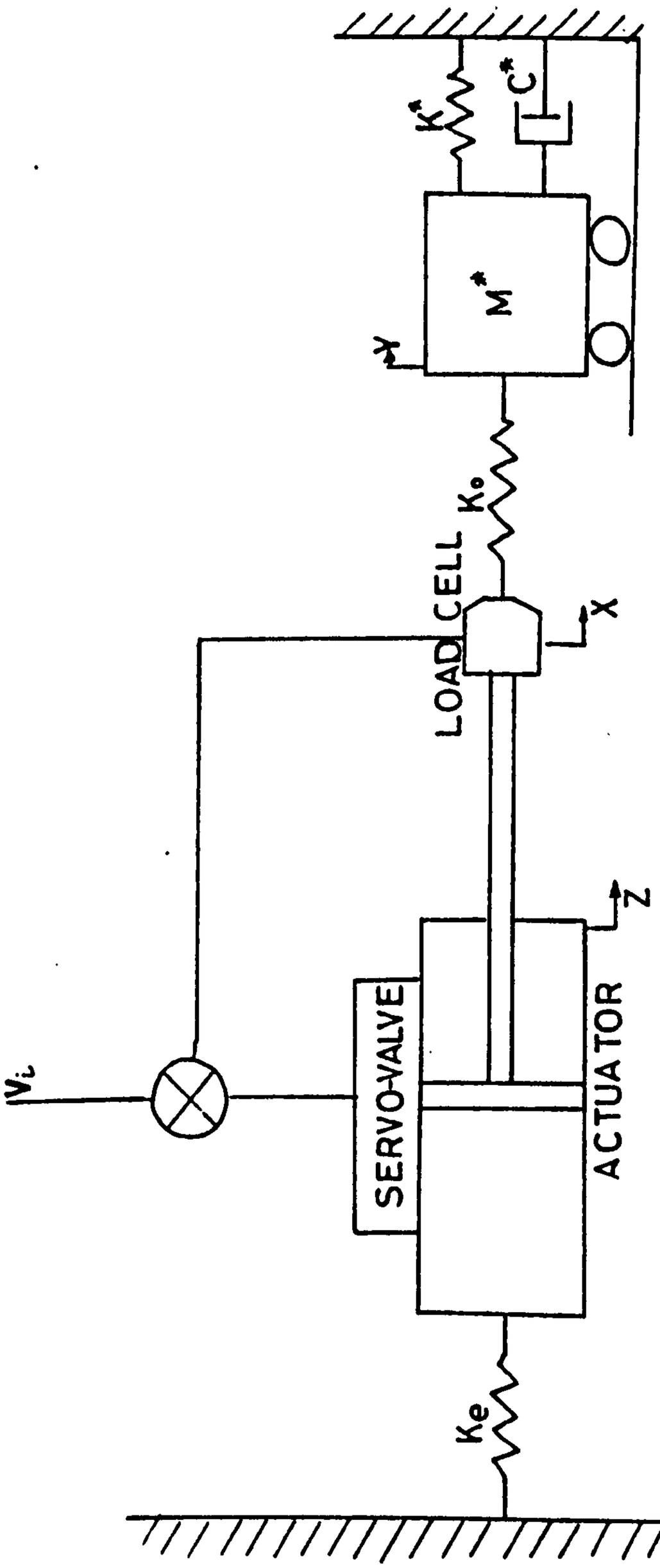

SIMPLIFIED DIAGRAM OF THE SYSTEM FOR CASE 1

FIGURE 44

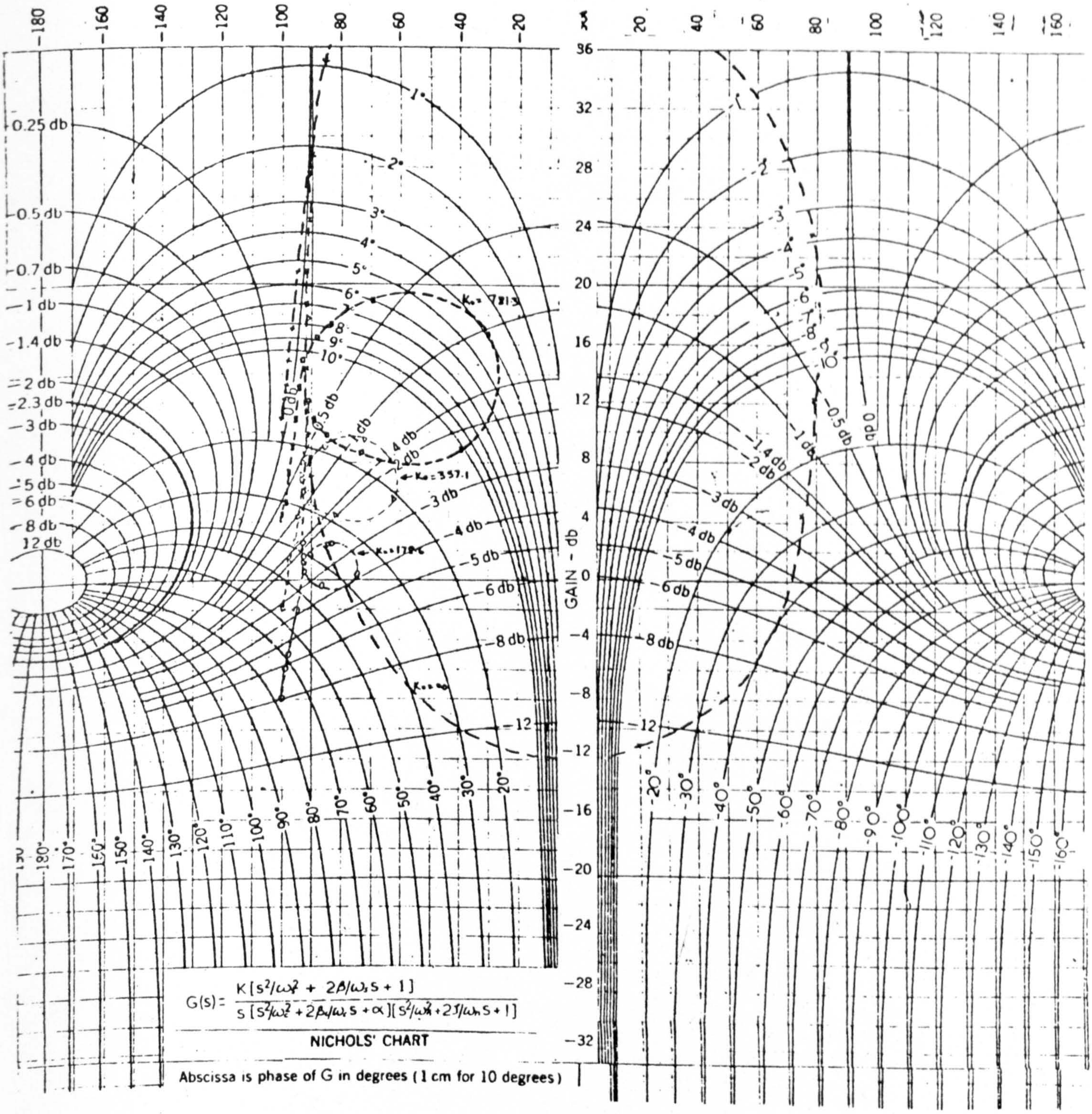

NICHOLS PLOTS OF G(s) FOR VARIOUS VALUES OF Ko

FIGURE 45

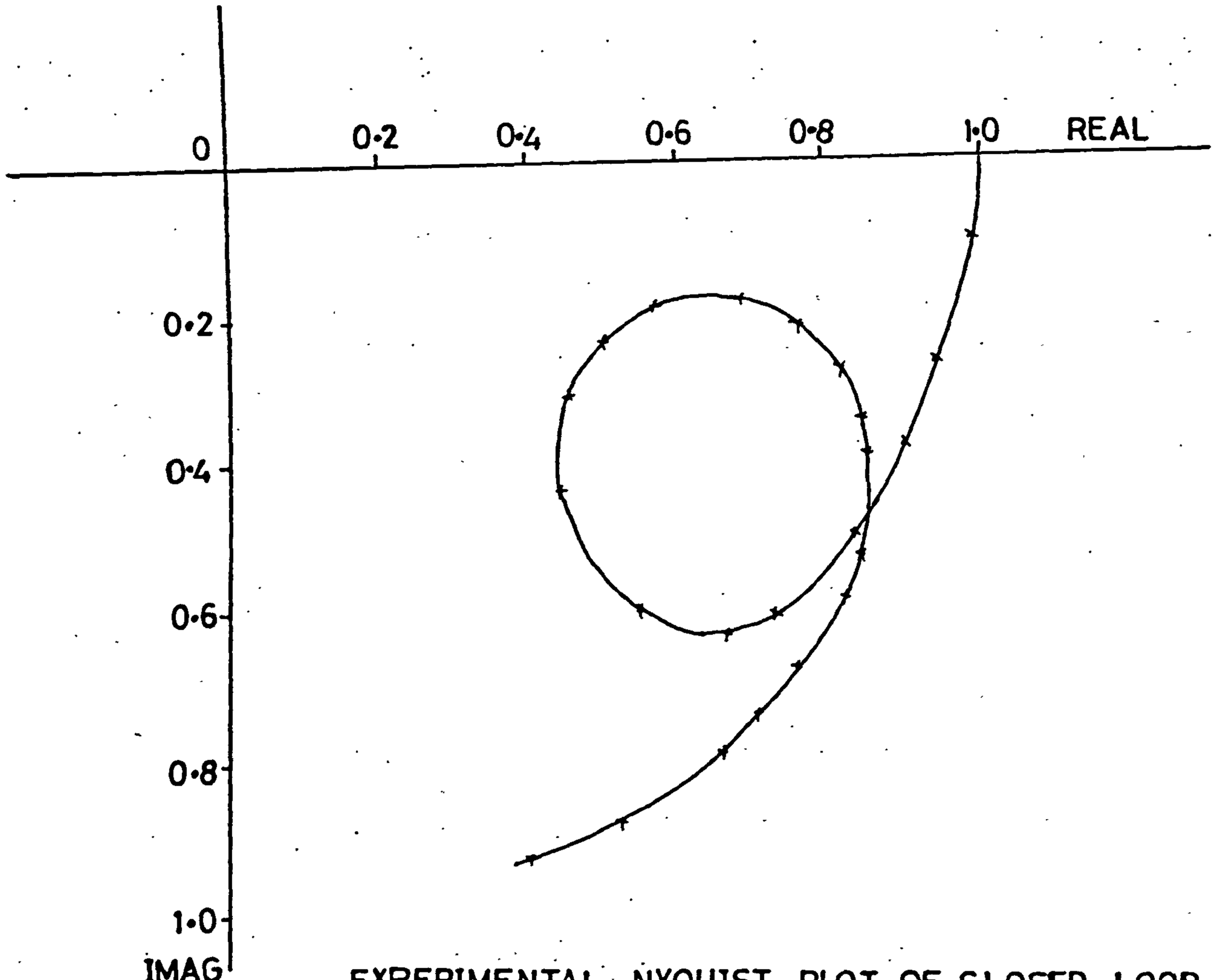

EXPERIMENTAL NYQUIST PLOT OF CLOSED LOOP TRANSFER FUNCTION

FIGURE 46

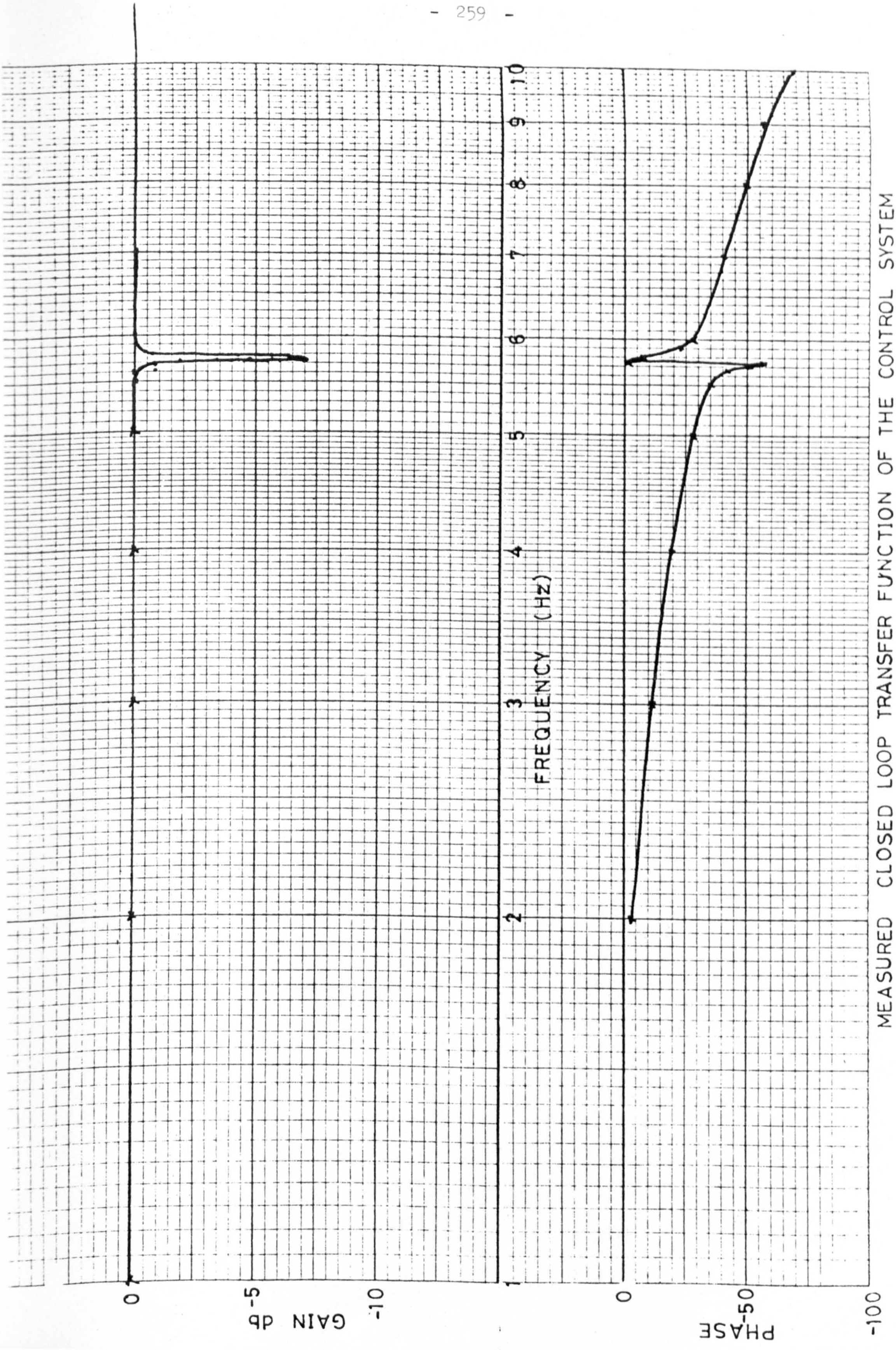

FIGURE 47 MEASURED CLOSED LOOP TRANSFER FUNCTION OF THE CONTROL SYSTEM

$$G(s) = \frac{K[s^2/\omega_f^2 + 2\beta/\omega_s s + 1]}{s[s^2/\omega_c^2 + 2\beta_d/\omega_c s + \alpha][s^2/\omega_n^2 + 2\zeta/\omega_n s + 1]}$$

A ∞
B 781.6 LB/IN
C 357.1 LB/IN
D 178.6 LB/IN

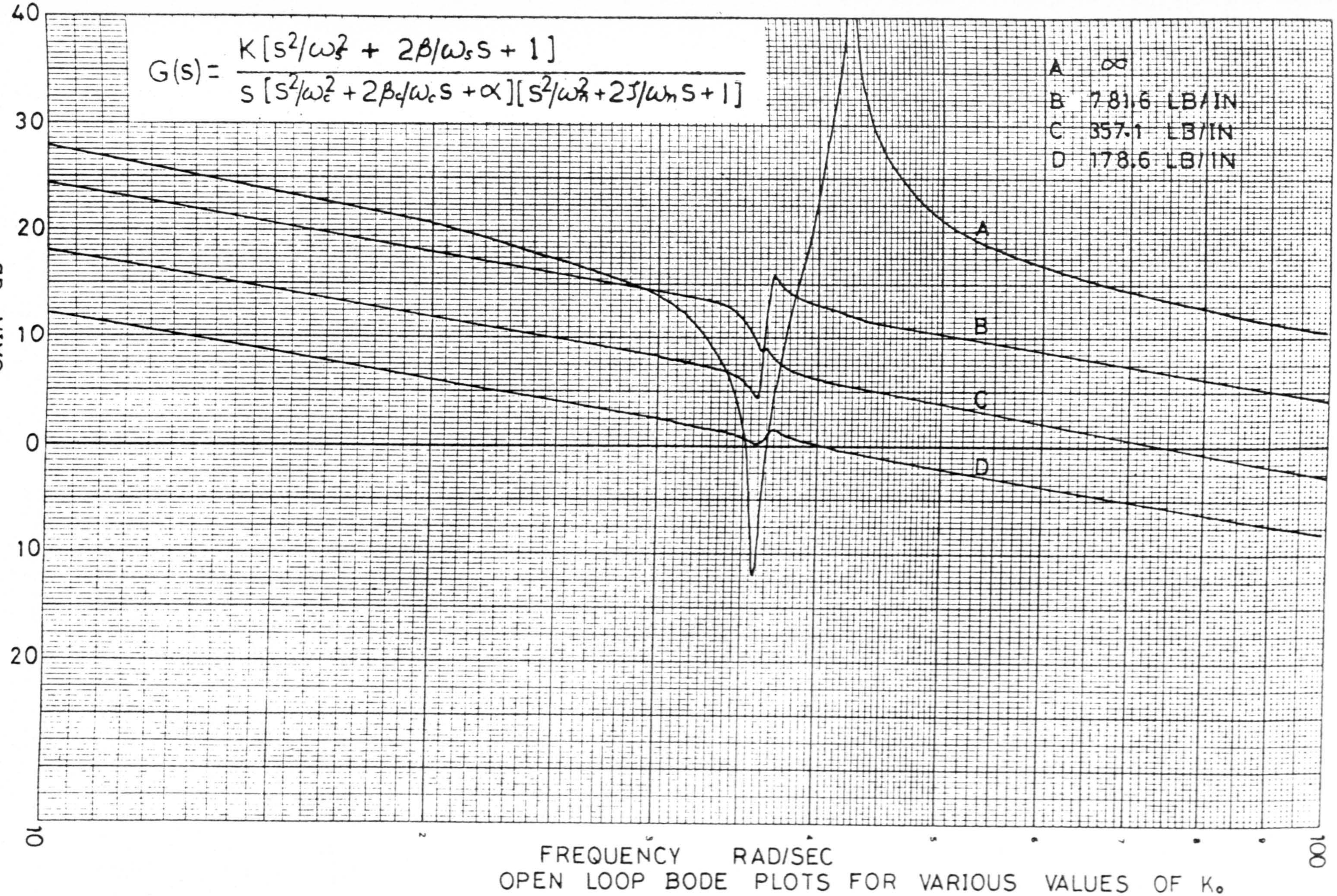

OPEN LOOP BODE PLOTS FOR VARIOUS VALUES OF K_o

FIGURE 48

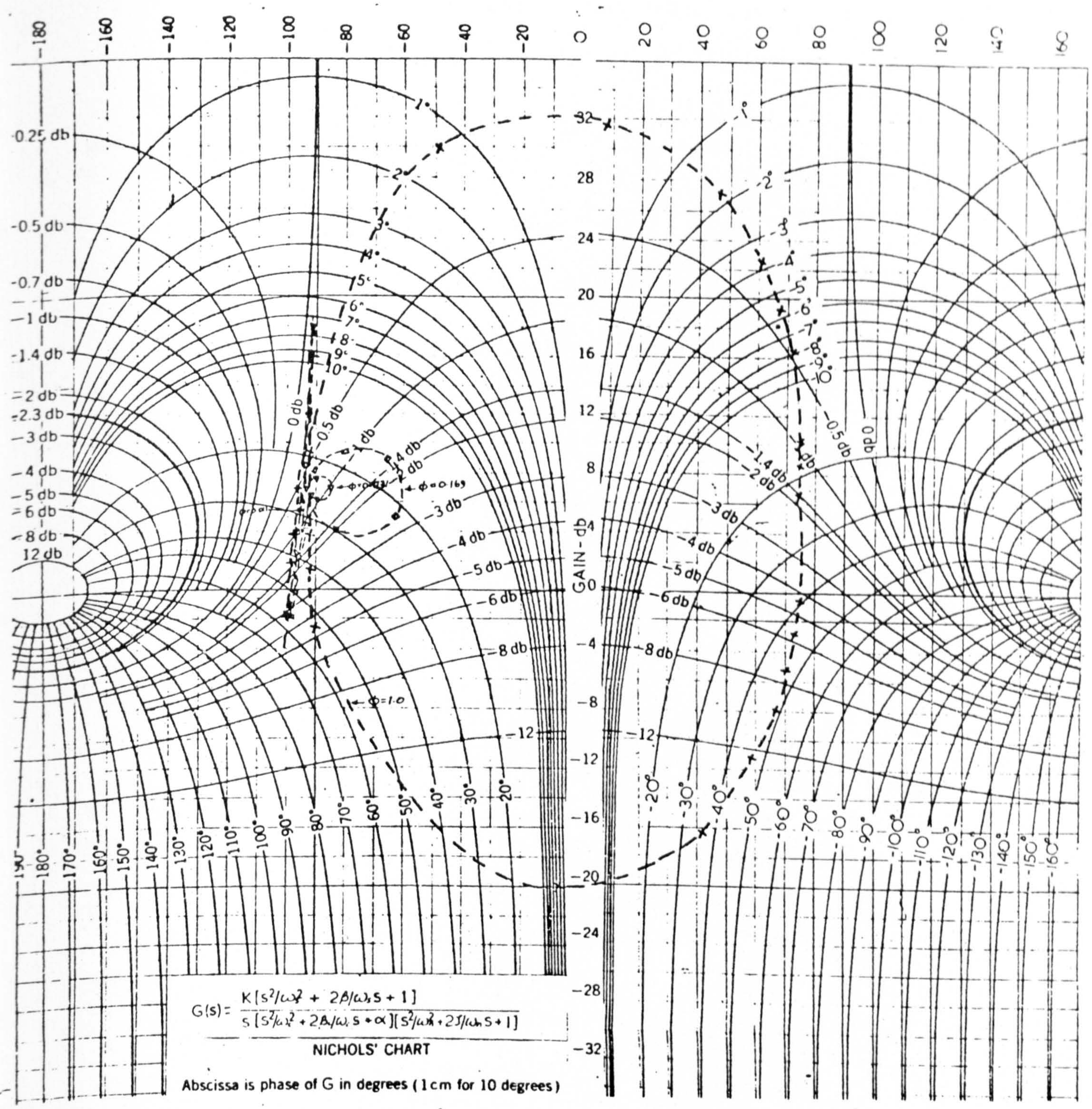

EFFECT OF ϕ ON G(s)

FIGURE 49

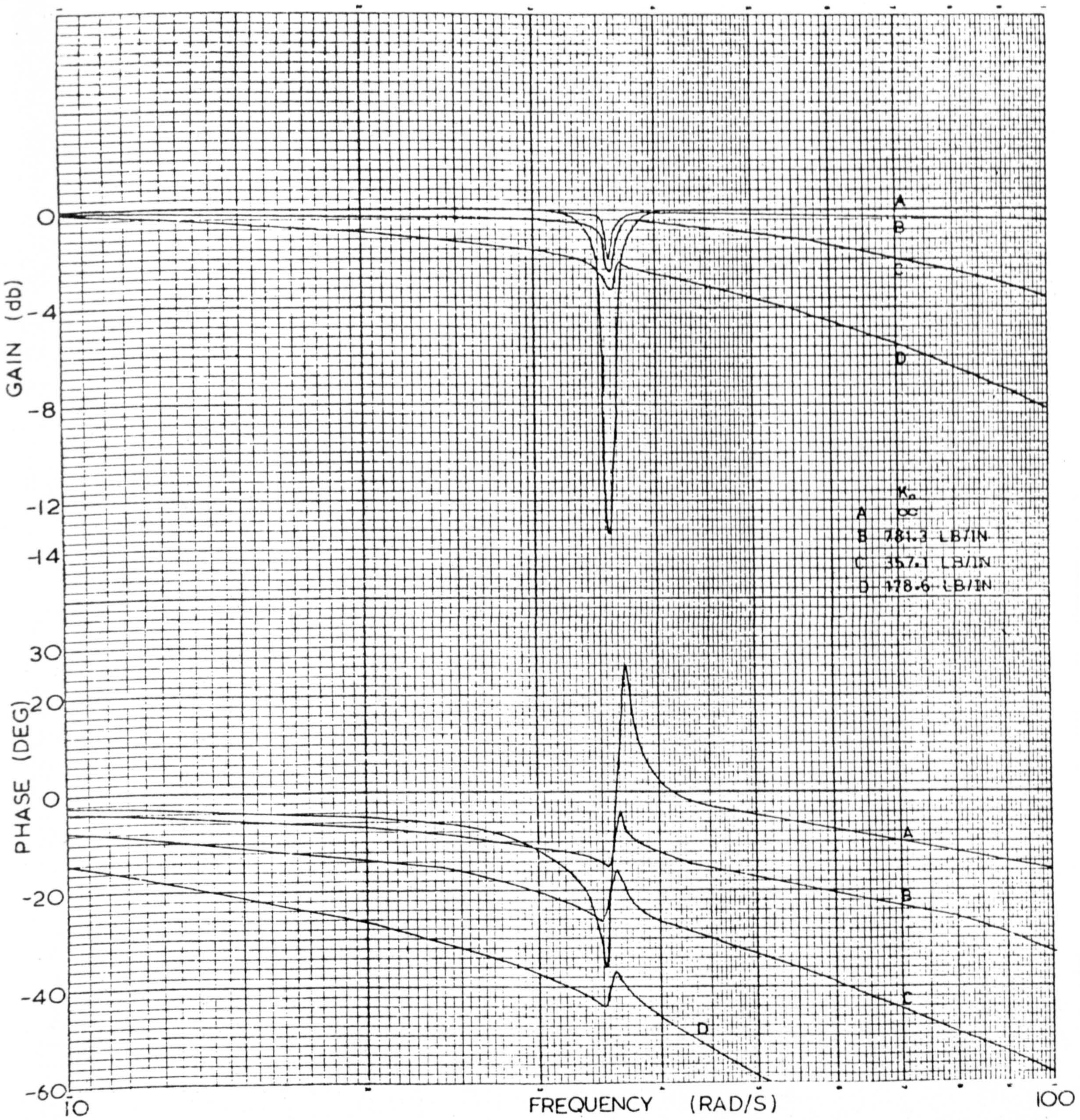

EFFECT OF K_o ON G_c (s)

FIGURE 50

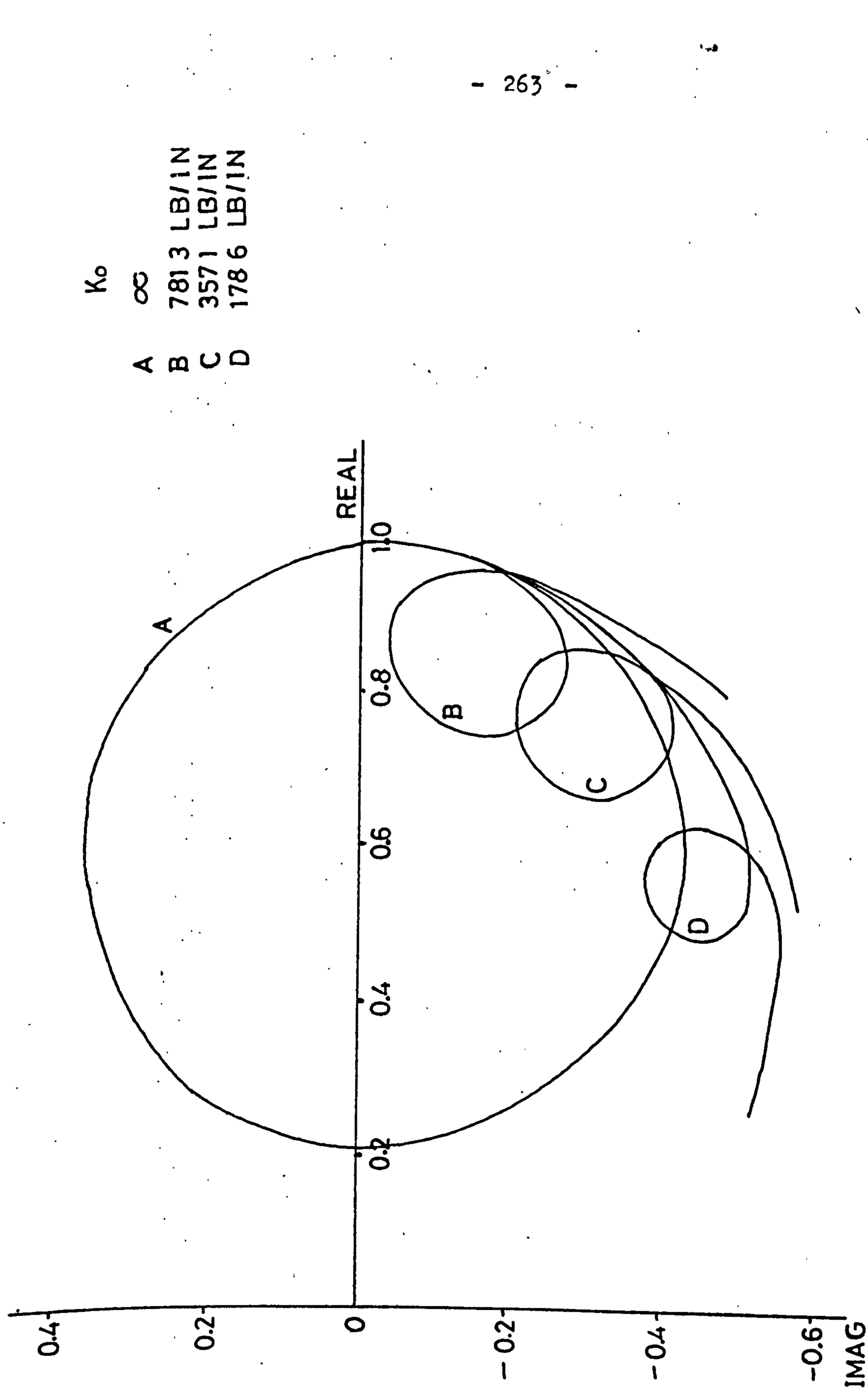

THEORETICAL NYQUIST PLOTS OF $G_c(s)$ FOR VARIOUS VALUES OF K_o

FIGURE 51

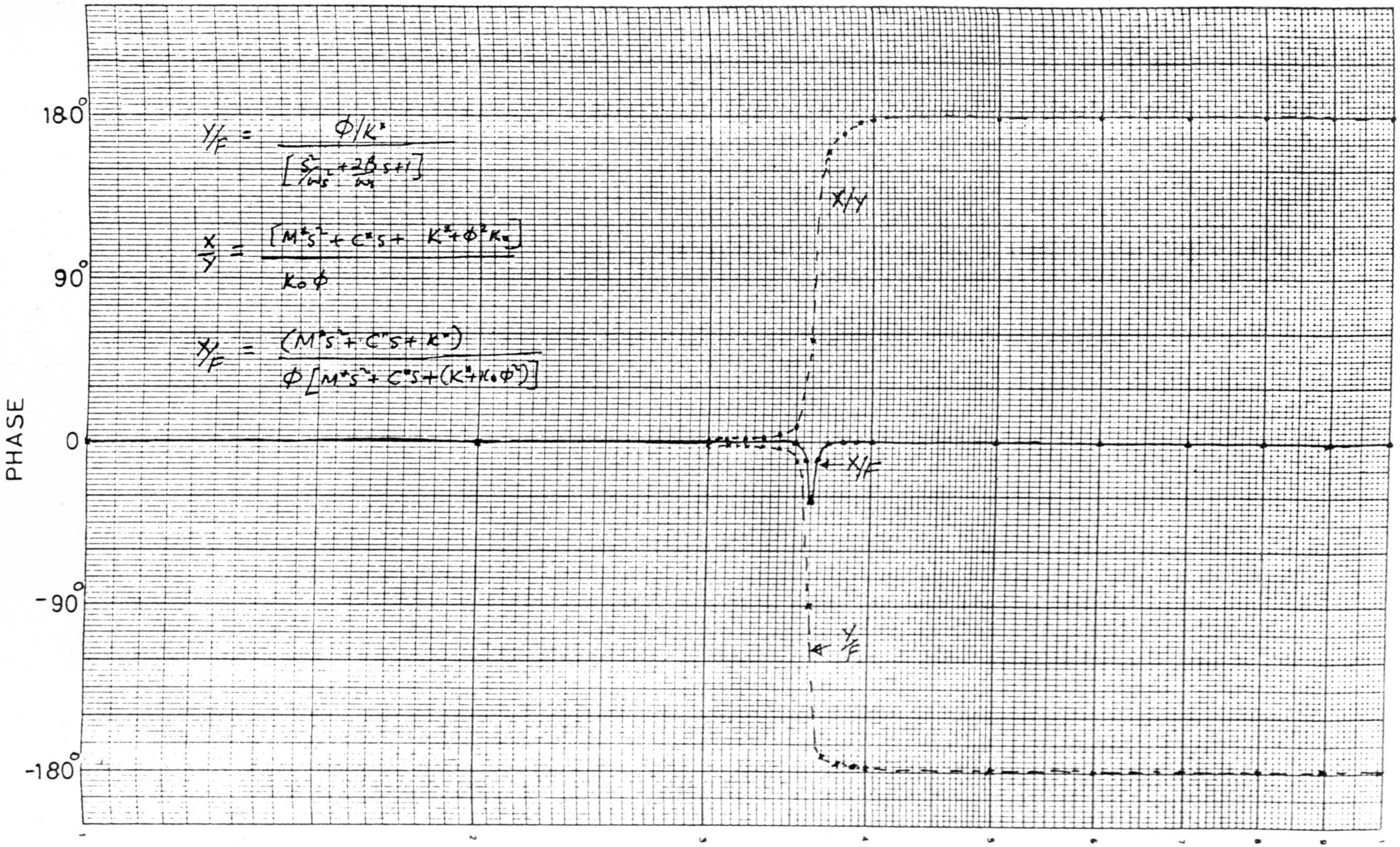

VARIATION OF PHASE WITH FREQUENCY

FIGURE 52

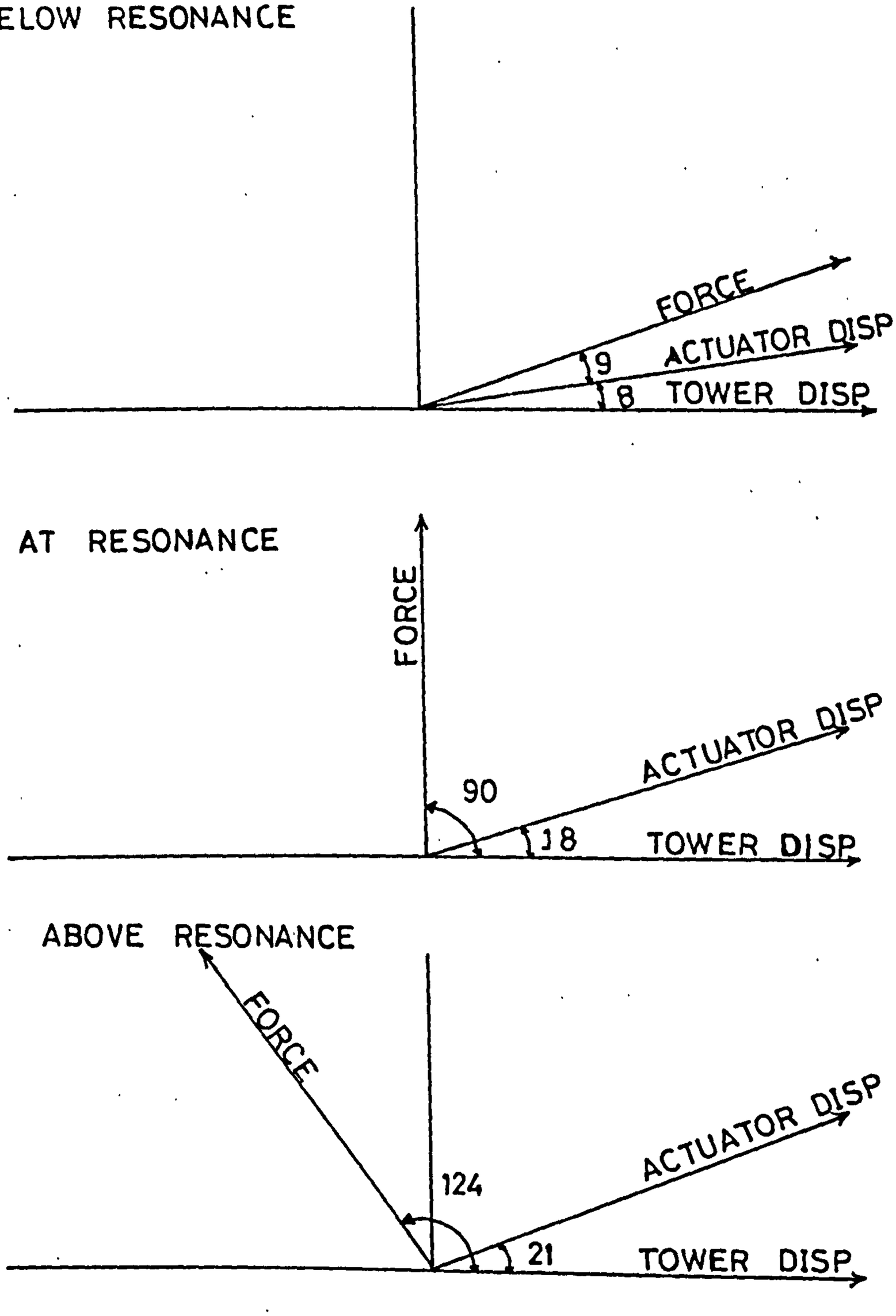

MEASURED PHASE BETWEEN DISPLACEMENTS AND FORCE

FIGURE 53

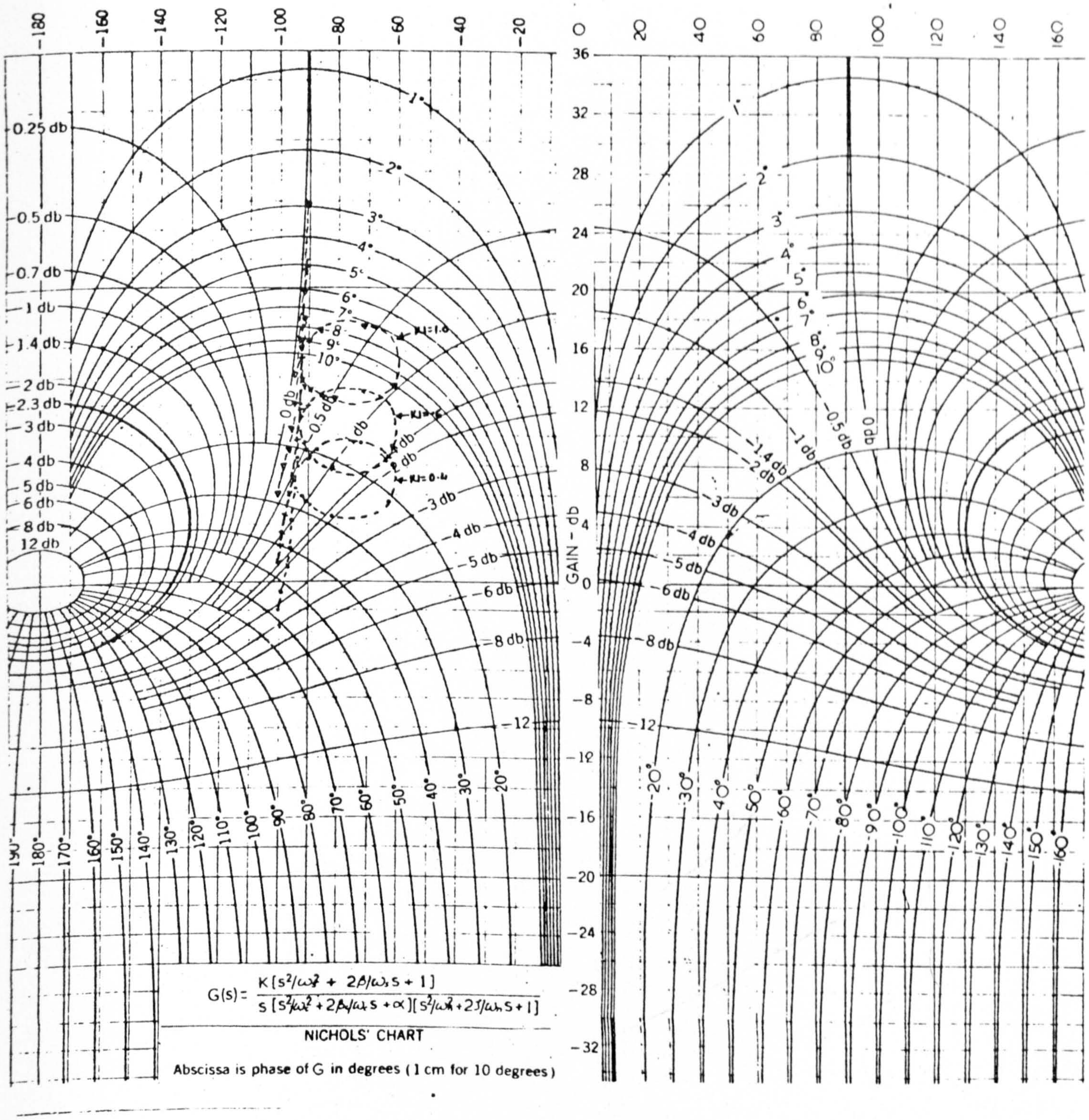

EFFECT OF LOOP GAIN ON G(s)

FIGURE 54

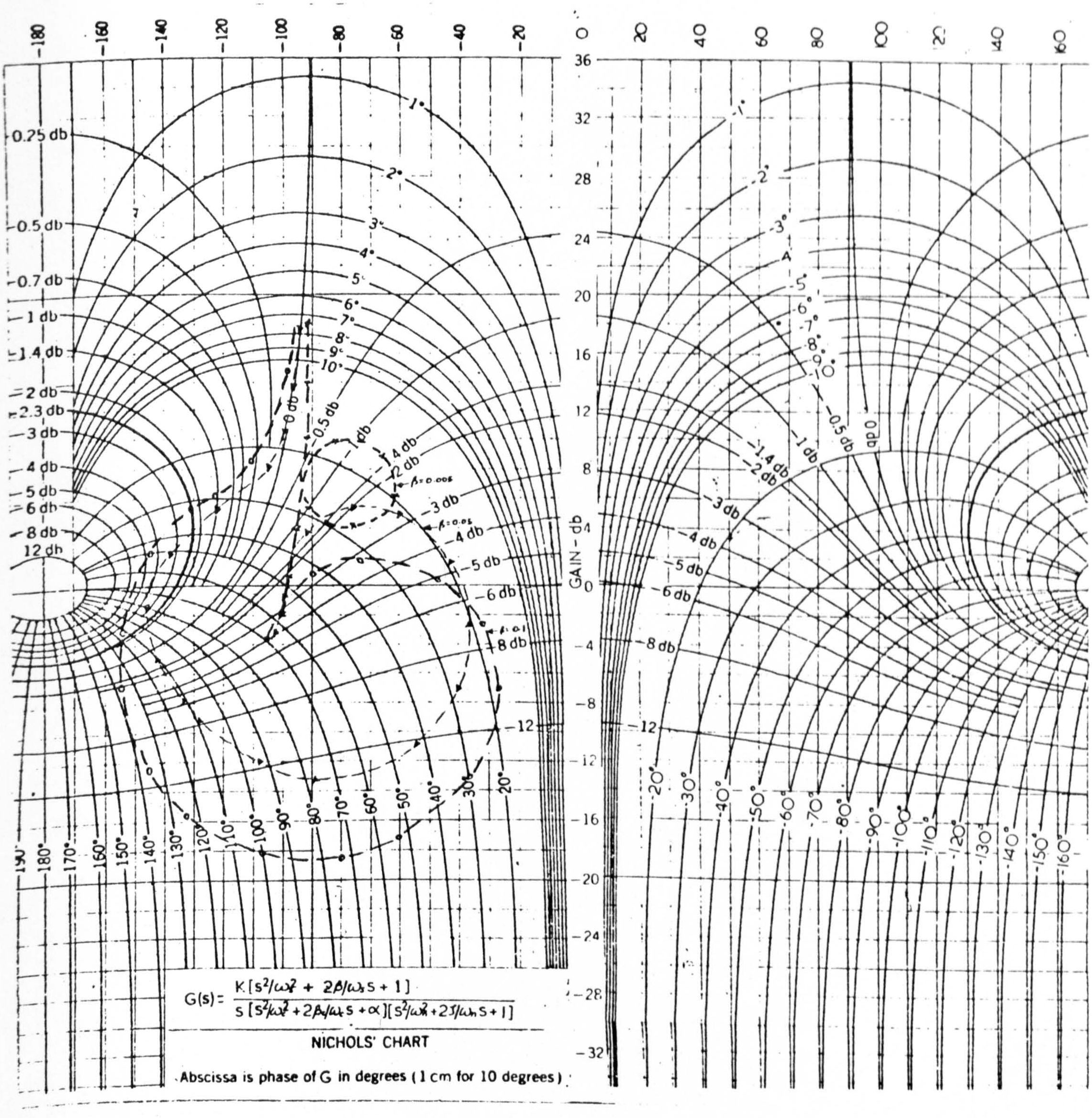

EFFECT OF β ON G(s)

FIGURE 55

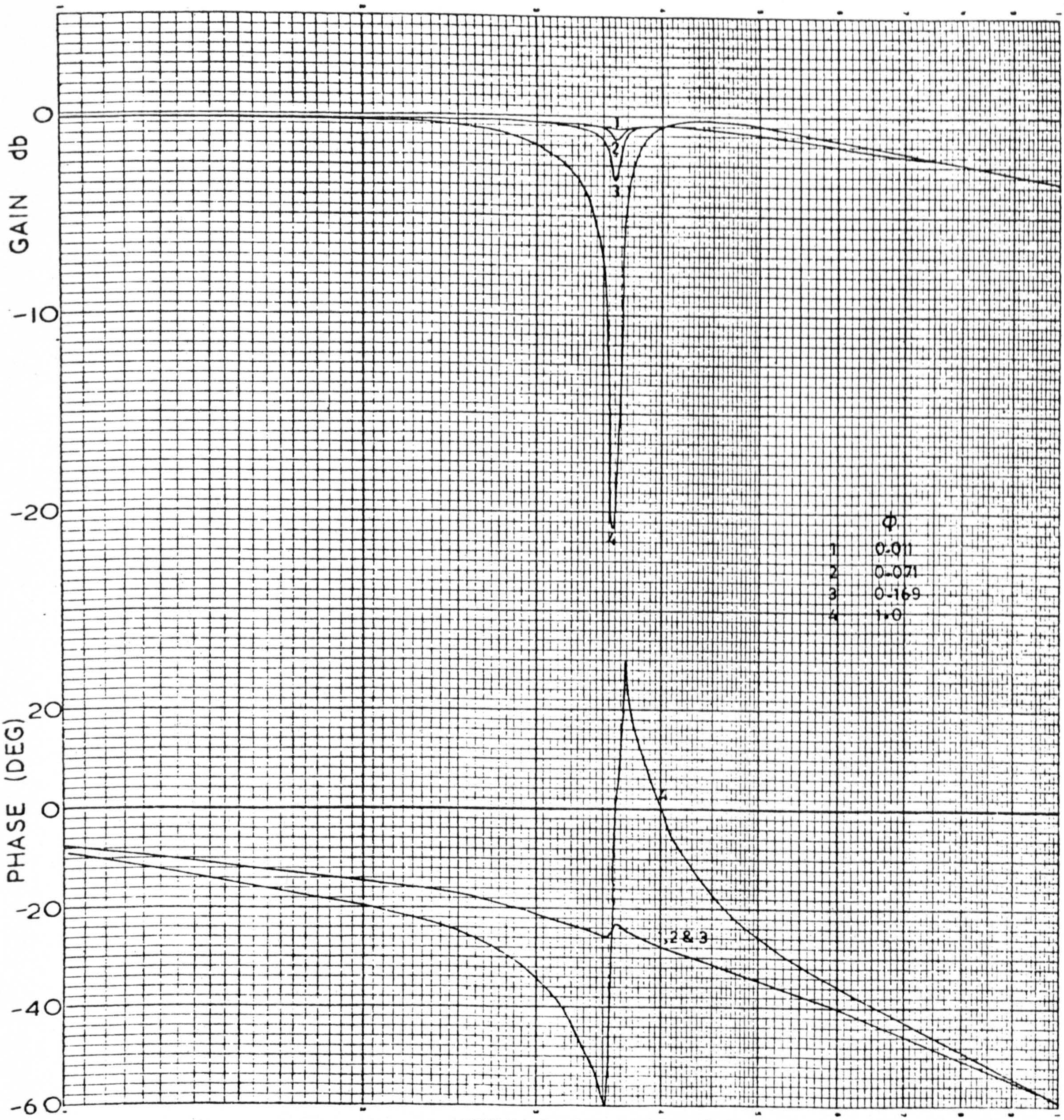

EFFECT OF ATTACHMENT POSITION ON $G_c(s)$

FIGURE 56

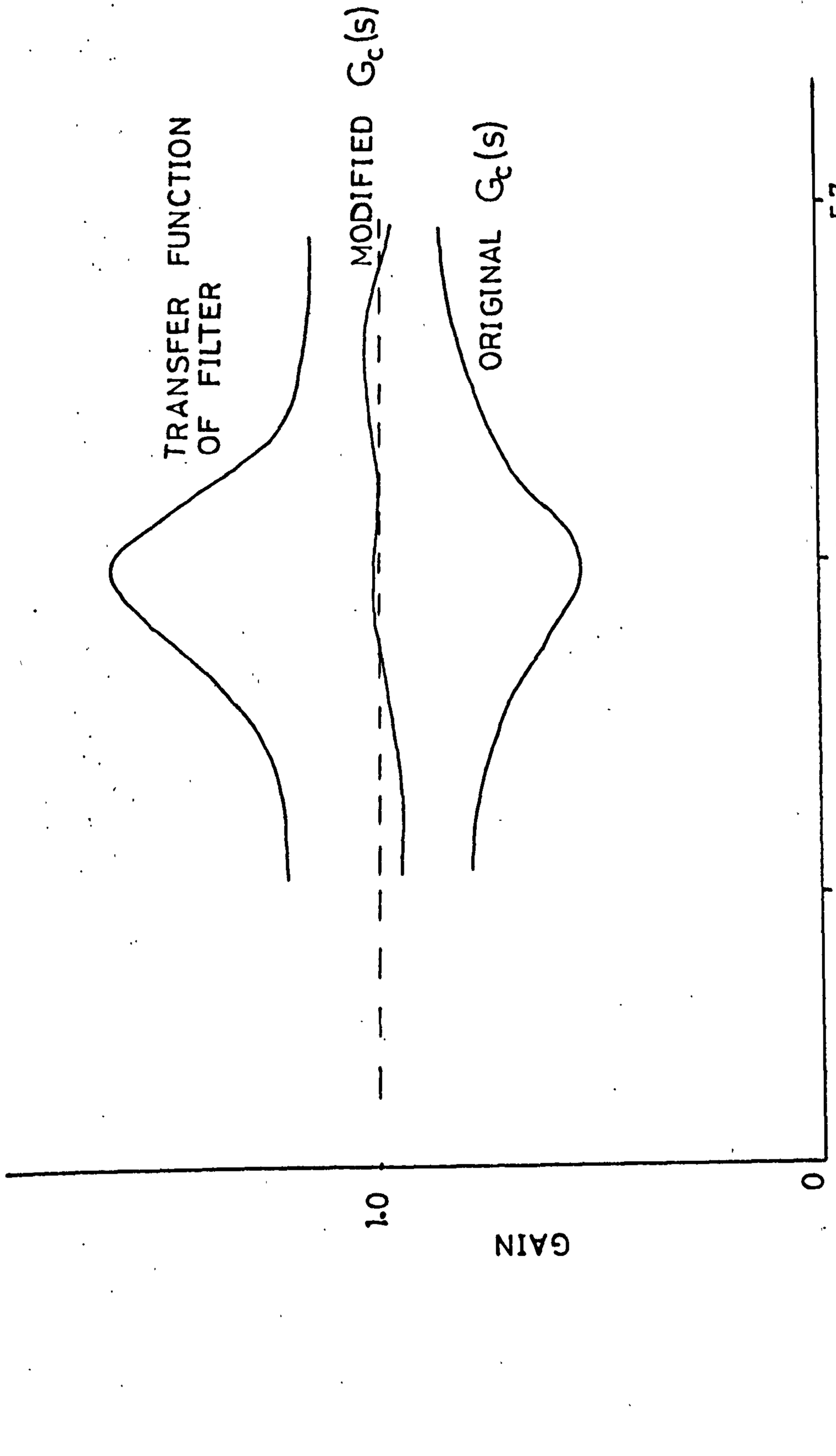
GAIN
1.0
0
5.5
5.6
5.7
FREQUENCY Hz
CLOSED LOOP TRANSFER FUNCTIONS
ORIGINAL $G_c(s)$
MODIFIED $G_c(s)$
TRANSFER FUNCTION OF FILTER

FIGURE 57

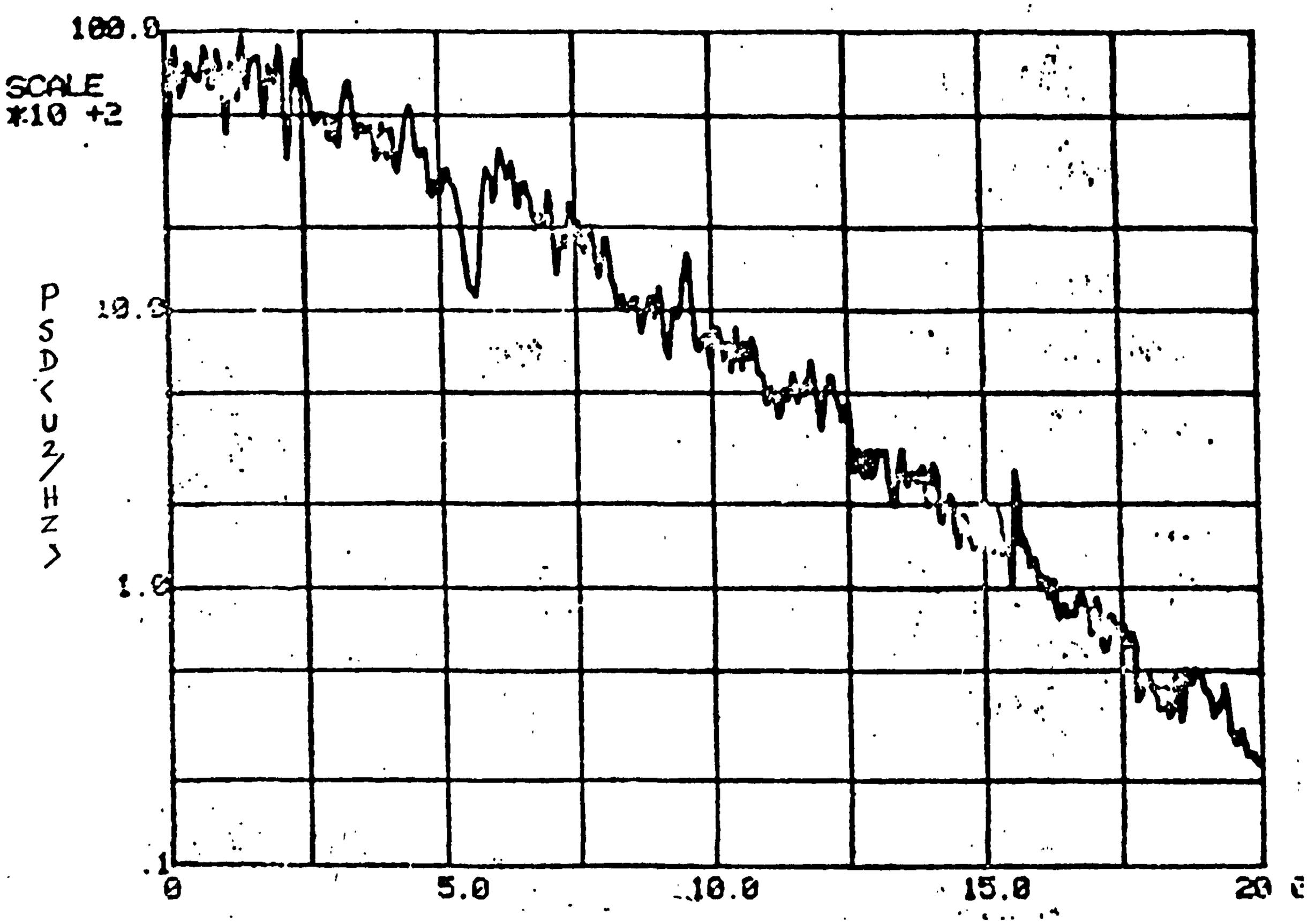

POWER SPECTRAL DENSITY OF FORCE INPUT TO THE TOWER
WITH RIGID CONNECTION

FIGURE 58

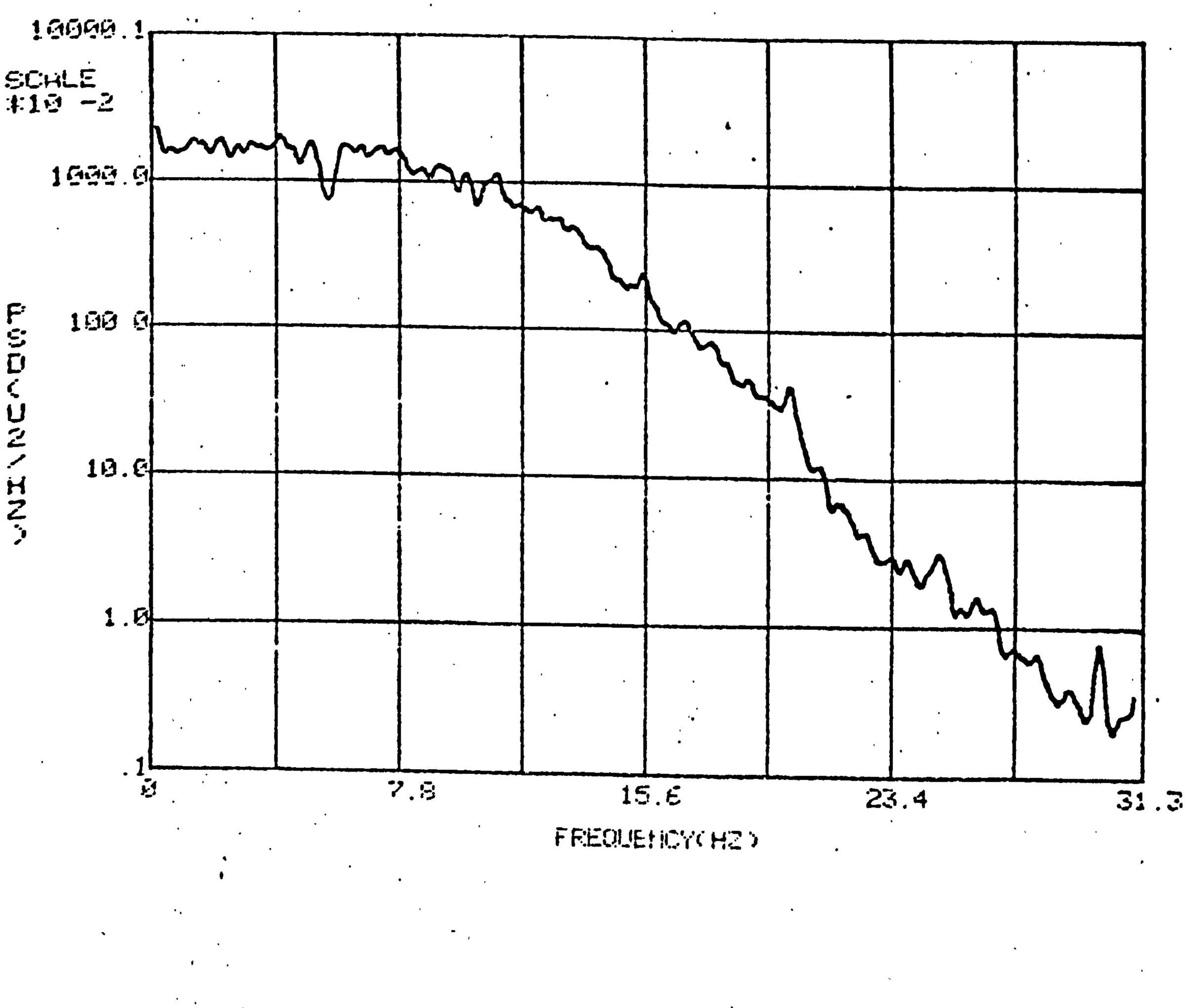

POWER SPECTRAL DENSITY OF FORCE INPUT TO THE TOWER
WITH ELESTIC CONNECTION - WITHOUT FILTER

FIGURE 59

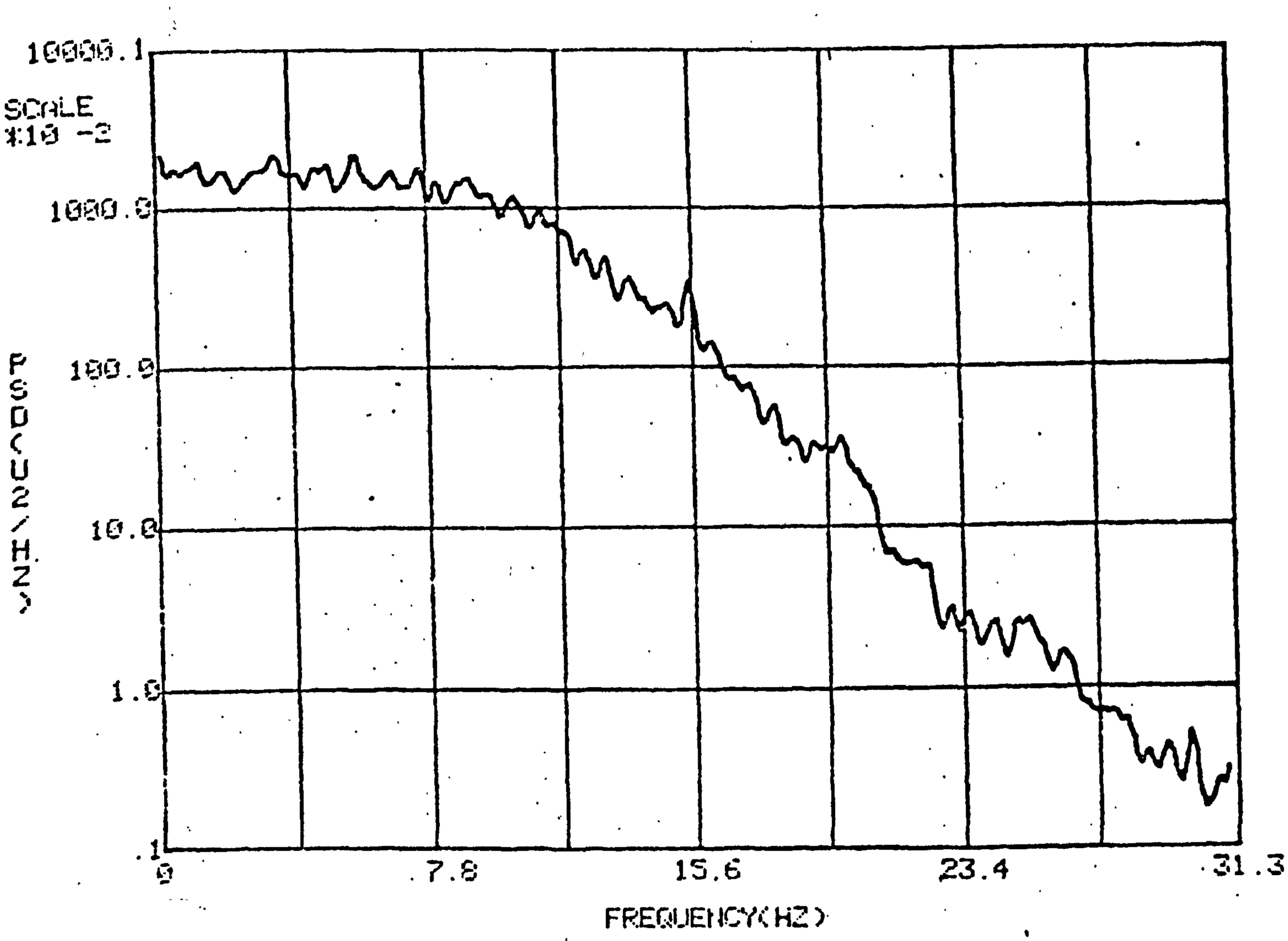

POWER SPECTRAL DENSITY OF FORCE INPUT TO THE TOWER
WITH ELASTIC CONNECTION - WITH FILTER

FIGURE 60

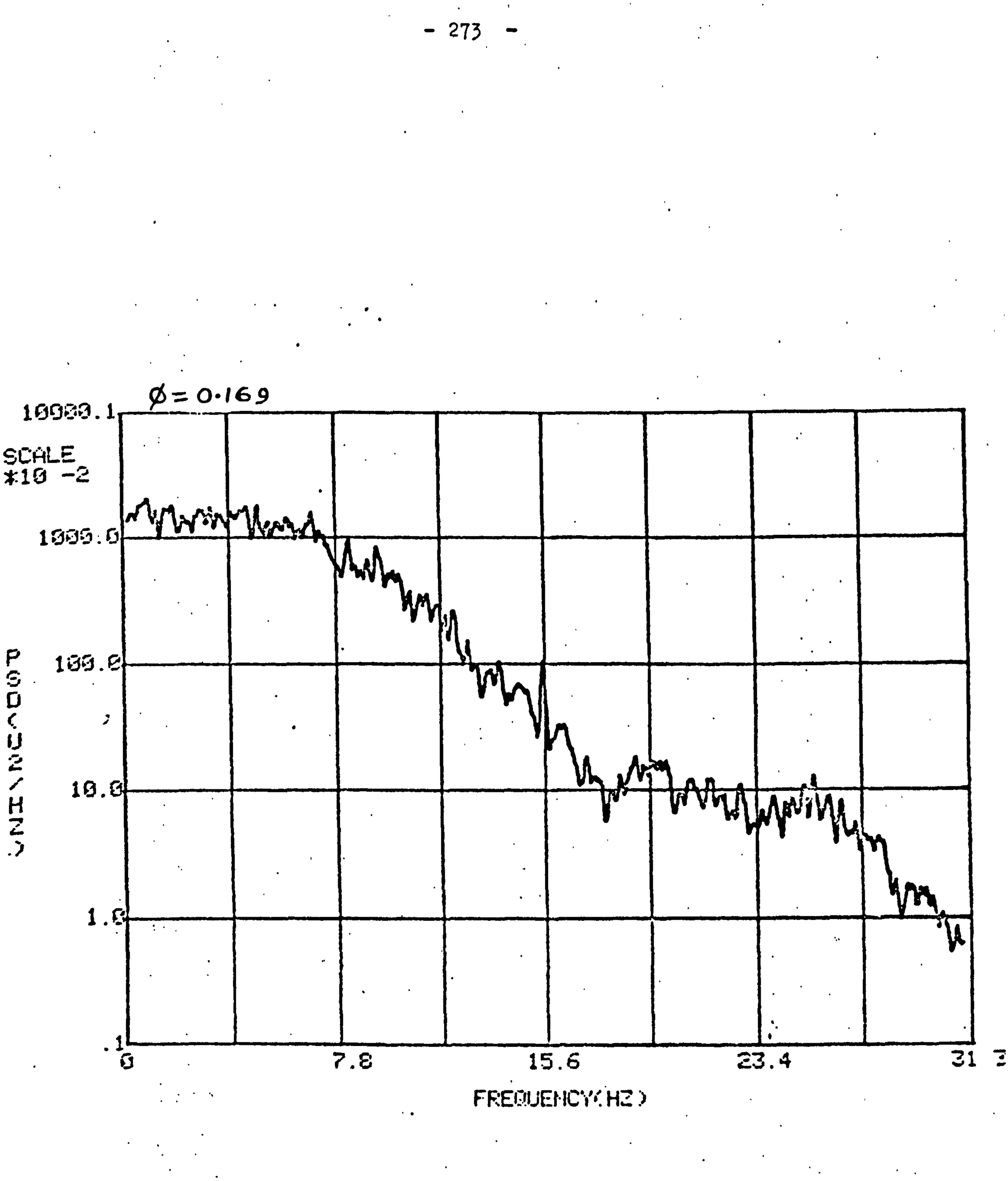

POWER SPECTRAL DENSITY OF FORCE WITH FILTER
K_o = 178.6 lb/in

FIGURE 61

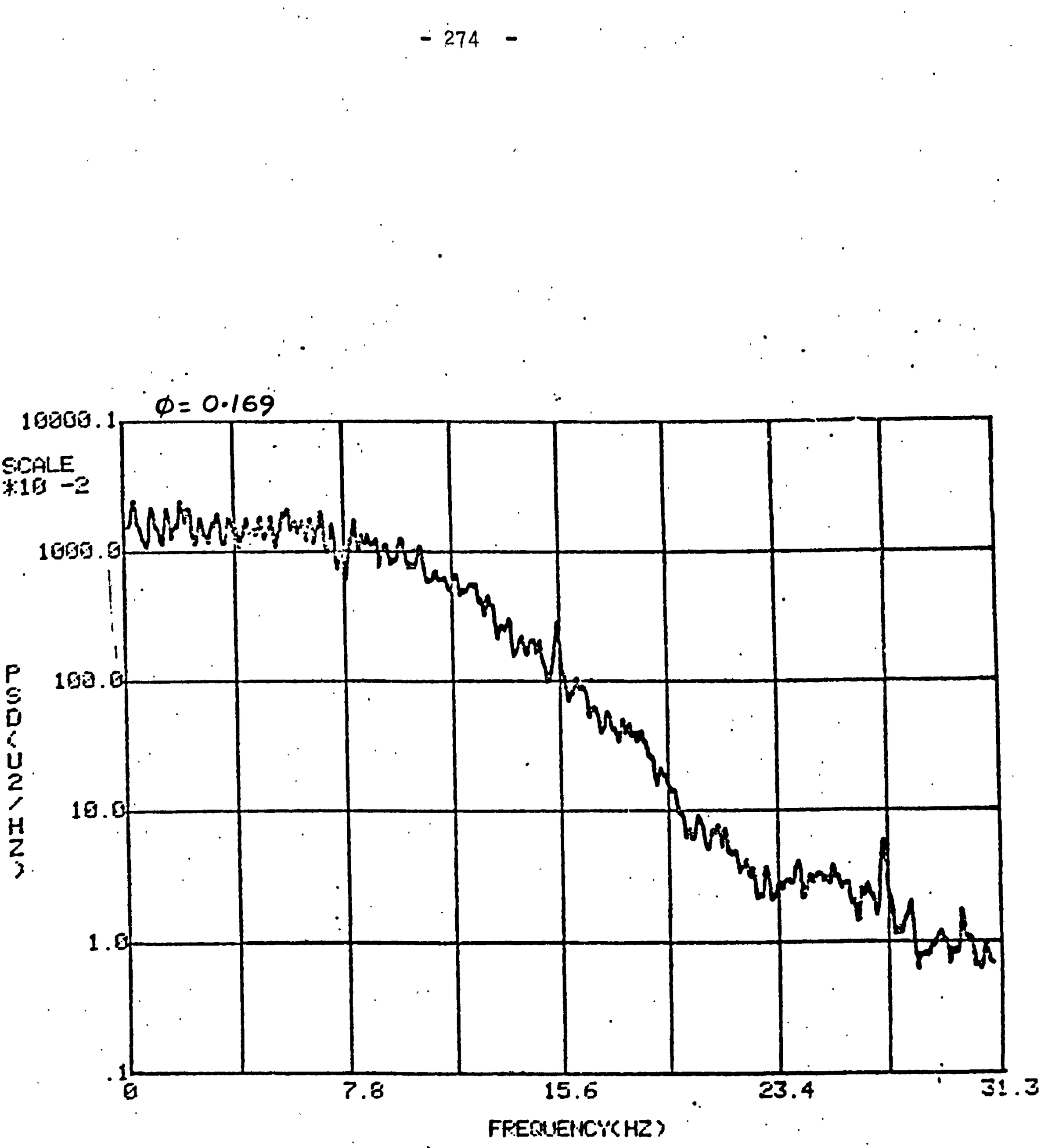

POWER SPECTRAL DENSITY OF FORCE WITH FILTER
K_o = 357.1 lb/in

FIGURE 62

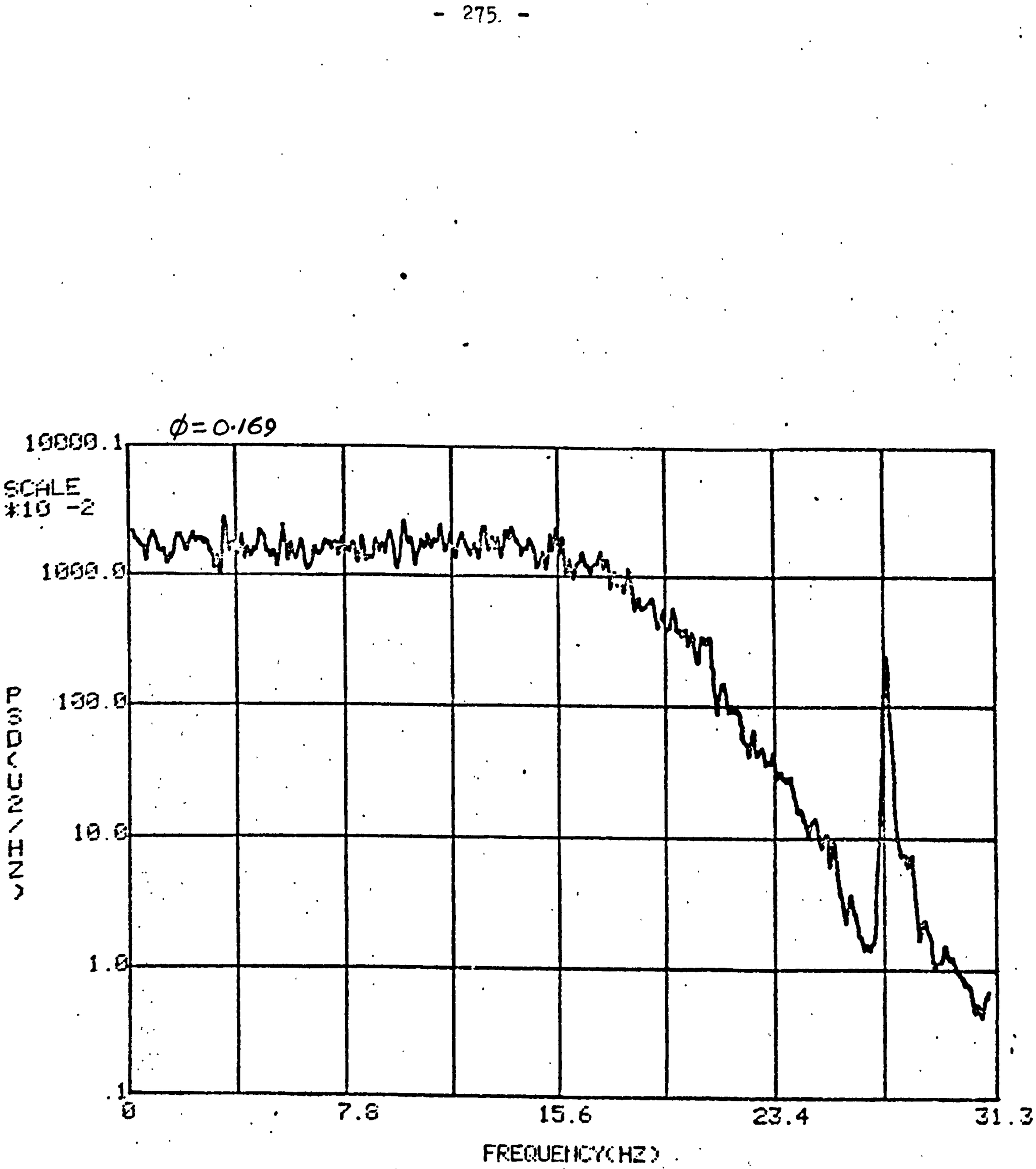

POWER SPECTRAL DENSITY OF FORCE WITH FILTER
K_o = 781.3 lb/in

FIGURE 63

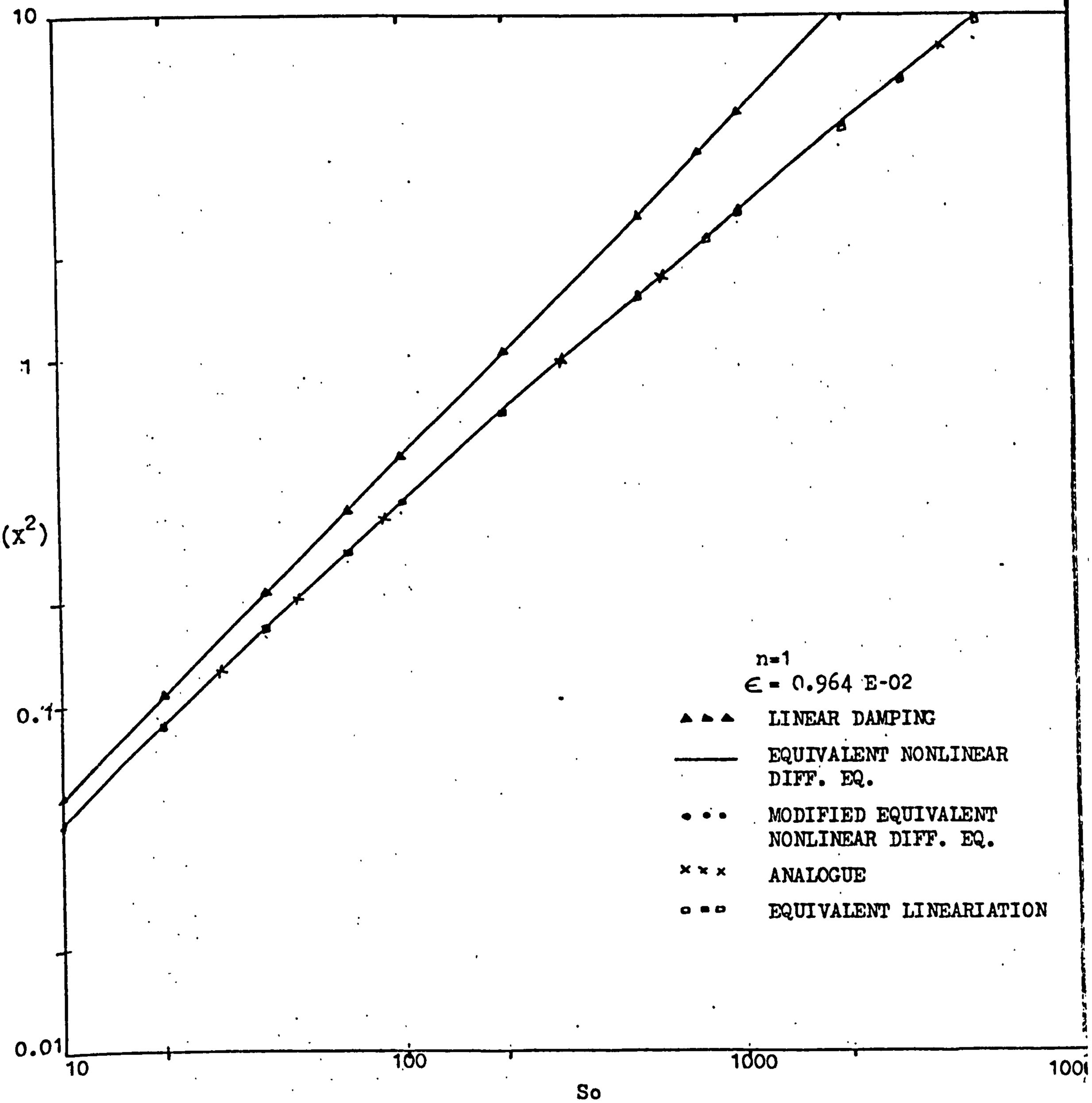

So

MEAN SQUARE RESPONSE VERSUS P.S.D. OF EXCITATION

FIGURE 64a

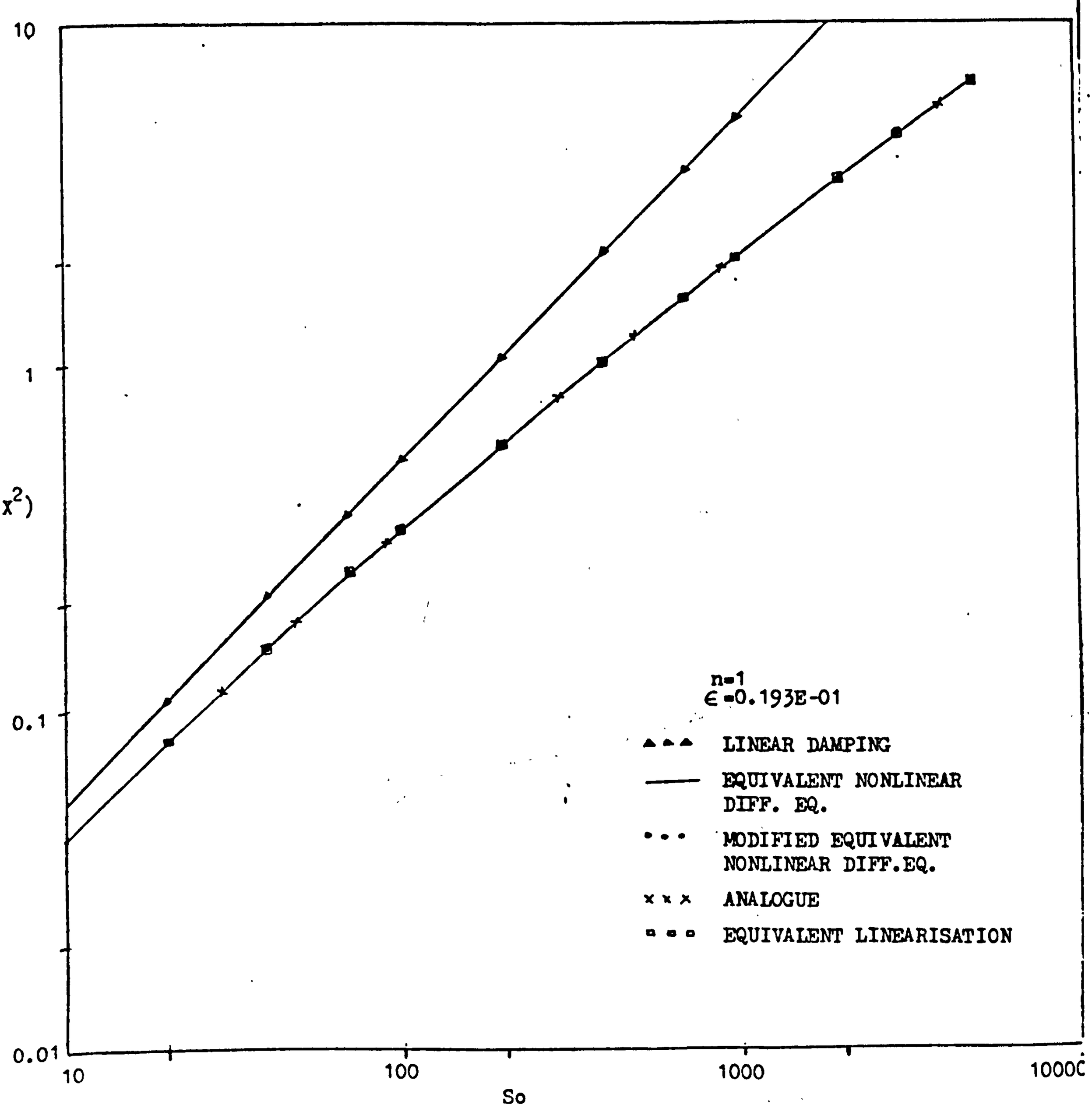

MEAN SQUARE RESPONSE VERSUS P.S.D. OF EXCITATION

FIGURE 64b

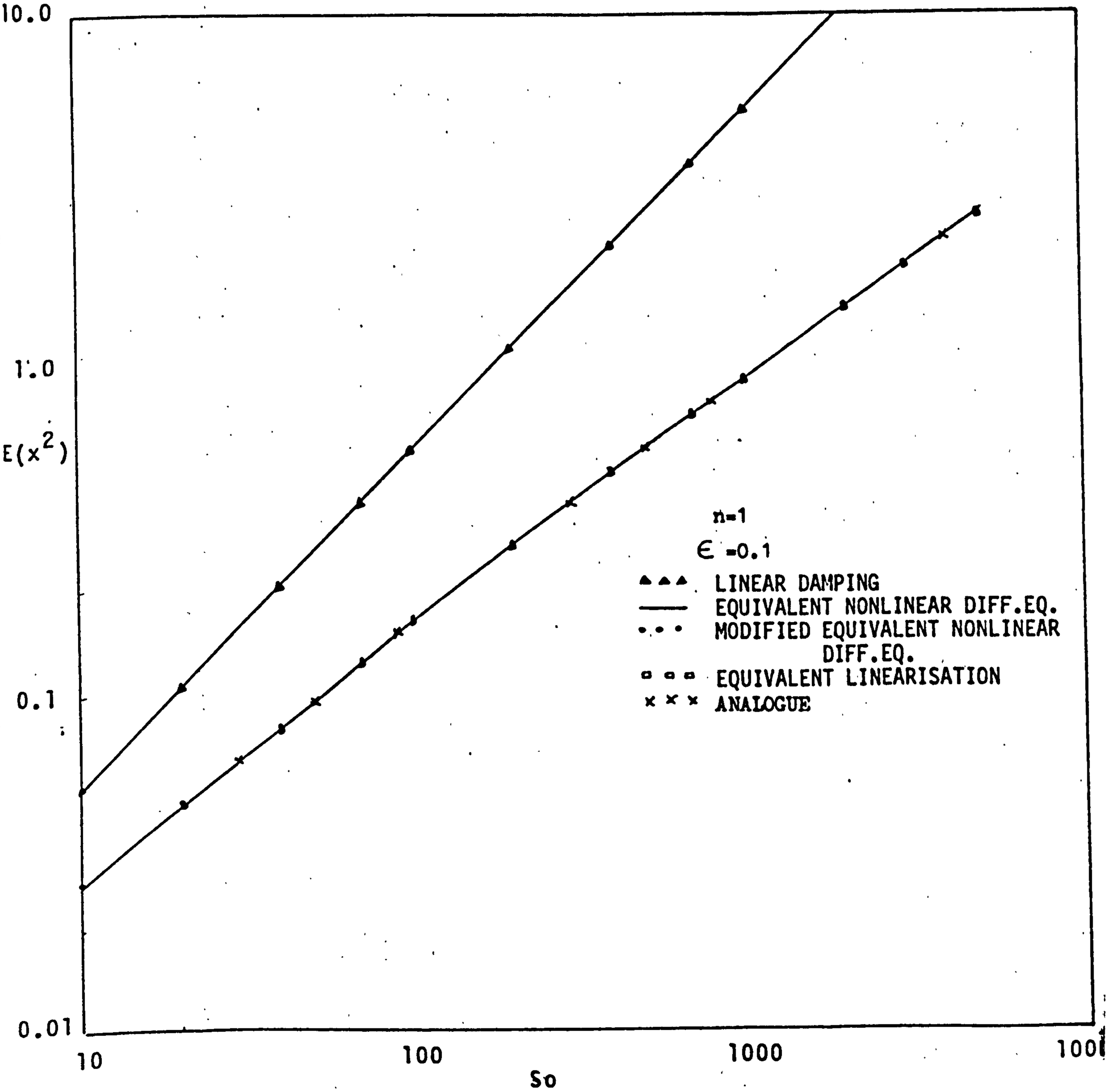

MEAN SQUARE RESPONSE VERSUS PSD OF EXCITATION

FIGURE 64c

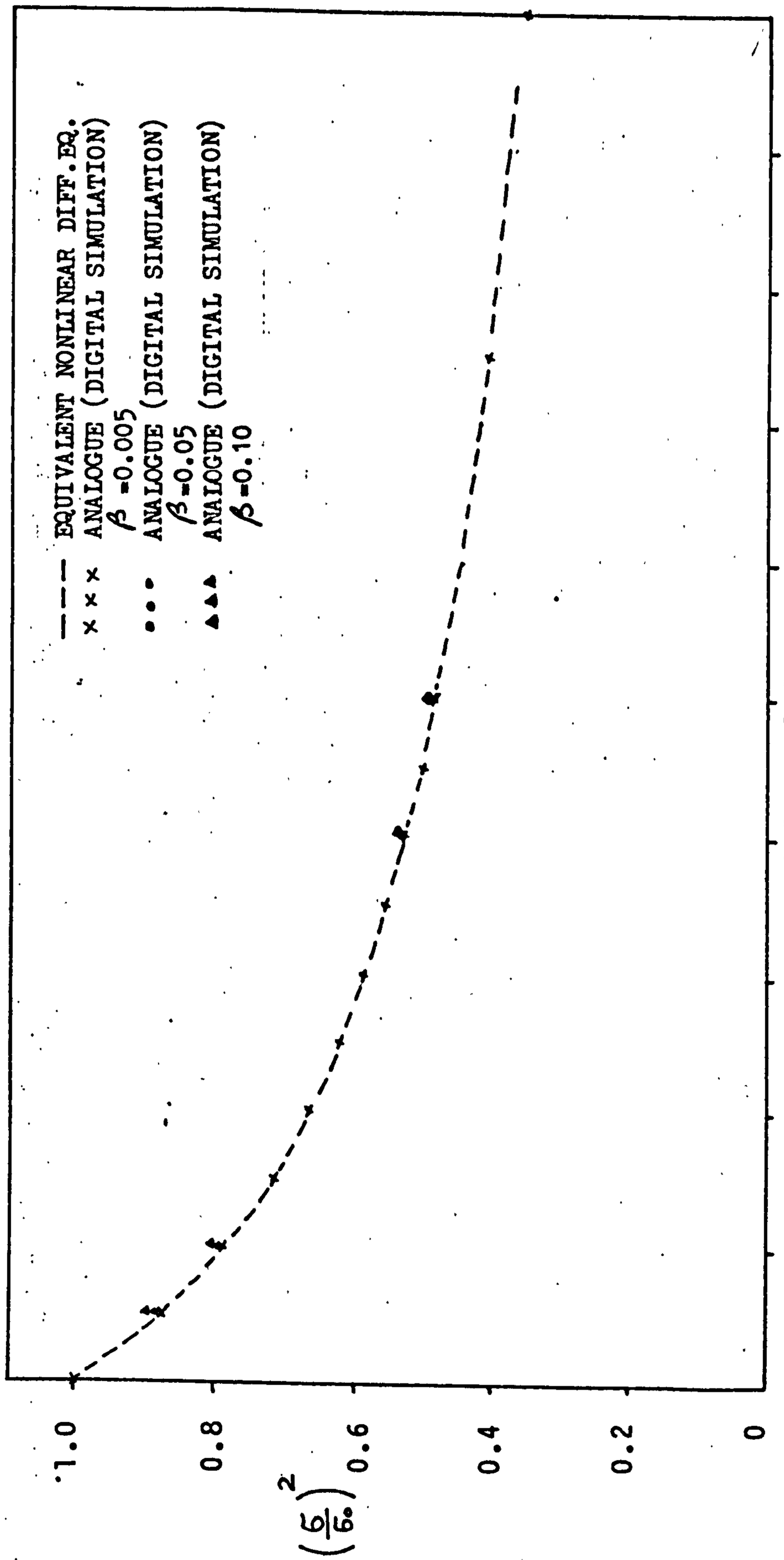

COMPARISON BETWEEN ANALOGUE AND THEORY (ENL) FOR $n=1$
FIGURE 65a

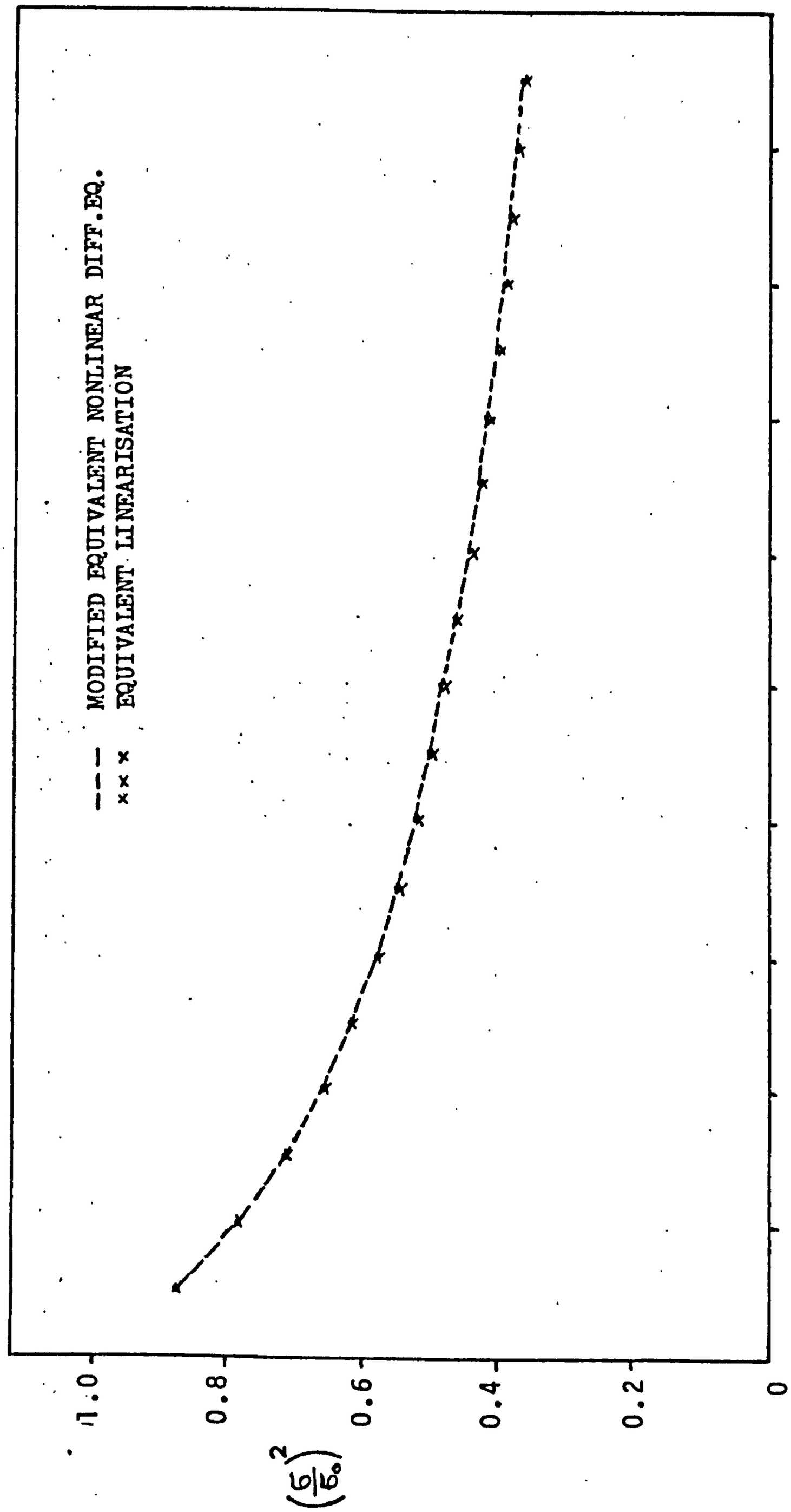

COMPARISON BETWEEN APPROXIMATE THEORETICAL SOLUTIONS

FIGURE 65b

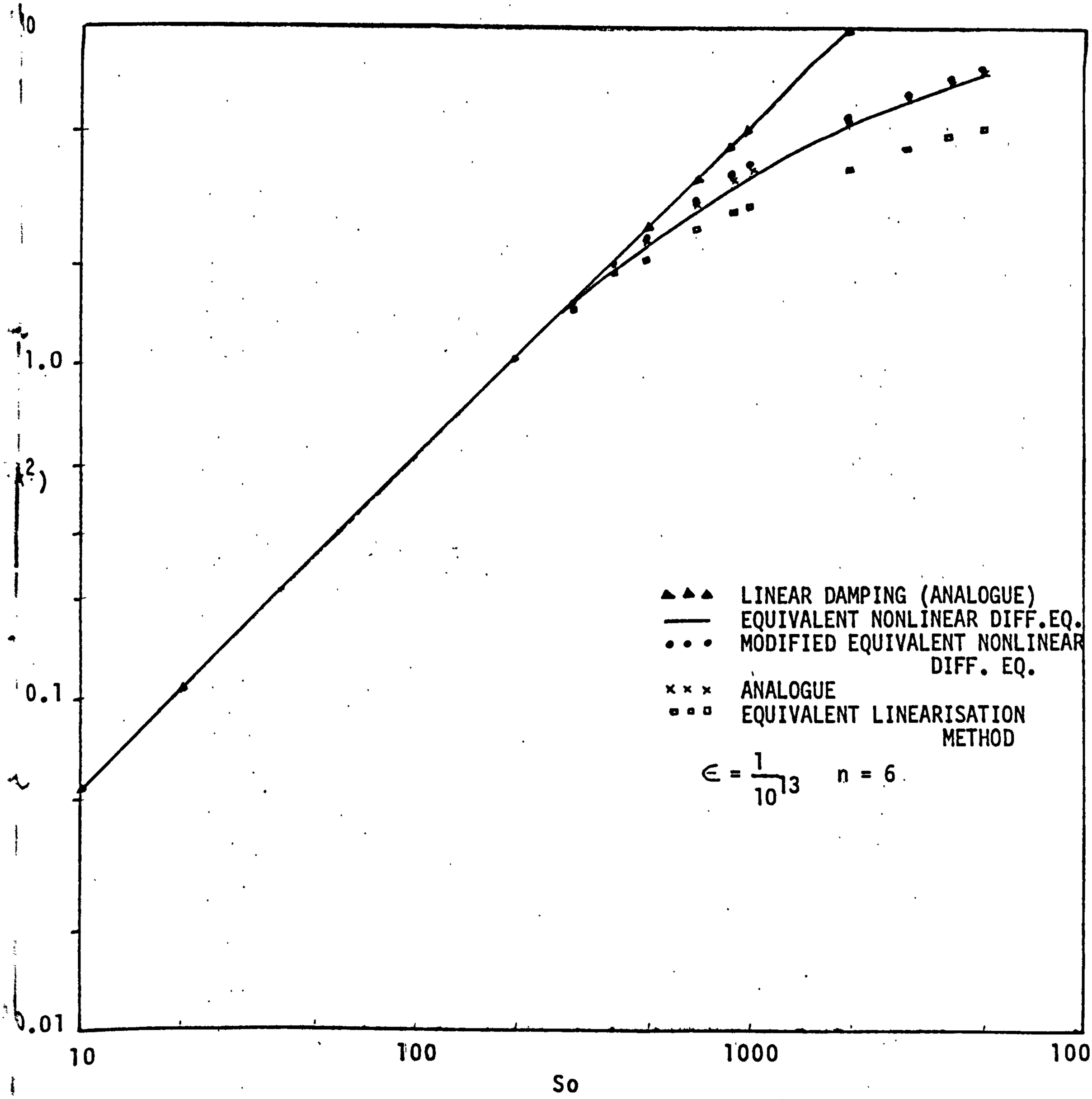

MEAN SQUARE RESPONSE VERSUS PSD OF EXCITATION (n=6)

FIGURE 66a

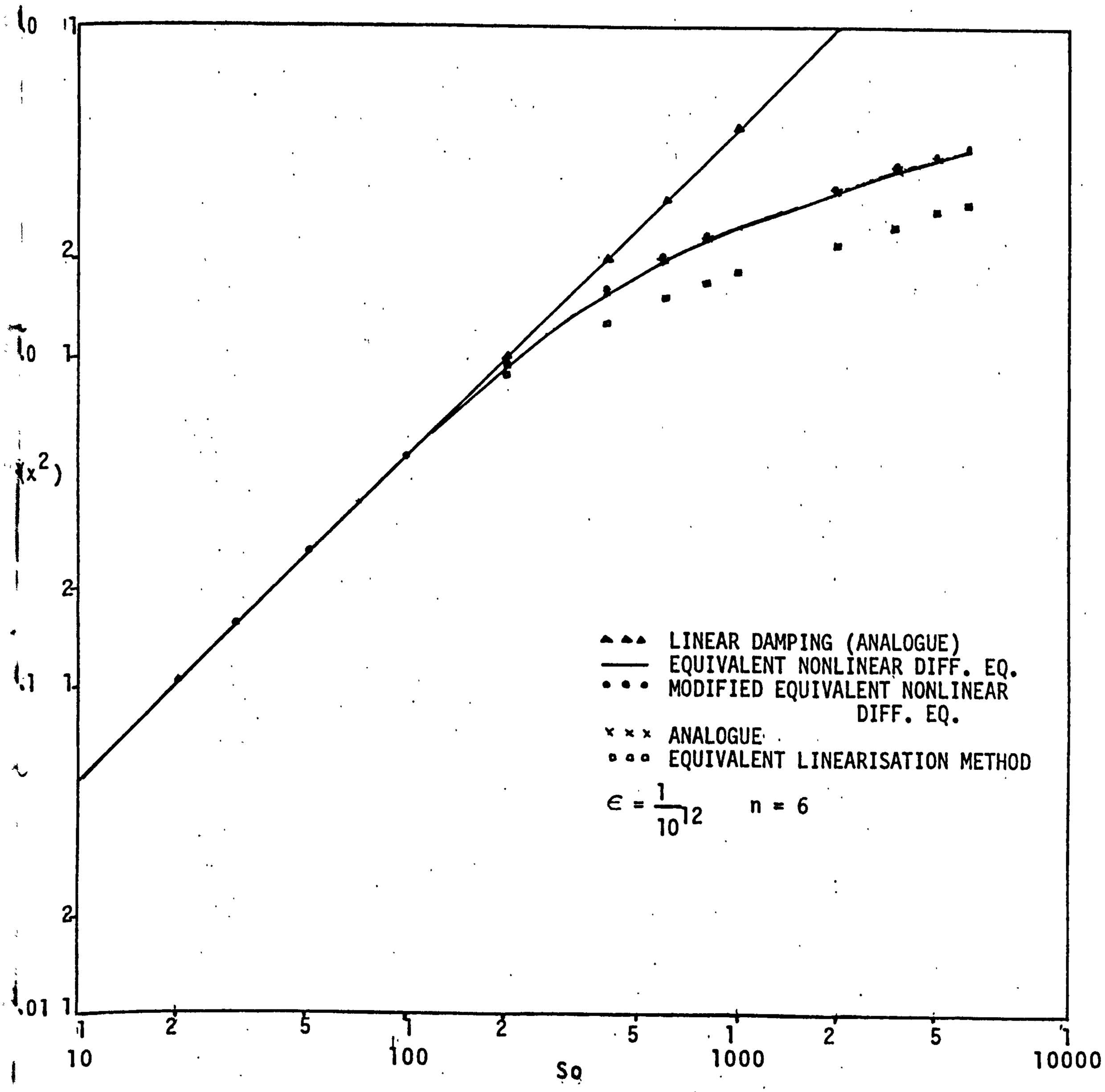

MEAN SQUARE RESPONSE VERSUS PSD OF EXCITATION

FIGURE 66b

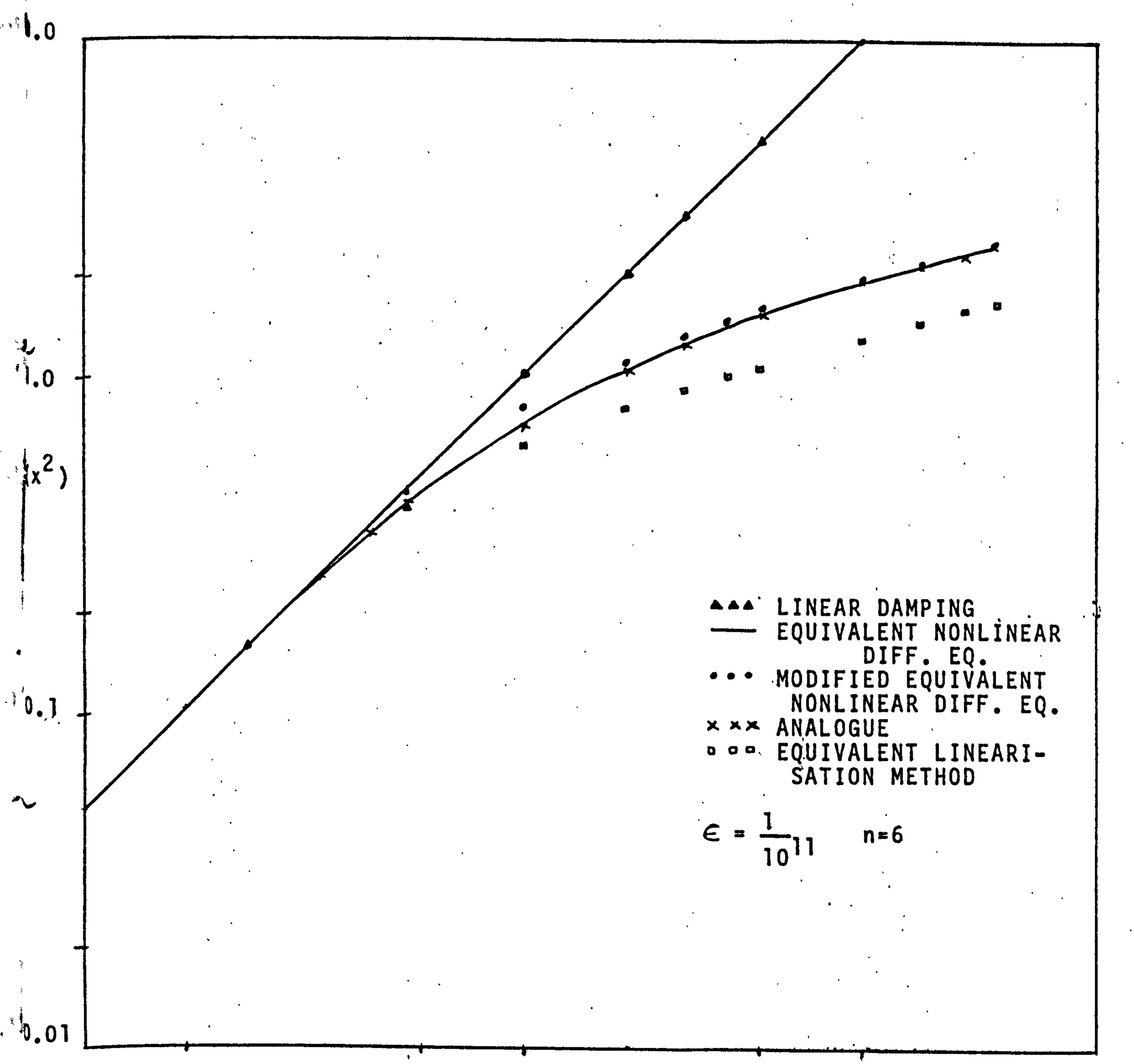

MEAN SQUARE RESPONSE VERSUS PSD OF EXCITATION

FIGURE 66c

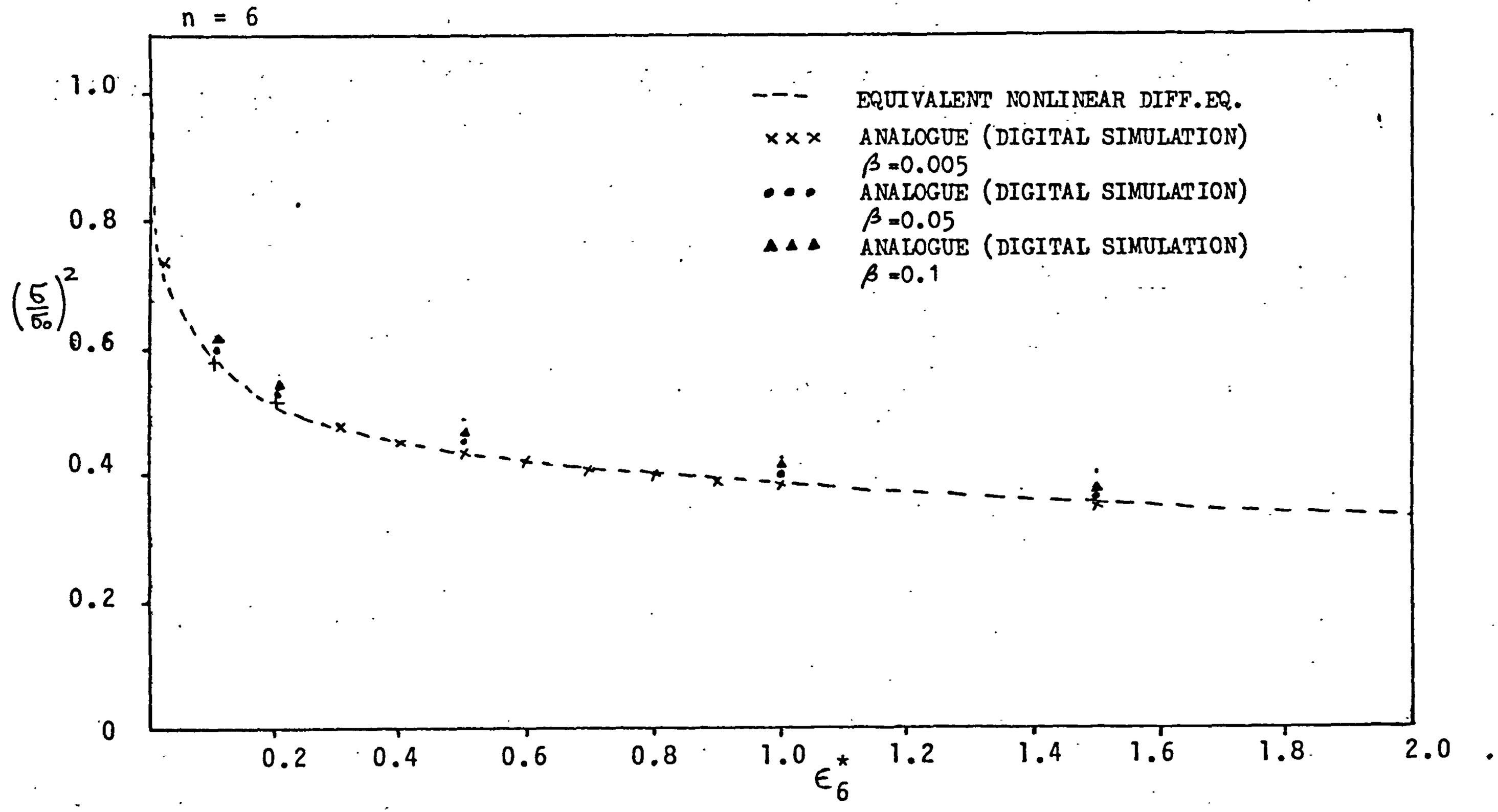

COMPARISON BETWEEN ANALOGUE AND THEORY (ENL) FOR n=6

FIGURE 67a

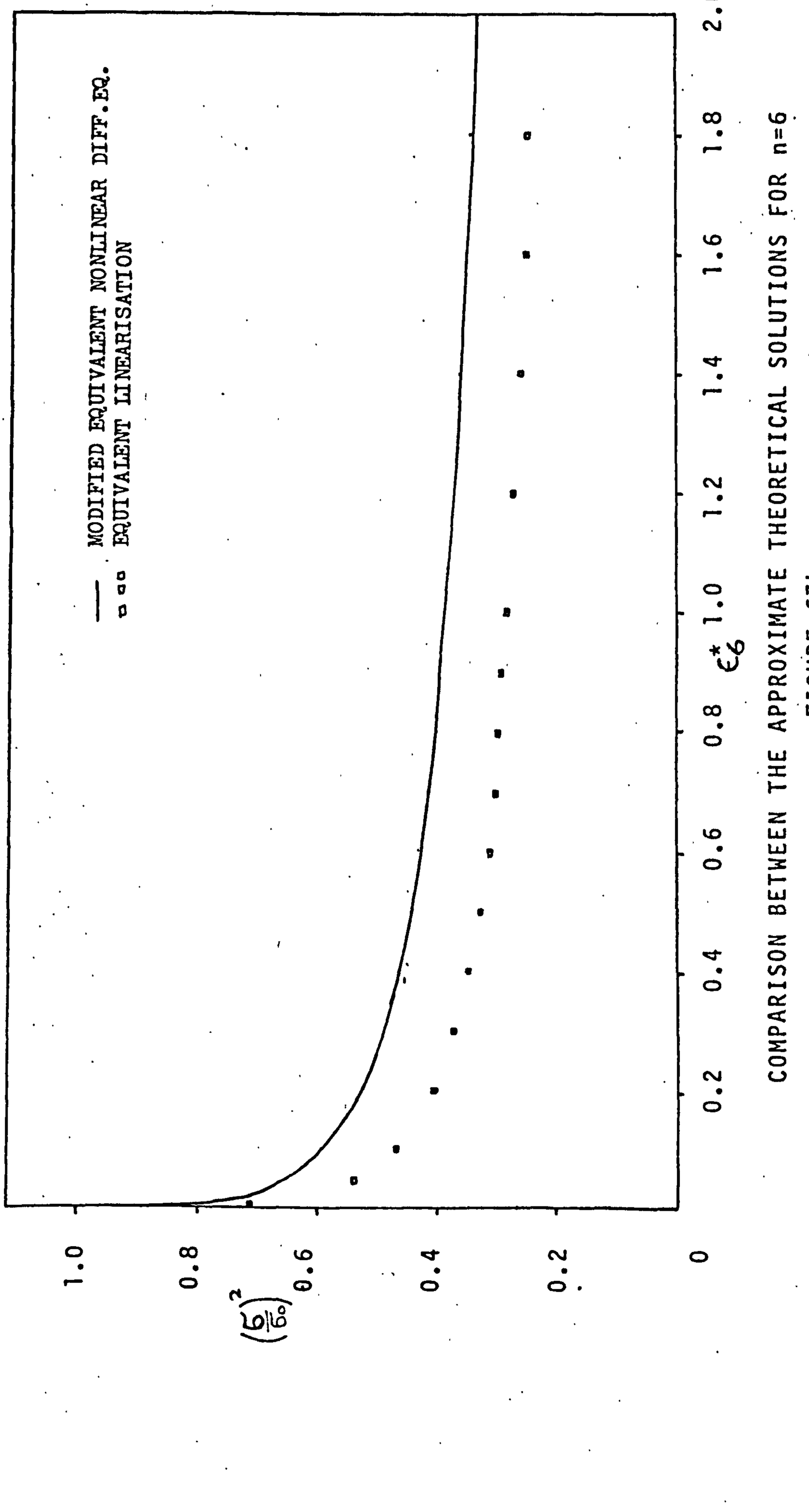

COMPARISON BETWEEN THE APPROXIMATE THEORETICAL SOLUTIONS FOR n=6

FIGURE 67b

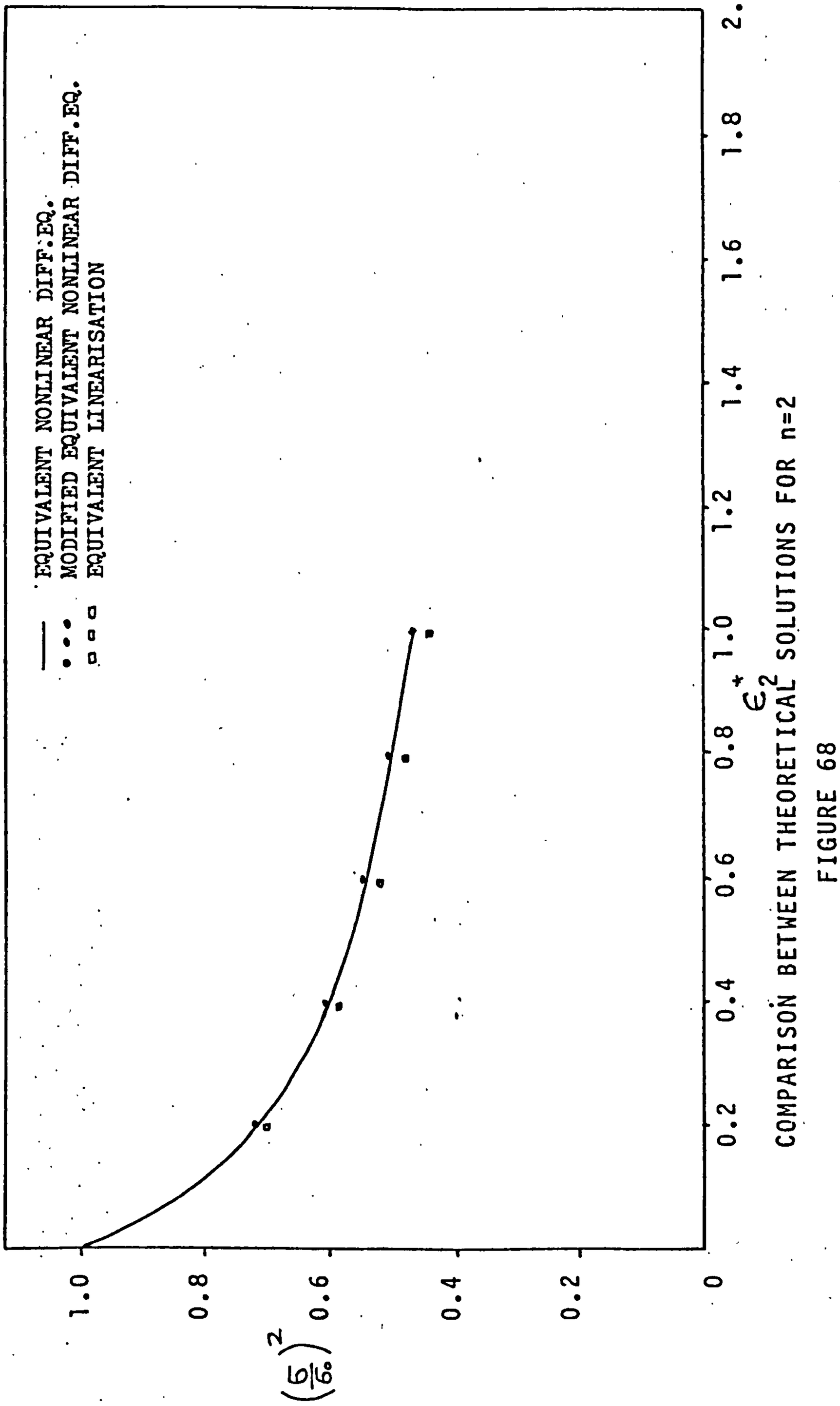
EQUIVALENT NONLINEAR DIFF.EQ.
MODIFIED EQUIVALENT NONLINEAR DIFF.EQ.
EQUIVALENT LINEARISATION
COMPARISON BETWEEN THEORETICAL SOLUTIONS FOR n=2
ϵ_2^+
$(\theta/\theta_0)^2$
0
0.2
0.4
0.6
0.8
1.0
1.2
1.4
1.6
1.8
2.0

FIGURE 68

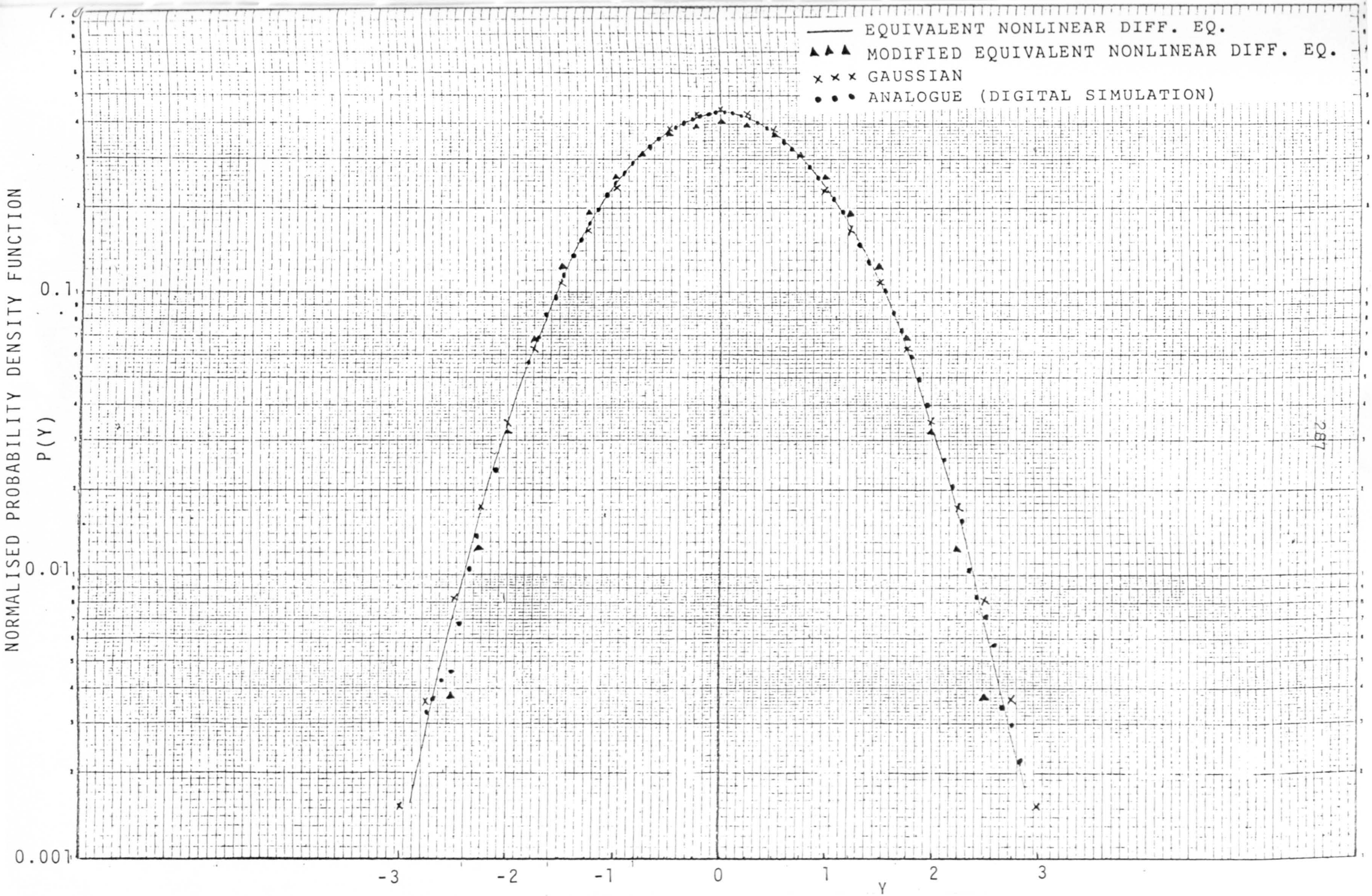

PROBABILITY DENSITY FUNCTION COMPARISON FOR N=1 ε^*=0.2
FIGURE 69a

EQUIVALENT NONLINEAR DIFF. EQ.
MODIFIED EQUIVALENT NONLINEAR DIFF. EQ.
GAUSSIAN
ANALOGUE (DIGITAL SIMULATION)

NORMALISED PROBABILITY DENSITY FUNCTION P(Y)

0.1
0.01
0.001

-3 -2 -1 0 1 2 3
Y

PROBABILITY DENSITY FUNCTION COMPARISON FOR N=1 ε^*=1.0
FIGURE 69b

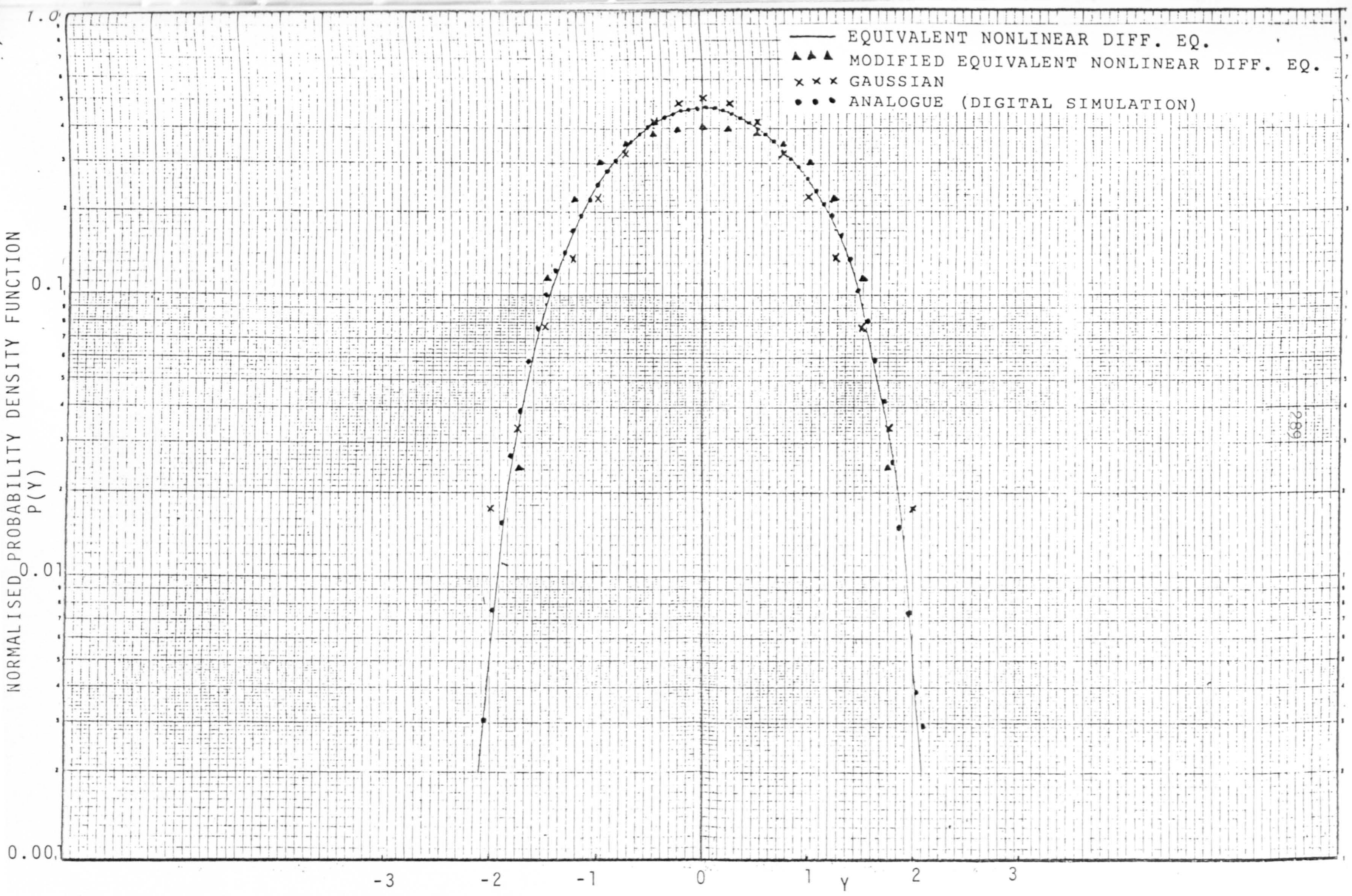

PROBABILITY DENSITY FUNCTION COMPARISON FOR N=6 $\varepsilon^*=0.1$
FIGURE 70a

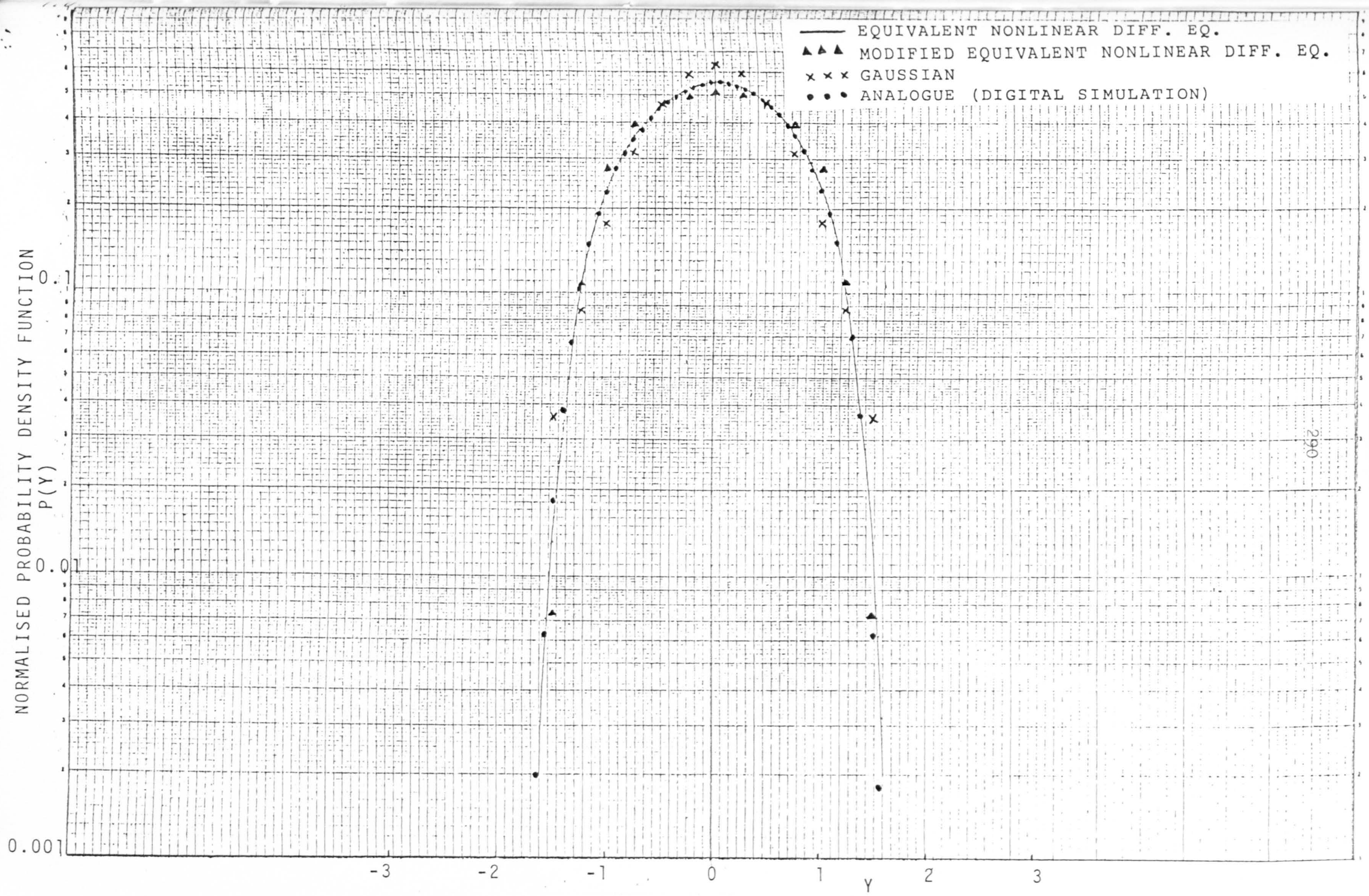

PROBABILITY DENSITY FUNCTION COMPARISON FOR N=6 ε^*=1.0
FIGURE 70b

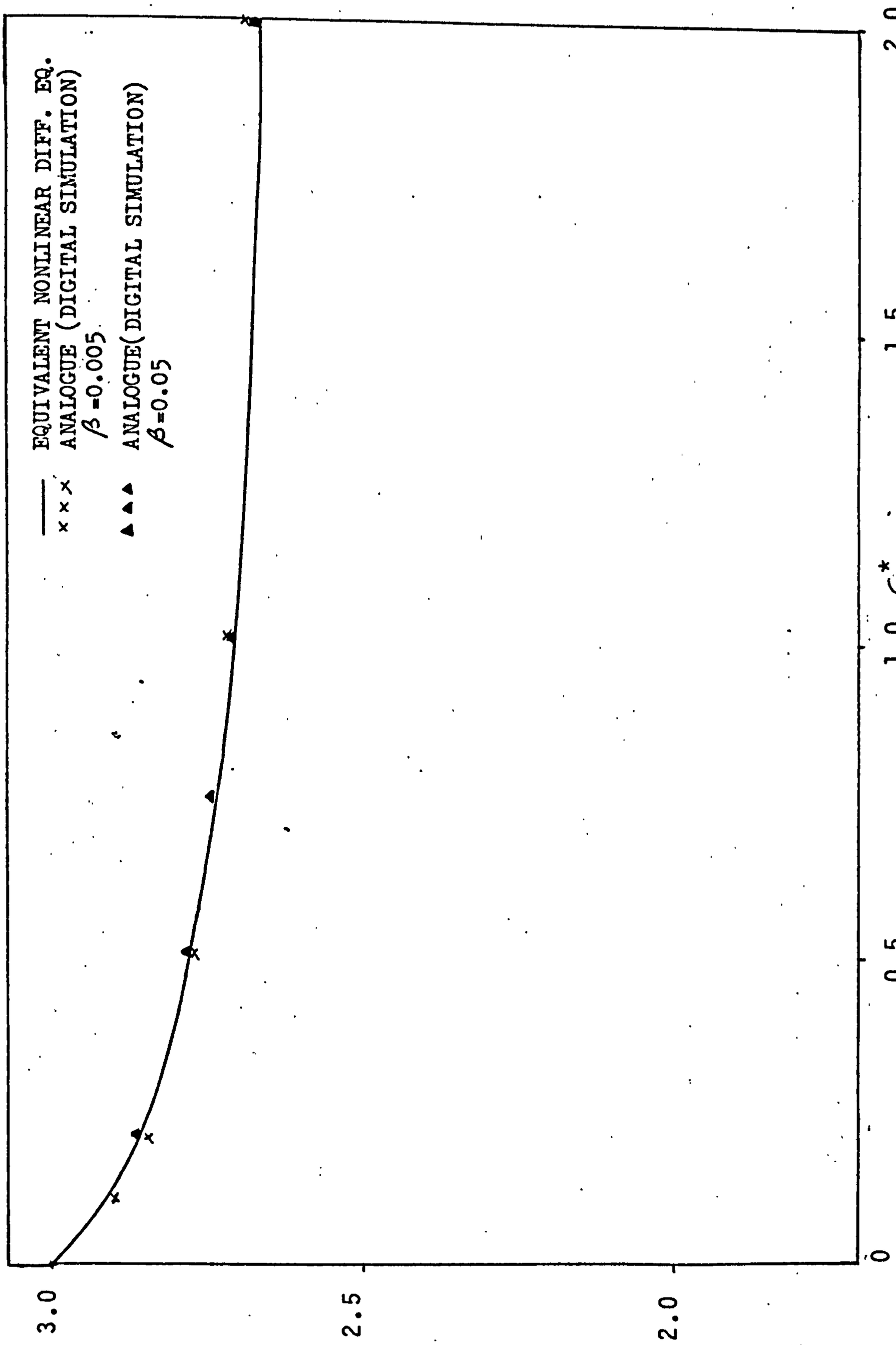

FIGURE 71a

(a4)

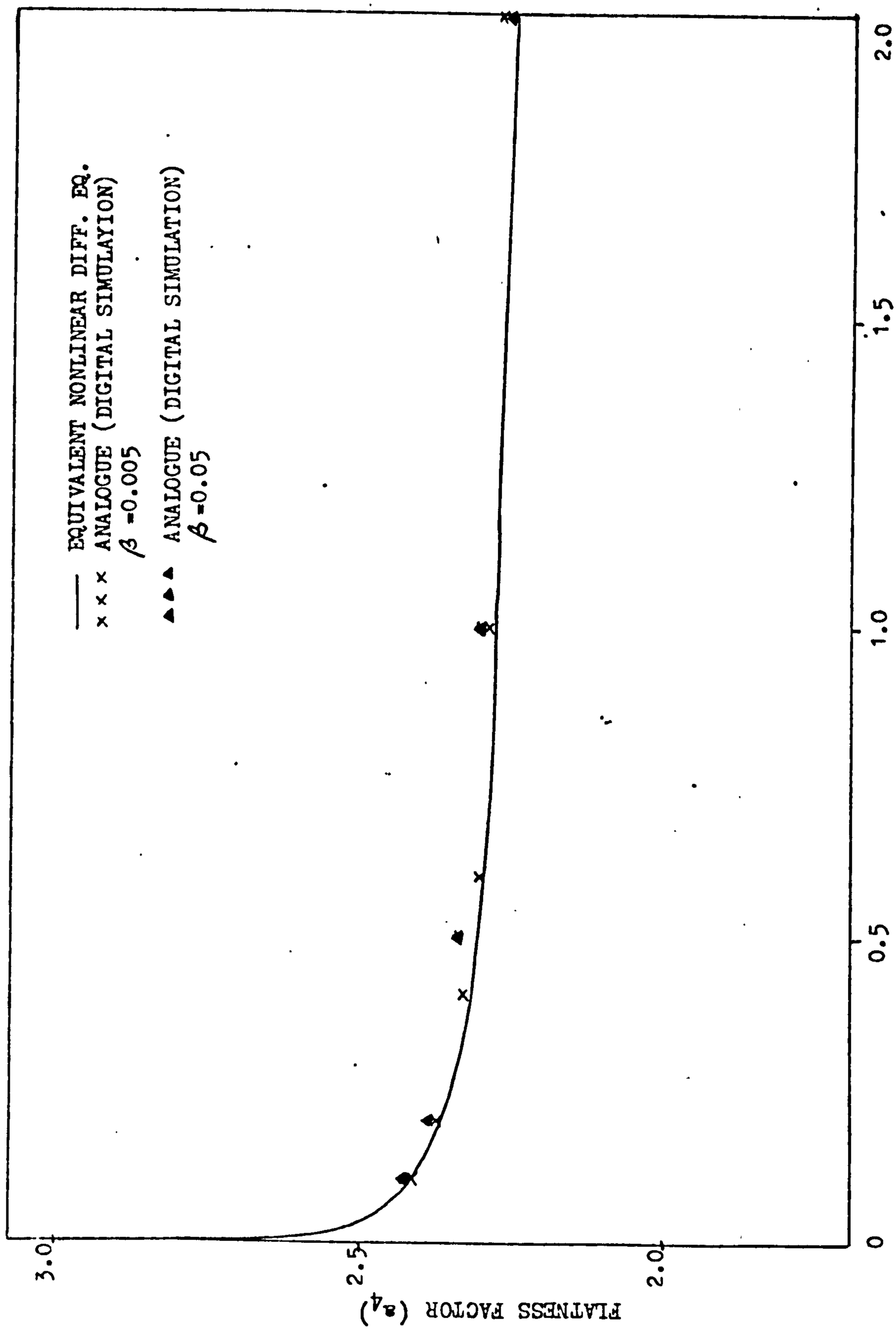

FIGURE 71b FLATNESS FACTOR FOR VARIOUS VALUES OF FOR n=6

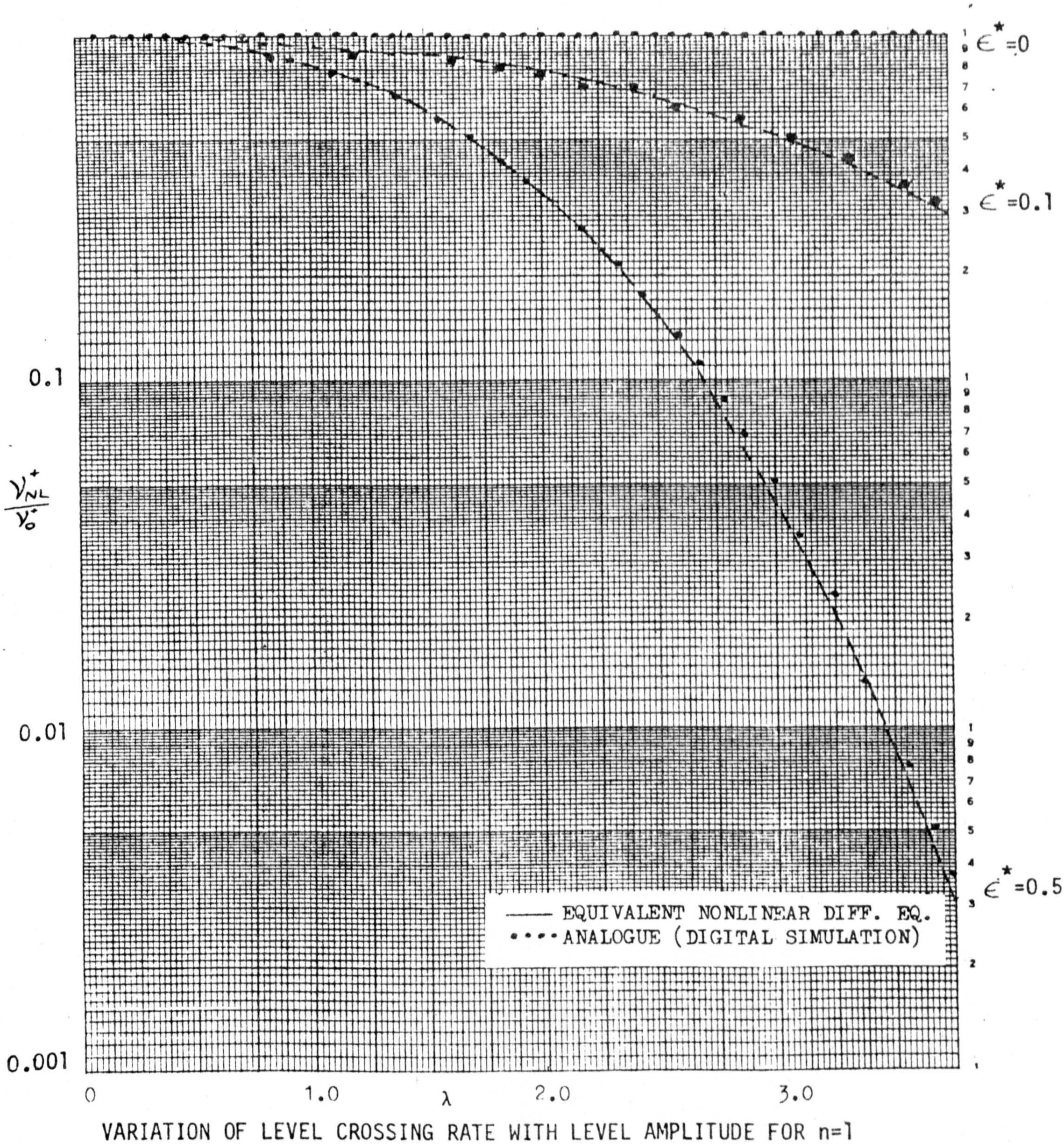

VARIATION OF LEVEL CROSSING RATE WITH LEVEL AMPLITUDE FOR n=1

FIGURE 72a

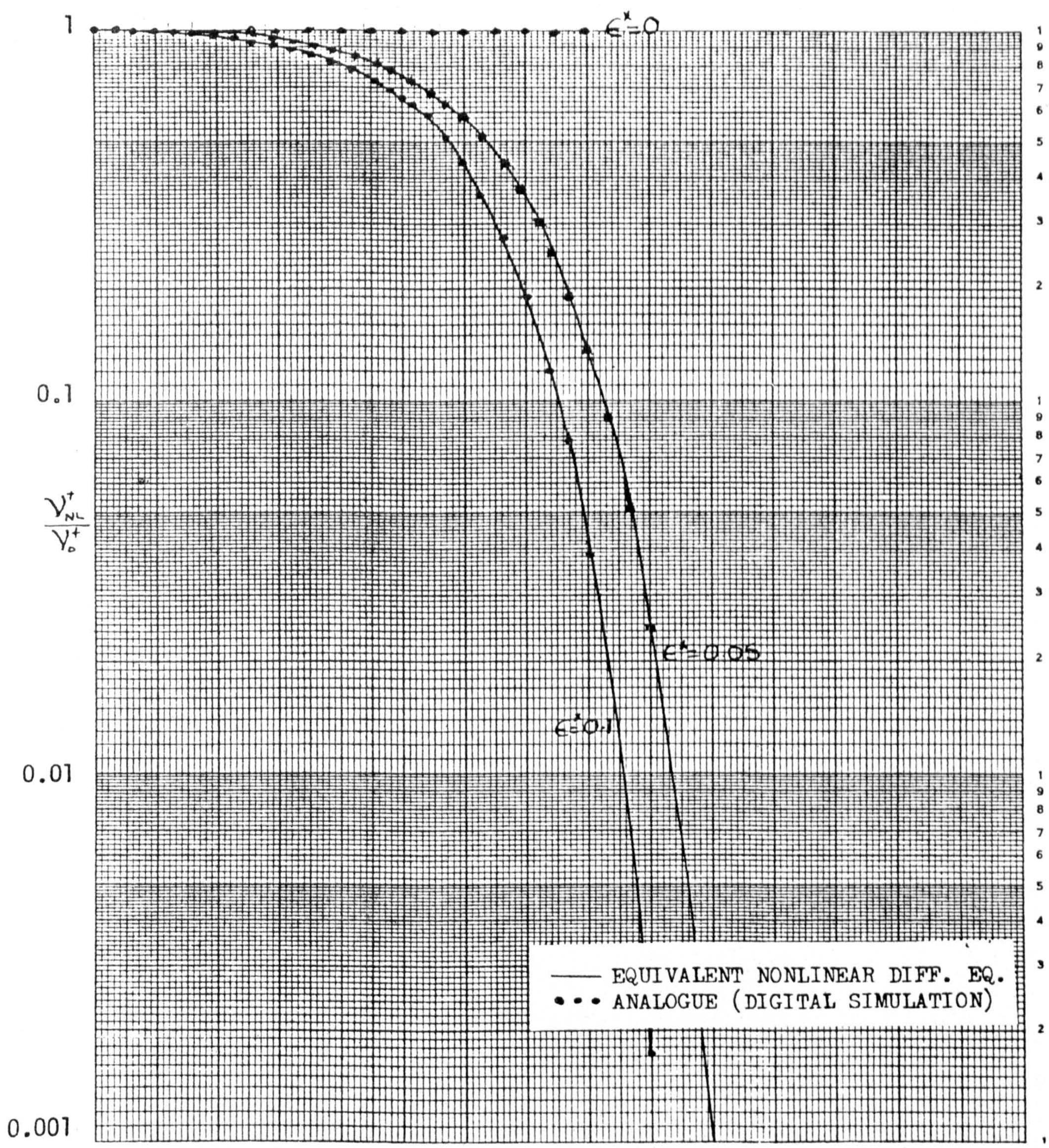

VARIATION OF LEVEL CROSSING RATE WITH LEVEL AMPLITUDE
FOR n=6

FIGURE 72b

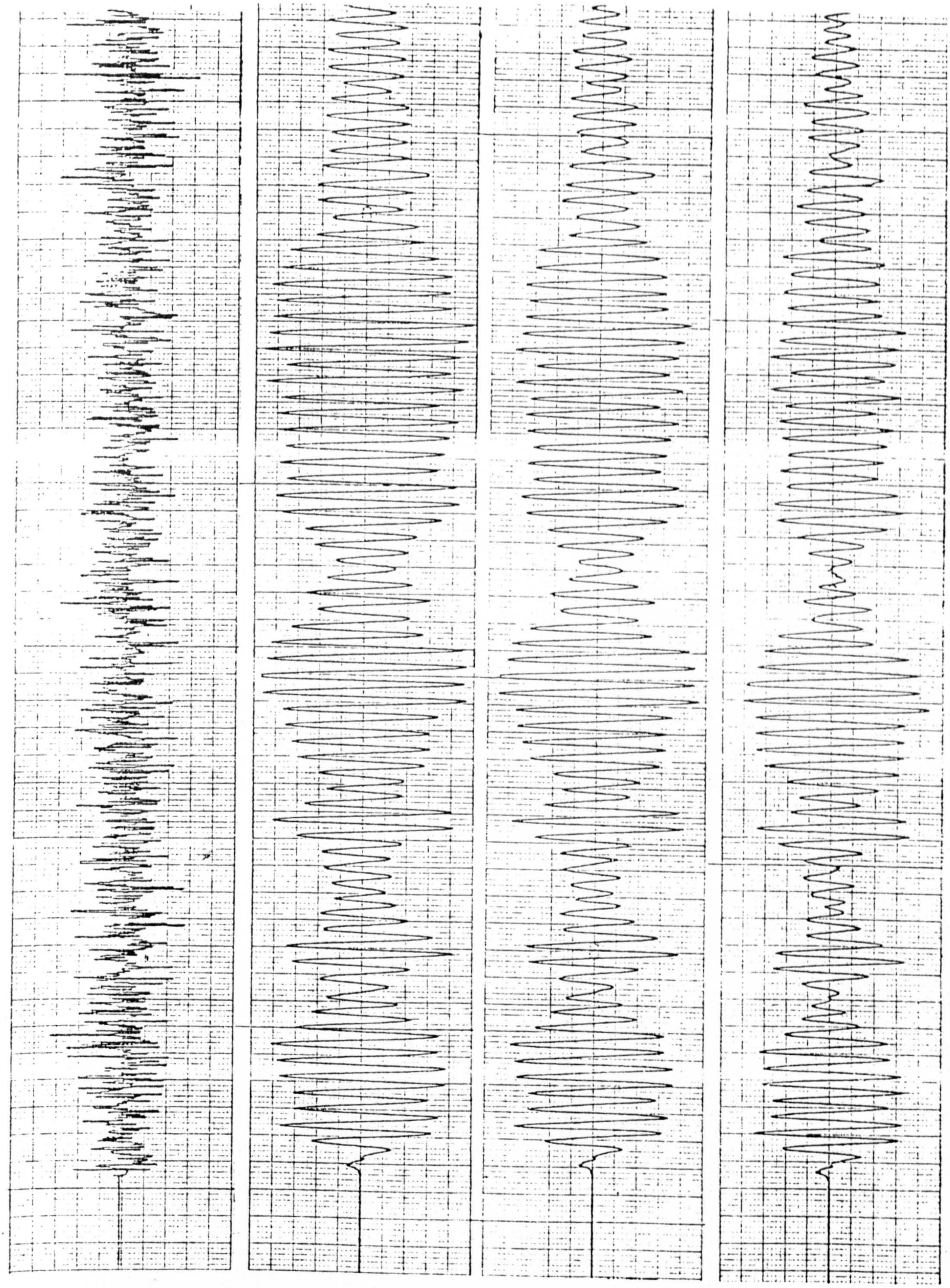

TIME HISTORIES FOR VARIOUS VALUES OF ϵ^* FOR n=1 So = 1000

FIGURE 73a.

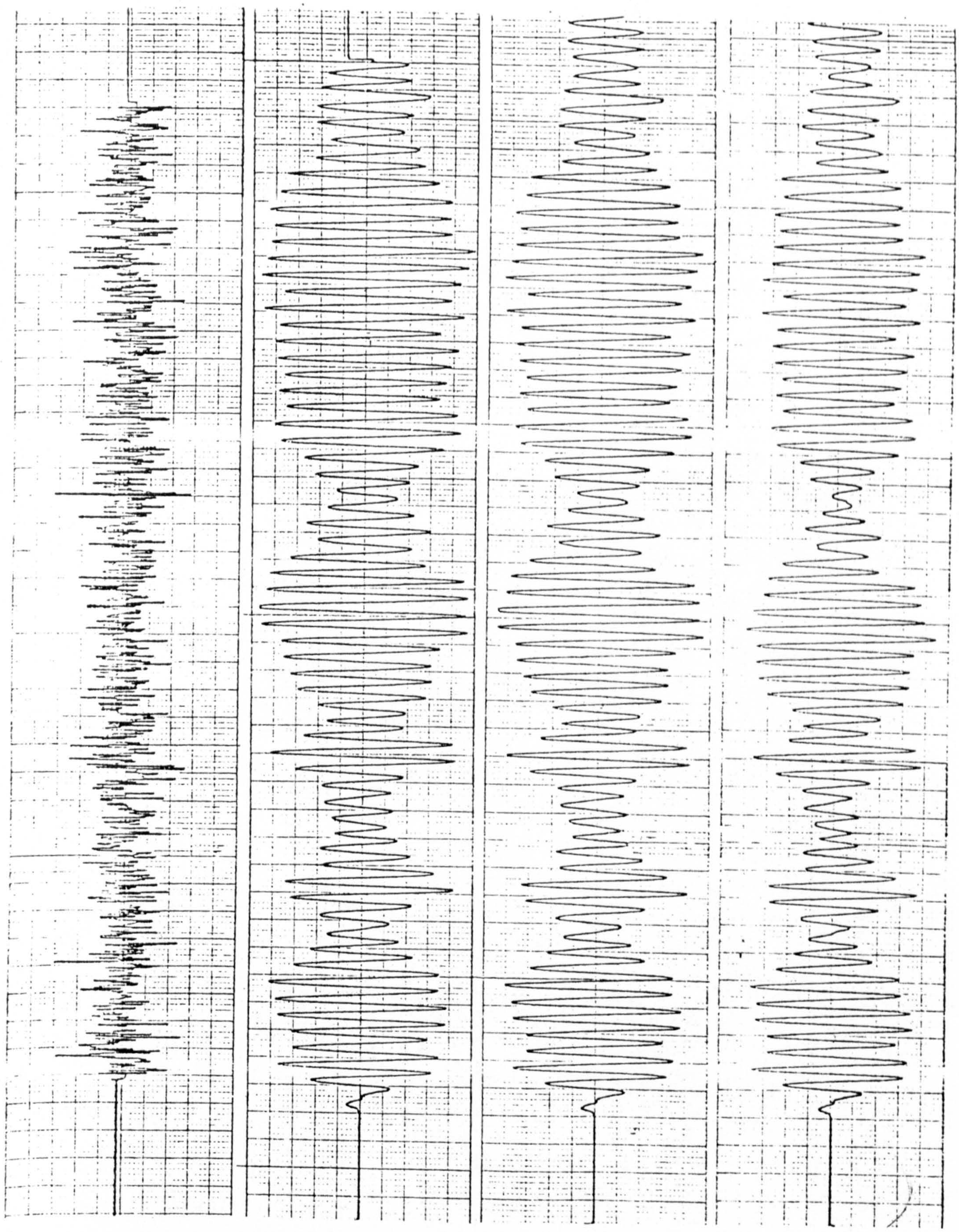

TIME HISTORIES FOR VARIOUS VALUES OF ϵ^* for n=6

FIGURE 73b

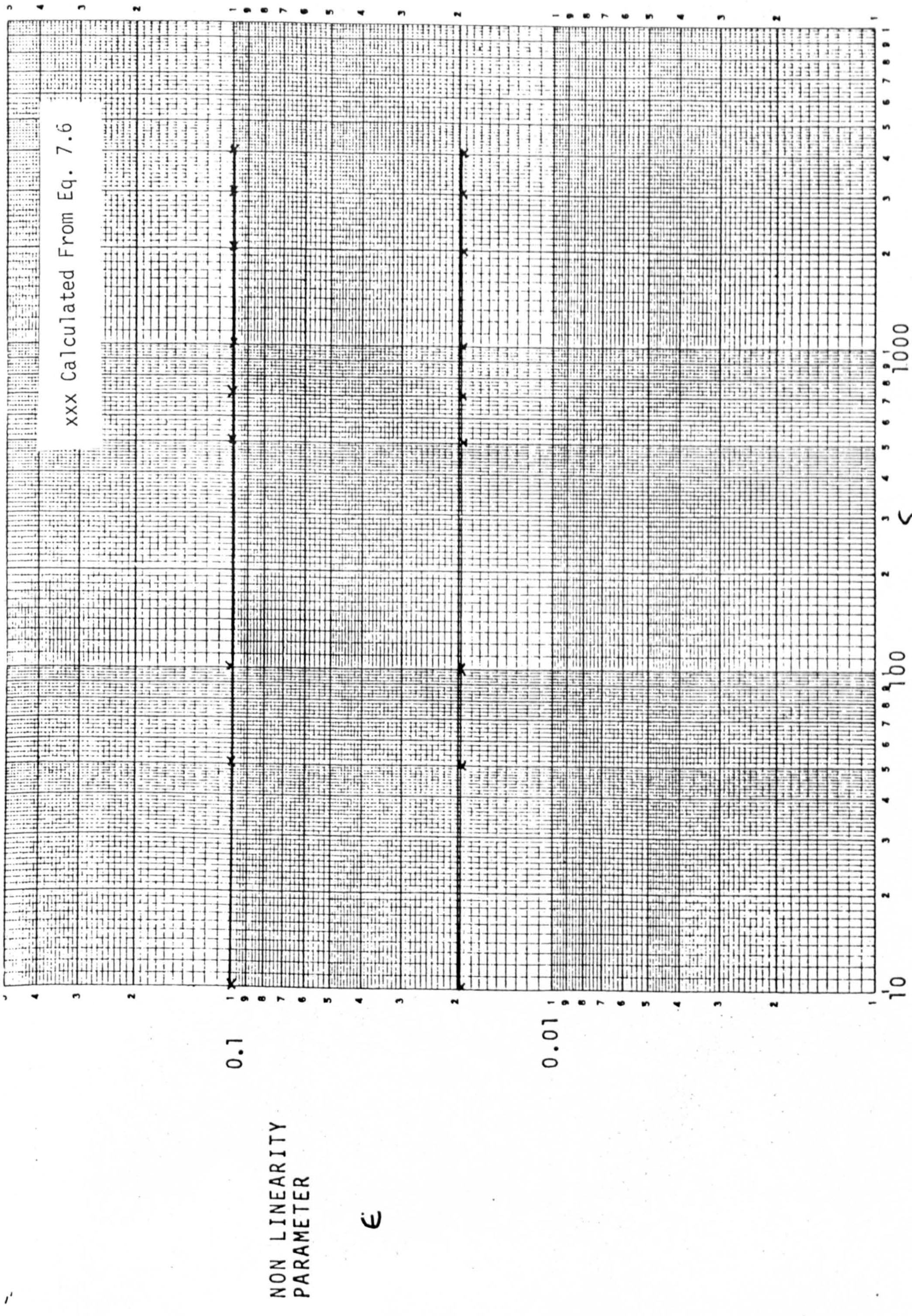
xxx Calculated From Eq. 7.6
NON LINEARITY PARAMETER CALCULATED USING MENL METHOD
FIGURE 74
NON LINEARITY PARAMETER
ε
So
1000
100
10
1
0.1
0.01

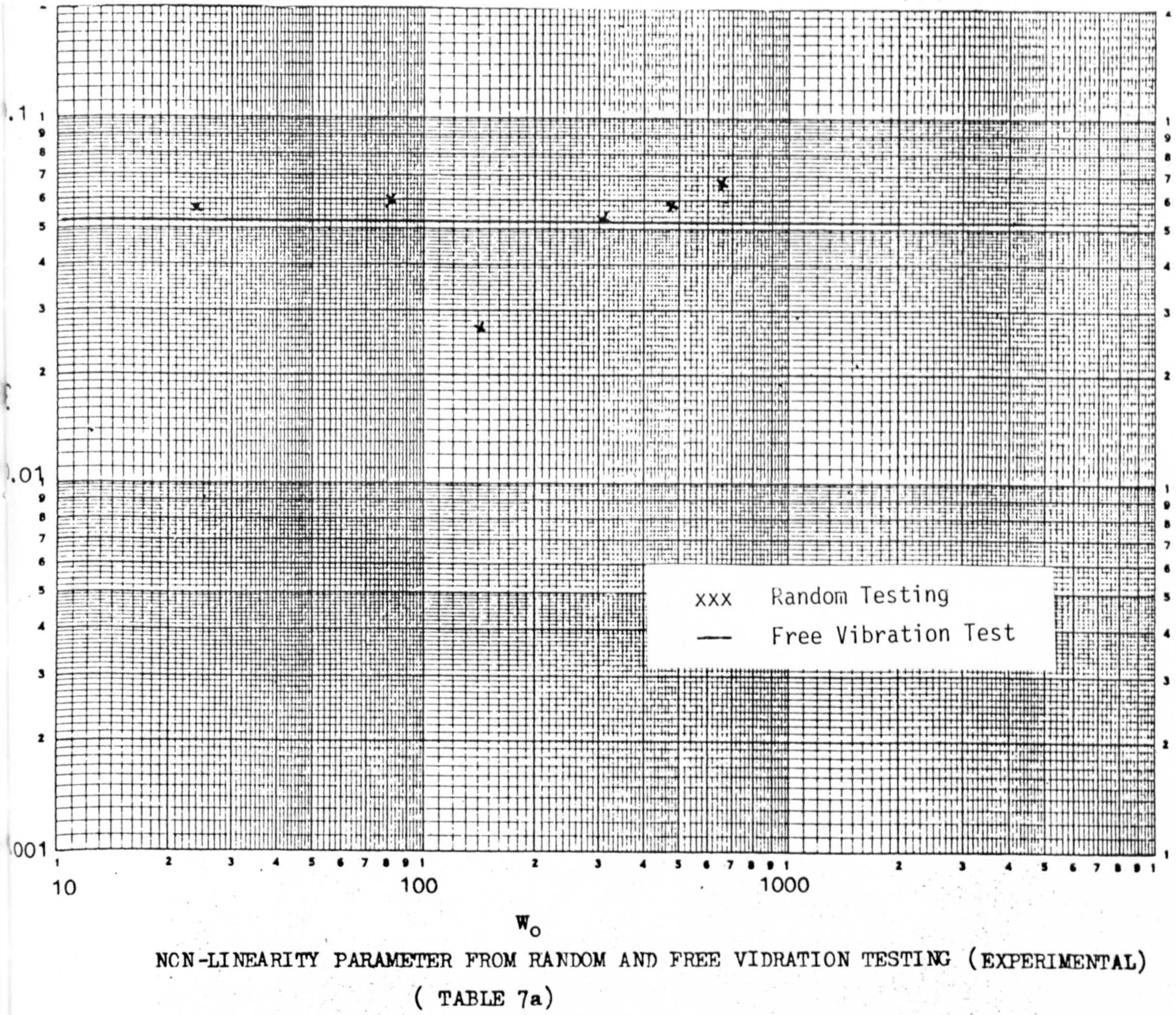

W_o

NON-LINEARITY PARAMETER FROM RANDOM AND FREE VIBRATION TESTING (EXPERIMENTAL)

(TABLE 7a)

FIGURE 75a

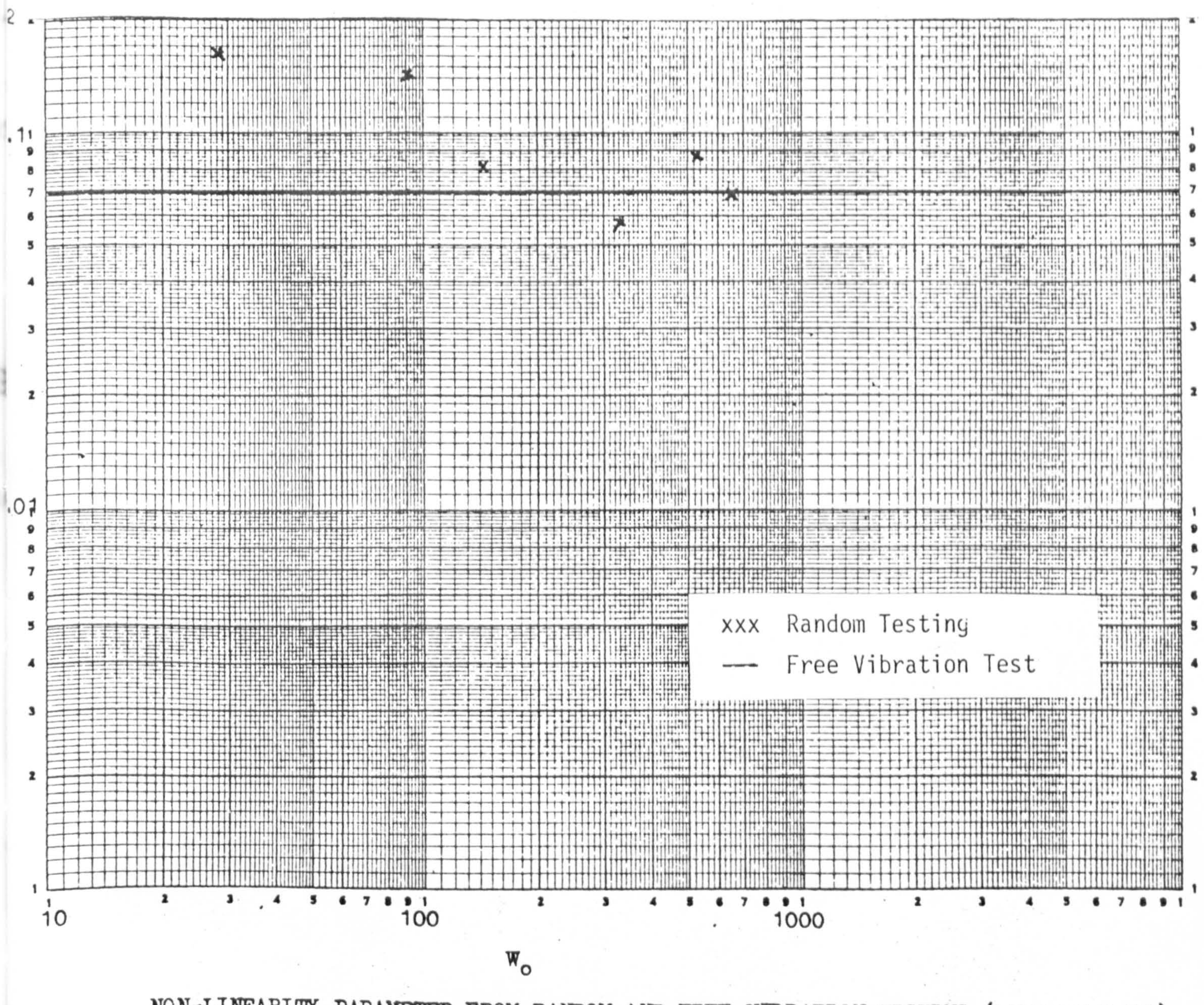

NON-LINEARITY PARAMETER FROM RANDOM AND FREE VIBRATION TESTING (EXPERIMENTAL)

(TABLE 7b)

FIGURE 75b